The University of Brighton
in collaboration with
Biocompatibles UK Ltd.

Hypoxia as a Target for Drug Combination Therapy of Liver Cancer

A thesis submitted in partial fulfilment of the requirements of the University of Brighton for the degree of Doctor of Philosophy

Cressida Jane Bowyer

2/20/2012

Abstract.

Oxygen is a requirement for almost all living organisms and adaptations to oxygen shortage are essential for surviving periods of oxygen deprivation, known as hypoxia. Cells have evolved a range of mechanisms which increase the supply of oxygen and facilitate metabolic alterations that enable the cell and the organism to maintain functionality under hypoxic conditions. Hypoxia is a hallmark of solid tumours and is associated with increased malignancy and mortality in hepatocellular carcinoma (HCC). Transarterial chemoembolisation therapy (TACE) using doxorubicin is the current standard of care for intermediate HCC, although response rates are poor. Drug eluting bead transarterial chemoembolisation (DEB-TACE) shows improved response rates over TACE. More recently, rapamycin has come under scrutiny as an effective therapy against HCC. Embolisation therapies have been shown to induce hypoxia in HCC, leading to the escape of hypoxia-adapted cancer cells from therapy. The principal transcription factor which orchestrates responses to hypoxia is hypoxia inducible factor 1 (HIF-1**)**. Laboratory and clinical evidence support the hypothesis that HIF-1 activity contributes to cancer progression and increased mortality. Targeting HIF-1 therefore presents an opportunity for improving outcomes of cancer therapy.

A hypoxic model of HCC was established, and used to characterise the responses of the cell line HepG2 to chemotherapeutic agents in both normoxic and hypoxic conditions. Firstly, the time and concentration dependent effects of doxorubicin, rapamycin and both drugs in combination on the viability of HepG2 cells cultured under both normoxic and hypoxic conditions were investigated. SDS-PAGE and Western Blotting was then used to evaluate the responses of HIF-1α, NFkB, S6K and Akt expression to doxorubicin, rapamycin and both drugs in combination in cells cultured under both normoxic and hypoxic conditions. Finally, the anti-tumour effects of doxorubicin, rapamycin and both drugs in combination were investigated *in vivo* using an ectopic xenograft murine model of HCC.

The *in vitro* evidence presented in this thesis demonstrates that a concentration of doxorubicin relevant to clinical concentrations following DEB-TACE effectively inhibits the viability of both normoxic and hypoxic liver cancer cells. Also presented is *in vitro* evidence that low dose rapamycin inhibits the viability of both normoxic, and to a lesser extent, hypoxic liver cancer cells. The addition of low dose rapamycin to doxorubicin was consistently observed to have an additive effect on the inhibition of cell viability. Protein analysis demonstrated that low dose rapamycin inhibits the hypoxia stimulated accumulation of HIF-1α, as does high dose doxorubicin. However, inhibition of HIF-1α was attenuated when the two drugs were used in combination. Cytotoxic effects are not, therefore, wholly dependent on inhibition of HIF-1α. Inhibition of HIF-1α by each drug alone appears to be due to different mechanisms. This study also showed *in vivo* that combinations of doxorubicin DEB-TACE with either rapamycin DEB-TACE or oral rapamycin are more effective than either treatment alone at reducing tumour burden in a mouse model of HCC. Two clinical trials are now underway to investigate the combination of doxorubicin DEB-TACE and low dose oral rapamycin to treat HCC.

List of Abbreviations and Acronyms.

4EBP-1	eukaryotic initiation factor 4E binding protein 1
ABC	adenosine triphosphate -binding cassette transporter
ADP	adenosine diphosphate
AFP	alpha-fetoprotein
AMP	adenosine monophosphate
APS	ammonium persulphate
ARNT	aryl hydrocarbon receptor nuclear translocator
Asp	asparagine
ATCC	American Type Culture Collection
ATP	adenosine triphosphate
BCLC	Barcelona Clinic Liver Cancer staging systems
BSA	bovine serum albumin
CAD	C-terminal transactivation domain
cAMP	cyclic adenosine monophosphate
CBP	cyclic adenosine monophosphate binding protein
CLIP	Cancer of the Liver Italian Program
cTACE	conventional transarterial chemoembolisation
DAPI	4', 6-diamidino-2-phenylindole
DEB-TACE	drug-eluting bead chemoembolisation
DMSO	dimethyl sulfoxide
DNA	deoxyribonucleic acid
DTT	dithiothreitol
EASL	European Association for the Study of the Liver
ECL	enhanced chemiluminescence
EDTA	ethylenediaminetetraacetic acid
EGTA	ethylene glycol tetraacetic acid
elF4F	elongation factor 4E
EPAS	endothelial per arnt sim domain protein
ETC	electron transport chain
FAT	focal adhesion targeting region of focal adhesion kinase
FDA	Food and Drug Administration
FIH-1	factor-inhibiting HIF-1α
FKBP12	FK506 (tacrolimus) binding protein 12
HBV	hepatitis B virus
HCV	hepatitis C virus
HCC	hepatocellular carcinoma
HEAT	Huntingtin, elongation factor 3, protein phosphatase 2A and PI3 kinaseTOR1
HIF	hypoxia-inducible Factor
HLH	helix-loop-helix
HRE	hypoxia response element
HRP	horseradish peroxidase
IkB	inhibitor kappa B
IAP-2	inhibitor of apoptosis 2
IgG	immunoglobulin G
IKK	IkB kinase
IPAS	inhibitory Per Arnt Sim
IRES	internal ribosome entry site
LDH-A	lactate dehydrogenase A
MDR	multi drug resistance
MAPK	mitogen-activated protein kinase
MEM	Minimum Essential Medium
mRNA	messenger ribonucleic acid
mTOR	mammalian target of rapamycin

mTORC1	mammalian target of rapamycin complex 1
mTORC2	mammalian target of rapamycin complex 2
MTS	3(4,5 dimethylthiazol-2-yl)-5-(3-carboxymethoxyphenyl)-2-(4 sulfophenyl)2H tetrazolium
NAD	N-terminal transactivation domain
NADH	nicotinamide adenine dinucleotide
NADPH	nicotinamide adenine dinucleotide phosphate
NFkB	nuclear factor kappa-light-chain-enhancer of activated B cells
NHE	Na-H exchange
NMRI	National Medical Research Institute
ODD	oxygen degradation domain
OLT	orthotopic liver transplantation
PAS	per arnt sim
PBS	phosphate-buffered saline
PDGFR	platelet-derived growth factor receptor
PDH	pyruvate dehydrogenase
PDK-1	pyruvate dehydrogenase kinase 1
PEI	perctaneous ethanol injection
PES	phenazine ethosulfate
Pgp	P-glycoprotein
pH	potential of hydrogen
PHD	prolyl-hydroxylase
PI3K	phosphoinositide 3-kinase
PIKK	phosphatidyl inositol 3' kinase-related kinases
PIP2	phosphotidylinositol (4, 5)-biphosphate
PIP3	phosphotidylinositol (3, 4, 5)-biphosphate
PS	performance status
PTEN	Phosphotase and Tensin Homolog Deleted on Chromosome 10
PVA	poly vinyl alcohol
PVDF	polyvinylidene fluoride
PVI	portal vein invasion
PVT	portal vein thrombosis
Raptor	regulatory associated protein of mTOR
REDD1	regulated in development and DNA damage responses
RFA	radiofrequency ablation
RNA	ribonucleic acid
Rictor	raptor independent companion of mTOR
ROS	reactive oxygen species
S6K	S6 kinase
SDS	sodium dodecyl sulphate
SDS-PAGE	sodium dodecyl sulphate-polyacrylamide gel electrophoresis
SEM	standard error of the mean
Ser	serine
siRNA	small interfering RNA
TACE	transarterial chemoembolisation
TAE	transarterial embolisation
TEMED	tetramethylethylenediamine
Thr	threonine
Tris	tris (hydroxymethyl) aminomethane hydrochloride
TNM	tumour node metastasis
TOP2	topoisomerase II
TRITC	tetramethylrhodamine-5-(and 6)-isothiocyanate
TSC1/TSC2	Tuberous sclerosis protein 1/Tuberous sclerosis protein 2
VEGF	vascular endothelial growth factor
VHL	von Hippel-Lindau

Acknowledgments.

Many thanks to my academic supervisors Dr Wendy Macfarlane and Dr Gary Phillips, to my industrial supervisor Professor Andrew Lewis, and to Professor Andrew Lloyd for their support, guidance and motivation throughout my PhD research. Also thanks to other members of staff at The University of Brighton for help and advice, especially Dr Iain Allan, Dr Marcus Allen, Dr Andrew Overall, Dr Peter Bush and Christopher Morris. Thanks also to friends and fellow PhD students.

Biggest thanks, and lots of hugs and kisses, have to go to my children Daisy, Harry and Alfie, for putting up with me often being elsewhere, in mind and in body. I hope you enjoy your University years as much as I have enjoyed mine.

Declaration

I declare that the research contained in this thesis, unless otherwise indicated within the text, is the original work of the author. The thesis has not been previously submitted to this or any other university for a degree, and does not incorporate any material already submitted for a degree.

Signed

Date

List of Figures.

List of Tables.

Chapter 1

Introduction.

1.1 Liver Cancer.

1.1.1 Epidemiology, Etiology, Diagnosis and Treatment.

Hepatocellular carcinoma (HCC), or primary liver cancer, is the sixth most common cancer worldwide, and the third most common cause of cancer death. More than half a million new cases are diagnosed each year. The prognosis is generally poor, with survival rates of between 3 and 5%, and the number of deaths per year is almost equal to the number of new cases. The major risk factors for HCC are infection with the hepatitis B or hepatitis C virus (HBV, HCV). Indeed, 75% of all cases are a result of hepatitis infection. The incidence of HCC is highest in Asian and African countries, where chronic HBV infection is the predominant risk factor, and the incidence of HCC mirrors the prevalence of HBV infection (Parkin *et al*., 2005, Zhu *et al*., 2011). In Europe, North America and Japan chronic HCV infection and alcoholic cirrhosis are the predominant risk factors, and HCC is the leading cause of death for cirrhotic patients (Parkin *et al*., 2005, Bruix *et al*., 2006, Di Bisceglie, 1995).

Exposure to the aflatoxin is a risk factor in sub-Saharan Africa, Southeast Asia, and China (Liu and Wu, 2010). Aflatoxin is a deoxyribonucleic acid (DNA) damaging agent produced by the fungus *Aspergillus*, which grows on food stored in warm and damp conditions (Sanyal *et al*., 2010).

The diverse etiologies of HCC mean that determining the prognosis and treatment plan for patients is not straightforward. The extent of underlying liver disease, as well as the tumour stage, needs to be taken into account when deciding on treatment modalities, and clinical staging systems are used for patient assessment. The staging

systems most commonly used for HCC are the Okuda, the tumour node metastasis (TNM), the Cancer of the Liver Italian Program (CLIP) score and the Barcelona Clinic Liver Cancer staging systems (BCLC). The Child-Pugh score, as summarised in Table 1.1, is used to measure liver function.

Score	1	2	3
Ascites	Absent	Slight	Moderate
Hepatic encephalopathy	Absent	Mild/transient	Hepatic coma
Bilirubin (μM/L)	< 34	34 - 51	>51
Albumin (g/L)	>35	35 - 28	< 28
Prothrombin (sec)*	< 4	4 – 6	>6
Child A: score 5-6 (well compensated). 1 yr survival = 100%, 2 yr survival = 85%. Child B: score 7-9 (functional compromise). 1 yr survival = 81%, 2 yr survival = 57%. Child C: score 10-15 (decompensated). 1 yr survival = 45%, 2 yr survival = 35%.			

*Difference between patient and control.

Table 1.1 Child Pugh Classification of Liver Function.
The Child Pugh classification assesses five clinical measures of liver disease. Each measure is scored from 1 to 3, with 3 indicating the most pathological. Liver disease is then classified into Child-Pugh class A to C, according to the added score from the assessment of liver damage.

The BCLC links the patient's general state of health, Child Pugh classification, and extent of tumour spread with a treatment algorithm, and this staging system has now become the international standard (Bruix *et al*., 2006, Pons *et al*., 2005). Figure 1.1 illustrates the staging system algorithm. Surveillance of patients with cirrhosis or hepatitis is crucial if patients are to be diagnosed early enough for curative treatments (Wong *et al*., 2008, Wong *et al*., 2000, Mok *et al*., 2005). The European Association for the Study of the Liver (EASL) recommends surveillance using ultrasound and serum alpha-fetoprotein (AFP) every 6 months.

If HCC is detected early enough, the treatment options are surgical resection, liver transplantation, and percutaneous ablation. Percutaneous ablation is the destruction of neoplastic cells by ethanol or acetic acid or by temperature (radiofrequency, laser,

microwave, and cryoablation). The 5-year survival rates for early stage treatments are 70 - 90% (Rampone *et al*., 2009, Granito and Bolondi, 2009).

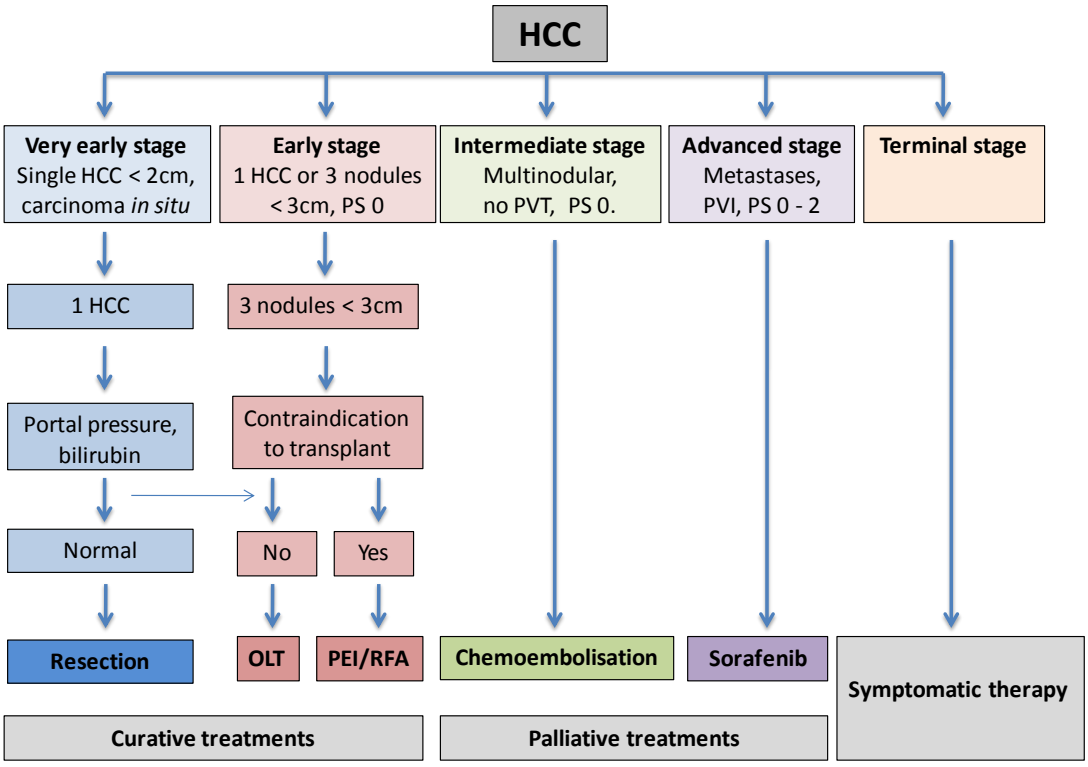

Figure 1.1 The Barcelona Clinic Liver Cancer (BCLC) Staging Classification and Treatment Schedule.
The BCLC links the stage of the disease to a specific treatment strategy.PS, performance status; OLT, orthotopic liver transplantation; PEI, perctaneous ethanol injection; PVI, portal vein invasion; PVT, portal vein thrombosis; RFA, radiofrequency ablation.

The treatment option that has shown best patient outcome and survival benefit for intermediate stage HCC is transarterial chemoembolisation (TACE) (Biselli *et al*., 2005, Takayasu *et al*., 2006, Lee *et al*., 2006, Kaibori *et al*., 2006, Molinari *et al*., 2006, Bruix *et al*., 2006, Llovet and Bruix, 2003). TACE is the current standard-of-care for intermediate stage HCC, and shows 1, 2 and 3 year survival rates of 80%, 65% and 50% respectively (Bruix *et al*., 2006, Bruix *et al*., 2004, Raoul *et al*., 2011). For advanced stage patients, sorafenib is the new standard of care (Keating and Santoro, 2009). Sorafenib is a small molecule multi-kinase inhibitor and has been

shown to improve survival times, but by months rather than years. Survival rates at one, two and three years are 29%, 16% and 8% respectively (Llovet *et al*., 2008, Cheng *et al*., 2009). End stage patients are treated symptomatically and have a life expectancy of less than 6 months (Granito and Bolondi, 2009).

The introduction of screening programmes for those at risk of developing HCC has resulted in more cases being diagnosed at an early stage, when curative treatments are possible (Sangiovanni *et al*., 2004). However, the majority of cases are not diagnosed until intermediate or advanced stage, by which time the treatment options are limited and the prognosis is poor (Colombo and Sangiovanni, 2003).

1.1.2 Transarterial Chemoembolisation (TACE).

Transarterial embolisation (TAE) is a technique used to treat HCC, and exploits both the fact that the liver tumour is fed by the hepatic artery whilst the normal liver tissue is fed by the portal vein (Breedis and Young, 1954), and that HCCs are typically highly vascularised (Ackerman, 1972).

TACE was first pioneered by Yamada in the 1980s (Yamada *et al*., 1980, Yamada *et al*., 1983) in an attempt to improve the dismal treatment outcomes associated with systemic chemotherapies. TACE combines tumour embolisation with delivery of chemotherapeutic agent(s) directly to the blood vessels feeding the tumour, thus increasing the intratumoural concentration and of the drug(s) whilst decreasing systemic concentration (Biolato *et al*., 2010). The embolic blocks the flow of blood to the tumour, starving tumour cells of oxygen and nutrients. There is minimal damage to paranchymal liver tissue since this tissue receives 75% of its blood supply *via* the portal vein, whereas the tumour derives 95% of its blood supply from the hepatic artery (Bruix *et al*., 2004). Typically, the protocol for conventional TACE (cTACE) consists of the catheter-based intra-arterial injection of a chemotherapeutic

iodised oil emulsion followed by injection of an embolic material (Liapi and Geschwind, 2010). TACE therapy allows a complete local tumour control of 25-35% and improved survival in patients with intermediate HCC, according to BCLC classification, when compared to systemic therapies. As an adjunctive therapy prior to liver resection TACE allows 70% tumour control (Vogl et al., 2009). TACE using the anthracycline antibiotic doxorubicin is the standard of care for the treatment of unresectable HCC (Biolato et al., 2010; Bruix et al., 2004).

1.1.3 Drug-eluting Bead Chemoembolisation (DEB-TACE).

Drug-eluting bead transarterial chemoembolisation (DEB-TACE) is a refinement of TACE, and provides a one-step procedure for both embolisation and drug delivery. The most successful embolic microsphere developed to date in terms of doxorubicin loading and release is the DC Bead (Biocompatibles UK). For HCC, the bead is available pre-loaded with doxorubicin (DEBDOX™). DEB-TACE allows a controlled, localised and sustained release of the drug to the tumour bed, with reduced systemic doxorubicin and an improved safety profile compared to cTACE (Varela et al., 2007, Lewis and Holden, 2011, Lewis et al., 2007). DEB-TACE also addresses some of the issues with regard to a lack of standardisation in the treatment of intermediate stage HCC. The only other commercially available DEB is the HepaSphere™, from Merit Medical Systems Inc.

The DC Bead actively sequesters doxorubicin from a non-ionic solution, due to an active ion-exchange process between the negatively charged sulfonate moieties on the microspheres with the positively charged amine region of the doxorubicin molecule. Drug elution is dependent on ion exchange with blood plasma ions after delivery of the microspheres (Lewis and Holden, 2011).

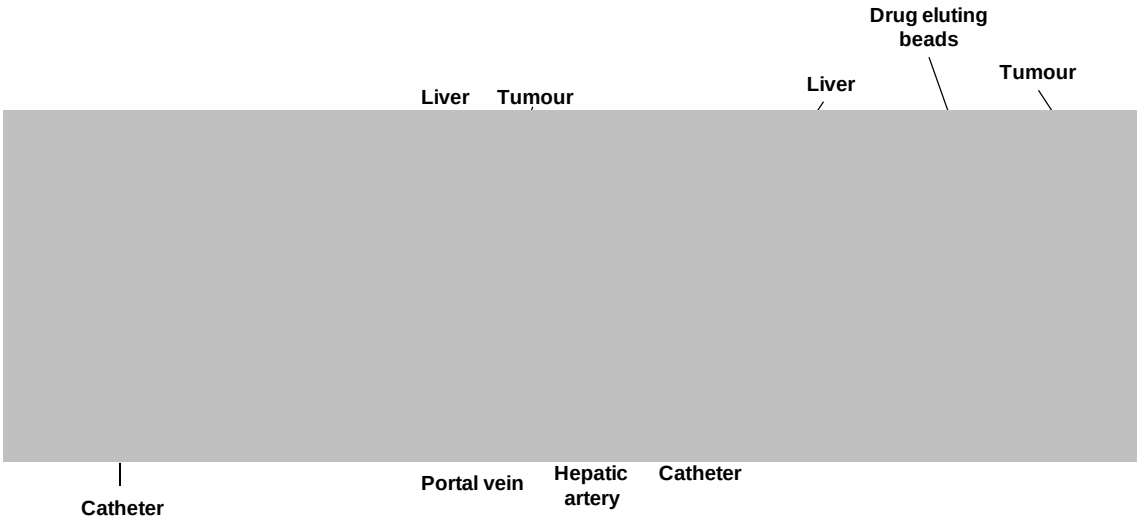

Figure 1.2 Schematic Outlining the Procedure for DEB-TACE.
A catheter is inserted into the femoral artery and directed to the liver using contrast media and X- ray equipment. Drug eluting beads are then injected into the capillaries feeding the tumour *via* the catheter. The procedure is normally carried out under local anaesthetic. Image adapted with permission from Biocompatibles UK Ltd.

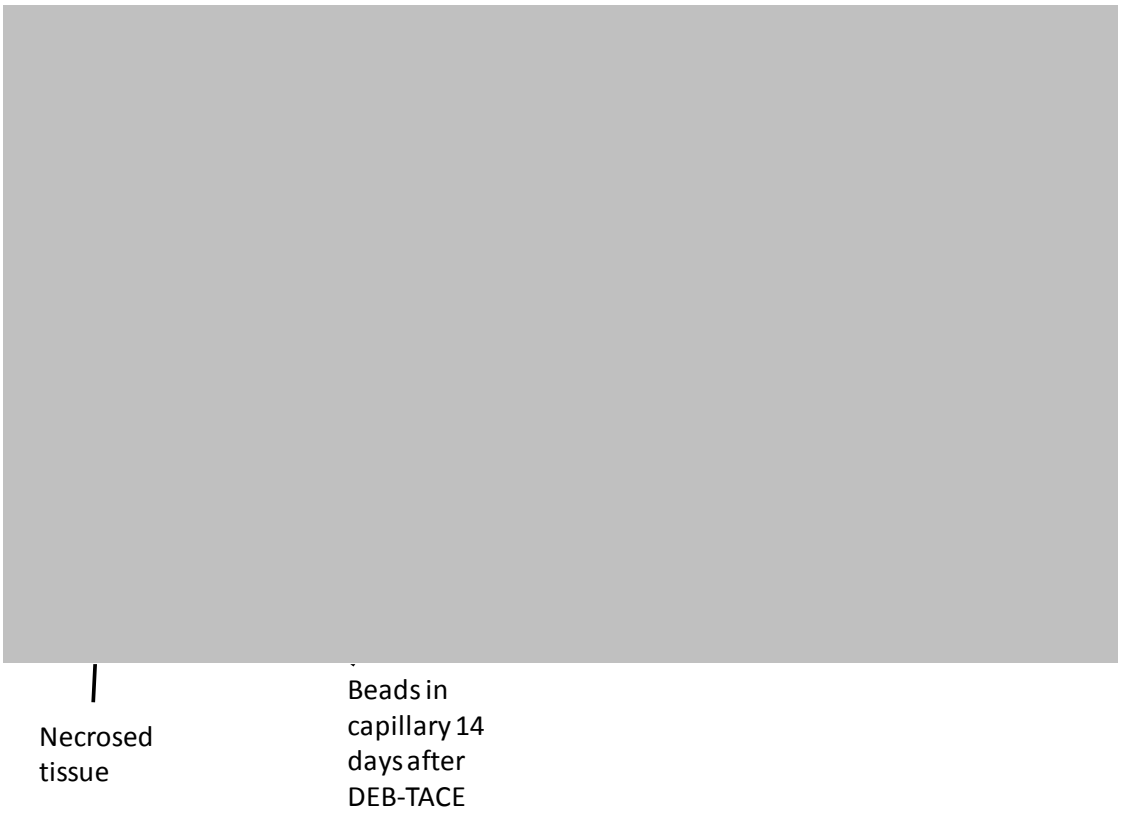

Figure 1.3 *In Vivo* Images of DEB-TACE.
A) An X-ray image of a chemoembolisation procedure. B) and C) histological analysis of DC Beads 14 days after DEB-TACE, in a rabbit Vx-2 model of hepatic arterial embolisation (Hong *et al*., 2006).

To deliver the beads to the tumour bed, a catheter is inserted into the femoral artery and directed to the liver. The beads are then injected *via* the catheter into the capillaries feeding the tumour. The procedure, outlined in Figures 1.2 and 1.3(A), is normally carried out under local anaesthetic, without the need for overnight hospitalisation. Figure 1.3 (B) and (C) show *in vivo* imaging of beads after DEB-TACE in a rabbit model.

Results so far from clinical trials, including the results of a randomised phase II trial (PRECISION V), show that DEB-TACE using DEBDOX shows a significant survival advantage, higher rates of complete response, and significant differences in objective response and disease control in patients with advanced HCC when compared with cTACE (Dhanasekaran et al., 2010, Liapi and Geschwind, 2011, Lammer et al., 2010, Reyes et al., 2009). The incidence of doxorubicin-related adverse events was significantly lower with DEBDOX compared to cTACE (Lammer et al., 2010). TACE using DEBDOX also demonstrated improved local response, fewer recurrences, and a longer time to progression when compared with bland embolisation using unloaded DC Beads (Malagari et al., 2010). DEB-TACE is a minimally invasive treatment that is becoming more widely used as a treatment for unresectable HCC, as an adjunctive therapy prior to resection and as a bridge therapy to maintain patients on transplant waiting lists (Carter and Martin Ii, 2009, Liapi and Geschwind, 2011, Lewis and Holden, 2011). The results of ongoing clinical trials will, in the future, contribute to the optimisation of treatment strategies.

1.2 Cellular Oxygen Supply and Hypoxia.

Adequate supplies of oxygen are essential for the normal functioning of all multicellular organisms/metazoan species. The principle energy source for the

majority of cellular processes is adenosine triphosphate (ATP). Oxidative phosphorylation is the process by which cells generate ATP from the catabolism of glucose and fatty acids, and the oxygen molecule is the metabolic substrate for this cellular respiration, acting as the terminal electron acceptor.

Low cellular oxygen concentrations, known as hypoxia, can compromise cell function and lead to cell death and tissue damage. However, oxygen molecules are potentially toxic, since they can cause oxidative damage to macromolecules within the cell. The control of oxygen homeostasis is thus essential for maintaining cellular and therefore whole organism viability.

The physiological oxygen tension within healthy human tissue varies according to the organ, but generally lies within the range 20 – 120 mmHg (Vaupel *et al*., 1989). Cells in different tissues experience different oxygen tensions, and cells within one tissue experience a range of oxygen tensions, depending on both distance from the nearest blood supply - the diffusion distance of oxygen through tissue is estimated to be around 150 μm (Coleman *et al*., 2002) - and the oxygenation status of that blood supply. For instance, the pressure of O_2 of the blood supply to the liver ranges from 95–105 mmHg in the hepatic artery, 50-65 mmHg in the portal vein, 35-45 mmHg in the sinusoids and 30– 40 mmHg in the central vein (Lee *et al*., 2007). The different oxygen tensions that each cell experiences in a healthy liver are all perceived as normal – indeed, the oxygen gradient along the sinusoid is the regulatory factor which creates the zonation of metabolic functioning within the sinusoid (Vollmar and Menger, 2009). Sensitive and adaptive mechanisms for sensing intracellular oxygen concentrations and responding to change are vital in order to maintain oxygen homeostasis. Adaptations to fluctuating oxygen levels need to be flexible and capable of responding to subtle changes.

Hypoxia occurs when oxygen tensions are ≤ 7 mmHg, usually as a result of decreased partial pressure of oxygen in the blood (hypoxeamia) or a decrease in the oxygen carrying capacity of the blood (anaemia) (Vaupel and Harrison, 2004). Molecular responses to hypoxia result in the increased expression of genes involved in adaptations to hypoxia, and the promotion of a range of physiological responses and adaptations that allow cells to survive in a hypoxic environment. These target genes play critical roles in angiogenesis, metabolism, cell proliferation and cell survival. The master regulator of adaptations to hypoxia is the transcription factor hypoxia-inducible factor (HIF) (Wang and Semenza, 1993).

1.2.1 Hypoxia-inducible Factor 1 (HIF-1).

HIF-1 was first identified by Gregg Semenza in 1992 whilst he was studying erythropoietin gene expression (Semenza and Wang, 1992). HIF is a highly conserved DNA binding protein (Iyer *et al*., 1998) that activates the expression of genes containing a hypoxia response element (HRE) (Wang and Semenza, 1993). HIF is a heterodimer comprising of two sub-units, α and β. Both sub-units belong to the Per-Arnt-Sim (PAS) family of helix-loop-helix (HLH) proteins (Wang and Semenza, 1995). HIF activity is regulated by the abundance of the HIF-α sub-unit. To date, three HIF-α isoforms have been described, with HIF-1α being the best characterised. In this study, we have concerned ourselves with the activity of HIF-1α. HIF-1α is constitutively expressed, but under normoxic conditions is subject to oxygen-dependent hydroxylation and ubiquitination that determines proteasomal degradation (Huang *et al*., 1998). Under hypoxic conditions the HIF-1α sub-unit stabilises, accumulates within the cell and translocates to the nucleus. Here it heterodimerises with HIF-1β, recruits the co-activators p300/cAMP binding protein (CBP) and becomes transcriptionally active (Wang and Semenza, 1993). This

response is rapid and its intensity correlates to the severity of hypoxia (Jiang *et al*., 1996). HIF-1β (also known as aryl hydrocarbon receptor nuclear translocator ARNT) is also constitutively expressed, and its stability is independent of oxygen tension. HIF-1β is involved in a wider range of cellular processes than HIF-1α *via* interaction with other proteins (Maxwell *et al*., 2001, Semenza *et al*., 1997, Swanson *et al*., 1995).

In addition to mediating cellular responses to oxygen shortage, there is increasing evidence that HIF-1 may be involved in preventing premature cell senescence, and in innate host defence mechanisms (Welford *et al*., 2006, Zarember and Malech, 2005, Lukashev *et al*., 2006). HIF-1 also plays an essential role in embryonic development (Huang *et al*., 2010).

1.2.2 HIF-α Isoforms.

In mammals, three isoforms of HIF-α have been identified – HIF-1α, HIF-2α (also known as Endothelial PAS domain protein or EPAS) and HIF-3α (also known as inhibitory Per Arnt Sim or IPAS). These are encoded by the genes *HIF1A, EPAS1, HIF3A* respectively. The HIF-1α, HIF-2α isoforms are structurally similar in their DNA binding and dimerisation domains, and regulation of gene expression by HIF-2α is similar to that of HIF-1α (Wiesener *et al*., 1998, O'Rourke *et al*., 1999). They differ in their transactivation domains, implying that they may have unique target genes (Heidbreder *et al*., 2003, Wiesener *et al*., 2003, Tian *et al*., 1997). HIF-3α lacks the transactivation domain found in factors containing either the 1α or 2α subunits and appears to inhibit transcriptional activation induced by hypoxia (Hirota and Semenza, 2006). HIF-1α is ubiquitously expressed, whereas expression of HIF-2α is cell specific (Loboda *et al*., 2010). In this study we have focussed on the abundance of HIF-1α in response to hypoxia.

1.2.3 The Structure of HIF-1α.

HIF-1α and HIF-1β belong to the Per Arnt Sim (PAS) sub-family of the HLH family of transcription factors. Both contain basic HLH motifs and a PAS domain, which are involved in DNA binding and dimerisation. The α sub-unit contains an oxygen degradation domain (ODD) and two transactivation domains – the N-terminal transactivation domain (NAD) and the C-terminal transactivation domain (CAD) (Figure 1.4) (Wang and Semenza, 1995, Chapman-Smith *et al*., 2004).

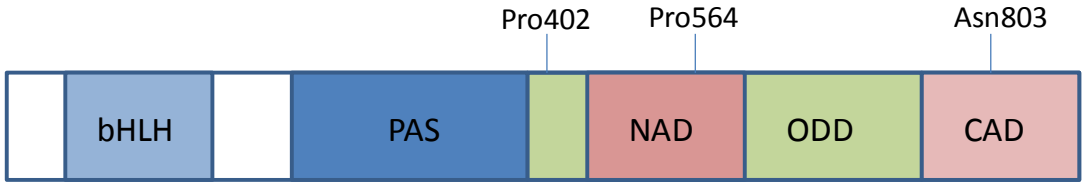

Figure 1.4 Schematic Showing Simplified Structure of HIF-1α and Hydroxylation Sites.
bHLH, basic helix-loop helix domain; CAD, C-terminal transactivation domain; NAD, N-terminal transactivation domain; ODD, oxygen degradation domain; PAS, Per Arnt Sim domain. Pro402, Pro 564 are the prolyl hydroxylation sites. Asn803 is the asparaginyl hydroxylation site.

1.2.4 Prolyl Hydroxylation Promotes the Degradation of HIF-1α.

In normoxic conditions HIF-1α is identified for ubiquitination and degradation *via* enzymatic hydroxylation of proline residues. The region of HIF-1α in which this takes place is known as the ODD. The ODD extends from amino acids 401 – 603 and contains proline residues at positions 402 and 564 (Bruick and McKnight, 2001, Huang *et al*., 1998) (Figure 1.5). Three HIF prolyl-hydroxylases (PHDs) have been identified (Jaakkola *et al*., 2001, Ivan *et al*., 2001). The hydroxylation promotes interaction with the von Hippel-Lindau (VHL) ubiquitylation complex (Ivan *et al*., 2001). The pVHL binds to the ODD and HIF-1α is ubiquinated by the VCB E3 ubiquitin-ligase complex. This labels the protein complex for proteasomal

degradation (Masson *et al*., 2001, Kamura *et al*., 2000, Iwai *et al*., 1999). Either or both of the residues can be hydroxylated, but hydroxylation of both residues is required for efficient degradation (Masson *et al*., 2001). The hydroxylation reaction requires oxygen, 2-oxogluterate and Fe (II). In hypoxic conditions (oxygen concentration < 6%), prolyl hydroxylation decreases and HIF-1α stabilises and accumulates (Ivan *et al*., 2001, Maxwell *et al*., 1999).

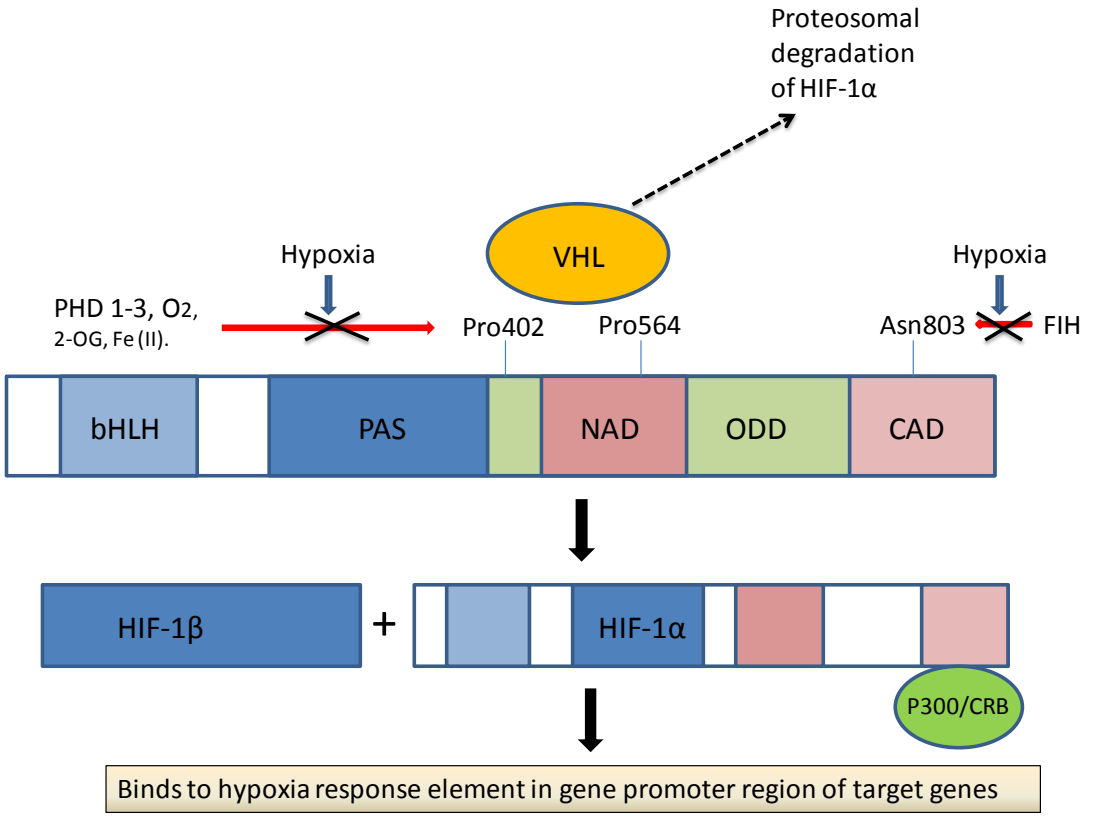

Figure 1.5 Schematic Outlining the Regulation of HIF-1α in Hypoxia.
Under normoxic conditions PHDs 1-3 and FIH hydroxylate HIF-1α on proline and asparagine residues respectively. The hydroxylation of the proline residue promotes interaction with the VHL/E3 ubiquitin ligase complex and consequent proteosomal degradation. Hydroxylation of the asparagine residue prevents recruitment of p300/CBP. Under hypoxic conditions the enzymes are inactive, and the α sub-unit stabilises and dimerises with the β sub-unit. p300/CBP is recruited and HIF-1 binds to HREs in the promoter region of target genes.

1.2.5 Asparagine Hydroxylation Inhibits Transcriptional Activation of HIF-1.

The C-terminus of HIF-1α contains a CAD and an NAD. The CAD contains a conserved asparagine residue at position 803 (Kaelin and Ratcliffe, 2008) (Figure 1.5). This is the region where recruitment of the transcriptional co-activator p300/CBP takes place, facilitating the binding of HIF-1 to the HRE in the promoter of hypoxia-response genes. In normoxic conditions factor-inhibiting HIF-1α (FIH-1) catalyses the hydroxylation of the asparagine (Asp) residue (McNeill *et al*., 2002, Lando *et al*., 2002). This hydroxylation prevents the recruitment of the co-activator and inhibits C-TAD activation (Mahon *et al*., 2001). The reaction requires 2-OG and Fe (II) (Lando *et al*., 2002), so that in hypoxia the hydroxylation does not occur and the CAD is activated. FIH-1 is abundant and ubiquitous in all cell types (Stolze *et al*., 2004).

1.2.6 HIF Prolyl-hydroxylases (PHDs).

The PHDs are highly conserved iron and 2-oxoglutarate dependant dioxygenases. Three PHD enzymes have been identified – PHD1, PHD2 and PHD3 (Jaakkola *et al*., 2001, Ivan *et al*., 2001). They have similar sequence and structure, with a catalytic core that brings the binding sites for Fe (II) and 2-OG together. PHD1 and PHD2 both have a C-terminal catalytic domain and an N terminal extension. PHD2 has a zinc finger in the N terminal. PHD3 lacks the N terminal extension (Choi *et al*., 2005). All three PHDs can hydroxylate Pro564, but only PHD1 and PHD2 hydroxylate Pro402 (Epstein *et al*., 2001). Several facts suggest that PHD2 is the most important of the three isoforms. Firstly, the activity of each PHD is dependent on its concentration within the cell, and PHD2 is the most abundant form. Secondly, PHD2 is ubiquitously expressed, whereas PHD1 and PHD3 are more tissue specific. For instance, PHD1 is highly expressed in the testes and PHD3 is highly expressed in

the heart (Lieb *et al*., 2002). Suppression of PHD2 using small interfering ribonucleic acid (siRNA) increases levels of HIF-1α in normoxic cells (Berra *et al*., 2003). Thirdly, PHD2 knockout mice are embryonically lethal, whilst PHD1 and PHD3 knockout mice are viable (Takeda *et al*., 2006). Finally, PHD2 seems to regulate HIF-1α more than HIF-2α, and PHD3 seems to regulate HIF-2α more than HIF-1α (Aprelikova *et al*., 2004). Since HIF-1α is ubiquitous and HIF-2α is tissue-specific, we can conclude that PHD2 has broader activity.

There are a number of negative feedback mechanisms regulating PHD activity. Hypoxia induces the expression of PHD2 and PHD3 in a HIF-1 dependant manner (Berra *et al*., 2003), perhaps to cap the levels of stabilised HIF-1 within the cell, or to protect against damage caused by reoxygenation (D'Angelo *et al*., 2003). Hypoxic preconditioning is known to protect cells against reoxygenation damage (D'Angelo *et al*., 2003). On the other hand, PHDs are degraded by Sian 1 and 2, and this degradation is enhanced by hypoxia because transcription of Sian 1 and 2 is increased in hypoxia in a HIF-1 independent manner (Nakayama and Ronai, 2004).

1.2.7 HIF-1 Activates the Transcription of Hypoxia Response Genes.

HIF-1 binds to hypoxia-responsive elements containing the recognition sequence 5'–RCGTC – 3' on target genes (Semenza *et al*., 1991, Semenza *et al*., 1994), initiating or upregulating (and in some cases downregulating) their expression (Semenza *et al*., 1997, Greijer *et al*., 2005). The target genes are physiologically relevant to overcoming hypoxia, operate at systemic, local and intracellular levels and include genes whose products are involved in cell proliferation, cell survival, cell motility, cell adhesion, apoptosis, angiogenesis, erythropoeisis, potential of hydrogen (pH) regulation and glucose metabolism (Greijer *et al*., 2005, Hirota and Semenza, 2006).

Microarray analyses have shown that there are hundreds of genes that respond to hypoxia, more than 50% of which are HIF-1 dependant (Elvidge *et al*., 2006).

1.3 Hypoxia and Cancer.

Tumour hypoxia is a positive factor for the growth of solid tumours, and is associated with malignant progression and a poor prognosis (Semenza, 2007a, Bos *et al*., 2003). Cells undergoing hypoxia escape necrosis and undergo a range of phenotypic adaptations. These adaptations not only allow the cells to survive the hypoxic environment, but may also increase the potential malignancy of the residual tumour cells. Intratumoural hypoxia and the hypoxic phenotype are implicated in drug resistance and tumour progression, and chemoresistance to doxorubicin can be attributed in part to the upregulation of hypoxia response genes (Semenza, 2007a, Semenza, 2000b, Vaupel and Harrison, 2004, Tomida and Tsuruo, 1999). Increased understanding of the pathophysiological responses to hypoxia will contribute to improved treatment regimes and treatment outcomes.

1.3.1 Hypoxia and Adaptations to Hypoxia in Solid Tumours.

When a solid tumour grows to 1 – 2 mm in diameter, the core becomes hypoxic, HIF-1 is activated and neo-vascularisation occurs. This tumour-driven angiogenesis is a requirement for continued cell proliferation and tumour growth (Kerbel, 2000). However, the vascularisation is poor, comprising of leaky and malformed blood vessels which are unable to supply the rapidly proliferating tumour mass with sufficient oxygen and nutrients. Whilst the central core of a tumour becomes anoxic and consequently necrotic, micro-regions of hypoxia persist within the tumour and HIF-1 continues to stabilise. The activity of HIF-1 increases as the oxygen concentration decreases. Hypoxia-inducible genes controlling cell proliferation and

survival, cell metabolism, cell invasiveness, metastatic potential and angiogenesis are all activated. Consequently, hypoxic tumours may have a more malignant phenotype (Harris, 2002). The metabolic alterations to cancer cells in hypoxia result in an increasingly acidic extracellular milieu (Vaupel *et al*., 1989). The relationship between oxygen pressure and local pH is represented in Figure 1.6.

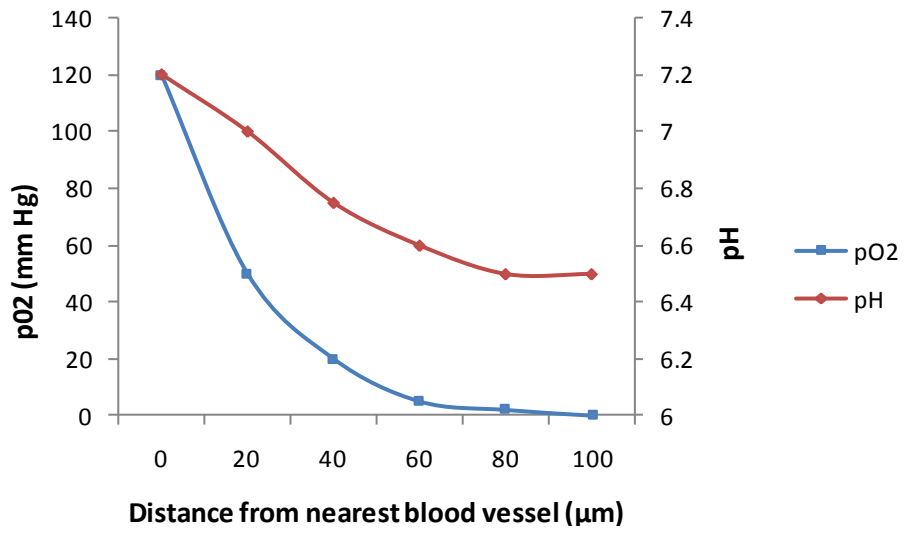

Figure 1.6 Graph showing intratumoural oxygen concentration and pH in relation to the nearest tumour blood vessel.
Oxygen concentration decreases and acidity increases as distance from the nearest blood vessel increases. Adapted from Vaupel (Vaupel *et al*., 1989).

Hypoxia is associated with resistance to both chemotherapies and radiotherapy, and hypoxia is positively correlated with a poor prognosis in many cancers (Hockel and Vaupel, 2001, Lee *et al*., 2006). HIF-1α knock-out studies have demonstrated that HIF-1 is a positive factor in tumour growth and proliferation (Zhang *et al* 2004; Helton *et al* 2005; Dang *et al* 2006; Li *et al* 2006; Luo *et al* 2006). HIF-1α overexpression is associated with angiogenesis, metastases, resistance to radio- and chemotherapies, malignant progression and a poor prognosis (Hockel and Vaupel, 2001, Semenza, 2000b).

Intrinsic and acquired drug resistance present major challenges for the treatment of cancers. Both tumour microenvironment and the cellular phenotype contribute to chemoresistance. HIF-1α expression is upregulated in many cancer cell lines even under normoxic conditions, either as a result of clonal selection, gain-of-function mutations, loss-of-function tumour suppressors or the influence of growth factors and cytokines and hypoxia and HIF-1α have been shown to contribute to chemoresistance in a range of cancers and cancer cell lines (Sullivan *et al*., 2008, Unruh *et al*., 2003, Rohwer *et al*., 2010, Daskalow *et al*., 2010, Jung *et al*., 2010, Nardinocchi *et al*., 2009a).

1.3.2 Hypoxia as a Consequence of Embolisation Therapy.

A negative, but inevitable, consequence of embolisation therapy is the creation of hypoxic regions within the tumour. Tumour hypoxia is associated with tumour growth, malignant progression, and resistance to therapies, and the escape of tumour cells from TACE therapy can potentially increase the aggressiveness of the tumour (Guo et al., 2004, Guo et al., 2002, Gupta et al., 2006, Kim et al., 2001, Liao et al., 2003, Liao et al., 2004, Shao et al., 2002). Both animal and human studies have reported increased HIF-1α levels in plasma and in liver tumour tissue samples post-TACE, and this increase is thought to be a result of hypoxia induced by the procedure (Liang et al., 2009, Liang et al., 2010b, Virmani et al., 2008, Rhee et al., 2007). Anti-sense HIF-1α has been shown to increase chemosensitivity and reduce hypoxia-stimulated cell migration (Song et al., 2006, Sun et al., 2009).

One of the effectors of HIF-1 is the endothelial cell mitogen vascular endothelial growth factor (VEGF) (Semenza et al., 2006). VEGF initiates a sequence of molecular events resulting in angiogenesis, which is a requirement for tumour growth. Increased proliferation of vascular endothelial cells post-TACE has been

reported (Kim et al., 2001), and increased VEGF has been reported within liver tumours and in plasma samples post-TACE (Li et al., 2003, Li et al., 2004, Wang et al., 2008a, Liang et al., 2010b, Liang et al., 2010a). High plasma VEGF levels post-TACE are associated with the development of metastases (Xiong et al., 2004), a poor treatment response and shorter survival times (Sergio et al., 2008, Poon et al., 2004, Shim et al., 2008).

In short, hypoxia is a major cause of tumour resistance to chemotherapy and is a positive factor for tumour progression. There is a growing body of evidence to support the hypothesis that embolisation therapies cause hypoxia and the activation of HIF-1; and that inhibition of HIF-1 and/or its effectors may improve treatment outcome. There is, therefore, a need to develop therapies which address both normoxic and hypoxic regions within a tumour. Targeting hypoxic tumour cells is a logical next step to improving treatment outcome.

1.4 Doxorubicin.

Doxorubicin is an anthracycline antibiotic that is widely used as a chemotherapeutic agent for the treatment of a range of cancers, including breast cancer, soft tissue sarcomas, childhood solid tumours and lymphomas. TACE using doxorubicin is the standard of care for HCC. The use of doxorubicin-eluting embolic beads is a new development of the TACE procedure (Lewis and Holden, 2011).

Anthracyclines are antibiotics derived from the bacterial species *Streptomyces* and are highly toxic to mammalian cells, displaying both anti-proliferative and cytotoxic effects. Doxorubicin (also known as Adriamycin™) is a metabolite of a mutated strain of the wild-type bacterium *S. peucetius*. During the 1950's *S. peucetius* was

cultured from a soil sample taken from the grounds of a 13th century castle in Italy (Figure 1.7). The bacterium produces a red pigmented antibiotic, daunorubicin,

Figure 1.7 Castel del Monte, Puglia, Italy.
The bacterium *Streptomyces peucetius* was cultured from a soil sample taken from the grounds of Castel del Monte in the 1950s. Stock photograph from TPGIMAGES.

which was found to have strong antitumoural activity in mice. By 1967, the cardiotoxic effects of daunomycin had been recognised (Tan *et al*., 1967). Mutating the bacterial species to *S. peucetius* var. *caesius* resulted in the accumulation of a slightly different antibiotic which proved to have a higher therapeutic index than daunorubicin (Bonadonna *et al*., 1969), although the cardiotoxic effects were still apparent. This toxicity limits both the single and cumulative doses of the drug (Young *et al*., 1981).

The chemical structure of doxorubicin comprises a four ring aglycone region linked to an amino sugar daunosamine by a glycosidic bridge (Figure 1.8).

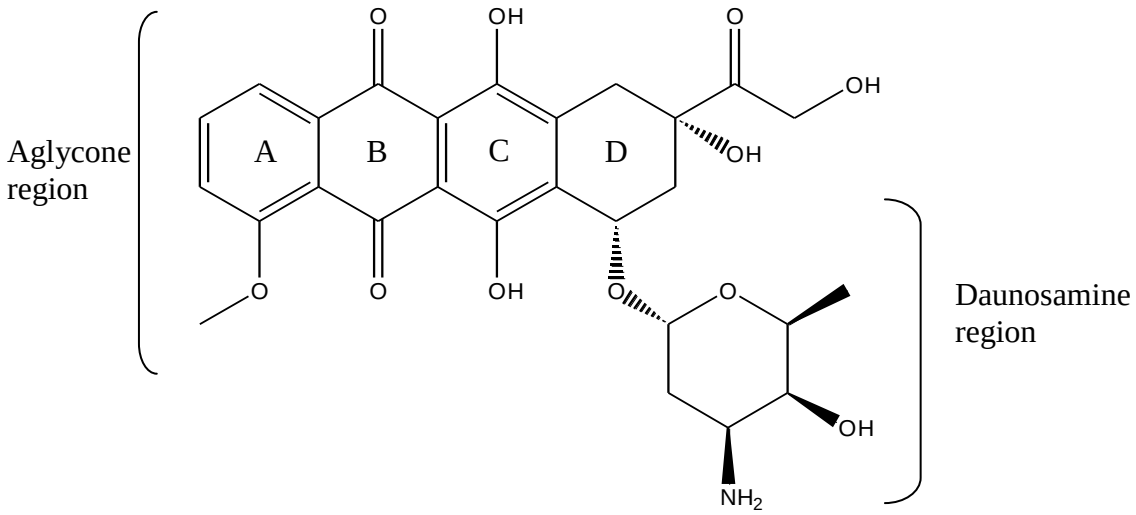

Figure 1.8 The Chemical Structure of Doxorubicin.
The chemical formula for doxorubicin is $C_{27}H_{29}NO_{11}HCl$, and the molecular weight is 579.98. Doxorubicin consists of a water insoluble tetracycline aglycone and a water soluble daunosamine sugar. Ring C is a quinone group, which activates to a semiquinone radical after reduction. Ring B is a hydroquinone and can be activated to a semiquinone radical after oxidation. During anaerobic reduction, the sugar group is split off and C7-deoxyaglycone is formed.

1.4.1 Mode of Action of Doxorubicin.

There are a number of different mechanisms by which doxorubicin is cytotoxic to eukaryotic cells. Different mechanisms of action are apparently activated at different drug concentrations, and the presence or absence of oxygen may also influence the mechanisms and degree of cytotoxicity. The interaction of doxorubicin with cells is complex, and is outlined below.

1.4.1.1 Doxorubicin Intercalation with Deoxyribonucleic Acid.

DNA contains the genetic information for the development and functioning of, with the exception of viruses, all living organisms. The genetic information in DNA is stored as a code made up of four chemical bases: the purines adenine (A) and guanine (G), and the pyrimidines cytosine (C) and thymine (T). The DNA bases pair up with each other, A with T and C with G, to form units called base pairs. Each base

is also attached to a 5 carbon sugar. The sugars are linked by phosphate groups that form a phosphodiester bond between carbons 3 and 5 of adjacent sugars. Together, a base, sugar, and phosphate are called a nucleotide. The sugar and phosphate residues form the backbone of a DNA strand. DNA strands exist in a double helix formation, with two anti parallel DNA strands being stabilised by hydrogen bonding between the complimentary base pairs.

Doxorubicin complexes with double stranded DNA by intercalation (Pigram *et al*., 1972). Rings B and C of the doxorubicin core (Figure 1.8) intercalate between G-C and C-G DNA base pairs, causing the base pairs above and below the drug molecule to buckle. Doxorubicin is stabilised within the DNA by the interactions between the electron-deficient quinone rings and the electron-rich purine-pyrimidine bases (Quigley *et al*., 1980, Patel *et al*., 1981). The daunosamine sugar and the carbonyl side chain linked to Ring D remain in the minor groove. The positively charged daunosamine interacts with the phosphate backbone of the DNA and Ring A protrudes into the major groove of the double helix. This distorts the tertiary structure of the DNA helix (Cullinane and Phillips, 1990). Intercalation inhibits the action of DNA and RNA polymerases and nucleotide replication, and protein synthesis and cell proliferation are inhibited (Neidle, 1979). The inhibition of RNA synthesis is a potential mechanism of anthracycline toxicity to non-dividing cells. It has been well established that doxorubicin inhibits DNA and RNA synthesis in cells, although the extent of the effects are cell specific (Gewirtz, 1999). Whether or not this inhibition translates to a cytotoxic or cytostatic outcome is less straightforward.

1.4.1.2 Doxorubicin Cross-linking of DNA.

Doxorubicin forms covalent adducts with cellular DNA, and this has been reported at drug concentrations of 50 μM (Sinha and Chignell, 1979). DNA cross-linking can

occur as a consequence of adduct formation, and this inhibits DNA replication. The ability of doxorubicin to form adducts with DNA correlates strongly to its cytotoxicity in certain cell lines, and fewer cross-links are found in drug-resistant cells compared to drug sensitive cells even when the intracellular drug concentrations are the same (Swift *et al*., 2006).

1.4.1.3 Doxorubicin is a Topoisomerase II Poison.

The primary mechanism for the cytotoxicity of doxorubicin at clinical concentrations is likely to be due to interference with the ubiquitous enzyme topoisomerase II (TOP2). This enzyme belongs to the topoisomerase family of enzymes, which are required for DNA replication, DNA transcription and chromosome segregation and therefore essential for cell survival (Wang, 2002, Nitiss, 2009).

1.4.1.3.1 The Role of Topoisomerase II in the Cell.

In order to be packaged into cells, DNA has to be supercoiled. DNA molecules are negatively supercoiled, since complimentary strands of negatively coiled DNA are more easily separated than those of positively coiled DNA (Boles *et al*., 1990). During replication, as the replication fork moves along the DNA, positive supercoiling of the DNA occurs ahead of the replication machinery. Similar problems arise during transcription, when RNA polymerases move along the separated DNA strand. The accumulation of positive supercoils makes strand separation more difficult and interferes with the processes of replication and translation (Wang, 2002).

Topoisomerases are responsible for maintaining the correct topological arrangement of DNA molecules, and regulate positive and negative supercoiling as well as knotting and tangling of DNA. Topoisomerase I (TOP1) enzymes generate a

transient break in one strand of a DNA duplex, and then either pass the other strand through the break (a single stranded passage reaction), or rotate it around the break, thus relieving twists in duplex DNA (McClendon and Osheroff, 2007). TOP2 enzymes generate a break in both strands of the DNA duplex, and then pass another intact DNA duplex through the gap. This is known as a double stranded passage reaction (Berger and Wang, 1996). TOP2 enzymes relieve over- or under-winding of the DNA helix ahead of or behind the replication fork, and resolve tangles and knots (known as catananes) between DNA duplex molecules (Osheroff, 1989, Osheroff *et al*., 1991).

1.4.1.3.2 The Catalytic Cycle of Topoisomerase II.

TOP2 enzymes are homodimeric, and an active tyrosyl residue in each subunit cleaves the phosphate backbone of opposite DNA strands of a DNA molecule, leaving a 4-base 5' overhang on each strand. TOP2 forms a covalent bond between the tyrosyl residue and the newly cut 5' end of the DNA phosphodiester backbone (Sander and Hsieh, 1983). This cleaved DNA is known as the G (gate) segment. The energy of the phosphate bond is retained within the phosphotyrosine bond, and is available for religation (Nitiss, 2009). TOP2 binds ATP and undergoes a conformational change such that the intact DNA helix, known as the T (transporter) segment, is passed through the cleaved DNA helix. ATP hydrolysis enables the release of the nucleic acids, and the cut ends religate (Lindsley and Wang, 1993, Lindsley and Wang, 1991).

1.4.1.3.3 Doxorubicin Interaction with Topoisomerase II.

TOP2 mediated strand breaks are transient intermediates in the catalytic cycle, and low levels are well tolerated. Doxorubicin is a TOP2 poison – that is, it increases the

concentration of TOP2 cleavage complexes within the cell to levels that are toxic. Intercalating TOP2 poisons have a high binding affinity for DNA. It is the ability of doxorubicin to intercalate DNA that enables the drug to stabilise the TOP2-DNA complex. Doxorubicin interacts with TOP2 at the protein-DNA interface by non-covalent bonding and inhibits the ability of TOP2 to religate the cleaved DNA strands (Wilstermann and Osheroff, 2003). In the presence of doxorubicin, TOP2 remains locked to the 5' cut ends of the DNA molecule (Tewey *et al*., 1984). This then increases the concentration of DNA cleavage complexes within the cell. Cleavage complexes are recognised by DNA surveillance and tracking machinery such as replication and transcription complexes. When a nucleic acid tracking system encounters a cleavage complex, it converts the transient break to a permanent one, and this then activates a range of repair pathways. The repair process involves the removal of the cleavage complex, and this results in a permanent double strand break. If the number of permanent double strand breaks is such that the cell is overwhelmed, apoptotic cell death pathways are triggered (Fortune and Osheroff, 2000). The repair of double strand breaks is by homologous recombination and non-homologous end joining. These repair processes are imperfect and can generate chromosomal translocations and other DNA aberrations (Aratani *et al*., 1996). Such aberrations can lead to the development of therapy related secondary leukaemias, most notably acute myeloid leukaemia (Kantidze and Razin, 2007, Felix, 1998).

The concentration of TOP2 is higher in rapidly proliferating cells than in quiescent cells, with levels peaking in G2/M phase, hence the efficacy of doxorubicin against neoplastic cells (Sullivan *et al*., 1987, Sinha, 1995). Drug sensitivity correlates with cellular TOP2 levels and drug resistant cancer cells have been shown to have reduced activity and/or decreased levels of TOP2 and a reduction in the number of strand

breaks (Beck *et al*., 1993, Pommier *et al*., 2010). Suppressing the expression of TOP2α using RNA interference has confirmed that reduction in TOP2 levels increases the resistance of cells to doxorubicin (Burgess *et al*., 2008).

1.4.1.4 Doxorubicin and Free Radical Formation.

Doxorubicin has a quinone ring (Figure 1.8), and this acts as an electron acceptor. As a result the quinones are converted to semiquinone free radicals which can induce DNA damage themselves as well as interacting with molecular oxygen to yield superoxides, hydroxyl radicals and peroxides. The formation of these reactive oxygen species (ROS) causes oxidative damage to cell components, cell membranes and DNA. The redox-cycling of doxorubicin has been observed in the cytoplasm, mitochondria, endoplasmic reticulum and nucleus of cells, and clearly influences the cytotoxicity of the drug (Doroshow, 1983, Goodman and Hochstein, 1977, Berlin and Haseltine, 1981, Rowley and Halliwell, 1983).

The ROS-dependent cytotoxicity of doxorubicin is reliant on the tumour cell being able to carry out the reductive reactions which activate ROS production, and this requires the presence of molecular oxygen (Teicher *et al*., 1981). However, under hypoxic conditions, doxorubicin does have the ability to generate aglycone free radicals. The redox-cycling of doxorubicin is slower under hypoxic conditions, but the aglycone free radicals that are generated can potently alkylate cellular DNA, and create DNA strand breaks. Under hypoxic conditions, the semiquinone free radical loses its sugar moiety and converts to the inactive metabolite C7-deoxyaglycone. This tautomerises to C7-quinone methide which is a DNA-alkylating species (Averbuch *et al*., 1985).

In the presence of oxygen, the reduced form of doxorubicin is known to cause lipid peroxidation of cell and mitochondrial membranes (Mimnaugh *et al*., 1985a,

Mimnaugh *et al*., 1985b). However, the evidence for doxorubicin-induced lipid peroxidation as a contributing factor to tumour cytotoxicity is inconclusive (Gewirtz, 1999).

1.4.1.5 Doxorubicin Damages the Cell Membrane.

Doxorubicin interacts directly with cell surface proteins and disrupts membrane structure and signal transduction pathways. Doxorubicin binding to cell surfaces can have a direct or an indirect effect on cell survival (Tritton, 1991).

1.4.1.6 Doxorubicin Interferes with HIF-1 Signalling.

Topoisomerase poisons other than doxorubicin (topotecan, etoposide, NSC 644221) have been reported to attenuate responses to hypoxia by decreasing levels of HIF-1α or by inhibiting its transcriptional activity (Creighton-Gutteridge *et al*., 2007, Choi *et al*., 2009). Since the investigations reported in this thesis began, doxorubicin has been shown to prevent the binding of HIF-1 to the promoter regions of hypoxia response genes (Lee *et al*., 2009a).

1.5 Rapamycin.

Rapamycin (also known as sirolimus) is a macrolide compound belonging to the class of secondary metabolites known as polyketides. Rapamycin is produced by the bacterium *Streptomyces hygroscopicus.* This organism was first isolated from a soil sample collected from the Polynesian island Rapa Nui (also known as Easter Island) in 1970, hence the name rapamycin (Figure 1.9) (Neuhaus *et al*., 2001).

Colleagues have previously shown that rapamycin can successfully be loaded onto poly vinyl alcohol (PVA) microspheres, either alone or in combination with doxorubicin (Forster 2009), and this provides the rationale for our choice of drugs in this investigation. Rapamycin (Figure 1.10) is a mammalian target of rapamycin

Figure 1.9 Huge statues, known locally as Moai, on Rapa Nui.
The bacterium *Streptomyces hygroscopius* was first isolated from a soil sample from the Polynesian island of Rapa Nui in 1970. Photograph Copyright free.

(mTOR) inhibitor which has antifungal, immunosuppressant and antineoplastic properties. It has been used as an immunosuppressant for more than ten years, and, in the majority of cases, is well tolerated. The immunosuppressant activity of rapamycin results from the inhibition of T cell activation. It is widely used to prevent the rejection of kidney and liver transplants. Rapamycin inhibits the proliferation of vascular smooth muscle cells, and for this reason it is used as an antirestenosis drug in coronary artery stents (Namur *et al*., 2010). mTOR has been implicated in the pathology of a range of diseases, including cancers, cardiovascular disease, neurological disorders and diabetes, and is thought to play an important role in the regulation of aging and lifespan (Tsang *et al*., 2007).

A number of clinically active rapamycin analogues – known as rapalogues – are now available. Rapalogues have improved pharmacological properties, and include

everolimus, temsirolimus, deferolimus, biolimus, picrolimus and zotarolimus. The structure of rapamycin is shown below (Figure 1.10).

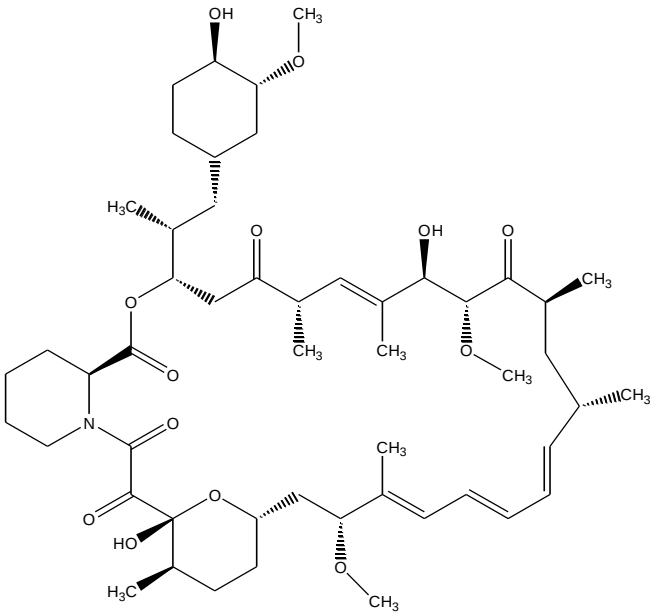

Figure 1.10 The Chemical Structure of Rapamycin.
The chemical formula for rapamycin is $C_{51}H_{79}NO_{13}$, and the molecular weight is 914.18. Rapamycin is a macrocyclic lactone antibiotic.

1.5.1 The PI3K/Akt/mTOR Pathway.

In order to understand the mechanism of action of rapamycin, it is necessary to have an understanding of the PI3K/Akt/mTOR pathway, which is outlined in Figure 1.11. The PI3K/Akt/mTOR pathway is a cell survival pathway that orchestrates cellular responses to nutrients, growth factors, cytokines, mitogens, hormones and stress. Activation of the pathway results in increased cell growth and proliferation and an inhibition of apoptosis.

At the top of the signalling cascade are members of the phosphoinositide 3-kinase family (PI3K), which are activated by the binding of the relevant ligands to their membrane-bound receptors. PI3K localises to the membrane and catalyses the

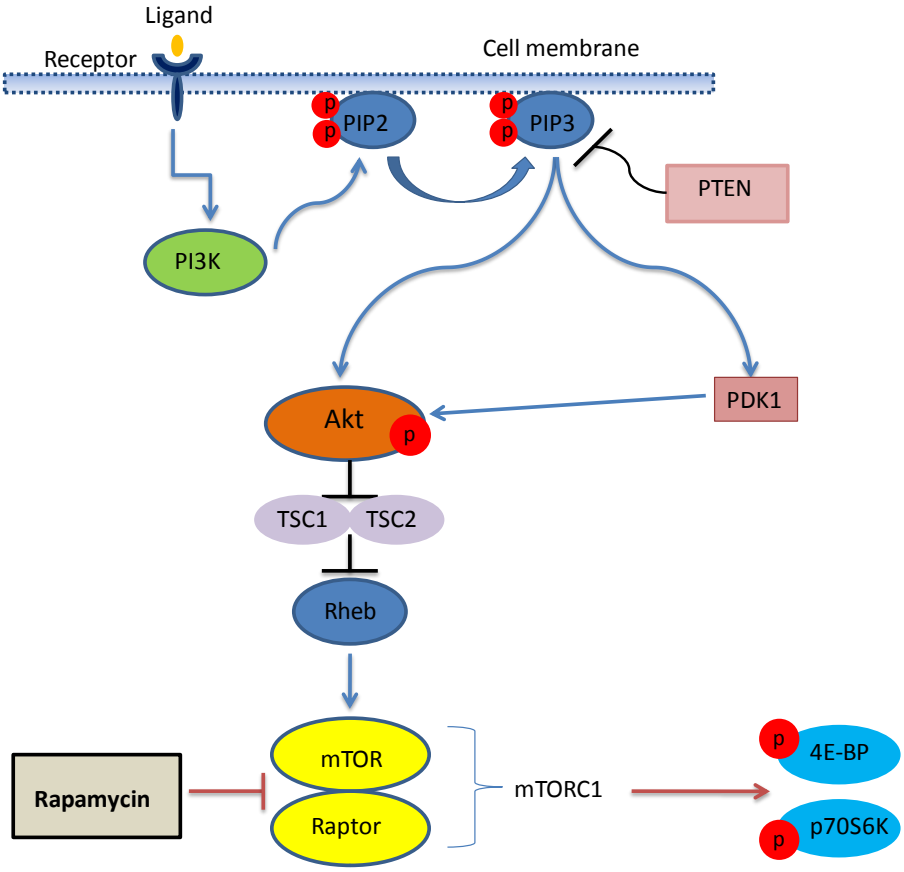

Figure 1.11 The PI3K/Akt/mTOR Pathway.
PI3K is activated by the binding of the relevant ligands to membrane-bound receptors. PI3K localises to the membrane and catalyses the conversion of PIP2 to PIP3. PIP3 binds to Akt, and Akt subsequently translocates to the cell membrane, whereupon it is phosphorylated and activated by PDK-1. Akt activates mTOR *via* phosphorylation of the protein at ser2448. mTOR binds to Raptor to form mTORC1 The downstream effectors of mTORC1 are S6 kinase (S6K), the ribosomal protein S6 and the eukaryotic initiation factor 4E binding protein 1 (4EBP-1). Both regulate the translation of mRNAs encoding proteins involved in cell growth. PTEN negatively regulates the PI3K pathway *via* dephosphorylation of PIP2 and PIP3. TSC1/TSC2 negatively regulates mTOR *via* Rheb. Akt can also activate mTOR *via* the inactivation of TSC.

conversion of phosphotidylinositol (4, 5)-biphosphate PIP2 to phosphotidylinositol (3, 4, 5)-biphosphate PIP3. PIP3 binds to Akt, and Akt subsequently translocates to the cell membrane, whereupon it is phosphorylated at Thr^{308} by 3'-phosphoinositide-dependant kinase 1 (PDK-1). Akt takes centre stage in the PI3K/Akt/mTOR pathway, with a vast array of effectors under its control. The outcomes of Akt

activation all result in anti-apoptotic and pro-proliferative cell survival strategies (Jiang and Liu, 2008b, Dancey, 2006, Foster and Fingar, 2010).

1.5.1.1 Phosphotase and Tensin Homolog Deleted on Chromosome 10 (PTEN).

PTEN is a tumour suppressor protein and antagonist of the PI3K pathway (Maehama and Dixon, 1999). PTEN dephosphorylates PIP2 and PIP3, thereby negatively regulating the activation of Akt. PTEN prevents uncontrolled cell growth by inducing cell cycle arrest and apoptosis, and is thought to interfere with cell migration, cell adhesion and angiogenesis. Mutations to PTEN result in constitutively active Akt (Maehama and Dixon, 1998, Maehama and Dixon, 1999, Chu and Tarnawski, 2004, Jiang and Liu, 2008a). PTEN mutations are frequently found in liver cancers, and are critically involved in the progression of HCC (Chen *et al*., 2009a, Dong-Dong *et al*., 2003, Hu *et al*., 2003, Ma *et al*., 2005, Mi *et al*., 2006, Peyrou *et al*., 2010, Sieghart *et al*., 2007, Tian *et al*., 2010a, Tian *et al*., 2010b, Wan *et al*., 2003, Zhou *et al*., 2009). Loss of PTEN facilitates the expression of HIF-1 gene expression *via* activation of Akt (Zundel *et al*., 2000) and increases the transcriptional activity of HIF-1 (Emerling *et al*., 2008).

1.5.1.2 Involvement of the Tuberous Sclerosis Tumour Suppressor Complex TSC1/TSC2.

TSC1/TSC2 is a tumour suppressor protein which is a negative regulator of mTORC1. Hypoxia activates TSC1/TSC2 by two separate pathways, one of which is HIF-dependent. HIF-dependent activation of TSC1/TSC2 depends on REDD1 mediated shuttling of the protein 14-3-3. 14-3-3 is an inhibitory protein which binds to phosphorylated TSC2. Activation of Akt causes phosphorylation of TSC2. This promotes the association of TSC2 with 14-3-3, and inhibits TSC1/TSC2 function. Under hypoxic conditions, HIF-1 induces the expression of REDD1. REDD1

preferentially binds to 14-3-3, thereby activating the TSC1/TSC2 complex, which then inhibits mTORC1. Hypoxia-induced negative regulation of mTORC1 results in a decrease in mRNA translation and protein synthesis, and suppression of cell growth and proliferation (Brugarolas *et al*., 2004, DeYoung *et al*., 2008, Sofer *et al*., 2005).

1.5.1.3 Akt Signalling to mTOR.

Akt can activate mTOR directly by phosphorylating the protein at Ser^{2448} or indirectly *via* the inactivation of the tuberous sclerosis protein complex TSC (Jiang and Liu, 2008a). The consequences of hyperactive mTOR signalling are demonstrated in the disease tuberous sclerosis complex, which is characterised by mutations to one of the two genes *tsc1* or *tsc2*. As previously mentioned, TSC1/TSC2 are negative regulators of mTORC1. The loss of function of either TSC1 or TSC2 results in the formation of multiple benign tumours and possibly the development of early-onset renal cell carcinoma (Nass and Crino, 2008).

1.5.2 Structure of mTOR.

mTOR (Figure 1.12) is a 289 kDa serine/threonine kinase which belongs to the PI3K-related protein kinase family and regulates levels of protein translation in response to nutrients, growth factors, energy and stress. mTOR has a catalytic C terminal kinase domain, a FK506-binding protein 12 (FKBP12) rapamycin binding domain, a C terminal repressor domain and FAT-C-terminus domain. The kinase domain phosphorylates serine (Ser) or threonine (Thr) residues in protein substrates. The FKBP12-rapamycin binding domain is specific to TOR and not other members of the PIKK family, hence the specificity of rapamycin (Choi *et al*., 1996, Chen and Fang, 2002).

Upon activation, mTOR is known to form at least two complexes – mTOR complex 1 (mTORC1) and mTOR complex 2 (mTORC2). In the mTORC1 complex mTOR is bound to regulatory associated protein of mTOR (Raptor) and the mTOR-interacting protein mLST8. In the mTORC2 complex mTOR is bound to Raptor independent companion of mTOR (Rictor), mLST8 and at least two other accessory proteins.

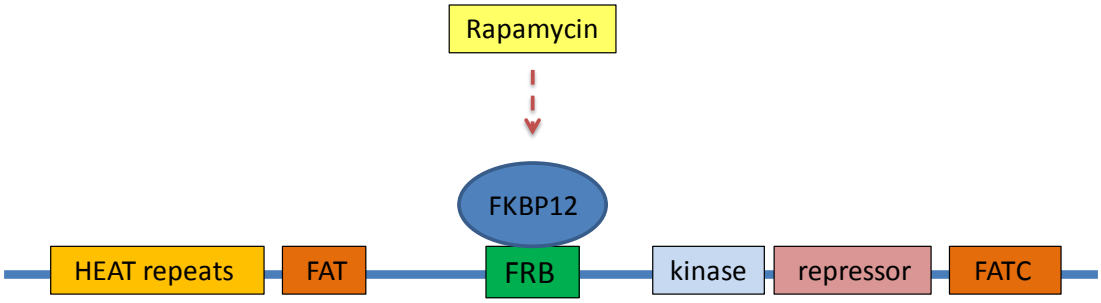

Figure 1.12 Schematic showing the basic structure of mTOR.
HEAT repeats, N terminus FAT region, FKBP12-rapamycin binding domain, C terminal kinase domain, C terminal repressor domain and FAT-C-terminus domain.

mTORC1 responds to nutrients and growth factors and ultimately results in increased cell proliferation. mTORC2 only responds to growth factors and appears to be involved in actin organisation (Houghton and Huang, 2004, Huang and Houghton, 2003). mTORC2 positively feeds back to Akt *via* phosphorylation of Akt at Ser^{473} (Sarbassov *et al.*, 2005).

1.5.3 Downstream Effectors of mTORC1.

The downstream effectors of mTORC1 are S6 kinase (S6K), the ribosomal protein S6 and the eukaryotic initiation factor 4E binding protein 1 (4EBP-1). Both regulate the translation of mRNAs encoding proteins involved in cell growth.

Phosphorylation of S6K at Thr^{389} by mTORC1 activates the ribosomal protein S6 and increases the translation of mRNAs that have a 5' tract of oligopyramidine (5'TOP) motif and increases the synthesis of ribosomal proteins and translation factors. mTORC1 also phosphorylates the elongation factor 4E (elF4F) inhibitor 4EBP-1. Upon phosphorylation, 4EBP-1 dissociates from elF4E and allows elF4E to associate with the 5'-CAP of RNAs and so promotes cap-dependant protein synthesis (Dufner *et al*., 1999, Dufner and Thomas, 1999).

When nutrients and growth factors are present, mTOR is activated and protein translation is upregulated. The cell mass increases and the cell cycle moves from the G1 phase to the S phase, thus increasing the rate of cell proliferation. In the absence of these ligands, protein translation is downregulated and energy is conserved. Cells are arrested at the G1 phase and apoptosis increases (Houghton and Huang, 2004).

1.5.4 Mode of Action of Rapamycin.

The biological activity of rapamycin is a consequence of the fact that it contains an mTOR-binding region and a FKBP12-binding region. When rapamycin enters the cytosol, FKBP12 binds to rapamycin with high affinity. The resulting FKBP12-rapamycin complex binds specifically and irreversibly to mTOR and prevents downstream signalling (Huang *et al*., 2003).

mTORC1 is inhibited by FKBP12-rapamycin. Components which are specific to mTORC2 are thought to prevent the FKBP12-rapamycin complex from binding to mTOR. If exposure to rapamycin is prolonged, however, the complex binds to newly synthesised mTOR before it assembles into mTORC2 (Houghton and Huang, 2004, Huang and Houghton, 2003), and recent reports suggest that rapamycin inhibits mTORC2 under certain conditions and in specific cell types (Barilli *et al*., 2008, Sarbassov *et al*., 2006). Rapamycin thus inhibits protein synthesis by blocking

mTORC1 signalling *via* S6K and 4E-BP1. Without a sufficient increase in cell size and mass, the cell cycle arrests at the G1 stage and apoptosis is increased (Mita *et al*., 2003).

1.5.5 Rapamycin and HIF-1.

Oxygen concentration is the primary determinant of HIF-1 activation. However, the extent of HIF-1 activation is partly modulated through the PI3/Akt/mTOR pathway, and hyperactive Akt is a positive factor for HIF-1 dependent signalling pathways. Rapamycin has been observed to interfere with HIF-mediated cell signalling pathways (Jiang and Liu, 2008b, Guba *et al*., 2002, Hudson *et al*., 2002, Zhong *et al*., 2000).

1.5.6 The PI3K/Akt/mTOR Pathway and Cancer Cells.

The anticancer activity of rapamycin was first recognised by the National Cancer Institute in the 1970s but was not extensively investigated until the late 90s. The PI3K/Akt/mTOR pathway is deregulated in many cancers and hyperactivity is implicated in tumourigenesis. The mechanisms of deregulation are numerous, and include loss of PTEN, amplification or gain of function mutations to PI3K, Akt or growth factor receptors, and exposure to carcinogens (LoPiccolo *et al*., 2008). The net result is an increase in cell proliferation and an increased resistance to apoptosis. Hyperactive Akt signalling may also result in increased HIF-1 activation. For instance, PTEN deficient cells display an exaggerated HIF-1 response to hypoxia, and this may contribute to the aggressiveness of PTEN deficient tumours (Zundel *et al*., 2000).

If cancer cells are dependent on mTOR signalling for survival, there is a potential role for mTOR inhibitors in the treatment of cancers with mutations to the

PI3K/Akt/mTOR pathway (Tsang *et al*., 2007). A number of preclinical and clinical trials of rapamycin and rapalogs against cancers including renal cell carcinoma, mantle cell lymphoma, and breast and endometrial cancers have had some encouraging results, particularly against some cancers with mutations to PTEN and Akt (O'Donnell *et al*., 2008, Okamoto *et al*., 2010, Hudes *et al*., 2009, Slomovitz *et al*., 2010, Yao *et al*., 2008, Hess, 2009, Motzer *et al*., 2010, Lu *et al*., 2008). Other trials however, have shown only modest or short lived responses with no significant improvements (Huang *et al*., 2003, LoPiccolo *et al*., 2008).

1.5.7 Protein Phosphatase and Tensin Homolog (PTEN).

Mutations or deletions to the tumour suppressor PTEN lead to hyperactivation of the PI3K/Akt/mTOR pathway. PTEN is a tumour suppressor protein and antagonist of the PI3K pathway (Maehama and Dixon, 1999). PTEN modifies other proteins by removing phosphate groups. It functions as a tumour suppressor by negatively regulating the Akt signalling pathway, and mutations to PTEN result in constitutively active Akt. PTEN prevents uncontrolled cell growth by inducing cell cycle arrest and apoptosis, and is thought to interfere with cell migration, cell adhesion and angiogenesis (Maehama and Dixon, 1998, Maehama and Dixon, 1999, Chu and Tarnawski, 2004, Jiang and Liu, 2008a).

PTEN mutations are frequently found in liver cancers, and are critically involved in the progression of HCC (Chen *et al*., 2009a, Dong-Dong *et al*., 2003, Hu *et al*., 2003, Ma *et al*., 2005, Mi *et al*., 2006, Peyrou *et al*., 2010, Sieghart *et al*., 2007, Tian *et al*., 2010a, Tian *et al*., 2010b, Wan *et al*., 2003, Zhou *et al*., 2009). The loss of PTEN facilitates the expression of HIF-1 gene expression via activation of Akt (Zundel *et al*., 2000) and increases the transcriptional activity of HIF-1 (Emerling *et al*., 2008).

We know that in HepG2 cells PTEN is barely detectable (Ma *et al*., 2005, Zhang *et al*., 2004) and that this results in increased synthesis of HIF-1α (Zundel *et al*., 2000, Zhong *et al*., 2000). Overexpressing PTEN in HepG2 cells decreases the activation of HIF-1 and suppresses angiogenesis, migration and invasiveness (Tian *et al*., 2010a, Tian *et al*., 2010b, Sze *et al*., 2011). The loss of PTEN therefore contributes to tumour cell survival under hypoxic conditions. Decreased PTEN in tumour biopsy specimens correlated with tumour progression and a poor prognosis in HCC (Hu *et al*., 2003, Chen *et al*., 2009a, Dong-Dong *et al*., 2003, Sze *et al*., 2011, Mi *et al*., 2006). Recently, an association has been found between PTEN haplotypes and susceptibility to HCC (Ding *et al*., 2011).

1.6 Combination Therapies for the Treatment of HCC.

The combination of standard chemotherapeutic agents with one (or more) of the recently identified molecular targeted therapies in the treatment of HCC presents opportunities to improve patient outcome. The rationale for combination chemotherapy is to use drugs that have different mechanisms of action, and reduce chemoresistance. For instance, the targeted drug may restore the apoptotic pathway in cells, thus allowing the traditional chemotherapeutic to cause apoptosis.

Recent research indicates that rapamycin will be most effective when used in combination with other chemotherapeutics or other molecular inhibitors (Huynh *et al*., 2009, LoPiccolo *et al*., 2008, Wang *et al*., 2008c, Piguet *et al*., 2008).

1.7 Nuclear Factor Kappa-light-chain-enhancer of Activated B Cells (NF-kB).

Nuclear factor kappa-light-chain-enhancer of activated B cells (NFkB) is a family of transcription factors which mediate cell proliferation, apoptosis and immune responses. It also mediates cellular responses to hypoxia, and the involvement of

NFkB in responses to hypoxia is now starting to be investigated. NFkB consists of a family of seven transcription factors, divided into two subfamilies – the Rel proteins and the NFkB proteins. The Rel protein subfamily includes p65 (aka RelA), and the NFkB protein subfamily includes the p105/p50 (aka NFkB1) and the p100/p52 (aka NFkB2) isoforms. NFkB subfamily proteins have long C-terminal domains which inhibit their activity, and are only able to bind to DNA in their shorter forms (e.g. p105 to p50). Members of the NFkB subfamily only activate transcription when they dimerise with one of the Rel subfamily. The p50-RelA heterodimer is the major NFkB dimer in many cells (Gilmore, 2006).

Two pathways have been described for NFkB activation – the canonical (or classical) pathway and the non-canonical (or alternative) pathway. The non-canonical pathway activates NFkB complexes during B- and T-cell development, and will not be considered in this study. In the canonical pathway, NFkB signalling is regulated by inhibitor kB (IkB) proteins. Inactive NFkB dimers, such as p50/RelA, are bound to IkB, and maintained in the cytosol. In response to a range of extracellular signals, IkB kinase (IKK) complexes phosphorylate IkB and induce its degradation. This then frees the NFkB dimer, which translocates to the nucleus and activates expression of its target genes. A third pathway is thought to involve translocation of homodimers of p50 to the nucleus (Gilmore, 2006).

Due to the number of different NFkB isoforms and IkBs, the complexity of their regulatory pathways, and the influence of post-translational modifications, the phenotypic effects of NFkB activation are not well understood (Perkins, 2006). NFkB is upregulated in HCC, and is associated with both pathogenesis and chemoresistance (Arsura and Cavin, 2005, He and Karin, 2011, Luedde and Schwabe, 2011).

1.8 Apoptosis.

Apoptosis can be defined as 'programmed cell death'. It is an energy requiring process and occurs in response to severe cell damage or cellular stress, including the formation of radical oxygen species, which can also initiate apoptosis (Kim and Park, 2003). Apoptosis is regulated by a caspase cascade, and is characterised by chromatin condensation, membrane blebbing, cytoplasmic shrinking, the formation of apoptotic bodies and DNA fragmentation. Caspases are cysteine proteases which are activated when cleaved. Both initiator and effector caspases determine the fate of the cell, and apoptosis is tightly regulated. The principal anti-apoptotic proteins are Bcl-2 and Bcl-xL and the principal pro-apoptotic proteins are Bax, Bad, Bak and Bid (Piret *et al*., 2002b).

1.8.1 Hypoxia and Apoptosis.

Hypoxia can induce both pro and antiapoptotic responses, depending on the severity and duration of oxygen depletion. Severe hypoxia $\leq$ 0.5% oxygen concentration results in pro-apoptotic responses due to the stabilisation of p53 (Santore *et al*., 2002) whereas moderate/mild hypoxia results in anti-apoptotic cellular survival responses such as angiogenesis and in some cases cell proliferation (Carmeliet *et al*., 1998). Severe hypoxia causes genetic instability and a high mutation rate, and apoptosis prevents the accumulation of cells carrying such mutations (Reynolds *et al*., 1996). Anoxic cells lack the energy required for apoptosis and undergo necrotic cell death. The apoptotic cascade in hypoxia is to some extent directly regulated by HIF-1 (Erler *et al*., 2004, Sowter *et al*., 2001). Pro-apoptotic proteins upregulated by HIF-1 include BNIP3 and NIX, which are both Bcl-2 binding proteins, and therefore inhibit the antiapoptotic activity of Bcl-2 (Goda *et al*., 2003). Conversely, hypoxia also induces expression of antiapoptotic proteins such as IAP-2 (*via* the transcription

factor NFkB) and downregulates the expression of the pro-apoptotic protein Bax (Dong *et al*., 2003). Disturbances to the inner mitochondrial membrane in hypoxia can also result in apoptosis. Oxygen depletion decreases the membrane potential at the inner membrane of the mitochondria. This activates Bax and Bak and initiates the caspase cascade (Saikumar *et al*., 1998).

As already discussed, solid tumours contain regions of both chronic and intermittent hypoxia. Some of these cells may be resistant to apoptosis, and are selected for. In addition to being resistant to hypoxia-induced apoptosis, these cells are also less sensitive to apoptosis induced by chemotherapeutics causing DNA damage, and apoptosis-resistant cells are a hallmark of solid of tumours (Chresta *et al*., 1996).

1.9 Tumour Suppressor Protein p53.

The tumour suppressor p53 is a pro-apoptotic protein and transcription factor that is activated in response to cellular stress, such as hypoxia, DNA damage and osmotic shock. Nuclear accumulation of p53 occurs in response to DNA damage. p53 activates the transcription of proteins that are involved in damage repair or apoptosis. When intracellular levels of p53 are low to moderate, the cell cycle is arrested at the G1 phase and DNA damage repair takes place. However, if levels of p53 are high, apoptotic cell death pathways are triggered. p53 is implicated in oncogenic transformation, and cancer cells which have mutated p53 are resistant to chemo- and radio-therapies (Bold *et al*., 1997). Fifty percent of tumours have been shown to have mutated or deleted p53 (Hammond and Giaccia, 2002), which protects from drug-induced apoptosis. Doxorubicin induces apoptosis as a consequence of DNA damage *via* p53 dependant mechanisms (Lee *et al*., 2002).

1.9.1 Regulation of p53.

In unstressed cells, p53 is bound to its negative regulator, the protein Mdm2. This binding promotes ubiquitination of p53 and the protein complex undergoes proteosomal degradation. In stressed cells the N-terminal end of p53 is phosphorylated by protein kinases and Mdm2 binding is disrupted, and p53 accumulates. Transcriptional co-activators p300/CRB are recruited, allowing the DNA binding domain of p53 to interact with the promoters and/or repressors of downstream genes (Piret *et al*., 2002b).

1.9.2 p53 and HIF-1.

The relationship between p53 and HIF-1 is complicated. There is a direct physical interaction between HIF-1α and p53. p53 only accumulates in response to hypoxia when hypoxia is severe and prolonged and appears to play a role in the regulation of HIF-1α. Two p53 binding sites have been identified within the ODD of HIF-1α. p53 stabilises HIF-1α and this promotes Mdm2-dependant degradation of HIF-1α (Chen *et al*., 2003, Sanchez-Puig *et al*., 2005). HIF-1 induces apoptosis by directly interacting with and stabilising wild-type p53. p53 activates the proapoptotic proteins Bax and Bak (Greijer and van der Wall, 2004).

Both HIF-1 and p53 require recruitment of the co-activator p300 in order to be transcriptionally active, and it has been suggested that competition for p300 attenuates transcriptional activity of HIF-1 (Blagosklonny *et al*., 1998). p53 induced by hypoxia is reported to be transcriptionally inactive, although it can still induce apoptosis, probably by associating with co-repressors (Koumenis *et al*., 2001). The inactivity could be explained by losing the competition with HIF-1 for co-activator p300. However, since severe hypoxia also causes DNA damage, which causes further stabilisation of p53, it is possible that with increasing severity of hypoxia the

competitive balance shifts in favour of p53, and p53 becomes transcriptionally active and HIF-1 attenuated (Kaluzova *et al*., 2004).

1.10 Cell Respiration.

Cell respiration is the process by which cells harvest energy from organic compounds and store it in the chemical bonds of adenine tri-phosphate (ATP). ATP is then used by the cell to provide the energy required for cellular processes to take place.

1.10.1 ATP.

ATP is a nucleic acid which has a ribose sugar attached to the nitrogenous base adenine. This sugar has three phosphate groups attached, each of which has a negative charge. Because of the proximity of these negative charges to each other, strong bonds are needed to hold the phosphate groups in place. If these bonds are broken, phosphate groups are uncoupled from the molecule and the bond energy is released. The cell uses hydrolysis to dephosphorylate ATP, resulting in the release of usable energy and the conversion of ATP to either adenine di-phosphate (ADP) (when only one phosphate group is removed) or adenosine monophosphate (AMP) (when two phosphate groups are removed).

1.10.2 Glucose Metabolism in the Presence of Molecular Oxygen.

In the presence of oxygen, mammalian cells generate ATP by the complete oxidation of glucose to water and carbon dioxide. This catabolic pathway comprises of a series of oxidation and reduction reactions that take place within the cytosol and the mitochondria. There are three major steps to aerobic cell respiration – glycolysis, the Krebs Cycle and the electron transport chain (ETC). The theoretical net energy gain is 38 molecules of ATP for each molecule of glucose.

1.10.3 Glycolysis.

Glycolysis takes place in the cytosol. In glycolysis one 6-carbon molecule of glucose is phosphorylated and converted to two 3-carbon molecules of pyruvate. The phosphorylation of glucose is catalysed by hexokinase enzymes. Splitting the glucose molecule is catalysed by a series of glycolytic enzymes. The pyruvate is then shunted towards the mitochondria for entry into the Krebs Cycle and the ETC.

1.10.4 Glucose Metabolism in the Absence of Molecular Oxygen.

In the absence of oxygen, ATP production comprises two stages – glycolysis and fermentation. Both of these take place in the cytosol. The end product is lactic acid. ATP levels are maintained and cells can continue to survive and proliferate in the absence of oxygen. Anaerobic respiration is much less efficient than aerobic respiration with a net gain of only 2 ATP molecules for every molecule of glucose. The pyruvate molecules generated in glycolysis are reduced to lactic acid. The increased conversion of pyruvate to lactic acid in hypoxic cells is known as the Pasteur Effect (Krebs, 1972).

Hypoxic cells increase the uptake of glucose molecules by upregulating the expression of glucose transporters and glycolytic enzymes in a HIF-1 dependant manner (Semenza, 2003). The glycolytic enzymes rapidly convert the glucose into pyruvate. HIF-1 also upregulates lactate dehydrogenase A (LDH-A) which shunts the pyruvate towards anaerobic glycolysis and conversion to lactic acid in the cytoplasm (Papandreou *et al*., 2006). Aerobic metabolism of pyruvate requires pyruvate dehydrogenase (PDH) and HIF-1 upregulates the expression of PDK1 which inhibits PDH (Kim and Dang, 2006).

1.10.5 Glucose Metabolism in Tumour Cells.

Cancer cells metabolise glucose through a cytoplasmic glycolytic pathway, even when molecular oxygen is available to the cell. This phenomenon is known as the Warburg Effect (Kim and Dang, 2006). Anaerobic metabolism is far less efficient than aerobic metabolism, and requires a much higher flux of glucose molecules. This increase in energy consumption explains why cancer patients suffer from cachexia (Dills, 1993). HIF-1 facilitates anaerobic glycolysis by upregulating enzymes as described in 1.10.4, and ATP production in cancer cells is HIF-dependent (Brahimi-Horn and Pouyssegur, 2006).

1.11 Using Hypoxic Culture Conditions for *In Vitro* Research.

It is now a well established fact that hypoxia influences tumour biology and intracellular pathways, including those that control proliferation, cell cycling and apoptosis. These changes will clearly have an impact on the effects of chemotherapeutic agents. The importance of pre-clinical *in vitro* research on cells cultured within a hypoxic environment is now apparent. Indeed, some of the disparities between *in vitro* and *in vivo* responses to cancer treatments may be due to the fact that much of the *in vitro* work has been carried out at an oxygen concentration of 21%.

1.12 Summary.

As discussed above, solid tumours contain regions of hypoxia, and this is associated with chemo- and radiotherapy-resistance, and a shift to a more malignant phenotype. HCCs have hypoxic regions, and this is associated with a poor outlook. TACE is the standard of care for intermediate HCC, although response rates are not good. There is a concern that, as well as creating regions of anoxia leading to tumour necrosis, the

escape from embolisation therapies of tumour cells in hypoxic regions could result in a residual population of aggressive cancer cells which are then clonally selected for.

Cellular responses to hypoxia are regulated principally by the transcription factor HIF-1. Targeting HIF-1 thus provides a therapeutic opportunity. Recent research has shown that doxorubicin interferes with HIF signalling pathways. Rapamycin is also thought to interfere with HIF signalling, by inhibiting the rate of synthesis of HIF-1α. The use of systemic low dose rapamycin to treat HCC is presently under clinical investigation.

The use of doxorubicin loaded DEBs for the treatment of HCC facilitates the sustained delivery of high concentrations of drug straight to the tumour bed, with minimal systemic exposure. Rapamycin can also be loaded onto DEBs, both on its own or in addition to doxorubicin.

1.13 Aims of the Thesis.

In this thesis we have investigated the response of the human HCC cell line HepG2 to doxorubicin and rapamycin, both as single agents and in combination. *In vitro* assessment of cytotoxicity was carried out in cells cultured under both normoxic and hypoxic conditions. Western Blotting was then employed in order to elucidate the mechanisms of action of the two drugs, and highlight differences in the expression of relevant proteins in normoxic and hypoxic cells. *In vivo* assessment of the anti-tumour activity of the drugs was carried out using an ectopic human HCC xenograft mouse model.

In summary, the aims of this thesis were as follows:

- to develop a hypoxic *in vitro* model of liver cancer
- to assess the cytotoxicity of doxorubicin and rapamycin, both as single agents and in combination, towards the human HCC cell line HepG2 cultivated *in vitro* under both 21% and 1% oxygen concentrations;
- to analyse changes in expression of relevant proteins in these cells;
- to investigate the anti-tumour activity of the drugs *in vivo*, using an ectopic human HCC xenograft mouse model.

Chapter 2

Materials and Methods.

2.1 Cell Culture.

Cell culture is a well established laboratory technique and one of the major tools at the disposal of cell and molecular biologists. Cells isolated from tissues are proliferated *ex vivo*, and this provides a model system for the study of cell physiology and biochemistry; and for investigating the effects of drugs and toxic compounds.

2.1.1 Cell Line.

The cell line used in all experiments was the human hepatocellular liver carcinoma cell line HepG2. The cells are derived from the liver tissue of a fifteen year old Caucasian male with a well differentiated HCC, and are extensively used for *in vitro* investigations of liver cancer. The cells have an epithelial morphology, and are anchorage-dependent. The cells were purchased frozen from ATCC Cell Biology Collection (ATCC, HB-8065, UK).

2.1.2 Culture Conditions.

Specific culture conditions vary with cell type. However, all cells in culture require a substrate that supplies the essential nutrients that are required for growth and proliferation; the presence of growth factors; and regulation of temperature and gases. Cells in culture should be passaged during the log phase of growth, before they reach confluence.

Here, cell culture in normoxic conditions was carried out under aseptic conditions inside a laminar flow cell culture hood (HERA Safe, Heraeus). All equipment was sterilised before use, and the hood was swabbed down with 70% industrial

methylated spirits. HepG2 cells were cultured in Minimum Essential Medium (MEM) + Earle's salts + L-Glutamine (PAA Laboratories, GmBH) supplemented with 10% Foetal Bovine Serum Heat Inactivated (PAA Laboratories, GmBH,) and 1% Non-essential Amino Acids (PAA Laboratories, GmBH), all of which were warmed to 37°C before use. The cells were seeded onto T75 tissue culture coated flasks (NUNC™, Denmark) and incubated at 37°C, 95% air and 5% CO_2. Cells were passaged when confluence reached 70%, using a sub-cultivation ratio of 1:6. All experiments used cells between passage numbers 96 and 125.

2.1.3 Passage Protocol.

The media was aspirated from the flask, and 5 ml of trypsin-EDTA (0.05% / 0.02% in PBS) (PAA Laboratories, GmBH) was added in order to detach the cells. The flask was incubated for 10 minutes at 37°C. Microscopy was used to confirm that the cells had detached from the surface of the flask. 10 ml of complete media was then added to the flask in order to neutralise the trypsin and the cell suspension was removed to a centrifuge tube. The cell suspension was centrifuged at 300 g for 5 minutes (Heraeus, Multifuge 3S). The supernatant was removed and discarded, and the pellet was resuspended in 1 ml of media. 10 µl of cell suspension was removed and added to 90 µl of PBS, providing a 1:10 dilution of the cell suspension to determine the cell count. 15 µl of the 1:10 dilution was pipetted onto a haemocytometer slide and the cells were counted. The appropriate fraction of cell suspension was then added to a new T75 flask, and fresh media was added to a total volume of 20 ml. Microscopy was used to confirm the presence of cells in the flask, and the flask was placed in the incubator.

2.2 Hypoxic Incubations.

In vitro experiments attempt to mimic the *in vivo* environment as closely as possible. However, most cell culture is carried out at 21% oxygen, which in most cases does not mirror the physiological oxygen concentration within the relevant tissue.

In this study a hypoxic glove box was used for hypoxic cell culture in order to investigate the responses of cells that may be refractory to embolisation therapy. The glove box allows the oxygen environment to be tightly regulated, and cell culture and manipulation of cells can be carried out under maintained oxygen concentrations. An

Figure 2.1 The COY Hypoxic Glove Box.
The glove box allows cell culture and manipulation of samples in an oxygen controlled environment, with temperature, humidity and CO_2 control. Oxygen, nitrogen and carbon dioxide cylinders supply gas feeds to the glove box. HEPA atmosphere filtration ensures sterility, and an internal fan ensures uniform gas distribution. The oxygen concentration is maintained using an oxygen sensor and controller, with an automatic purge control. Samples are introduced through a transfer chamber airlock which is purged to equilibrate to the O_2 level within the glove box. An internal humidified incubation box prevents media from drying out during long incubation periods. Manipulation of samples is carried out through sealed arm ports so that the internal atmosphere is not compromised.

oxygen concentration of 1% was selected because it represents

a) an oxygen concentration at which HepG2 cells adapt to hypoxic conditions. At concentrations lower than 0.5%, the cells undergo apoptosis, and at concentrations less than 0.1% the cells undergo necrosis

   and

b) an oxygen concentration that represents an *in vivo* niche, where cells that experience embolisation-induced hypoxia are exposed to doxorubicin as it elutes from the bead (Namur *et al*., 2010).

For hypoxic incubations the cells were cultured inside a hypoxic glove box (COY Laboratory Products Inc. MI. USA) (Figure 2.1) set to 1% oxygen, 5% carbon dioxide, 94% nitrogen. Any media used in the hypoxic condition was placed inside the chamber for 24 hours before use in order that the liquid phase could equilibrate to the gas phase.

2.3 Verification of Stabilisation of HIF-1α in Hypoxic Culture Conditions.

Two methods were utilised to confirm that HIF-1α had stabilised and translocated to the nucleus in HepG2 cells exposed to 1% oxygen – SDS-PAGE and Western Blotting (see 2.5 for method and Chapter 6 for results); and immunohistochemistry.

2.3.1 Immunohistochemistry.

Specific proteins in cultured cells can be labelled using antibodies conjugated to fluorophore reporter systems. The presence or absence of these proteins can then be investigated using fluorescence microscopy. A nuclear counter stain allows visualisation of all the cells in the sample. Here, levels of HIF-1α in normoxic and hypoxic HepG2 cells were compared.

HepG2 cells were seeded onto chamber slides (Fisher Scientific, UK) at a seeding density of 2 x 10^5 per well and incubated in normoxic conditions until confluence was 60%. The cells were then incubated at either 21% oxygen or 1% oxygen for 24 hours. The cells were fixed with 3.7% formalin at room temperature for 20 minutes, and washed in PBS. Cells were blocked for 15 minutes using blocking buffer (0.7% glycerol, 0.2% Tween-20, 2% BSA, in PBS). Blocking buffer was removed and HIF-1α antibody diluted 1:750 in blocking buffer was added to the chamber slides. The slides were incubated overnight at 4°C, and then washed with wash buffer (0.7% glycerol, 0.4% Tween-20, 2% BSA, in PBS). A tetramethylrhodamine-5-(and 6)-isothiocyanate fluorescein isothiocyanate (TRITC) conjugated secondary antibody (Sigma, UK), diluted 1:200 in blocking buffer, was added to the chamber slides. The slides were protected from light, and subjected to agitation for 1 hour at room temperature. Secondary antibody was removed and cells washed in wash buffer at room temperature for 1 hour. Cells were counter-stained with 4', 6-diamidino-2-phenylindole (DAPI) (Gibco, UK), and viewed by confocal microscopy at x 100 magnification.

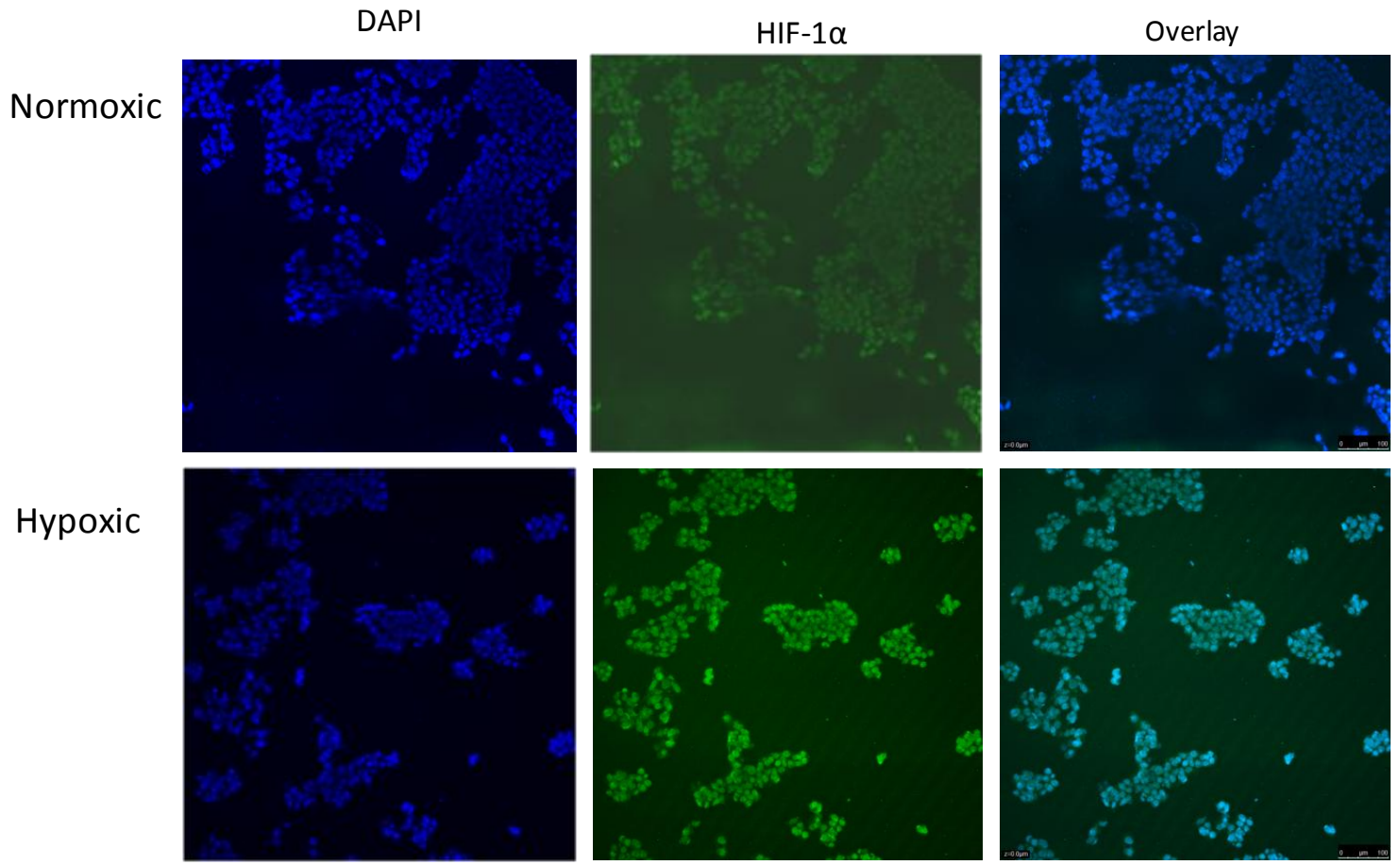

Figure 2.2 Immunohistochemistry Staining for HIF-1 in Normoxic and Hypoxic HepG2 cells.
Cells were seeded onto chamber slides HepG2 cells were seeded onto chamber slides and incubated under normoxic conditions until confluence was 60%. The cells were then incubated under normoxic or hypoxic conditions for 24 hours. The cells were incubated overnight with antibodies to HIF-1α, and then incubated with TRITC conjugated secondary antibody. DAPI staining was used to visualise the nucleus. Images are taken at x100 magnification. HIF-1α is absent in normoxic cells and present in hypoxic cells.

2.4 The 3 - (4, 5 dimethylthiazol - 2 - yl) - 5 - (3 - carboxymethoxyphenyl) - 2 - (4 sulfophenyl) 2H - tetrazolium, inner salt (MTS) Cytotoxicity Assay.

The MTS assay is a cell-based assay, the end point measure of which indicates the number of viable cells in culture (Cory *et al.*, 1991). MTS assays are widely used for pharmacological studies to investigate the effects of cytotoxic compounds on cell viability and cell proliferation. The assay relies on the assumption that the number of viable cells is directly proportional to the coloured formazan product.

Here the CellTiter 96® Aqueous One Solution Proliferation Assay (Promega, UK) was used to determine the chemosensitivity of HepG2 cells to treatment with doxorubicin, rapamycin and both in combination under both normoxic and hypoxic culture conditions. The CellTiter 96® Aqueous One Solution Proliferation Assay is a colorimetric assay which depends on the cellular reduction of the tetrazolium compound MTS to the coloured product formazan. The reagent contains the tetrazolium compound MTS together with an electron coupling reagent (phenazine ethosulfate; PES), which combine to form a stable solution. The conversion of MTS to formazan is due to the activity of mitochondrial dehydrogenase enzymes within metabolically active cells.

Metabolic activity in cells produces reducing agents nicotinamide adenine dinucleotide (NADH) and nicotinamide adenine dinucleotide phosphate (NADPH). These reducing compounds donate their electrons to the electron coupling reagent PES, and this then reduces the MTS to formazan. The formazan product is soluble in tissue culture medium. The quantity of formazan product is measured by the amount of absorbance at 490 nm, and this measure is directly proportional to the number of living cells in culture (Cory *et al.*, 1991). The sensitivity of the assay is approximately 1 x 10^3 cells/well in a 96-well plate (Promega Protocols and Applications Guide).

Cell titrations were carried out under both normoxic and hypoxic conditions to validate the assay. The optimal seeding density and optimal MTS reagent incubation period, such that absorbance readings across the time course of the experiment fell within the linear range of the assay, was found to be 1 x 10^4 cells/well and the optimal and 2 hours respectively (data not shown). These values were used in all experiments.

Control wells containing media and cytotoxic compound(s) but no cells were included in the experimental design. The mean control absorbance was subtracted from each of the absorbance readings to yield a corrected absorbance.

2.4.1 Determining the Effect of Doxorubicin, Rapamycin or a Combination of Both on Cell Viability.

2.4.1.1 Seeding the 96-well Plates.

HepG2 cells were grown to 70% confluence in a T75 flask, and harvested and counted as previously described. The cells were resuspended in media to a concentration of 5 x 10^4 cells/ml. Cells were seeded onto six 96-well tissue culture coated plates in 200 µl aliquots to provide a cell seeding density of 1 x 10^4 cells/well. The plates were incubated under normoxic conditions for 24 hours to allow the cells to equilibrate.

2.4.1.2 Exposure of Cells to Doxorubicin, Rapamycin or a Combination of Both.

Three 96-well plates were removed to hypoxic conditions and three 96-well plates remained in normoxic conditions. The media was aspirated from the plates and replaced with 200 µl of the appropriate concentration of drug(s) in solution. Six replicate wells were prepared for each drug concentration. Two control wells, containing no cells, were prepared for each drug concentration. The plates were

incubated for either 24, 48 and 72 hours, under either normoxic or hypoxic conditions as appropriate (Figure 2.4).

2.4.1.3 Measuring Cell Viability using the MTS Assay.

After the required incubation period, 40 µl of MTS assay reagent was added to each of the wells. This was carried out under normoxic or hypoxic conditions, as appropriate. The plates were incubated for a further two hours.

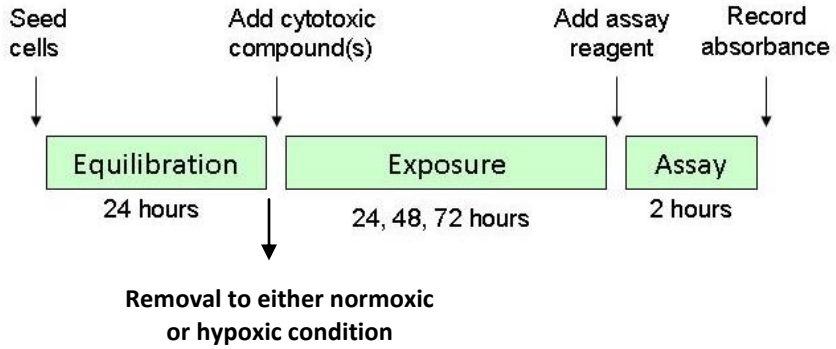

Figure 2.3 Schematic showing timeline for the cytotoxicity assay.
HepG2 cells were seeded onto 96-well plates and incubated for 24 hours to equilibrate. Plates were removed to either normoxic or hypoxic conditions. Cells were exposed to cytotoxic compounds and incubated for 24, 48 and 72 hours. MTS assay reagent was added and the cells were incubated for a further 2 hours. The absorbance at 490 nm was recorded.

The absorbance at 490 nm was read using a multiwell plate reader (BioTek, UK). The mean control absorbance was calculated for each experimental condition. The mean control absorbance for each experimental condition was then subtracted from each of the six absorbance readings for the same experimental condition. The mean absorbance for each experimental condition was then calculated. The effect of the drug(s) for each experimental condition was calculated as percentage change in mean absorbance compared to the untreated control.

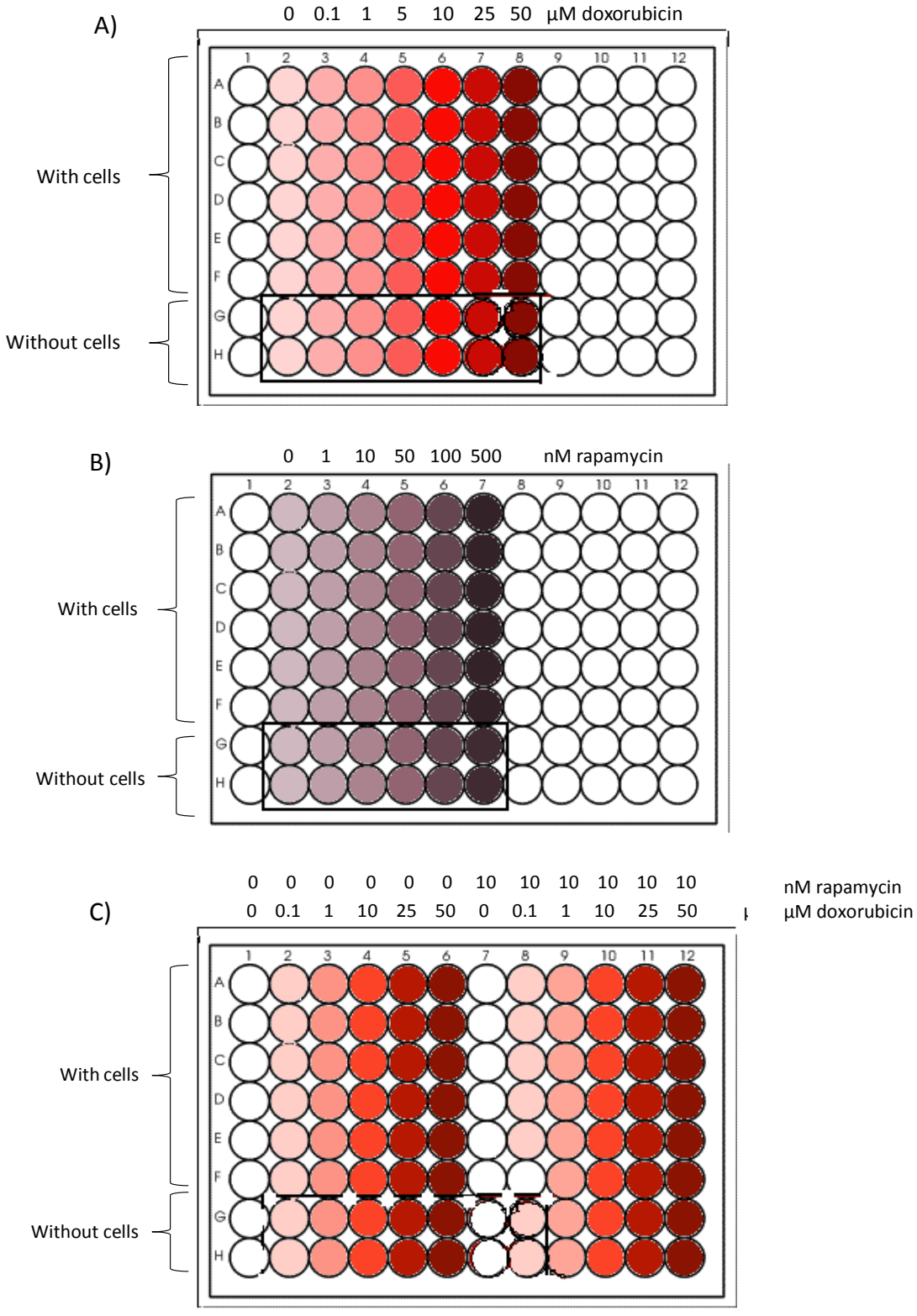

Figure 2.4 Schematic showing the layout of the 96 well plates for MTS assay. A) doxorubicin alone B) rapamycin alone and C) doxorubicin and rapamycin combinations. The last two wells in each column do not contain cells, and provide control absorbance readings.

2.5 Preparation of Drug Solutions.

2.5.1 Preparation of Doxorubicin Solutions.

Doxorubicin hydrochloride (> 98% purity; Zhejiang Hisun Pharmaceuticals, China) was supplied dissolved in sterile H_2O at a concentration of 50 mg/ml. The stock solution was stored at 4˚ C in a glass vial. Doxorubicin hydrochloride can be stored for 6 - 12 months at 4˚ C without loss of potency (Hoffman *et al*., 1979).

For each experiment dilutions of doxorubicin hydrochloride in media were made up fresh from the stock solution, under sterile conditions, in either normoxic or hypoxic conditions as appropriate.

2.5.2 Preparation of Rapamycin Solutions.

Rapamycin (> 99% purity, LC Laboratories, Massachusetts, USA) was supplied at 60 mg/ml in the solvent dimethyl sulfoxide **(**DMSO). Since the drug is poorly soluble in media, a 10 mM solution of rapamycin was prepared in DMSO. A cell proliferation assay had previously been carried out using the highest concentration of DMSO seen by the cells in order to demonstrate that there were no cytotoxic effects from the diluent itself (data not shown).

Fresh dilutions of rapamycin were made up for each experiment. Rapamycin as supplied was stored long term at − 20˚C. Rapamycin/DMSO was stored at 4˚ C protected from light for up to 4 weeks.

2.5.3 Preparation of Doxorubicin/Rapamycin Combination Solutions.

Solutions of doxorubicin were prepared as described in 2.3.1. A 10 µM solution of rapamycin in media was made up from the 10 mM rapamycin/DMSO stock described in 2.3.2. Appropriate amounts of the 10 µM solution were used to spike the doxorubicin solutions to a final rapamycin concentration of 10 nM.

2.6 Preparation of Nuclear and Cytoplasmic Cell Extracts for SDS-PAGE and Western Blotting.

2.6.1 Treating the Cells.

HepG2 cells were seeded onto T75 flasks and incubated under normoxic conditions until confluence reached 60%. The flasks were then removed to either normoxic or hypoxic conditions. The media was aspirated off, and replaced with concentrations of drug as described in the figure legends. The cells were incubated for 24 hours under either normoxic or hypoxic conditions, as appropriate.

2.6.2 Harvesting the Cells.

The media was aspirated from cells under normoxic or hypoxic conditions as appropriate. Cells were washed twice using 2 mls of phosphate-buffered saline (PBS) (Sigma Aldrich, UK). PBS (1.5 ml) was added to the flask and the cells were dislodged from the flask using a cell scraper. The cell suspension was removed to a microcentrifuge tube (Eppendorf UK) using a Gilson pipette and centrifuged at 13,000 rpm for three minutes. The supernatant was discarded.

2.6.3 Preparation of Nuclear and Cytoplasmic extracts.

The cell pellet was resuspended in 400 µl of Buffer A (10mM Hepes pH 7.9, 10mM potassium chloride, 0.1mM EDTA pH 8.0, 0.1mM EGTA pH 8.0, 1mM DTT, 1x protease inhibitor cocktail (Roche, UK) and incubated on ice for fifteen minutes. 25 µl of 10% NP-40 was added. The mixture was vortexed for 30 seconds and centrifuged for 45 seconds. Aliquots of the cytoplasmic extract supernatant were removed to Eppendorf tubes and snap frozen in liquid nitrogen. The pellet was resuspended in 50 µl of Buffer C (20mM Hepes pH 7.9, 400mM sodium chloride, 1mM EDTA pH 8.0, 1mM EGTA pH 8.0, 1mM DTT, 5% glycerol, 1x protease inhibitor cocktail) and incubated for 1 hour at 4°C with vigorous shaking. The

mixture was then centrifuged at 13,000 rpm for thirty seconds. Aliquots of the nuclear extract were removed to Eppendorf tubes and snap frozen in liquid nitrogen. Nuclear and cytoplasmic extracts were stored at − 20°C. When probing for phosphorylated proteins, phosphotase inhibitor cocktail (10 mM sodium flouride, 10 mM sodium molybdate, 10 mM β-glycerophosphate, 10 mM sodium vanadate and 10 mM p nitrophenyl phosphate) was added to buffer A.

2.6.4 Determining the Protein Concentration of Cell Extracts using the Bradford Assay.

A protein assay is used to measure the protein concentration of a solubilised protein. This measure is then used to ensure that equal amounts of protein are analysed when performing quantitative comparisons of protein expression between different experimental conditions, for instance in Western Blotting. The dye-binding assay used here is based on the method of Bradford (Bradford, 1976), and depends on the fact that a differential colour change occurs in response to varying protein concentrations. The intensity of the colour can be quantified by measuring the absorbance at 595 nm using a spectrophotometer. Comparison with a standard curve allows the protein concentration to be determined.

A stock solution of protein assay dye reagent was prepared by diluting one part Bio-Rad assay dye (BioRad, UK) with four parts distilled deionised water. A standard curve was prepared by measuring the absorbance at 595 nm of known concentrations of bovine serum albumin (BSA) (BioRad, UK). An aliquot (3 µl) of cell extract was added to 1 ml of stock solution and briefly vortexed. The mixture was incubated at room temperature for fifteen minutes and transferred to a cuvette. The absorbance of the cell extract was determined spectrophotometrically at 595 nm. The protein

concentration of the cell extract was calculated by comparison with the standard curve.

2.7 Sodium Dodecyl Sulphate-polyacrylamide Gel Electrophoresis and Western Blotting.

Protein expression in HepG2 cells was analysed using sodium dodecyl sulphate-polyacrylamide gel electrophoresis (SDS-PAGE) and Western Blotting. Briefly, protein samples were denatured and coated with negative charge. The samples were loaded onto wells in a polyacrylamide gel. The gel was placed into the SDS-PAGE apparatus, the wells were positioned at the negative electrode side. Application of a voltage pulls the samples towards the positively charged electrodes. Since smaller proteins move more easily through the gel (have a greater electrophoretic mobility), the proteins were size-fractionated. A molecular ladder was run alongside the samples to determine size (kDa). The proteins fixed as bands in the gel matrix were transferred to a membrane. The membrane was then probed using a primary antibody raised against the protein of interest. The antibody-antigen complex was detected using a secondary antibody-enzyme conjugate. The membrane was then incubated in a substrate solution, and the conjugated enzyme catalyzed the conversion of the substrate into a visible product that precipitated at the blot site. The intensity of the signal in different samples was compared using densitometry analysis, and changes in protein expression between different experimental conditions were quantified.

2.7.1 Preparation of Samples for SDS-PAGE.

Before the cell extracts were applied to the gel they were incubated with SDS sample buffer. This contains SDS which breaks up hydrophobic interactions to denature the proteins, and coats the proteins with negative charge; and β-mercaptoethanol which further denatures the proteins by reducing the disulfide bonds.

Using the results from the protein assay, the volume of cell extract equivalent to 20 µg of protein was calculated using Excel. This was mixed with sterile water to a total volume of 10 µl. An equal volume of SDS sample buffer (95% Laemmli sample buffer (BioRad Laboratories Inc. UK), 5% β-mercaptoethanol (BioRad Laboratories Inc. UK) was added. The samples were mixed by gently pipetting and incubated at room temperature for 10 minutes.

2.7.2 Separation of the Proteins by Gel Electrophoresis.

The proteins were separated by running on a 10% SDS-PAGE gel (resolving gel; 10% acrylamide/Bis mix, 0.38 M Tris-HCl pH 8.8, 0.0001% SDS, 0.0001% APS, 0.00005% TEMED in H_2O. Stacking gel; 5% acrylamide/Bis mix, 0.125 M Tris-HCl pH 6.8, 0.0001% sodium dodecyl sulphate (SDS), 0.0001% ammonium persulphate (APS), 0.0001% TEMED in H_2O) for 60 minutes at 150 V/50 mA in SDS running buffer (3g/l Tris Base, 14.4 g/l glycine, 1 g/l SDS) (Bio-Rad Mini Protean 3 Cell, Bio-Rad UK). A molecular marker was run alongside the protein samples (Bio-Rad Precision Plus Protein Kaleidoscope standards, Bio-Rad, UK).

2.7.3 Transferring the Protein to a Polyvinylidene Fluoride Membrane.

The proteins were transferred from the gel onto a polyvinylidene fluoride (PVDF) membrane (Immobilon-P membrane, Millipore Corp.) using a semi-dry electro-blotting apparatus (TRANS-BLOT®, Bio-Rad, UK).

The apparatus was wiped down with distilled water then methanol before use. Filter paper was pre-soaked in transfer buffer (3.0 g/l Tris base, 14.4 g/l glycine). The PVDF membrane was pre-soaked in methanol for 30 seconds, water for two minutes and transfer buffer for five minutes. A sandwich of thick filter paper (BioRad Laboratories Inc. UK), gel, PVDF membrane and another layer of thick filter paper

were placed onto the anode plate of the electro-blotting apparatus. A roller was used to remove air bubbles. The top of the apparatus (the cathode plate) was put on, and the apparatus was run at 60 mV for 30 minutes (45 minutes for two gels). When the current was applied, the proteins were electrophoresed out of the gel and onto the membrane.

2.7.4 Blocking the Membrane.

In order to prevent non-specific binding of the primary antibody to membrane proteins, the membrane was blocked using a dilute protein solution. The proteins in the solution attach to the membrane proteins, where cell proteins have not attached. During optimisation of Western Blotting, different blocking agents at varying concentrations were tested, and the blocking protocol varies somewhat for the different proteins that were investigated. See Table 2.1 for details. Membranes were incubated in blocking buffer for 1 hour at room temperature with gentle agitation. Following blocking, the membranes were washed 3 times for 5 minutes in wash buffer (200 mM Tris-HCl pH 7.6, 29.2 g/l NaCl, 0.05% Tween 20).

2.7.5 Incubation of the Membrane with Primary and Secondary Antibody.

Primary antibodies bind to specific antigens with high affinity. Secondary antibodies bind to a primary antibody, according to the host species in which the primary was raised. Secondary antibodies can be conjugated to reporter enzymes to allow detection and quantification of protein in a sample.

The membrane was placed in a Falcon tube, with the protein side facing inwards. Primary antibody solution in wash buffer (5 ml) was added, and the membrane was incubated overnight with rotation at 4°C. The membrane was then washed twice quickly, once for fifteen minutes and twice for five minutes in large volumes of wash

buffer. The primary antibodies, the antibody dilutions and the diluent used are detailed in Table 2.1.

The membrane was placed in a Falcon tube, with the protein side facing inwards. An aliquot of secondary antibody solution (5 ml) was added, and the membrane was incubated for one hour at room temperature. The membrane was then washed twice quickly, once for fifteen minutes and twice for five minutes in large volumes of wash buffer. The secondary antibodies, the antibody dilutions and the diluent used are detailed in Table 2.1.

2.7.6 Visualising the protein.

Enhanced chemiluminescence (ECL) was used to visualise the protein bands (Amersham ECL Plus™ Western Blotting Detection Reagents, GE Healthcare, UK). Combined horseradish peroxidise (HRP) and peroxide catalysed oxidation of the Lumigen PS-3 substrate produces a chemiluminescent signal, which can be captured when the membrane is exposed to autoradiography film (HyperfilmTM ECL, GE Healthcare, UK).

The detection reagents were equilibrated to room temperature before use, and made up as specified by the manufacturers to a volume of 1 ml solution/10 cm^2 membrane. Any excess wash buffer was drained off the PVDF membrane. Detection mix was pipetted onto the membrane to thoroughly soak. After five minutes, the detection mix was wicked from the membrane, and the membrane was wrapped in saran wrap. The membrane was placed inside a Kodak cassette. Under darkroom conditions, the membrane was exposed to autoradiography film. The film was developed using an automatic developer (XoGraph Healthcare Ltd., UK).

2.7.7 Stripping and Reprobing the Membrane.

PVDF membranes can be stripped of signal, primary and secondary antibodies and the same blot can be reprobed for a different protein. In order to quantitatively evaluate protein expression between samples, the chemiluminescent signal from the target protein was compared to that of a structural protein on the same blot. The amount of structural protein is not expected to change between samples. This provides an internal standard and allows normalisation and standardisation of sample load. In addition, membranes probed for a specific phosphorylated protein were stripped and reprobed for total levels of the same protein, in order that the ratio of phosphorylated to total protein could be determined.

The blot was washed three times for five minutes, and incubated in stripping buffer (Restore Western Blot Stripping Buffer, Thermo Fisher Scientific Inc.) for fifteen minutes with shaking at 37°C. The wash was repeated. Checks were carried out to ensure complete removal of primary and secondary antibodies, after which the next antibody detection was carried out (as from 2.6.4).

2.7.8 Densitometry Analysis.

The blot was analysed using densitometry. This technique measures the intensity of the band, and thus the amount of protein transferred, in terms of optical density. Densitometry analysis was carried out on both the target protein and the structural protein, using FlouroChem software (Alpha Innotech, USA) and the amount of target protein was normalised to the amount of structural protein. This corrects for any difference in protein loading or protein transfer between the samples. Quantitative comparisons can then be made between different experimental samples.

* Non-fat dried milk powder diluted in wash buffer.

† Bovine serum albumin diluted in wash buffer.

Protein of interest	Intracellular location	Blocking protocol	1° antibody and antibody dilution	2° antibody and antibody dilution
HIF-1α	Nuclear	10% milk*	CS #3716 (Cell Signaling Tech., MA) 1:250 in wash buffer	CS#7074 Anti-rabbit IgG, HRP-linked (Cell Signaling Tech., MA) 1:1000 in 1% milk*
NFkB	Nuclear	10% milk*	ab7971 (abcam®, UK) 1:400 in wash buffer	CS#7074 Anti-rabbit IgG, HRP-linked (Cell Signaling Tech., MA) 1:1000 in 1% milk*
Lamin B1	Nuclear	10% milk*	ab16048 (abcam®, UK) 1:5000 in wash buffer	CS#7074 Anti-rabbit IgG, HRP-linked (Cell Signaling Tech., MA) 1:5000 in 1% milk*
S6k	Cytoplasmic	5% BSA†	ab24490 (abcam®, UK) 1:400 in wash buffer	CS#7074 Anti-rabbit IgG, HRP-linked (Cell Signaling Tech., MA) 1:5000 in 1% BSA†
phospho S6k	Cytoplasmic	5% BSA†	ab2571 (abcam®, UK) 1:250 in 5% BSA†	CS#7074 Anti-rabbit IgG, HRP-linked (Cell Signaling Tech., MA) 1:1000 in 1% BSA
Akt	Cytoplasmic	10% milk	CS#9272 (Cell Signaling Tech., MA) 1:1000	CS#7074 Anti-rabbit IgG, HRP-linked (Cell Signaling Tech., MA) 1:1000 in 1% milk
phospho Akt	Cytoplasmic	5% BSA†	CS#4058 (Cell Signaling Tech., MA) 1:1000 in 5% BSA†	CS#7074 Anti-rabbit IgG, HRP-linked (Cell Signaling Tech., MA) 1:1000 in 1% BSA
B actin	Cytoplasmic	5% BSA†	ab8226 (abcam®, UK) 1:2500	ab6789 Anti-mouse IgG, HRP-linked 1:5000 in 1% BSA†

Table 2.1 Primary and Secondary Antibodies used for Western Blotting.
This table details the blocking and antibody protocols for all Western Blotting.

2.8 *In Vivo* Animal Study.

The first step in *in vivo* pre-clinical testing of anti-cancer compounds typically involves the subcutaneous injection of human cancer cells into immunocompromised mice, thereby creating an ectopic xenograft tumour model. Assessment of tumour growth can be carried out externally using a caliper, and tumours can be excised *post mortem* for immunohistochemical analysis.

In this study the anti-cancer activity of doxorubicin-eluting beads, rapamycin eluting beads, rapadox eluting beads, oral rapamycin and combinations thereof was investigated in an ectopic xenograft human HCC mouse model. The experiments were carried out by EPO-GmbH under approved conditions.

2.8.1 Animal Species.

National Medical Research Institute (NMRI) nu/nu mice (Taconic M & B, Ry, DK), adult females weighing 20 g. These animals lack a thymus, and are unable to produce T-cells, so are immunodeficient. All experiments were approved by LAGeSo (State Office of Health and Social Affairs), Berlin.

2.8.2 HCC Xenograft Model.

The HCC cell line used was the HepG2 cell line. Cells were cultivated *in vitro* and harvested prior to implantation.

2.8.3 Preparation of Beads for Injection.

DC Bead microspheres (Biocompatibles UK) were loaded to a doxorubicin concentration of 25 mg/ml, a rapamycin concentration of 20 mg/ml, and a combination of both. The beads were then lyophilised and gamma sterilised (Isotron PLC, UK) and stored in vials containing 1 ml of bead.

A 3 ml aliquot of alginate solution (0.6% w/v, CellMed) was added to the vial, and mixed on a whirlimixer to hydrate the beads. The alginate acts as a viscosity modulator and stabilises the beads *in situ* post injection.

2.8.4 Preparation of Rapamycin for Gavage.

Rapamycin powder was fully dissolved in ethanol to a concentration of 10 mg/ml. This was then diluted to 0.01 mg/ml in drinking water. A dose of 1 mg/kg/day was administered by gavage.

2.8.5 Treatment Protocol.

Mice were randomly assigned to one of 7 treatment groups A – G, n = 3 per group. 1 x 10^7 HepG2 cells from culture were transplanted subcutaneously at day 0. Treatment started when the tumours were of palpable size, = day 23. 100 µl of bead/alginate mix was applied adjacent to the tumour by direct injection. Oral rapamycin was administered daily by gavage. See Table 2.2.

2.8.6 Assessment of Tumour Growth.

Tumour growth was measured twice per week in two perpendicular diameters using a caliper. Tumour volume was calculated using the ellipsoid volume formula where tumour volume = $\pi/6$ x length x width^2. This method has previously been shown to be the most accurate method for assessing the volume of subcutaneous tumours in nude mice (Tomayko and Reynolds, 1989).

2.8.7 Assessment of Toxic Effects.

The mice were inspected regarding signs of toxicity and behavioural changes immediately after application of the beads, and then twice daily. Body weight change was used as a parameter for toxicity. Mouse body weight was determined twice per

Table 2.2 Treatment Protocol for *In Vivo* Study.

Group	n	DEB	Oral rapamycin	Volume of injected alginate/DEB mix (ul)	Amount of drug (mg/ml bead)	Predicted maximum dose (mg)
A	3	-	-	-	-	-
B	3	Bland bead	-	100	-	0
C	3	Doxorubicin	-	100	25	0.8
D	3	Rapamycin	-	100	20	0.67
E	3	Rapadox	-	100	25 (dox), 20 (rapa)	0.8 (dox), 0.67 (rapa)
F	3	-	1 mg/kg/day	-	-	-
G	3	Doxorubicin	1 mg/kg/day	100	25	0.8

This table summarises the treatment schedules for each experimental condition.

week. Mice were euthanized at a moribund stage, or if the tumour was larger than 10% of total body weight.

2.8.8 Autopsies.

The tumours were removed and weighed. The tumours were shock frozen for future immunohistochemistry.

2.9 Statistical Analysis.

Statistical analysis was carried out using Excel and Minitab. For comparisons where data was normally distributed, T tests were applied. Where data was not normally distributed, the non-parametric equivalent, the Wilcoxon Signed-Rank test, was used. Where more than one comparison was carried out on a data set, the Bonferroni correction was applied, whereby the α level is divided by the number of comparisons made.

The α level defines the probability of making a Type I (false positive) error – i.e. rejecting the null hypothesis if it is true. Conventionally, α is set at 0.05, so that there is only a 5% chance of wrongly rejecting the null hypothesis. If more than one comparison is made within a data set the chance of making a Type I error increases. The Bonferroni correction is used when more than one statistical test is being performed simultaneously. The level of α is divided by the number of comparisons being made. If the p-value is less than or equal to α/n then the null hypothesis can be rejected. This maintains the family wise error rate within the data set, and the experiment wide critical value remains equal to α. The Bonferroni correction is fairly conservative, and decreases the chance of making a Type I error, but increases the chance of making a Type II error.

For analysing the data generated from the *in vivo* experiments (Chapter 7), where all the data was normally distributed, analysis of variance was used. Post hoc Bonferroni pairwise comparisons were used to directly compare different treatments.

Chapter 3

The Effects of Doxorubicin on HepG2 Cells Cultured *In Vitro* Under Normoxic and Hypoxic Conditions.

3.1 Introduction.

Tumour hypoxia is a positive factor for the growth of solid tumours, and is associated with malignant progression and a poor prognosis (Semenza, 2007a, Bos et al., 2003). The hypoxic phenotype is implicated in drug resistance and tumour progression (Semenza, 2007a, Semenza, 2000b, Vaupel and Harrison, 2004, Tomida and Tsuruo, 1999). TACE using the chemotherapeutic doxorubicin is the current standard of care for unresectable HCC. Doxorubicin-loaded DEB-TACE offers a survival advantage over cTACE and is becoming more widely used. There is, however, a concern that hypoxia which occurs as a result of embolisation therapy allows the escape of tumour cells from necrosis, and results in clonal selection for hypoxia-resistant cells and cells with a more aggressive phenotype. Recent reports suggest that doxorubicin can, to some extent, block hypoxia-induced survival pathways.

3.1.1 Doxorubicin.

Doxorubicin is an anthracycline antibiotic which, despite the lack of a clear survival benefit, has become the standard of care for inoperable HCC.

The cytotoxicity of doxorubicin against cancer cells is attributed to a number of different mechanisms, including - the intercalation of the drug in the DNA of dividing cells and the consequent inhibition of DNA and RNA synthesis; the activity of doxorubicin as a topoisomerase II poison; the generation of free oxygen radicals which damage DNA and cell membranes; and direct interaction with cell surface proteins (Aubel-Sadron and Londos-Gagliardi, 1984, Keizer *et al*., 1990, Zunino and

Capranico, 1990, Tritton, 1991, Pommier *et al*., 2010). The cytotoxicity of doxorubicin towards HepG2 cells has been demonstrated numerous times and continues to be demonstrated (Boulin *et al*., 2011).

3.1.2 Doxorubicin and HIF-1.

There have been reports that doxorubicin inhibits angiogenesis in HCC (Piguet *et al*., 2008) and in other cancers (Drevs *et al*., 2004, Quesada *et al*., 2005). The transcription factor HIF-1 induces angiogenesis as a response to hypoxia. Inhibition of HIF-1 signalling by Topoisomerase I poisons (Rapisarda *et al*., 2004a, Beppu *et al*., 2005, Puppo *et al*., 2008, Sapra *et al*., 2011a, Choi *et al*., 2009) and Topoisomerase II poisons (Yamazaki *et al*., 2006, Creighton-Gutteridge *et al*., 2007, Dai *et al*., 2010, Choi *et al*., 2009, Chang *et al*., 2003, Xie *et al*., 2007) has been reported in a number of different cell lines.

Since we started this investigation, one publication has shown that doxorubicin inhibits the transcription of HIF-mediated genes by blocking the binding of HIF-1 to the promoter region of hypoxia response genes in Hep3B cells and reduces tumour-derived angiogenesis and tumour vascularisation in xenograft murine tumour models (Lee *et al*., 2009a).

This concurs with findings that doxorubicin results in the downregulation of VEGF but not HIF-1α in HepG2 tumour models (Liu *et al*., 2008a). Doxorubicin was also found to inhibit both HIF-1 activity and VEGF expression in human ovarian cancer cells (Duyndam *et al*., 2007). The anthracyclines cinerubin and aclarubicin inhibit hypoxic induction of VEGF in HepG2 cells (Yamazaki et al., 2006). However, the same study reported no effect from doxorubicin on either HIF-1 transcriptional activity or VEGF expression (Yamazaki *et al*., 2006).

These findings provide a rationale for the anti-angiogenic effects of anthracycline therapy that have previously been reported and suggest that doxorubicin can, to some extent, block the cell survival pathways activated by hypoxia. Since chemoresistance to doxorubicin can be attributed in part to the phenotypic alterations that occur in response to hypoxia, there is a need to investigate the cytotoxicity of doxorubicin to tumour cells cultured under hypoxic conditions *in vitro*, and the effect of doxorubicin treatment on cell survival pathways induced by hypoxia.

3.1.3 Hypoxia, Doxorubicin and NFkB.

Cellular stresses such as hypoxia and doxorubicin-induced DNA damage have been reported to activate the transcription factor NFkB (REFS). NFkB regulates the transcription of HIF-1α.

3.1.4 Phosphorylation of S6K and Akt.

The PI3K/Akt/mTOR pathway regulates cellular responses to nutrients, growth factors and stress. Activation of the pathway results in increased cell proliferation and inhibition of apoptosis. Phosphorylation of Akt *via* PI3K is at thr^{308}, and Akt directly phosphorylates mTORC1 at ser^{2448}. Akt lies upstream of mTOR, and is negatively regulated by PTEN. Akt is positively regulated by mTORC2 via phosphorylation at ser^{473}. In order to conserve cellular energy, hypoxia downregulates mTORC1 activation via a different pathway involving the upregulation of REDD1 (Brugarolas *et al*., 2004). In cells with mutations to PTEN this mechanism may be dysregulated.

Activated mTORC1 phosphorylates S6K at thr^{389}. This then increases the number of ribosomal components involved in protein translation, and thus affects the rate of global protein synthesis.

3.2 Aims.

• To study the effects of doxorubicin in a time and concentration dependent manner on the viability of HepG2 cells under normoxic and hypoxic conditions.

• To evaluate the response of HIF-1α, NFkB, S6K and Akt expression in HepG2 cells under normoxic and hypoxic conditions.

3.3 Objectives.

Here the chemosensitivity of HepG2 cells cultured under normoxic and hypoxic conditions to the application of clinically relevant concentrations of doxorubicin hydrochloride was investigated. Cell viability was estimated using the CellTiter 96® Aqueous One Solution Proliferation Assay. Hypoxic culture conditions (oxygen = 1%) were established using the Coy Hypoxic Glove box, as described in the Methods section.

SDS-PAGE and Western Blotting were used to quantify the nuclear accumulation of HIF-1α and p50 NFkB; and the phosphorylation status of p70 S6K and Akt.

3.4. Results.

3.4.1 Cell Viability at 24 Hours.

The only doxorubicin treatment that had a significant effect at 24 hours was the 25 µM doxorubicin treatment, which significantly decreased the viability of cells cultured under normoxic conditions ($p = 0.009$, $\alpha/n = 0.01$) (Figure 3.1, Table 3.3). Cells cultured under hypoxic conditions were resistant to all doxorubicin concentrations at the 24 hour time point (Figure 3.1, Table 3.3 and 3.4).

3.4.2 Cell Viability at 48 Hours.

After 48 hours, 10 µM doxorubicin significantly decreased cell viability in cells cultured under normoxic conditions and in cells cultured under hypoxic conditions when compared to untreated controls ($p = <0.001$ and $p = <0.001$ respectively, $\alpha/n = 0.01$). Furthermore, the 25 µM doxorubicin treatment significantly decreased cell viability in normoxic cells and in hypoxic cells control ($p = <0.001$ and $p = 0.008$ respectively, $\alpha/n = 0.01$). However, whilst the 50 µM doxorubicin treatment significantly decreased cell viability in normoxic cells ($p = <0.001$, $\alpha/n = 0.01$), it had no significant effect on cell viability of hypoxic cells (Figure 3.2 and Tables 3.5 and 3.6). Under hypoxic conditions, 10 µM doxorubicin was more effective at decreasing cell viability than 25 µM ($p = <0.001$, $\alpha/n = 0.01$) (Table 3.6).

Both 10 µM and 25 µM doxorubicin treatments were more effective at decreasing cell viability in normoxic cells than in hypoxic cells ($p = 0.019$ and $p = 0.005$ respectively, $\alpha/n = 0.025$) (Table 3.7).

3.4.3 Cell Viability at 72 Hours.

After 72 hours, 5 µM doxorubicin significantly decreased cell viability in cells cultured under normoxic conditions when compared to untreated controls ($p =$

<0.001, α/n = 0.01). 10 µM doxorubicin significantly decreased cell viability in cells cultured under normoxic conditions and in cells cultured under hypoxic conditions when compared to untreated controls (p = <0.001 and p = <0.001 respectively, α/n = 0.01). The 25 µM doxorubicin treatment significantly decreased cell viability in normoxic cells (p = <0.001, α/n = 0.01) but had no significant effect on cell viability of hypoxic cells. However, 50 µM doxorubicin significantly decreased cell viability in normoxic cells and in hypoxic cells when compared to control (p = <0.001 and p = 0.002 respectively, α/n = 0.01) (Figure 3.3 and Tables 3.8 and 3.9). Under hypoxic conditions, 10 µM doxorubicin was more effective at decreasing cell viability than 25 µM (p = 0.007, α/n = 0.01) (Table 3.8 and 3.9).

A 10 µM doxorubicin treatment was significantly more effective at decreasing cell viability in normoxic cells than in hypoxic cells (p = 0.014, α/n = 0.025) (Table 3.10).

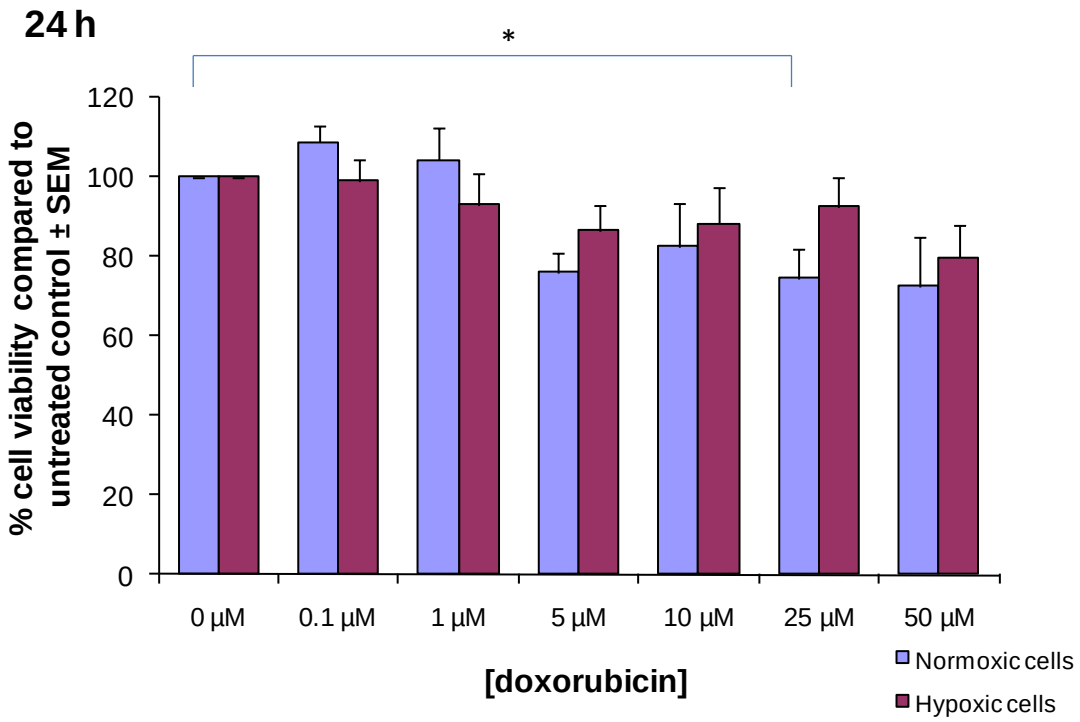

Figure 3.1 The Effects of 24 Hours Exposure to Doxorubicin on Viability of HepG2 Cells Cultured Under Normoxic and Hypoxic Conditions.
1 x 10^4 cells/200 µl were added to each well of a 96-well plate and incubated overnight at 37°C under normoxic conditions. The following day, the plates were removed to either normoxic or hypoxic conditions and exposed to doxorubicin, 6 replicate wells for each concentration. The plates were incubated under normoxic or hypoxic conditions for 24 hours. Cell viability was measured using MTS assay and normalised to untreated control. Data points represent mean of 6 separate experiments ± standard error of the mean, except for 5 µM concentrations which represent a mean of 3 separate experiments ± standard error of the mean and 50 µM concentrations which represent a mean of 4 separate experiments ± standard error of the mean. * denotes significant decrease in cell viability compared to control, where $p = < 0.01$, $\alpha/n = 0.01$.

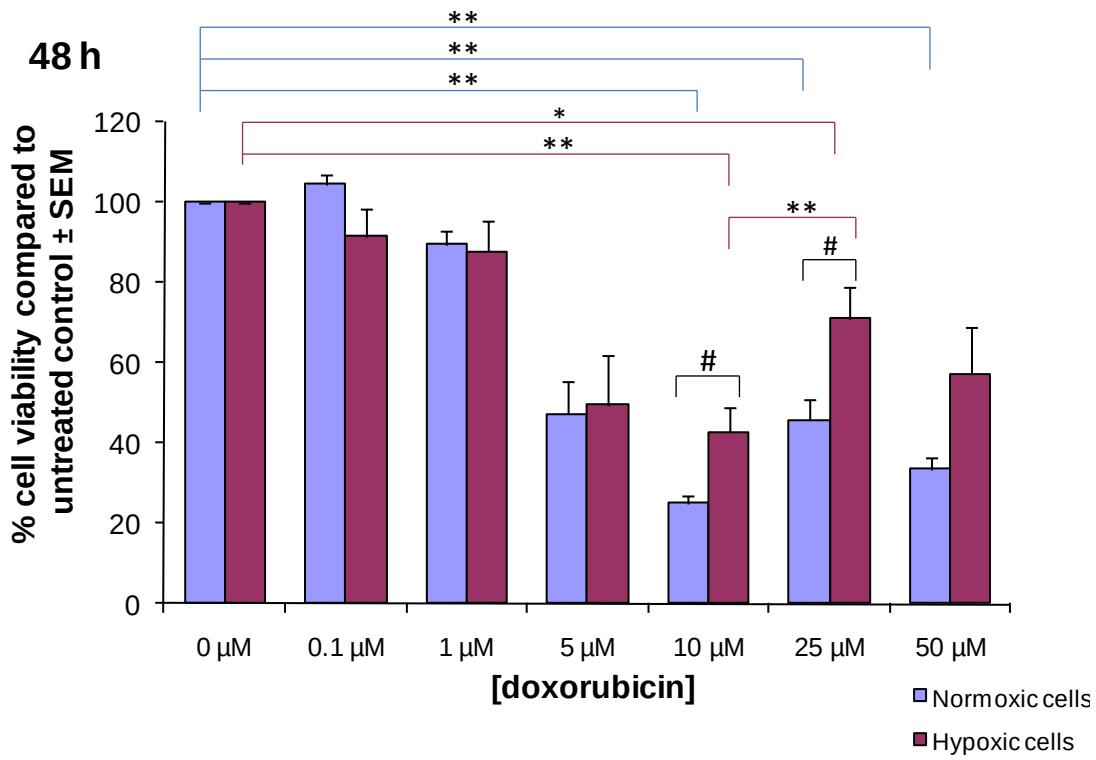

Figure 3.2 The Effects of 48 Hours Exposure to Doxorubicin on Viability of HepG2 Cells Cultured under Normoxic and Hypoxic Conditions.
1 x 10^4 cells/200 µl were added to each well of a 96-well plate and incubated overnight at 37°C under normoxic conditions. The following day, the plates were removed to either normoxic or hypoxic conditions and exposed to doxorubicin, 6 replicate wells for each concentration. The plates were incubated under normoxic or hypoxic conditions for 48 hours. Cell viability was measured using MTS assay and normalised to untreated control. Data points represent a mean of 6 separate experiments ± standard error of the mean for all doxorubicin concentrations, except for 5 µM concentrations which represent a mean of 3 separate experiments ± standard error of the mean and 50 µM concentrations which represent mean of 4 separate experiments ± standard error of the mean. * denotes significant decrease in cell viability compared to control, where $p = < 0.01$, $\alpha/n = 0.01$; ** denotes significant decrease in cell viability compared to control, where $p = < 0.001$, $\alpha/n = 0.01$; # denotes significant decrease in cell viability compared to control, where $p = < 0.025$, $\alpha/n = 0.025$.

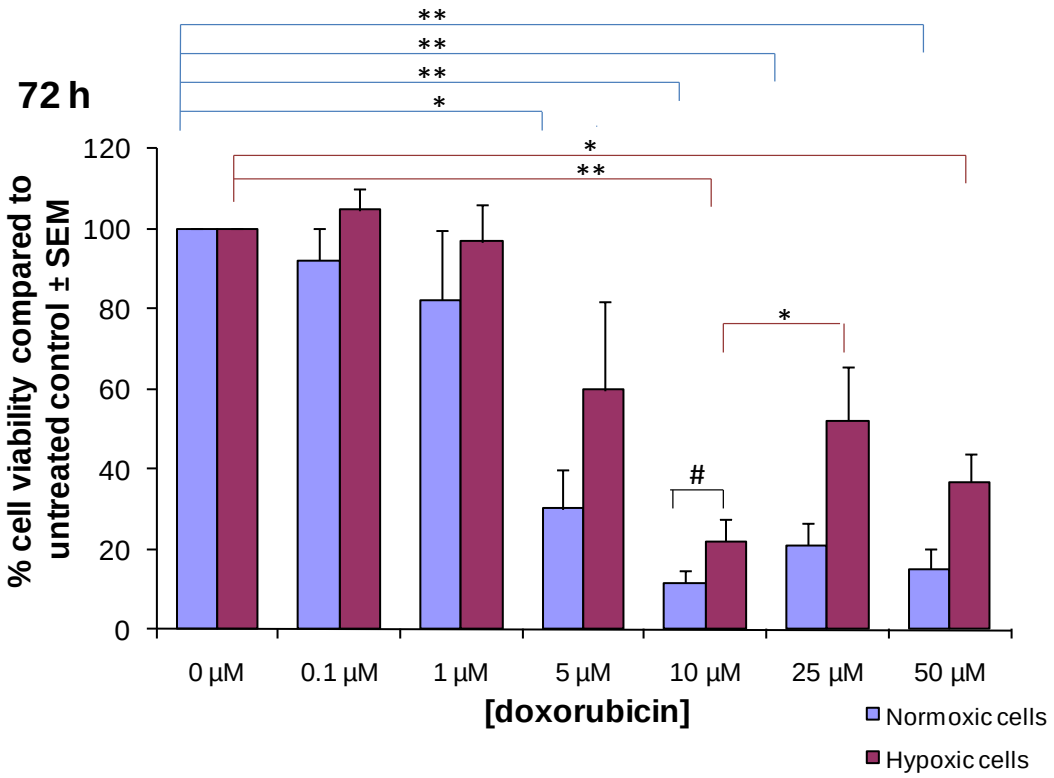

Figure 3.3 The Effects of 72 Hours Exposure to Doxorubicin on Viability of HepG2 Cells Cultured Under Normoxic and Hypoxic Conditions.
$1x10^4$ cells/200 µl were added to each well of a 96-well plate and incubated overnight at 37°C under normoxic conditions. The following day, the plates were removed to either normoxic or hypoxic conditions and exposed to doxorubicin, 6 replicate wells for each concentration. The plates were incubated under normoxic or hypoxic conditions for 72 hours. Cell viability was estimated using MTS assay and normalised to untreated control. Data points represent a mean of 6 separate experiments ± standard error of the mean, except for 5 µM concentrations which represent a mean of 3 separate experiments ± standard error of the mean and 50 µM concentrations which represent mean of 4 separate experiments ± standard error of the mean. * denotes significant decrease in cell viability compared to control, where $p = < 0.01$, $\alpha/n = 0.01$.** denotes significant decrease in cell viability compared to control, where $p = < 0.001$, $\alpha/n = 0.01$._# denotes significant decrease in cell viability compared to control, where $p = < 0.025$, $\alpha/n = 0.025$.

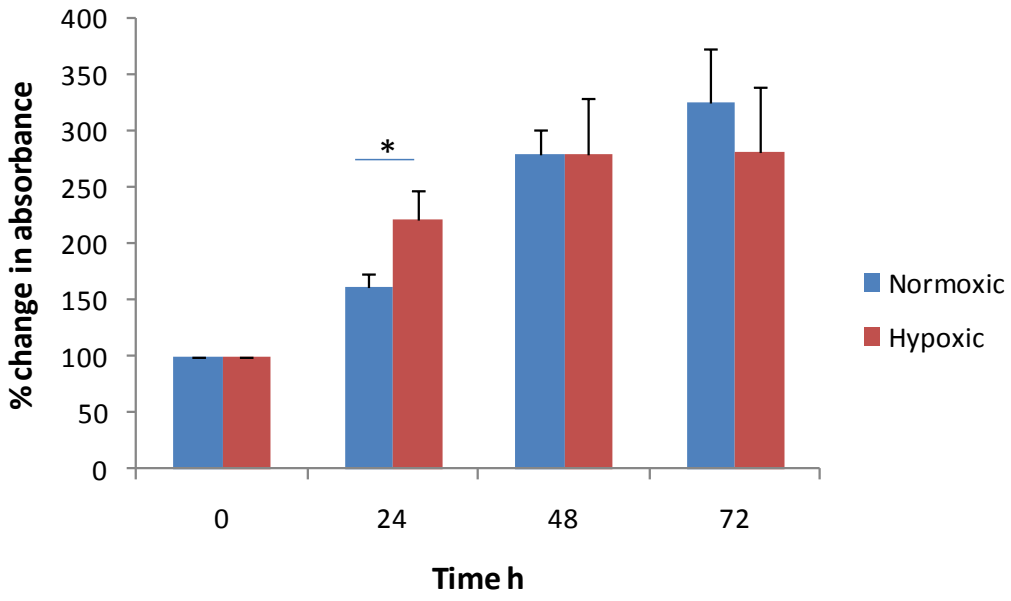

Figure 3.4 Cell Proliferation in Normoxic Compared to Hypoxic Cells.
1 x 10^4 cells in 200 µl aliquots were added to each well of a 96-well plate and incubated overnight at 37°C under normoxic conditions. The following day, the plates were removed to either normoxic or hypoxic conditions and the media was replenished. The plates were incubated under normoxic or hypoxic conditions for 24, 48 and 72 hours. Cell viability was measured using MTS assay and normalised to cell viability at 0 hours. Data points represent a mean of 6 separate experiments ± standard error of the mean. * denotes significant difference, p = < 0.05, using a two sample one tailed T test.

3.4.4 Statistical Analysis.

Comparison	p value normality	N.D.	Test used	p value	α/n	Significant
0 *vs.* 5 µM	0.109	Yes	One sample T	0.019	0.0125	No
0 *vs.* 10 µM	0.299	Yes	One sample T	0.082	0.0125	No
0 *vs.* 25 µM	0.606	Yes	One sample T	0.009	0.0125	Yes
0 *vs.* 50 µM	0.195	Yes	One sample T	0.057	0.0125	No

Table 3.1 Comparisons for Factor [drug] after 24 Hours of Treatment under Normoxic Culture Conditions.
For each doxorubicin concentration, the mean % cell viability compared to control readings from each of the replicate experiments were subjected to a normality test. For normally distributed (N.D.) data, a one sample T test was carried out, using a one tailed comparison, 100 vs. < 100. The significance level was adjusted for multiple tests using the Bonferroni correction, whereby the significance level is equal to α/n, where n = the number of tests carried out.

Comparison	p value normality	N.D.	Test used	p value	α/n	Significant
0 *vs.* 5 µM	0.332	Yes	One sample T	0.085	0.0125	No
0 *vs.* 10 µM	0.948	Yes	One sample T	0.124	0.0125	No
0 *vs.* 25 µM	0.788	Yes	One sample T	0.177	0.0125	No
0 *vs.* 50 µM	0.029	No	One sample Wilcoxon	0.100	0.0125	No

Table 3.2 Comparisons for Factor [drug] after 24 Hours of Treatment under Hypoxic Culture Conditions.
For each doxorubicin concentration, the mean % cell viability compared to control readings from each of the replicate experiments were subjected to a normality test. For normally distributed data, a one sample T test was carried out, using a one tailed comparison, 100 *vs.* < 100. For non-normally distributed data, a one sample Wilcoxon Rank test was carried out, using a one tailed comparison, 100 *vs.*<100. The significance level was adjusted for multiple tests using the Bonferroni correction, whereby the significance level is equal to α/*n*, where *n* = the number of tests carried out.

Comparison	p value normality	N.D.	Test used	p value	α/n	Significant
0 *vs.* 5 µM	0.065	Yes	One sample T	0.012	0.010	No
0 *vs.* 10 µM	0.479	Yes	One sample T	<0.001	0.010	Yes
0 *vs.* 25 µM	0.136	Yes	One sample T	<0.001	0.010	Yes
0 *vs.* 50 µM	0.068	Yes	One sample T	<0.001	0.010	Yes
10 *vs.* 25 µM	0.017	No	One sample Wilcoxon	0.030	0.010	No

Table 3.3 Comparisons for Factor [drug] after 48 Hours of Treatment under Normoxic Culture Conditions.
For each doxorubicin concentration, the mean % cell viability compared to control readings from each of the replicate experiments were subjected to a normality test. For normally distributed data, a one sample T test was carried out, using a one tailed comparison, 100 *vs.* < 100. For comparisons between different doxorubicin concentrations, a normality test was carried out on the differences between the mean % cell viability readings (differences = 25 µM - 10 µM). For non-normally distributed data, a one sample Wilcoxon Rank test was carried out, using a one tailed comparison, 0 *vs.*>0. The significance level was adjusted for multiple tests using the Bonferroni correction, whereby the significance level is equal to α/n, where n = the number of tests carried out.

Comparison	p value normality	N.D.	Test used	p value	α/n	Significant
0 *vs.* 5 µM	0.606	Yes	One sample T	0.029	0.010	No
0 *vs.* 10 µM	0.230	Yes	One sample T	<0.001	0.010	Yes
0 *vs.* 25 µM	0.117	Yes	One sample T	0.008	0.010	Yes
0 *vs.* 50 µM	0.456	Yes	One sample T	0.018	0.010	No
10 *vs.* 25 µM	0.179	Yes	One sample T	<0.001	0.010	Yes

Table 3.4 Comparisons for Factor [drug] after 48 Hours of Treatment under Hypoxic Culture Conditions.
For each doxorubicin concentration, the mean % cell viability compared to control readings from each of the replicate experiments were subjected to a normality test. For normally distributed data, a one sample T test was carried out, using a one tailed comparison, 100 *vs.* < 100. For comparisons between different doxorubicin concentrations, a normality test was carried out on the differences between the mean % cell viability readings (differences = 25 µM - 10 µM). For normally distributed data, a one sample T test was carried out, using a one tailed comparison, 0 *vs.*>0. The significance level was adjusted for multiple tests using the Bonferroni correction, whereby the significance level is equal to α/n, where n = the number of tests carried out.

Comparison	p value normality	N.D.	Test used	p value	α/n	Significant
0 *vs.* 5 µM	0.591	Yes	One sample T	0.010	0.010	Yes
0 *vs.* 10 µM	0.429	Yes	One sample T	<0.001	0.010	Yes
0 *vs.* 25 µM	0.380	Yes	One sample T	<0.001	0.010	Yes
0 *vs.* 50 µM	0.520	Yes	One sample T	<0.001	0.010	Yes
10 *vs.* 25 µM	0.177	Yes	One sample T	0.029	0.010	No

Table 3.5 Comparisons for Factor [drug] after 72 Hours of Treatment under Normoxic Culture Conditions.

For each doxorubicin concentration, the mean % cell viability compared to control readings from each of the replicate experiments were subjected to a normality test. For normally distributed data, a one sample T test was carried out, using a one tailed comparison, 100 *vs.* < 100. For comparisons between different doxorubicin concentrations (differences = 25 µM – 10 µM), a normality test was carried out on the differences between the mean % cell viability readings. For normally distributed data, a one sample T test was carried out, using a one tailed comparison, 0 *vs.* > 0. The significance level was adjusted for multiple tests using the Bonferroni correction, whereby the significance level is equal to α/*n*, where *n* = the number of tests carried out.

Comparison	p value normality	N.D.	Test used	p value	α	Significant
0 *vs.* 5 µM	0.067	Yes	One sample T	0.106	0.010	No
0 *vs.* 10 µM	0.059	Yes	One sample T	<0.001	0.010	Yes
0 *vs.* 25 µM	0.035	No	One sample Wilcoxon	0.030	0.010	No
0 *vs.* 50 µM	0.180	Yes	One sample T	0.002	0.010	Yes
10 *vs.* 25 µM	0.098	Yes	One sample T	0.007	0.010	Yes

Table 3.6 Comparisons for Factor [drug] after 72 Hours of Treatment under Hypoxic Culture Conditions.

For each doxorubicin concentration, the mean % cell viability compared to control readings from each of the replicate experiments were subjected to a normality test. For normally distributed data, a one sample T test was carried out, using a one tailed comparison, 100 *vs.* <100. For non-normally distributed data, a one sample Wilcoxon Rank test was carried out, using a one tailed comparison, 100 *vs.* < 100. For comparisons between different doxorubicin concentrations, a normality test was carried out on the differences between the mean % cell viability readings (differences = 25 µM – 10 µM). For normally distributed data, a one sample T test was carried out, using a one tailed comparison, 0 *vs.*>0. The significance level was adjusted for multiple tests using the Bonferroni correction, whereby the significance level is equal to α/*n*, where *n* = the number of tests carried out.

Comparison	[Dox]	p value normality	N.D.	Test used	p value	α	Significant
Normoxic *vs.* hypoxic	10 µM	0.619	Yes	One sample T	0.019	0.025	Yes
Normoxic *vs.* hypoxic	25 µM	0.679	Yes	One sample T	0.005	0.025	Yes

Table 3.7 Comparisons for Culture Conditions after 48 Hours Exposure to Doxorubicin.
The differences between the mean % cell viability readings for normoxic and hypoxic culture conditions at the same doxorubicin concentration were calculated (hypoxic – normoxic), and these differences were then subjected to a normality test. For normally distributed data, a one sample T test was carried out, using a one tailed comparison, 0 *vs.* > 0. The significance level was adjusted for multiple tests using the Bonferroni correction, whereby the significance level is equal to α/n, where n = the number of tests carried out.

Comparison	[Dox]	p value normality	N.D.	Test used	p value	α	Significant
Normoxic *vs.* hypoxic	10 µM	0.841	Yes	One sample T	0.014	0.025	Yes
Normoxic *vs.* hypoxic	25 µM	0.531	Yes	One sample T	0.031	0.025	No

Table 3.8 Comparisons for Culture Conditions after 72 Hours Exposure to Doxorubicin.
The differences between the mean % cell viability readings for normoxic and hypoxic culture conditions at the same doxorubicin concentration were calculated (differences = hypoxic – normoxic), and these differences were then subjected to a normality test. For normally distributed data, a one sample T test was carried out, using a one tailed comparison, 0 *vs.* > 0. The significance level was adjusted for multiple tests using the Bonferroni correction, whereby the significance level is equal to α/n, where n = the number of tests carried out.

3.4.5 50 µM Doxorubicin Attenuates Hypoxia Stimulated HIF-1α Nuclear Accumulation.

To determine the effect of doxorubicin treatment on hypoxia stimulated nuclear accumulation of HIF-1α, SDS-PAGE and Western Blotting was carried out on nuclear extracts from HepG2 cells cultured under normoxic and hypoxic conditions, and exposed to drug concentrations as shown, see Figure 3.8. The results confirmed that 24 hours incubation under hypoxic conditions resulted in a significant increase in the amount of HIF-1α in the nucleus of HepG2 cells ($p = 0.013$, $\alpha/n = 0.017$), see Figure 3.5 (Lane 4). Doxorubicin treatment of 10 µM had no significant effect on the nuclear accumulation of HIF-1α in hypoxic cells; see Figure 3.5 (Lane 5). However, the 50 µM treatment significantly reduced the amount of HIF-1α detected in the nucleus ($p = 0.003$), see Figure 3.5 (Lane 6). The 10 µM and 50 µM doxorubicin treatments had no effect on the amount of HIF-1α detected in the nucleus of normoxic cells.

3.4.6 Doxorubicin Activates NFkB p50 in Normoxic Cells. Hypoxia Activates NFkB p50, and Doxorubicin has no Effect on Hypoxia Stimulated Activation of NFkB p50.

To determine the effect of doxorubicin treatment on hypoxia stimulated nuclear accumulation of NFkB p50, SDS-PAGE and Western Blotting was carried out on nuclear extracts from HepG2 cells cultured under normoxic and hypoxic conditions, and exposed to drug concentrations as shown, see Figure 3.6. Doxorubicin treatment of normoxic HepG2 cells increased the amount of p50 NFkB in the nucleus (Lanes 1, 2 and 3). However, the increase was not significant (10 µM doxorubicin, $p = 0.087$; 50 µM doxorubicin, $p = 0.034$, $\alpha = 0.017$). Hypoxia also increased the amount of p50 NFkB in the nucleus of HepG2 cells ($p = 0.049$, $\alpha = 0.017$) (Lane 4). However,

doxorubicin treatment of hypoxic cells did not increase the amount of NFkB compared to the effects of hypoxia alone (Lanes 5 and 6).

3.4.7 Effects of Doxorubicin on p70 S6K and p70 S6K (phospho T389).

To determine the effect of doxorubicin treatment on S6K and the phosphorylation of S6K, SDS-PAGE and Western Blotting was carried out on cytoplasmic extracts from HepG2 cells cultured under normoxic and hypoxic conditions, and exposed to drug concentrations as shown, see Figure 3.7. Hypoxia had no effect on the ratio of phosphorylated S6K to total S6K (Panel A and Lanes 1 and 4). Similarly, doxorubicin had no effect on the ratio of phosphorylated S6K to total S6K in cells cultured under normoxic or hypoxic conditions (Panel A, Lanes 1 – 3 and 4 - 6). Levels of total S6K remained the same in normoxia and hypoxia and for all treatments (Panel B, Lanes 1 – 3 and 4 - 6).

3.4.8 Effects of Doxorubicin on Akt and Akt (phospho ser473).

Akt was observed to be activated in normoxic and hypoxic cells, see Figure 3.8. Hypoxia was not observed to have any effect on Akt phosphorylation (Lanes 1 and 3). Doxorubicin treatment was not observed to have any effect on Akt phosphorylation in either normoxic or hypoxic conditions (Lanes 1 – 3 and 4 – 6).

The total amount of Akt did not change in either normoxic or hypoxic conditions or with application of doxorubicin.

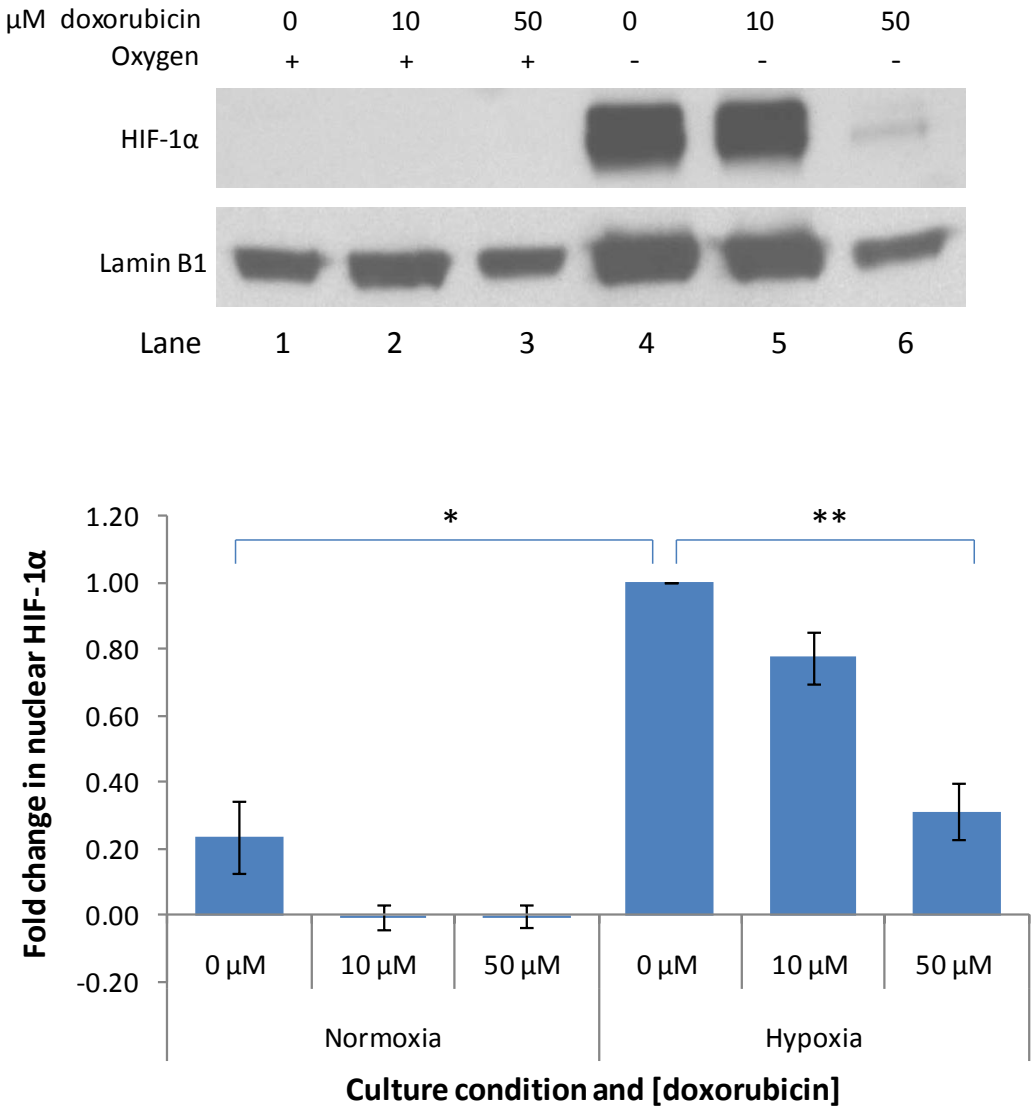

Figure 3.5 Nuclear Accumulation of HIF-1α after Doxorubicin Treatment. HepG2 cells were seeded onto T75 tissue culture flasks and incubated under normoxic conditions until 60% confluent. The cells were exposed to doxorubicin in normoxic or hypoxic conditions and incubated for 24 hours. The cells were harvested and nuclear extracts were prepared. Equal quantities of protein were fractionated on a 10% SDS-PAGE gel. The proteins were transferred to a PVDF membrane and probed with anti-HIF-1α antibodies. Proteins were visualised using chemiluminescent reagents. The membrane was stripped and reprobed using antibodies against the nuclear house-keeping protein Lamin B1. Protein levels were quantified using densitometry analysis. The amount of HIF-1α was normalised to Lamin. Fold change compared to untreated hypoxic cells was calculated. Data shown represents mean of 4 independent experiments ± standard error of the mean for hypoxic cells, and mean of 3 independent experiments ± standard error of the mean for normoxic cells. Statistical analysis was carried out using a one sample one tailed T test, 1 vs. < 1. * denotes a statistically significant result, p = < 0.05; ** denotes a statistically significant result, p = < 0.01.

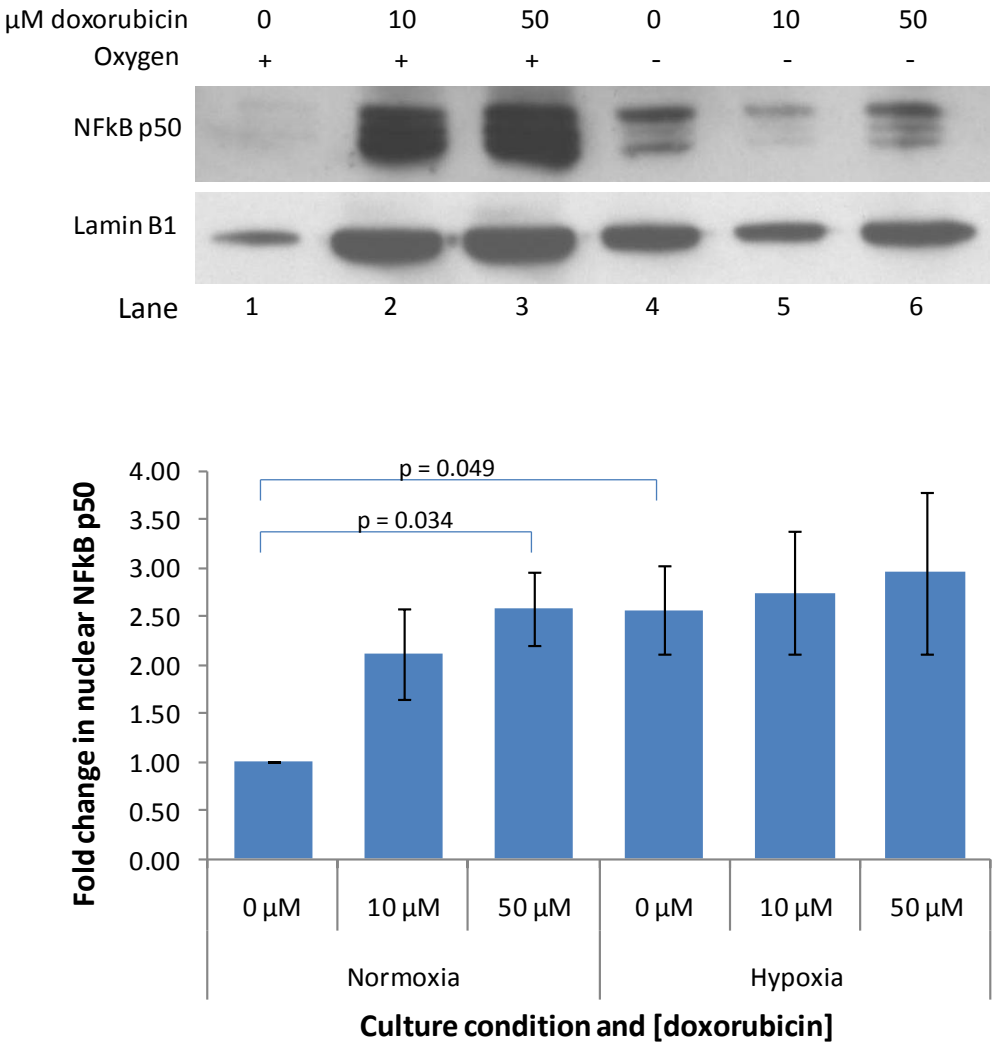

Figure 3.6 Nuclear Accumulation of NFkB p50 after Doxorubicin Treatment. HepG2 cells were seeded onto T75 tissue culture flasks and incubated under normoxic conditions until the cells reached 60% confluence. The cells were exposed to doxorubicin in normoxic or hypoxic conditions and incubated for 24 hours. The cells were harvested and nuclear extracts were prepared. Equal quantities of protein were fractionated on a 10% SDS-PAGE gel. The proteins were transferred to a PVDF membrane and probed with anti-NFkB p50 antibodies. Proteins were visualised using chemiluminescent reagents. The membrane was stripped and reprobed using antibodies against the nuclear house-keeping protein Lamin B1. Protein levels were quantified using densitometry analysis. The amount of NFkB p50 was normalised to Lamin. Fold change compared to untreated normoxic cells was calculated. Data shown represents mean of 3 separate experiments ± standard error of the mean.

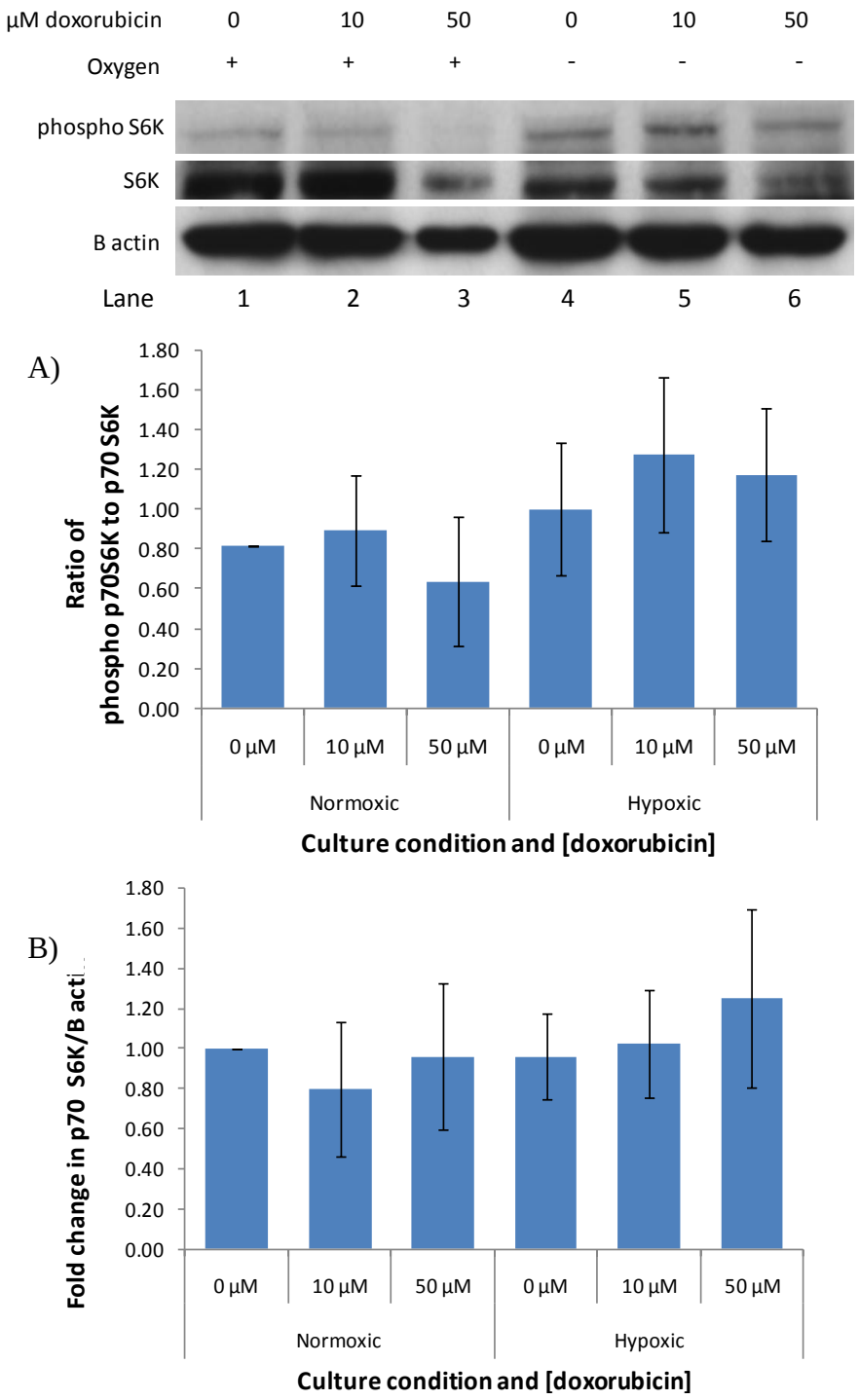

Figure 3.7 Cytoplasmic p70 S6K and p70 S6K (phospho T389) after Doxorubicin Treatment of Normoxic and Hypoxic Cells.
Cells were treated as described in Figure 6.1. Cytoplasmic extracts were prepared and fractionated on a 10% SDS-PAGE gel. The proteins were transferred to a PVDF membrane and probed with anti- p70 S6K (phospho T389) antibodies. Proteins were visualised and the membrane was stripped and reprobed using antibodies against total S6K, and antibodies against B actin. Protein levels were quantified using densitometry analysis. Ratio of p70 S6K (phospho T389) to total S6K was calculated, as was the amount of p70 S6K normalised to B actin. Data shown represents mean of 3 separate experiments ± standard error of the mean.

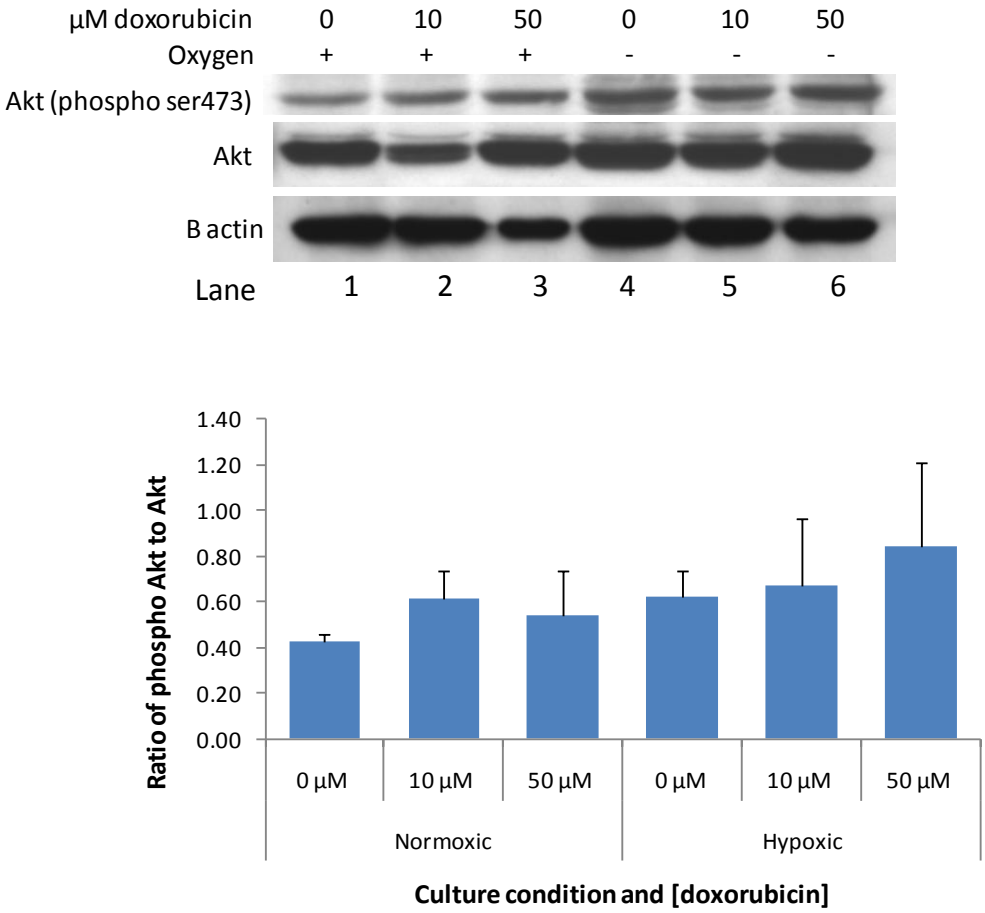

Figure 3.8 Cytoplasmic Akt and Akt (phospho ser473) after Doxorubicin Treatment of Normoxic and Hypoxic Cells.
Cells were treated as described in Figure 6.1. Cytoplasmic extracts were prepared and fractionated on a 10% SDS-PAGE gel. The proteins were transferred to a PVDF membrane and probed with anti- Akt (phospho ser473) antibodies. Proteins were visualised and the membrane was stripped and reprobed using antibodies against total Akt, and antibodies against B actin. Protein levels were quantified using densitometry analysis. Ratio of Akt (phospho ser473) to total Akt was calculated, as was the amount of Akt normalised to B actin. Data shown represents mean of 3 separate experiments ± standard error of the mean.

3.5 Discussion.

3.5.1 Poor Treatment Outcomes Observed in Clinic are Likely Due to Sub-Clinical Concentrations of Doxorubicin Reaching Tumour Cells.

It has been shown here that doxorubicin concentrations of < 5 μM do not exhibit cytotoxic effects against normoxic or hypoxic HepG2 cells (Chapter 3).

One explanation for the resistance to doxorubicin in the treatment of HCC after systemic administration is almost certainly due to the fact that intratumoural concentrations of doxorubicin are sub-clinical. Bolus administration of doses between 15 and 90 mg/m^2 give a maximal initial plasma concentration of approximately 5 μM (Brenner *et al* 1985; Greene *et al* 1983), with most initial plasma concentrations lying between 1 – 2 μM (Muller *et al* 1993; Speth *et al* 1987; Benjamin *et al* 1993; Creasey *et al* 1976). However, there is a rapid decline after 1 hour to plasma concentrations between 25 – 250 nM, which is the same range as achieved when doxorubicin is administered by continuous infusion (Greene *et al;* Muller *et al;* Speth *et al*). Experiments using three different tumour types in a mouse model showed that even when potentially lethal intraperitoneal doses of doxorubicin were administered, intratumoural concentrations of doxorubicin declined exponentially with distance from tumour blood vessels, with little or no doxorubicin detectable in many of the tumour cells (Primeau *et al*., 2005). *In vitro* data suggests that concentrations of 0.1 – 5 μM (Fornari *et al* 1996); at least 2 μM (Meriwether *et al* 1972); and in some cases up to 100 μM (Momparler *et al* 1976) are necessary for inhibition of DNA and RNA synthesis. As discussed in the introduction, different mechanisms of action are likely to be involved at different drug concentrations.

The delivery of doxorubicin to tumour cells is vastly improved when cTACE is used. Intratumoural drug concentration has been reported to be 60% of the injected dose (Raoul *et al*., 1992). Concentrations of doxorubicin within tumour tissue are 10 to

100 times higher after cTACE than after systemic application (Konno, 1990). Doxorubicin release from DC Bead after DEB-TACE has been reported as 52% at day 28, and 89% at day 90 (Namur *et al*., 2010). Low plasma concentrations after DEB-TACE compared to TACE suggest that tumour retention of doxorubicin is high (Hong *et al*., 2006). The loco-regional delivery of doxorubicin to HCCs therefore ensures that the tumour cells experience effective doses of chemotherapeutic.

3.5.2 Relevance of Results to DEB-TACE.

Here we have shown *in vitro* that there is a therapeutic window for doxorubicin of 10 µM (= 5.8 µg/ml), where the drug is cytotoxic to both normoxic and hypoxic HepG2 cells. Concentrations above 10 µM do not show increased cytotoxicity in normoxic cells. However, in hypoxic cells, concentrations above 10 µM have decreased cytotoxicity, even up to a concentration x 5 higher.

So how does this *in vitro* finding translate to the clinical setting? Three studies have looked at the release and tissue penetration of doxorubicin from DEBDOX in embolised swine liver. In one, using radioopaque beads, MicroCT and epiflourescent microscopy demonstrated that the concentration of doxorubicin into liver tissue at 1 to 4 hours post TACE reached a maximum of 150 µM within a distance of 10 µm from the bead. Doxorubicin concentration decreased with increasing distance from the bead and concentrations >10µM extended out to 250-350 µm from the bead surface. Necrosis was observed 24 hours post TACE and coincided with areas of high drug exposure (Reddy *et al*., 2010). Another study used fluorescence microscopy to image the distribution of doxorubicin in liver tissue after embolisation using DEBDOX 100 – 300 µm in diameter. Doxorubicin was detected up to 200 µm from the bead surface 2 hours after embolisation had taken place (Dreher *et al*., 2009). In another study, livers were sampled at day 28 and day 90 post TACE.

Fourier transform IR spectroscopy/mass spectrometry (FTIR-MS) was then used to image the amount of doxorubicin left in the beads. Results showed that 52% of the doxorubicin had eluted from the bead at day 28, and that 89% of doxorubicin had eluted from the bead at day 90 (Namur *et al*., 2010).

In fact, Namur *et al* (2008) had shown previously in an animal model that therapeutic doses of doxorubicin are released into liver tissue up to 90 days after application of DEBDOX (Namur *et al*., 2008a). Namur *et al* 2008 also looked at doxorubicin elution in liver explants from HCC patients who underwent TACE using DEBDOX prior to transplantation. Time between treatment and explantation ranged from one day to 36 days. For the 6 hour explant, doxorubicin was detected within the tumour up to a distance of 1.1 cm from the bead, with intratumoural concentrations of 6.4 µM. No necrosis was evident in this explant. Doxorubicin was detected up to 600 µm from the beads in all explants. The concentration of doxorubicin decreased with distance, by up to 70% between 20 µm and 600 µm from the bead. Since the limit of oxygen diffusion in tissue is 100 – 200 µm from the capillary, it is clear that cells experiencing hypoxia which has not occurred as a result of the embolisation itself, are in contact with the drug (Namur *et al*., 2011). The concentration of doxorubicin decreased with time, from one day to 9 – 14 days, and from 9 -14 days to 32 – 36 days after treatment in the Namur study. The tissue concentration of doxorubicin at day one was within the therapeutic window for both normoxic and hypoxic cells that we have identified *in vitro,* up to a distance of 600 µm from the bead. The extent of tumour necrosis correlated with penetration and concentration of doxorubicin, and necrotic/fibrotic tissue surrounded the beads at day 9 to day 36 explantation. Doxorubicin concentration in normal tissue in the Namur *et al* animal model was higher at time points and similar distances from the bead than doxorubicin

concentrations in HCCs. This is likely to be due to increased interstitial pressure in tumour compared to normal tissue.

A retrospective study by Citron *et al*, (2008), looked at the distribution of drug and the extent of tumour necrosis following TACE using doxorubicin-loaded LC Bead™. Seven patients received one treatment, two patients received > one treatment. Doses were 150 mg doxorubicin per treatment. CT scan was used to assess treatment response prior to explantation, and further analysis investigated necrosis, drug diffusion and the relationship between the two. Histological analysis demonstrated cytostatic drug concentrations in tissue surrounding the beads up to several hundred microns away. Complete tumour necrosis was observed in all but one of the patients, who was transplanted 8 hours after treatment. Complete tumour necrosis was observed after histological assessment in all but two patients – the patient transplanted 8 hours after treatment and another patient where histology revealed a small residual focus. No tumour recurrence occurred during 15 months of follow up, although 2 patients died; one from Hepatitis C related liver failure and one from multi-organ failure after candidal infection (Citron *et al*., 2008).

A recent study used contrast-enhanced ultrasonography (CEUS) to assess the efficacy of DEBDOX for the treatment of unresectable HCC. 10 patients were given a 4 ml dose of DEBs, preloaded with 25 mg doxorubicin/ml hydrated beads. After 2 days, necrosis ranged from 21% to 70%, with a mean of 44%. After 35 to 40 days this had increased significantly (= 0.0012) to necrosis ranging between 24% and 88%, with a mean of 52%. This suggests that during the first 2 days after treatment necrosis is evident, and that there is a sustained effect out to 40 days post TACE (Moschouris *et al*., 2010).

As discussed above, several clinical studies have now been published, citing improved treatment responses for DEB-TACE compared to cTACE (Lammer *et al*., 2010, Dhanasekaran *et al*., 2010, Ferrer Puchol *et al*., 2011); and compared to bland embolisation using unloaded beads (Malagari *et al*., 2010). Other data, as cited above, demonstrates that doxorubicin elution from ionic exchange microspheres *in vivo,* in both animal models and HCC explants, provides tissue and intratumoural drug concentrations that result in necrosis (Reddy *et al*., 2010, Namur *et al*., 2010, Citron *et al*., 2008, Moschouris *et al*., 2010). The response of tumour cells to DEB-TACE can be seen as soon as one day after embolisation and continues for at least 36 days afterward (Moschouris *et al*., 2010).

Here we have shown that concentrations above 5 µM are required for cell death in both normoxic and hypoxic cells. The reported intratumoural concentration of doxorubicin at distances up to 600 µm from the beads fits the therapeutic window that we have identified for both normoxic and hypoxic tumour cells. Viable hypoxic cells have been observed at distances of 50 – 250 µm from the nearest blood vessel (Sutherland, 1988). The drug is diffusing out to distances where cells are hypoxic, whether this hypoxia is due to distance from the nearest blood vessel or due to the embolisation procedure itself. Effects are time and dose dependent, and so the prolonged and sustained release of drug into the tumour associated with DEB-TACE is likely to provide optimal exposure of tumour cells to the drug.

3.5.3 Increased Doxorubicin Resistance in Hypoxic Cells.

The data here shows that hypoxia protects HepG2 cells from doxorubicin-induced cytotoxicity. This effect is seen at the 48 and 72 hour time points, at doxorubicin concentrations of 10, 25 and 50 µM (Figures 3.5 and 3.6). Hypoxia-induced

resistance to chemotherapeutics is well documented (Gupta and Costanzi, 1987, Kalra *et al*., 1993, Kennedy *et al*., 1983, Luk *et al*., 1990, Martin and McNally, 1980, Sakata *et al*., 1991, Sanna and Rofstad, 1994, Song *et al*., 2006, Tomida and Tsuruo, 1999, Wilson *et al*., 1989, Yamagata *et al*., 1992, Yamauchi *et al*., 1987, Sullivan *et al*., 2008, Unruh *et al*., 2003, Liu *et al*., 2008b, Jung *et al*., 2010, Rohwer *et al*., 2010) and interference with HIF-1α has been reported to reverse this (Chang *et al*., 2006, Liu *et al*., 2008a, Wang and Minko, 2004, Song *et al*., 2006, Nardinocchi *et al*., 2009a, Daskalow *et al*., 2010).

No data has been published to date on resistance to doxorubicin in HepG2 cells cultured *in vitro* under hypoxic conditions. However, a recent publication has shown that the unfolded protein response (UPR), which is activated in hypoxia, is activated in HCCs and protects against doxorubicin cytotoxicity to HepG2 cells *in vitro* (Al-Rawashdeh *et al*., 2010). Another study has shown that hypoxia protects against doxorubicin cytotoxicity in Huh-7 HCC cells (Jung *et al*., 2010).

As discussed in the introduction, the cytotoxicity of doxorubicin is due to a number of different mechanisms. Resistance to chemotherapies in hypoxic tumour cells is therefore likely to be multi-factorial. Oxygen is thought to be involved both directly and indirectly in mechanisms of action of doxorubicin (Teicher *et al*., 1981).

3.5.3.1 Reduced Drug Accumulation in Hypoxia - Influence of the Extracellular Milieu.

The interstitial fluid within solid tumours has increased acidity when compared to that of normal tissue, with a further increase in acidosis in hypoxic compartments *(*Vaupel *et al*., 1989; Chiche *et al*., 2010*).* Both glucose consumption and lactate production have been shown to increase by a factor of three in HepG2 cells exposed to severe hypoxia (Chevrollier *et al*., 2005). Doxorubicin is a weak base, and the

local pH affects the ionisation state of the drug. Increased acidity reduces the proportion of doxorubicin in the non-ionised, membrane-permeable form. As a consequence, there is a reduction in the accumulation of doxorubicin in hypoxic tumour cells (Mellor and Callaghan, 2011, Gerweck *et al*., 1999; De Milito and Fais, 2005, Raghunand *et al*., 1999).

3.5.3.2 Enhanced Drug Efflux Under Hypoxic Conditions.

Drug efflux has long been recognised as a major contributor to chemoresistance. Pgp is a transmembrane glycoprotein which functions as an efflux pump for a wide range of xenobiotics and is widely expressed in hepatocytes (Thiebaut *et al*., 1987). Hypoxia has been shown to increase the expression of Pgp in HepG2 cells and in other cell lines (Comerford *et al*., 2002, Zhu *et al*., 2005, Wartenberg *et al*., 2003).

3.5.3.3 Oxygen-Dependent Cytotoxicity. Free Radical Formation.

Doxorubicin-induced free radical DNA damage occurs at doxorubicin concentrations > 10 µM (Ubezio and Civoli, 1994; Benchekroun *et al*., 1993a, Benchekroun *et al*., 1993b). However, in hypoxic conditions, tumour cells may not be capable of carrying out these reductive reactions (Teicher *et al*., 1981). If this mechanism of cytotoxicity comes into effect above a threshold concentration, but is only seen in cells where the oxygen concentration is sufficiently high, this would explain the decrease in the cytotoxicity of doxorubicin towards hypoxic cells at higher drug concentrations.

3.5.3.4 Reduced Levels of Topoisomerase II in Hypoxic Cells.

Drug sensitivity correlates with cellular TOP2 levels and drug resistant cancer cells have been shown to have reduced activity and/or decreased levels of TOP2 (Beck *et al*., 1993, Hofmann and Mattern, 1993). Hypoxia has been shown to reduce

intracellular topoisomerase II levels and so reduce the cytotoxicity of TOP2 poisons (Sullivan and Graham, 2009).

3.5.3.5 Hypoxia and Apoptosis.

Hypoxia can induce both pro- and anti-apoptotic responses, depending on the severity and duration of oxygen depletion. The apoptotic cascade in hypoxia is to some extent directly regulated by HIF. (Goda *et al*., 2003, Sowter *et al*., 2001, Piret *et al*., 2005, Dong *et al*., 2003, Erler *et al*., 2004, Baek *et al*., 2000). In HepG2 cells hypoxia has been shown to protect from apoptosis (Sermeus *et al*., 2008; Piret *et al*., 2005).

3.5.4 The Nuclear Accumulation of HIF-1α in Response to Hypoxia and Doxorubicin.

This study investigated the effect of doxorubicin, an anthracycline and Topoisomerase II poison, on the amount of HIF-1α in the nucleus of HepG2 cells cultured under normoxic and hypoxic conditions, and found that a doxorubicin dose of 50 μM significantly attenuated nuclear HIF-1α found in cells cultured under hypoxic conditions. A dose of 10 μM however, had no significant effect.

Analysis of doxorubicin elution from embolisation particles following TACE demonstrates that concentrations of the drug may be as high as 150 μM up to 10 μm from the beads, whilst concentrations >10μM extend out to 250-350 μm from the beads (Reddy *et al*., 2010). Consequently, the high concentrations of doxorubicin which are found in cancer tissue close to the embolised blood vessel may be sufficient to block HIF-1 signalling in cells which experience hypoxia as a result of embolisation therapy itself, and inhibit the activation of hypoxia-induced survival pathways. Without the activation of compensatory mechanisms which enable a cell to adapt to hypoxia, the cells will undergo necrosis.

The investigations undertaken in this thesis have identified a therapeutic window of 10 µM doxorubicin, where the drug is more toxic to hypoxic HepG2 cells than a 50 µM dose. Hypoxic cells were found to be significantly more resistant to doxorubicin than normoxic cells at all effective concentrations. Whilst 50 µM doxorubicin attenuates the hypoxia stimulated nuclear accumulation of HIF-1α, a 10 µM application has no significant effect. It seems that the cytotoxicity of this critical 10 µM dose is not connected to the ability of doxorubicin to inhibit HIF-1α accumulation in the nucleus. However, it may well be connected to the ability of doxorubicin to inhibit HIF-1 transcriptional activity, and block hypoxia-induced survival pathways.

So why does a dose of 50 µM reduce HIF-1α levels? There are at least three possible explanations – firstly, doxorubicin increases the degradation of HIF-1α; secondly, doxorubicin decreases the translocation of HIF-1α to the cell nucleus; and thirdly, doxorubicin decreases the rate of transcription or translation of HIF-1α.

The degradation of HIF-1α is dependent on oxygen and intracellular iron in the form of Fe^{2+}. Under anaerobic conditions, the semiquinone free radical forms of doxorubicin catalyze the rapid release of iron from the intracellular iron storage molecule ferritin (Thomas and Aust, 1986). Free intracellular iron contributes to ROS formation and to the cytotoxic effects of doxorubicin *via* catalysation of the Fenton reaction. However, the degradation of HIF-1α depends not only on the presence of iron, but also on the presence of oxygen. Whether or not increased iron availability reduces the threshold oxygen concentration below which HIF-1α is stabilised has not yet been explored.

Levels of cytoplasmic HIF-1α were undetectable both before and after doxorubicin treatment (data not shown), so it would seem that the reduction in nuclear

accumulation of HIF-1α is not a result of a decrease in the translocation of the protein from the cytoplasm to the nucleus. The rate of transcription of *hif 1α* could be reduced due to a stalling of transcriptional machinery as a result of the formation of doxorubicin/DNA complexes (Sinha and Chignell, 1979). GL331 is a plant toxin derivative and Topoisomerase II poison (Lee and Huang, 2001) that has been shown to downregulate expression of HIF-1α mRNA by interfering with the binding of cellular components to the promoter region of the *HIF-1α* gene and so repressing its transcription (Chang *et al*., 2003).

Doxorubicin is known to inhibit global protein synthesis at the elongation step of translation (White *et al*., 2007). Topotecan is a topoisomerase I poison that inhibits the translation of HIF-1α mRNA (Rapisarda *et al*., 2004a, Puppo *et al*., 2008). Metronomic doses of Topotecan inhibit angiogenesis and tumour growth in glioma xenograft models (Rapisarda *et al*., 2004b) and topotecan can also block the expression of IGF-1 induced HIF-1α in normoxic cancer cells (Beppu *et al*., 2005). The topoismerase II poison NSC 644221 inhibits the translation of HIF-1α and expression of HIF target genes in cancer cells (Creighton-Gutteridge *et al*., 2007). Yamazaki's laboratory failed to observe any decrease in HIF-1α in HepG2 cells after doxorubicin treatment, although it should be noted that their group only tested concentrations of doxorubicin up to 0.5 μM (Yamazaki *et al*., 2006). Similarly, Lee's group (Lee *et al*., 2009a) failed to observe any decrease of HIF-1α in Hep3B cells treated with doxorubicin, but only tested concentrations up to 10 uM. However, Lee's group reported a downregulation of HIF-1 target genes after administration of 10 uM doxorubicin.

Further work is needed to elucidate the mechanism of HIF-1α inhibition by the higher dose of doxorubicin that we have observed here. Further work is also needed

to ascertain whether the lower dose of doxorubicin inhibits the transcriptional activity of HIF-1 on downstream genes in hypoxic HepG2 cells.

3.5.5 Activation of the Transcription Factor NFkB.

Activation of NF-kB is, in general, associated with upregulation of anti-apoptotic proteins, particularly in cancer cells. NF-kB is upregulated in HCC, probably as a result of hypoxia, and is associated with both pathogenesis and chemoresistance (Arsura and Cavin, 2005, He and Karin, 2011, Luedde and Schwabe, 2011).

In this study doxorubicin treatment of normoxic cells induced nuclear localisation of p50 NFkB. Doxorubicin treatment of normoxic cells induces p50 NFkB activation (Figure 3.6). Anthracyclines have been widely reported to activate NFkB, and doxorubicin-induced NFkB activation is associated with chemoresistance (Wang *et al*., 2003, Gruber *et al*., 2008), and inhibition of NFkB sensitises cells to doxorubicin (Wang *et al*., 2003, Chiao *et al*., 2002, Gangadharan *et al*., 2009, Bednarski *et al*., 2008, Ahn *et al*., 2008, Mi *et al*., 2008). Doxorubicin appears to activate NFkB *via* the canonical pathway and the degradation of IkB (Bednarski *et al*., 2008, Tapia *et al*., 2007).

This study also found that hypoxia induced nuclear translocation of NFkB (Figure 3.6). The mechanism of hypoxia-induced NFkB is not well described as yet. There are reports that hypoxia causes the activation of NFkB in an IKK-independent way (Koong *et al*., 1994a, Koong *et al*., 1994b) and also reports that it activates NFkB in an IKK-dependent way (Romano *et al*., 2004). Interestingly, hypoxic cells appeared to be protected from doxorubicin induced NFkB activation (Figure 3.6).

3.5.6 The Effects of Hypoxia and Doxorubicin on phosphorylation of p70 S6K.

The phosphorylation of p70S6K was not affected by culture conditions or doxorubicin treatments. Levels of total S6K remained the same across all experimental conditions (Figure 3.7).

3.5.7 The Effects of Hypoxia and Doxorubicin on phosphorylation of Akt.

The phosphorylation of Akt was not affected by culture conditions or doxorubicin treatments. Levels of Akt remained the same across all treatments and culture conditions. Phosphorylated Akt was observed across all experimental conditions. Phosphorylation at this site is known to be mediated by mTORC2.

3.6 Conclusions.

We have here identified a doxorubicin concentration of 10 µM that is effective against normoxic and hypoxic HCC cells. This concentration is commensurate with reported tissue and intratumoural concentrations of doxorubicin released by drug-eluting beads from both human and animal studies (Namur *et al*., 2008b, Namur *et al*., 2010, Reddy *et al*., 2010, Citron *et al*., 2008). The cytotoxicity of doxorubicin *in vitro* was also observed to be time and dose dependent, and this implies that the prolonged and sustained release of drug associated with DEB-TACE *in vivo* provides an effective method of drug delivery.

50 µM doxorubicin, but not 10 µM doxorubicin, attenuated the stabilisation of HIF-1α under hypoxic conditions. This suggests that the effectiveness of the 10 µM dose of doxorubicin towards hypoxic cells is not due to its activity preventing the stabilisation of HIF-1α. Doxorubicin induced nuclear localisation of NFkB in normoxic cells. Hypoxia alone also induced nuclear localisation of NFkB, with no further localisation observed after application of doxorubicin.

Recently there has been a great deal of interest in the use of the mTOR inhibitor rapamycin, and a number of rapalogs, in the treatment of HCC (Treiber, 2009). This came about after the observation that patients who were prescribed rapamycin as an immunosuppressant after liver transplantation had much lower rates of tumour recurrence than patients who were prescribed other immunosuppressants (Castroagudin *et al*., 2011). Rapamycin inhibits the mTOR pathway. mTOR is a central regulator of cell growth and angiogenesis, and the mTOR pathway is activated in 40-50% of patients with HCC (Sieghart *et al*., 2007). The following chapter will report on investigations into the effects of rapamycin on HepG2 cells cultured under normoxic and hypoxic conditions.

Chapter 4

The Effect of Rapamycin on the Viability of HepG2 Cells Cultured *In Vitro* under Normoxic and Hypoxic Conditions.

4.1 Introduction.

As the understanding of the molecular mechanisms and pathways involved in the initiation and progression of cancers increases, so opportunities have arisen to identify novel molecular targeted therapies in the fight against them. Pathways that are deregulated in cancer cells, and which may be essential for the survival of those cells, can be blocked or disrupted using agents that often have very specific targets.

The PI3K/Akt/mTOR pathway is deregulated in many cancers and hyperactivity is implicated in tumourigenesis (Liu *et al*., 2009, Treiber, 2009, Zhou *et al*., 2009, Villanueva *et al*., 2008). Tumours with hyperactive mTOR tend to be highly vascularised and the mTOR signalling pathway has been shown to be deregulated in 40-50 % of HCCs, and this is associated with a poor prognosis (Sahin *et al*., 2004, Zhou *et al*., 2009, Sieghart *et al*., 2007). If tumour cells are dependent on mTOR signalling for survival, there is a potential role for mTOR inhibitors in the treatment of cancers with deregulated PI3K/Akt/mTOR signalling (Tsang *et al*., 2007).

Hypoxia is a negative regulator of mTOR in many cell lines (Arsham *et al*., 2003). However, cells which carry mutations to the PTEN/PI3K/Akt pathway have been shown to retain mTOR activity even under hypoxic conditions (Kaper *et al*., 2006). HepG2 cells and human hepatocarcinoma tissues have reduced levels of PTEN (Zhang *et al*., 2004, Tian *et al*., 2010a).

4.1.1 Rapamycin.

Recently there has been a great deal of interest in the use of rapamycin and other mTOR inhibitors in the treatment of HCC. This came about after the observation that

patients who were prescribed rapamycin as an immunosuppressant after liver transplantation had much lower rates of tumour recurrence than patients who were prescribed other immunosuppressant drugs (Toso *et al*., 2010, Vivarelli *et al*., 2010b, Zhou *et al*., 2008, Zimmerman *et al*., 2008). Rapamycin is a bacteria-derived macrolide which has antifungal, immunosuppressant and anti proliferative properties. Although the anticancer activity of rapamycin was first recognised by the National Cancer Institute in the 1970s, it was not extensively investigated until the late 90s. Rapamycin has been shown to have anti-tumoural effects *in vitro* and *in vivo* (Semela *et al*., 2007, Zhang *et al*., 2007, Huynh *et al*., 2009a, Huynh *et al*., 2008b, Huynh *et al*., 2009b, Rizell *et al*., 2008, Wang *et al*., 2008b, Wang *et al*., 2009b, Wang *et al*., 2008c, Wang *et al*., 2009c, Heuer *et al*., 2009). The biological activity of rapamycin is due to inhibition of mTORC1. Results from pilot studies using rapamycin or its derivatives as a single agent for the treatment of HCC patients show promising results (Vivarelli et al., 2010a, Rizell et al., 2008, Zhu et al., 2011, Schoniger-Hekele and Muller, 2010, Hui et al., 2010). Clinical trials using rapamycin and rapalogs against a wide range of malignancies are currently underway (O'Donnell *et al*., 2008, Okamoto *et al*., 2010, Hudes *et al*., 2009, Slomovitz *et al*., 2010, Yao *et al*., 2008, Hess, 2009, Motzer *et al*., 2010, Lu *et al*., 2008).

4.1.2 Rapamycin and HIF-1α.

Some of the anticancer activity of appears to be due to inhibition of survival pathways induced by hypoxia. Rapamycin has been demonstrated to inhibit HIF-1α in a number of cancer cell types (Arsham et al., 2003, Wang et al., 2008b, Hudson et al., 2002, Jiang and Feng, 2004). mTOR activation enhances the rate of translation of HIF-1α (Land and Tee 2007), and mTOR is aberrantly activated in 40 – 50% of HCCs (Sieghart *et al*., 2007). Inhibition of mTOR using rapamycin inhibits tumour

growth and progression in HCC *in vivo* and *in vitro* (Heuer *et al*., 2009, Huynh *et al*., 2008a, Jimenez *et al*., 2009, Ong *et al*., 2009, Shirouzu *et al*., 2010, Varma and Khandelwal, 2007, Wang *et al*., 2008b, Wang *et al*., 2009b, Wang *et al*., 2006, Wang *et al*., 2008c, Zhang *et al*., 2007). There is therefore a need to investigate the cytotoxicity of rapamycin to tumour cells cultured under hypoxic conditions *in vitro.*

4.1.3 Rapamycin and S6K.

Rapamycin inhibits the formation of mTORC1 and blocks downstream signalling, thus reducing cell growth and proliferation. S6K is directly regulated by mTORC1 *via* phosphorylation of thr^{389}. Rapamycin therefore reduces the phosphorylation of S6K at this residue.

4.2 Aims.

• To study the effects of rapamycin in a time and concentration dependent manner on the viability of HepG2 cells under normoxic and hypoxic conditions, and identify the minimum effective concentration.

• To evaluate the response of HIF-1α and S6K expression in HepG2 cells under normoxic and hypoxic conditions.

4.3 Objectives.

Here the chemosensitivity of HepG2 cells cultured under normoxic and hypoxic conditions to the application of clinically relevant concentrations of rapamycin was investigated. Cell viability was estimated using the CellTiter 96® Aqueous One Solution Proliferation Assay. Hypoxic culture conditions (oxygen = 1%) were established using the Coy Hypoxic Glove box, as described in the Methods section. SDS-PAGE and Western Blotting were used to quantify the nuclear accumulation of HIF-1α and the phosphorylation status of p70 S6K.

4.4 Results.

4.4.1 Cell Viability at 24 Hours.

At the 24 hour time point, 100 nM rapamycin was found to be the lowest effective concentration for decreasing cell viability in normoxic cells ($p = 0.011$). Hypoxic cells were resistant up to 500 nM rapamycin (Figure 4.1).

4.4.2 Cell Viability at 48 Hours.

At the 48 hour time point, 10 nM rapamycin was found to be the lowest effective concentration for decreasing cell viability in normoxic cells ($p = 0.047$), and 100 nM rapamycin was found to be the lowest effective concentration for decreasing cell viability in hypoxic cells ($p = 0.023$) (Figure 4.2).

4.4.3 Cell Viability at 72 Hours.

At the 72 hour time point no decrease in cell viability was observed at any rapamycin concentration in either of the culture conditions (Figure 4.3). Cell proliferation was significantly less at 72 hours in hypoxic cells compared to normoxic cells ($p = 0.001$) (Figure 4.4).

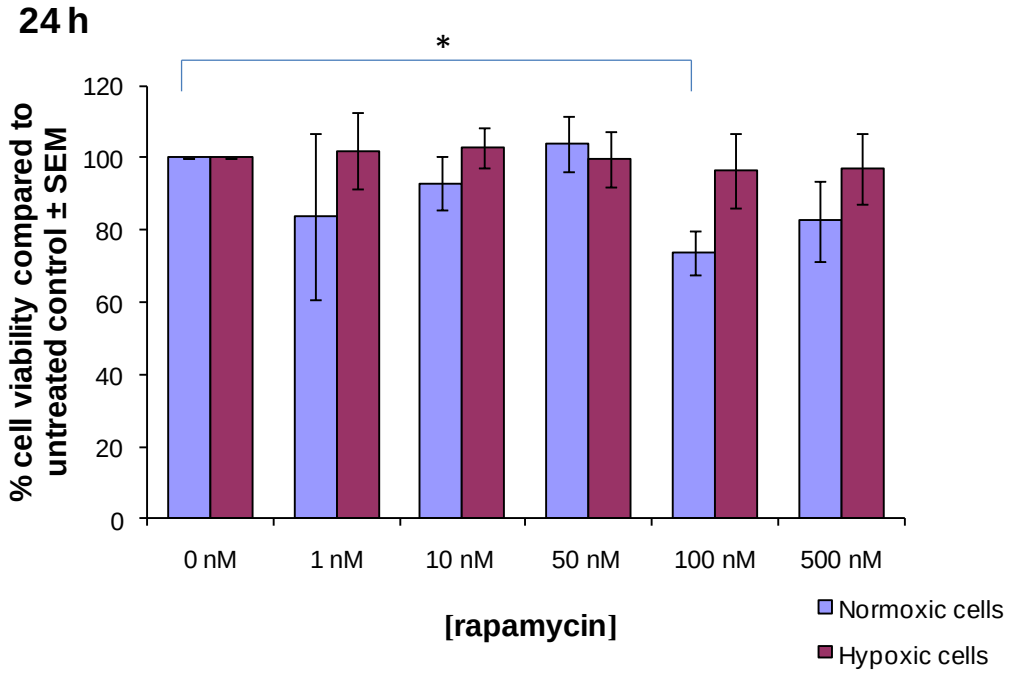

Figure 4.1 The Effects of 24 Hours Exposure to Rapamycin on the Viability of HepG2 Cells Cultured under Normoxic and Hypoxic Conditions.
$1x10^4$ cells/200 µl were added to each well of a 96-well plate and incubated overnight at 37°C under normoxic conditions. The following day, the plates were removed to either normoxic or hypoxic conditions and exposed to rapamycin, 6 replicate wells for each concentration. The plates were incubated under normoxic or hypoxic conditions for 24 hours. Cell viability was estimated using MTS assay and normalised to untreated control. Data points for normoxic conditions represents the mean of 6 separate experiments ± standard error of the mean for all rapamycin concentrations, except for 100 nM and 500 nM concentrations which represents the mean of 4 separate experiments ± standard error of the mean. Data points for hypoxic conditions represents the mean of 7 separate experiments ± standard error of the mean for all rapamycin concentrations, except for 100 nM and 500 nM concentrations which represents the mean of 5 separate experiments ± standard error of the mean. * denotes lowest effective rapamycin concentration that resulted in a significant decrease in cell viability compared to untreated control under same culture conditions using a one sample T test carried out using a one tailed comparison, 100 vs. < 100, p = < 0.05.

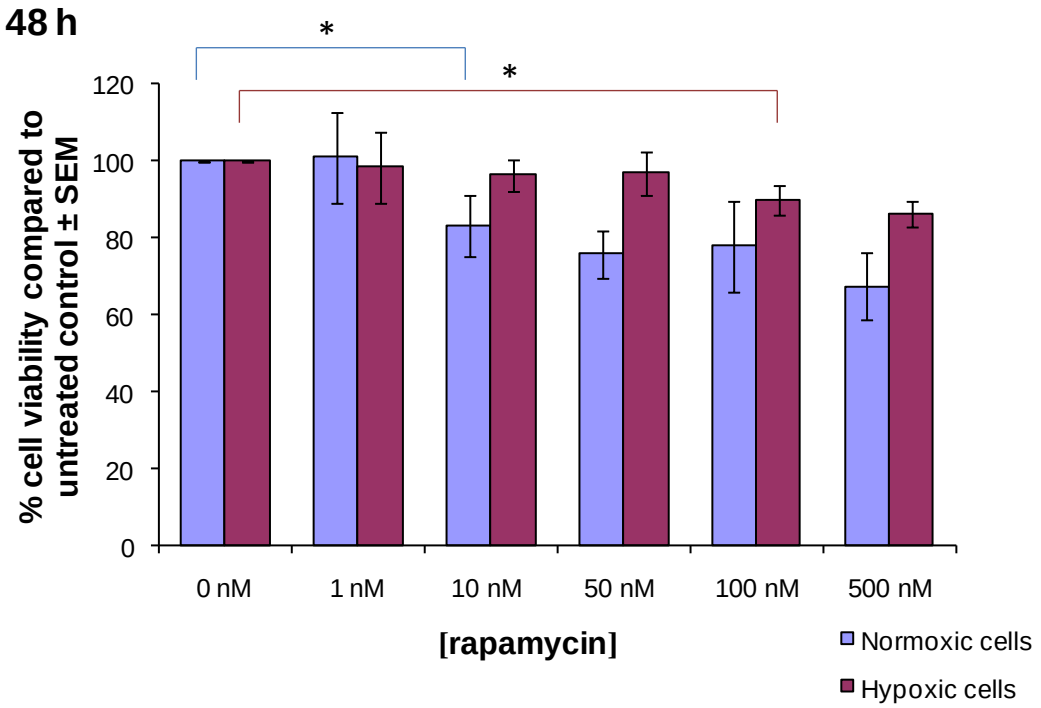

Figure 4.2 The Effects of 48 Hours Exposure to Rapamycin on the Viability of HepG2 Cells Cultured under Normoxic and Hypoxic Conditions.
$1x10^4$ cells/200 µl were added to each well of a 96-well plate and incubated overnight at 37°C under normoxic conditions. The following day, the plates were removed to either normoxic or hypoxic conditions and exposed to rapamycin, 6 replicate wells for each concentration. The plates were incubated under normoxic or hypoxic conditions for 48 hours. Cell viability was estimated using MTS assay and normalised to untreated control. Data points for normoxic conditions represents the mean of 6 separate experiments ± standard error of the mean for all rapamycin concentrations, except for 100 nM and 500 nM concentrations which represents the mean of 4 separate experiments ± standard error of the mean. Data points for hypoxic conditions represents the mean of 7 separate experiments ± standard error of the mean for all rapamycin concentrations, except for 100 nM and 500 nM concentrations which represents the mean of 5 separate experiments ± standard error of the mean. * denotes lowest effective rapamycin concentration that resulted in a significant decrease in cell viability compared to untreated control under same culture conditions using a one sample T test carried out using a one tailed comparison, 100 vs. < 100, p = < 0.05.

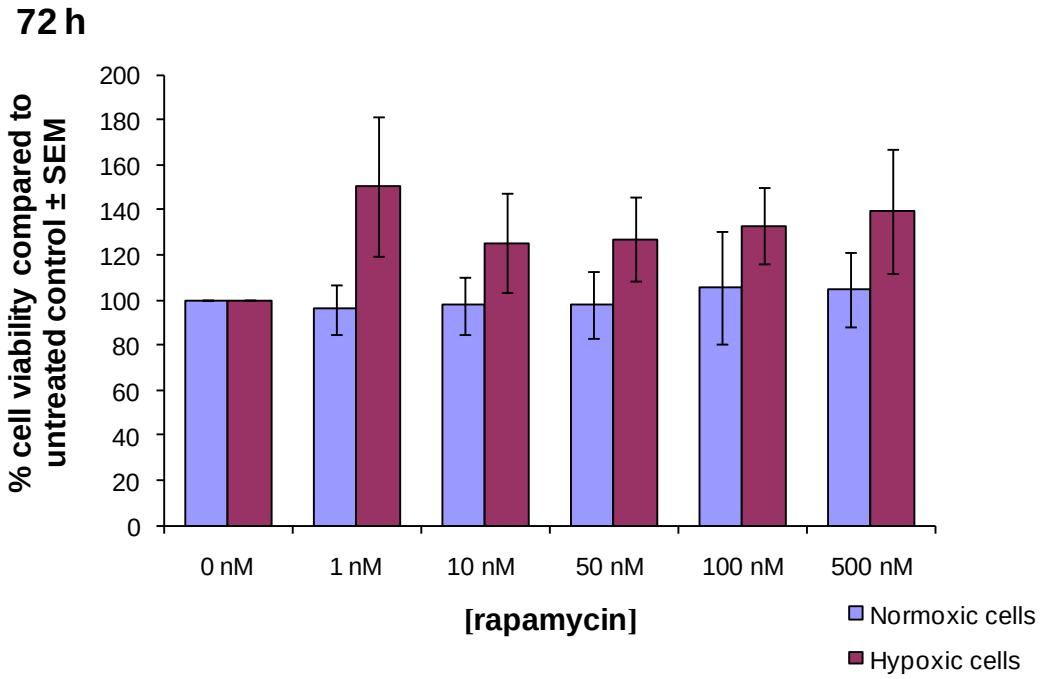

Figure 4.3 The Effects of 72 Hours Exposure to Rapamycin on the Viability of HepG2 Cells Cultured under Normoxic and Hypoxic Conditions.
1x104 cells/200 µl were added to each well of a 96-well plate and incubated overnight at 37°C under normoxic conditions. The following day, the plates were removed to either normoxic or hypoxic conditions and exposed to rapamycin, 6 replicate wells for each concentration. The plates were incubated under normoxic or hypoxic conditions for 72 hours. Cell viability was estimated using MTS assay and normalised to untreated control. Data points for normoxic conditions represents the mean of 6 separate experiments ± standard error of the mean for all rapamycin concentrations, except for 100 nM and 500 nM concentrations which represents the mean of 4 separate experiments ± standard error of the mean. Data points for hypoxic conditions represents the mean of 7 separate experiments ± standard error of the mean for all rapamycin concentrations, except for 100 nM and 500 nM concentrations which represents the mean of 5 separate experiments ± standard error of the mean.

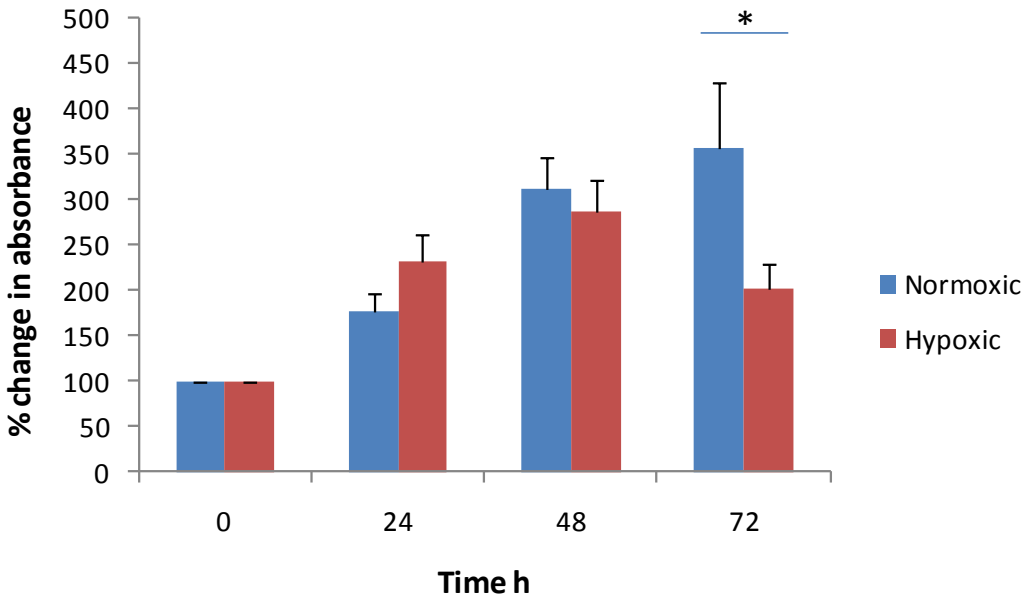

Figure 4.4 Cell Proliferation in Normoxic Compared to Hypoxic Cells.
1 x 10^4 cells/200 µl were added to each well of a 96-well plate and incubated overnight at 37°C under normoxic conditions. The following day, the plates were removed to either normoxic or hypoxic conditions and the media was replenished. The plates were incubated under normoxic or hypoxic conditions for 24, 48 and 72 hours. Cell viability was measured using MTS assay and normalised to cell viability at 0 hours. Data points represents the mean of 6 separate experiments ± standard error of the mean for normoxic cells and 7 separate experiments ± standard error of the mean for hypoxic cells. *denotes a significant difference, using a two sample one tailed T test, p = 0.001.

4.4.4 Rapamycin Attenuates Hypoxia Stimulated HIF-1α Nuclear Accumulation.

To determine the effect of rapamycin treatment on hypoxia stimulated nuclear accumulation of HIF-1α, SDS-PAGE and Western Blotting was carried out on nuclear extracts from HepG2 cells cultured under normoxic and hypoxic conditions, and exposed to drug concentrations as shown, see Figure 4.5. After 24 hours, both 10 nM rapamycin and 100 nM rapamycin treatments significantly reduced the amount of HIF-1α detected in the cell nucleus ($p = 0.021$ and $p = 0.005$ respectively), (Lanes 4, 5 and 6). The 10 nM and 100 nM rapamycin treatments had no effect on levels of HIF-1α detected in the nucleus of normoxic cells (Lanes 1, 2 and 3).

4.4.5 Effects of Rapamycin on Phosphorylation of S6K.

To determine the effect of rapamycin treatment on S6K and the phosphorylation of S6K, SDS-PAGE and Western Blotting was carried out on cytoplasmic extracts from HepG2 cells cultured under normoxic and hypoxic conditions, and exposed to drug concentrations as shown, see Figure 4.6. Again, hypoxia had no effect on phosphorylation of p70 S6K (Lanes 1 and 4). Rapamycin was observed to decrease the ratio of phosphorylated S6K to total S6K in both hypoxia and normoxia, although the results were not significant (Lanes 1 – 3 and 4 – 6). Levels of total S6K compared to B actin remained the same across all treatments in culture conditions.

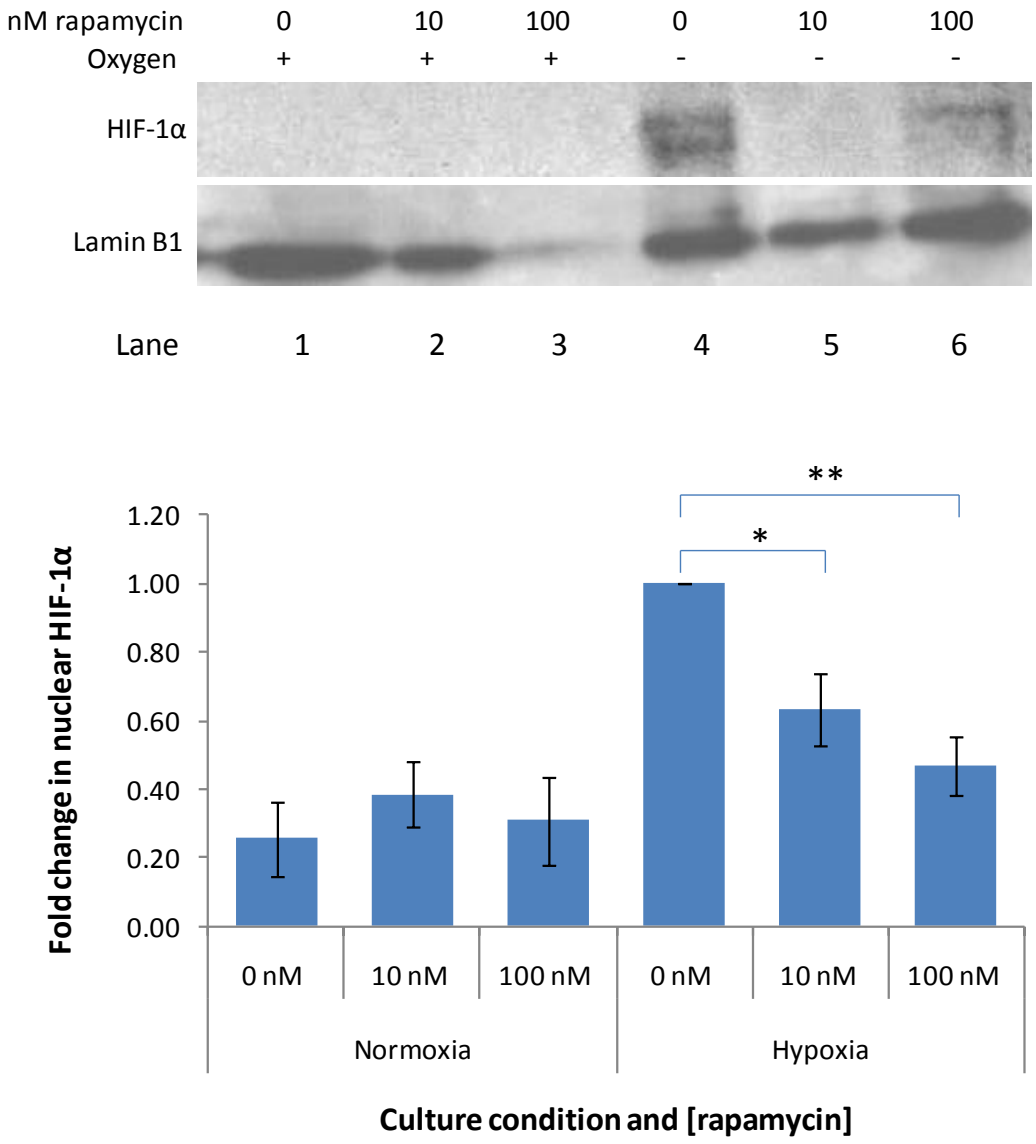

Figure 4.5 Nuclear Accumulation of HIF-1α after Rapamycin Treatment.
HepG2 cells were seeded onto T75 tissue culture flasks and incubated under normoxic conditions until 60% confluent. The cells were exposed to rapamycin in normoxic or hypoxic conditions and incubated for 24 hours. The cells were harvested and nuclear extracts were prepared. Equal quantities of protein were fractionated on a 10% SDS-PAGE gel. The proteins were transferred to a PVDF membrane and probed with anti-HIF-1α antibodies. Proteins were visualised using chemiluminescent reagents. The membrane was stripped and reprobed using antibodies against the nuclear house-keeping protein Lamin B1. Protein levels were quantified using densitometry analysis. The amount of HIF-1α was normalised to Lamin. Fold change compared to untreated hypoxic cells was calculated. Data shown represents mean of 4 independent experiments ± standard error of the mean for hypoxic cells, and mean of 3 independent experiments ± standard error of the mean. for normoxic cells. Statistical analysis was carried out using a one sample one tailed T test, 1 vs. < 1. * denotes a statistically significant result, p = < 0.05; ** denotes a statistically significant result, p = < 0.01.

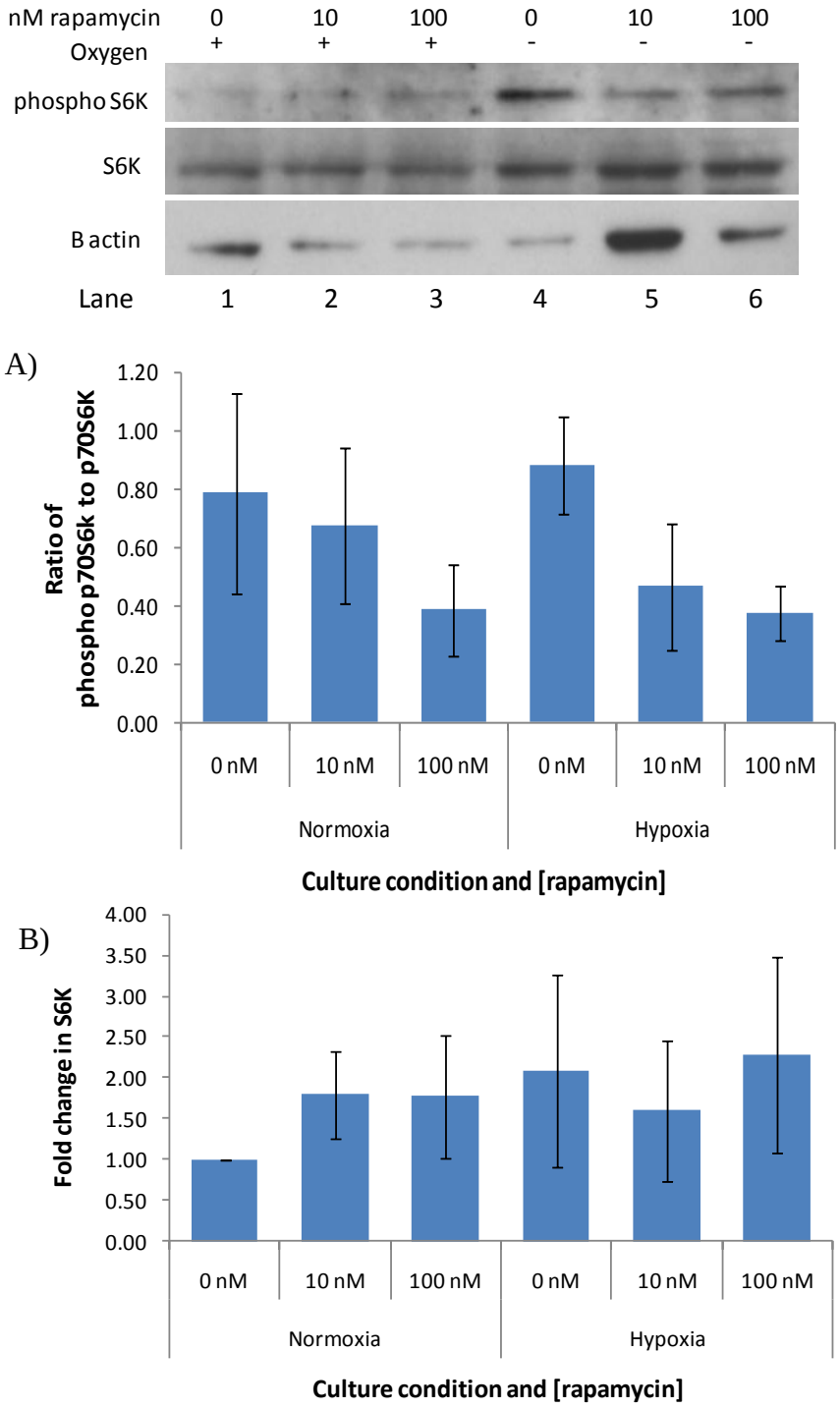

Figure 4.6 Cytoplasmic p70 S6K and p70 S6K (phospho T389) after Rapamycin Treatment of Normoxic and Hypoxic Cells.
Cells were treated as described in Figure 6.2. Cytoplasmic extracts were prepared and fractionated on a 10% SDS-PAGE gel. The proteins were transferred to a PVDF membrane and probed with anti- p70 S6K (phospho T389) antibodies. Proteins were visualised and the membrane was stripped and reprobed using antibodies against total S6K, and antibodies against B actin. Protein levels were quantified using densitometry analysis. Ratio of p70 S6K (phospho T389) to total S6K was calculated, as was the amount of p70 S6K normalised to B actin. Data shown represents mean of 3 separate experiments ± standard error of the mean.

4.4.6 Statistical Analysis.

Comparison	Test statistic for normality	N.D.	Test used	Test statistic	p value	Significant?
Untreated vs. 100 nM	0.647	Yes	One sample T	0.011	0.050	Yes

Table 4.1 Comparisons for Factor [drug] after 24 Hours of Treatment under Normoxic Culture Conditions.
To determine the lowest effective concentration of rapamycin, a one sample T test was carried out, using a one tailed comparison, 100 *vs*. < 100.

Comparison	Test statistic for normality	N.D.	Test used	Test statistic	p value	Significant?
Untreated vs. 10 nM	0.596	Yes	One sample T	0.047	0.050	Yes

Table 4.2 Comparisons for Factor [drug] after 48 Hours of Treatment under Normoxic Culture Conditions.
To determine the lowest effective concentration of rapamycin, a one sample T test was carried out, using a one tailed comparison, 100 *vs*. < 100.

Comparison	Test statistic for normality	N.D.	Test used	Test statistic	p value	Significant?
Untreated vs. 100 nM	0.373	Yes	One sample T	0.023	0.050	Yes

Table 4.3 Comparisons for Factor [drug] after 48 Hours of Treatment under Hypoxic Culture Conditions.
To determine the lowest effective concentration of rapamycin, a one sample T test was carried out, using a one tailed comparison, 100 *vs*. < 100.

4.5 Discussion.

4.5.1 Cell Viability after Rapamycin Treatment.

After 24 hours of treatment in normoxia, 100 nM rapamycin significantly inhibited the cell viability of HepG2 cells, and was observed to be more effective than 500 nM. Rapamycin had no significant effect on hypoxic cells.

After 48 hours, a rapamycin dose of 10 nM significantly inhibited the viability of HepG2 cells cultured under normoxic conditions (Figure 4.3). 10 nM rapamycin represents a clinically relevant dose, where clinical serum levels are between 5 – 10 nM after a 5 mg daily oral dose (McAlister *et al*., 2000, Kneteman *et al*., 2004). However, a 100 nM dose was required for significant inhibition of viability in hypoxic cells.

The findings for the normoxic cells are in line with other studies, as discussed below. A 2009 *in vitro* study demonstrated that low-dose rapamycin inhibited the growth of HepG2 cells at doses of 1, 5 and 10 nM. Cell growth was reduced by 15% to 35% at 48 and 72 hour time points. By 96 hours the growth inhibition was declining. There was a cut off dose of 20 nM, above which a decrease in growth inhibition was seen (Heuer *et al*., 2009). Heuer *et al*, 2009, hypothesised that there exists a rapamycin dose that reverses the mechanisms of action in treated cells, and above which increased dose results in a decreased inhibition of tumour cell growth.

A study by Schumacker *et al* 2002 found that a 5 nM application of rapamycin for 5 days caused G1 arrest in Hep3B and SKHep1 cells but not apoptosis (Schumacher *et al*., 2002). Similarly, when MHCC97H cells (highly metastatic) were treated with 10 nM rapamycin, growth arrest at occurred at G0/G1 stage, but no apoptosis was seen (Wang *et al*., 2006). A 2007 *in vitro* study found that rapamycin between 30 nM and 50 nM had a significant inhibitory effect on the growth of HepG2 cells via the

induction of apoptosis. The response was dose and time dependant up to 4 days (Zhang *et al*., 2007). The effect of rapamycin in the Zhang *et al* 2007 study was much more marked than our own and other findings, and interestingly, this was the only study which detected apoptosis.

After 72 hours, the inhibitory effect of the drug towards normoxic cells is no longer seen (Figure 4.4). Continuous low dose rapamycin has been shown to be more effective than higher dose bolus application *in vivo* (Guba *et al*., 2005). In one *in vitro* study, rapamycin was renewed every 48 hours, rather than a single application at the start of the experiment, and rapamycin induced a dose dependent inhibition of tumour cell proliferation in the HCC cell lines PLC5 and HuH for seven days (Shirouzu *et al*., 2010).

In the cells cultured under hypoxia, rapamycin appeared to have a stimulatory effect, although this was not statistically significant. Inhibition of mTORC1 can result in mTORC2 mediated phosphorylation and activation of Akt (Huang and Manning, 2009), although prolonged exposure to rapamycin is thought to attenuate this effect by inhibiting the assembly of mTORC2 (Sarbassov *et al*., 2006). This may be one reason why metronomic administration of rapamycin is more effective than higher intermittent doses, although the low concentrations used and the short half life (60 hours) of rapamycin may have an influence. Furthermore, the HepG2 cell line has little or no detectable PTEN protein (Zhang *et al*., 2004, Ma *et al*., 2005). PTEN functions by negatively counteracting PI3K signalling, and low PTEN expression is associated with liver malignancies (Peyrou *et al*., 2010). Hypoxia-induced mTOR inhibition is attenuated in cells lacking TSC2 or PTEN and cells retain mTOR activity and increased translation and protein synthesis under hypoxic conditions

(Kaper *et al*., 2006). Loss of PTEN facilitates the expression of HIF-1 gene expression via activation of Akt (Zundel *et al*., 2000).

Rapamycin is known to be a substrate for Pgp (Arceci *et al*., 1992), and hypoxia-induced overexpression of Pgp could potentially result in rapamycin resistance (Thews *et al*., 2008).

The intrinsic anti-tumour activity of rapamycin towards normoxic HepG2 cells due to the inhibition of mTORC1 is not apparent in the cells cultured under hypoxic conditions. Is this because the drug isn't getting into the cells, or because the pathway is different due to the cell responses to hypoxia? There is clearly a need to investigate the phosphorylation of proteins downstream of mTOR, and this will be addressed in Chapter 6.

4.5.2 The Nuclear Accumulation of HIF-1α in Response to Rapamycin.

Rapamycin significantly reduced the amount of HIF-1α detected in the nucleus of hypoxic HepG2 cells. 10 nM rapamycin and 100 nM rapamycin treatments both significantly inhibited the accumulation of HIF-1α in the nucleus of hypoxic cells, although the 10 nM treatment was not significantly more effective than the 100 nM treatment. This is in accordance with other studies. Wang *et al* (2009) found that 10 nM rapamycin decreased the expression of cobalt chloride-induced HIF-1α in a metastatic HCC cell line. Rapamycin was found to inhibit expression of HIF-1α in human embryonic kidney cells (Arsham *et al*., 2003), and in *in vivo* models of ovarian cancer and pancreatic cancer, which also showed a concomitant increase in tumour apoptosis and decreased tumour growth (Hudson *et al*., 2002, Jiang and Feng, 2004).

4.5.3 Hypoxia, Rapamycin and phosphorylation of p70 S6K.

In this study the effect of hypoxia on mTOR activity was investigated by analysing the phosphorylation status of the mTORC1 target S6K. Cell stressors, such as low oxygen, nutrient or iron availability, typically result in the downregulation of mTORC1 activity and inhibition of protein synthesis in order to conserve energy (Ellisen, 2005). Regulation of mTORC1 activity by hypoxia requires REDD1 and TSC2 (Brugarolas *et al*., 2004). However, the ability of cancer cells to survive in unfavourable environments is often due to mutation(s) to the PI3K/Akt/mTOR pathway, so that cells retain mTOR activity even under hypoxic conditions (Kaper *et al*., 2006). This investigation found that hypoxia had no effect on the ratio of S6K (phospho Thr389) to total S6K when compared to normoxia. This investigation also found that Akt was hyperphosphorylated in both normoxic and hypoxic cells. Activation of Akt was not affected by treatment with doxorubicin. Akt activation in HepG2 cells can be due to loss of PTEN which results in constitutive activation of the PI3K/Akt/mTOR pathway, and is associated with mTOR dependent HIF-1α translation (Zundel *et al*., 2000). In HepG2 cells PTEN is barely detectable (Ma *et al*., 2005, Zhang *et al*., 2004). In conclusion, hypoxia does not inhibit the mTOR pathway downstream of mTOR itself.

Next, the effect of rapamycin on mTORC1 activity was investigated by analysing the phosphorylation status of S6K. 10 nM and 100 nM rapamycin treatments inhibited phosphorylation of S6K in a dose dependent manner in both normoxic and hypoxic cells, although no significance was observed. Levels of total S6K remained the same under all conditions and treatments. Rapamycin appears to be inhibiting mTORC1 activity under both normoxic and hypoxic conditions. However, comparing the pattern of mTOR inhibition with the cell proliferation data (Chapter 4), we can see

that the inhibition of phosphorylation of S6K does not necessarily go hand-in-hand with a decrease in cell proliferation. A 2009 study interrogated a panel of tumorigenic hepatic cell lines, some of which were rapamycin resistant. They found that rapamycin was effective at blocking mTORC1 signalling via S6K in all the cell lines, and concluded that 'mechanisms of rapamycin resistance are not dependent on alterations in the direct actions of mTOR on its targets, but may be related to deregulation of the cell cycle' (Jimenez *et al*., 2009). Hypoxia is known to affect cell cycling, and the effects of hypoxia on cell cycling in HepG2 cells are complex (Koshiji and Huang, 2004).

Rapamycin was initially thought to inhibit mTORC1 exclusively (Jacinto *et al*., 2004), although recent research suggests that this is dependent on the duration and dosage (Sarbassov *et al*., 2006, Foster and Toschi, 2009). mTORC2 positively feeds back to Akt *via* phosphorylation of Akt at Ser^{473} (Sarbassov *et al*., 2005). In this study we observed that Akt was phosphorylated at this residue, but phosphorylation was not increased by the application of rapamycin (data not shown).

4.6 Conclusions.

This study has shown that treatment with rapamycin can inhibit the cell proliferation of both normoxic and hypoxic HepG2 cells, although hypoxic cells are less susceptible to mTOR inhibition. The lowest effective concentration against normoxic cells was 100 nM, and the lowest effective concentration against hypoxic cells was 100 nM. Using a single dose of rapamycin at time 0 leads to attenuation of the effect beyond 48 hours. Repeated administration every 24 hours warrants investigation. Rapamycin inhibited phosphorylation of S6K in a dose dependent manner in both normoxic and hypoxic cells, although not significantly. Rapamycin attenuated the stabilisation of HIF-1α under hypoxic conditions.

The effectiveness of chemotherapy can be improved by the administration of antitumour drugs in combination rather than as single agents (Forster, 2009). The use of molecular inhibitors in combination with traditional chemotherapeutics may facilitate the modulation of biochemical pathways in order to overcome chemoresistance in HCC (Boulin *et al*., 2011, Ferrer Puchol *et al*., 2011). In the following chapter, the activity of rapamycin and doxorubicin combinations against HepG2 cells cultured under normoxic and hypoxic conditions will be investigated.

Chapter 5

The Effects of Doxorubicin in Combination with Low Dose Rapamycin on the Viability of HepG2 Cells Cultured In Vitro under Normoxic and Hypoxic Conditions.

5.1 Introduction.

The combination of standard chemotherapeutic agents with one (or more) of the recently identified molecular targeted therapies in the treatment of HCC presents opportunities to improve patient outcome.

There have been quite a number of *in vitro* investigations into the effects of combinations of rapamycin (and rapamycin analogues) with other agents towards cancer cells. Doxorubicin and rapamycin combinations have been investigated *in vitro* and found to have synergistic or additive effects against leukaemias (Batista *et al*., 2011, Avellino *et al*., 2005); breast cancers (Mondesire *et al*., 2004, Steelman *et al*., 2008, Sokolosky *et al*., 2011a); T cell lymphoma (Huang *et al*., 2010); thyroid cancer (Lin *et al*., 2010); colon cancer (Sun *et al*., 2008, O'Reilly *et al*., 2011); mantle cell lymphoma (Haritunians *et al*., 2007); melanoma (Romano *et al*., 2004); cervical cancer (O'Reilly *et al*., 2011), lung cancer (O'Reilly *et al*., 2011), prostate cancer (Grunwald *et al*., 2002) and HCC (Piguet *et al*., 2008).

5.1.1 Rapamycin and Doxorubicin Combinations.

It has been shown *in vitro* that known clinical concentrations of doxorubicin in liver tumours post DEB-TACE may be effective against hypoxic as well as normoxic cells (Chapter 3), and that low dose rapamycin inhibited cell viability in normoxic cells, although doses tenfold higher were required to inhibit cell viability in hypoxic cells (Chapter 4). Combination therapies, where targeted therapies are administered in combination with standard chemotherapeutics, offer more of an opportunity to

interfere with activated signalling cascades which contribute to drug resistance, including pathways activated by hypoxia.

5.1.2 Rapamycin and Doxorubicin Combinations and HIF-1α.

Targeting HIF-1 in combination with doxorubicin has been to enhance the cytotoxicity of doxorubicin in a range of cancer types (Liang *et al*., 2010c, Liu *et al*., 2008a, Wang *et al*., 2010, Nardinocchi *et al*., 2009b, Du *et al*., 2010, Chen *et al*., 2009b). Doxorubicin and rapamycin combinations have been shown to be effective in an HCC model (Piguet *et al*., 2008), although the effects of the drug combination on HIF-1α were not investigated.

Using a combination of localised and sustained delivery of doxorubicin with metronomic low dose orally administered rapamycin *in vivo* may result in decreased activation of hypoxia-induced survival pathways and improved treatment responses. There is also scope for loading rapamycin onto DEBs (Forster, 2009). Locoregional delivery of rapamycin may show some of the same pharmacokinetic advantages as the locoregional delivery of doxorubicin. There is clearly a need to investigate the activity of doxorubicin/rapamycin combinations at clinically relevant concentrations towards HCC cell lines cultured *in vitro* under normoxic and hypoxic conditions.

5.2 Aims.

- To assess the cell viability of HepG2 cells cultured under normoxic and hypoxic conditions to rapamycin and doxorubicin in combination.
- To investigate the nuclear accumulation of HIF-1α in response to this combination.
- To investigate the nuclear accumulation of NFkB in response to this combination.

5.3 Objectives.

Here the chemosensitivity of HepG2 cells cultured under normoxic and hypoxic conditions to the application of clinically relevant concentrations of doxorubicin and rapamycin in combination was investigated. Cell viability was estimated using the CellTiter 96® Aqueous One Solution Proliferation Assay. Hypoxic culture conditions (oxygen = 1%) were established using the Coy Hypoxic Glove box, as described in the Methods section. SDS-PAGE and Western Blotting were used to quantify the nuclear accumulation of HIF-1α and NFkB.

5.3 Results.

5.3.1 Rapamycin and Doxorubicin Combination Treatments and Cell Viability.

To investigate the effects of combinations of doxorubicin and rapamycin against HCC, HepG2 cells were incubated with a range of doxorubicin concentrations with or without the addition of 10 nM rapamycin. Cell viability was measured after 24, 48 and 72 hours using the MTS assay.

After 24 hours (Figures 5.1 and 5.4), cell viability was observed to be less with the addition of rapamycin compared to doxorubicin alone, and this was consistent for all concentrations investigated. The decrease in cell viability was significantly more for the combinations where doxorubicin concentrations were 1 μM ($p = 0.006$) and 25 μM ($p = 0.008$) for normoxic cells, and 1 μM for hypoxic cells ($p = 0.043$). After 48 hours (Figures 5.2 and 5.5), cell viability was observed to be less with the addition of rapamycin compared to doxorubicin alone, and this was consistent for all concentrations investigated except 0.1 μM doxorubicin in hypoxic cells. The decrease in cell viability was significantly more for the combinations where doxorubicin concentrations were 1 μM ($p = 0.036$) for normoxic cells, but there was no significant effect for any of the hypoxic cells. After 72 hours, (Figures 5.3 and

5.6), cell viability was observed to be less with the addition of rapamycin compared to doxorubicin alone, and this was consistent for all concentrations investigated except 25 µM doxorubicin in normoxic cells. The decrease in cell viability was significantly more for the combinations where doxorubicin concentrations were 10 µM ($p = 0.004$) for hypoxic cells, but there was no significant effect for any of the normoxic cells. The additive effects of rapamycin were more pronounced at the 24 hour time point than at either of the other time points, and more pronounced in the normoxic cells than in the hypoxic cells.

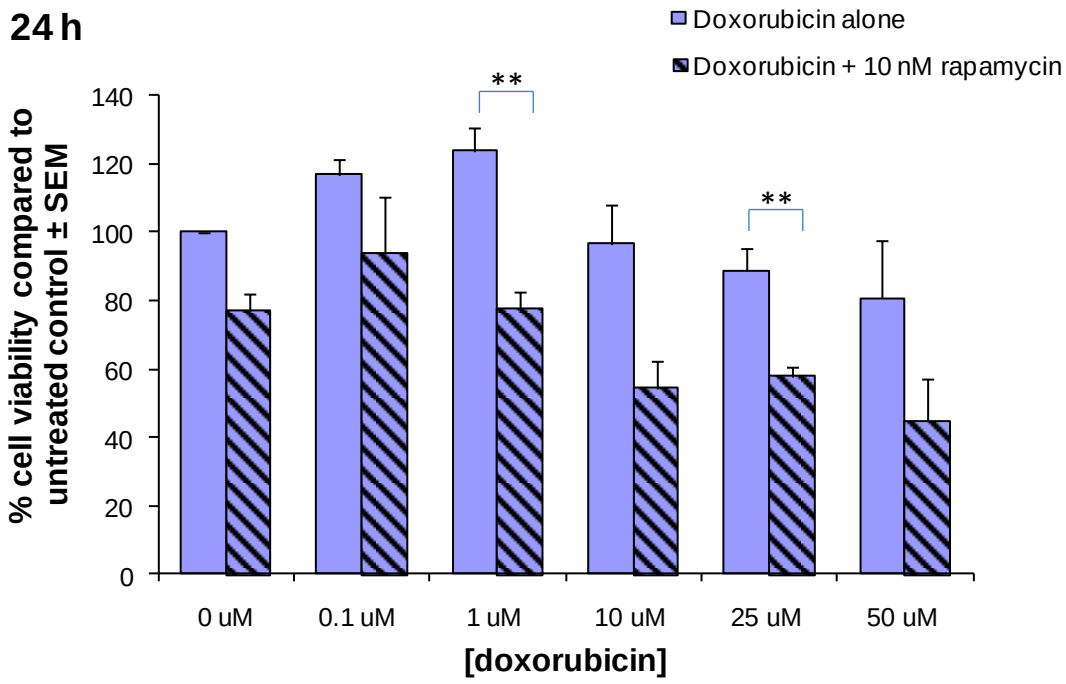

Figure 5.1 The Effects of 24 Hours Exposure to Varying Concentrations of Doxorubicin + 10 nM Rapamycin on the Viability of HepG2 Cells Cultured under Normoxic Conditions.

$1x10^4$ cells/200 µl were added to each well of a 96-well plate and incubated overnight at 37°C under normoxic conditions. The media was removed and replaced with a range of doxorubicin concentrations + 10 nM rapamycin. 6 replicate wells for each concentration. The plates were incubated under normoxic conditions for 24 hours. Cell viability was measured using MTS assay and normalised to untreated control. Data points represent mean of 3 separate experiments ± standard error of the mean. Statistical analysis was carried out using a one tailed paired t test. ** denotes a significant difference, $p = < 0.01$.

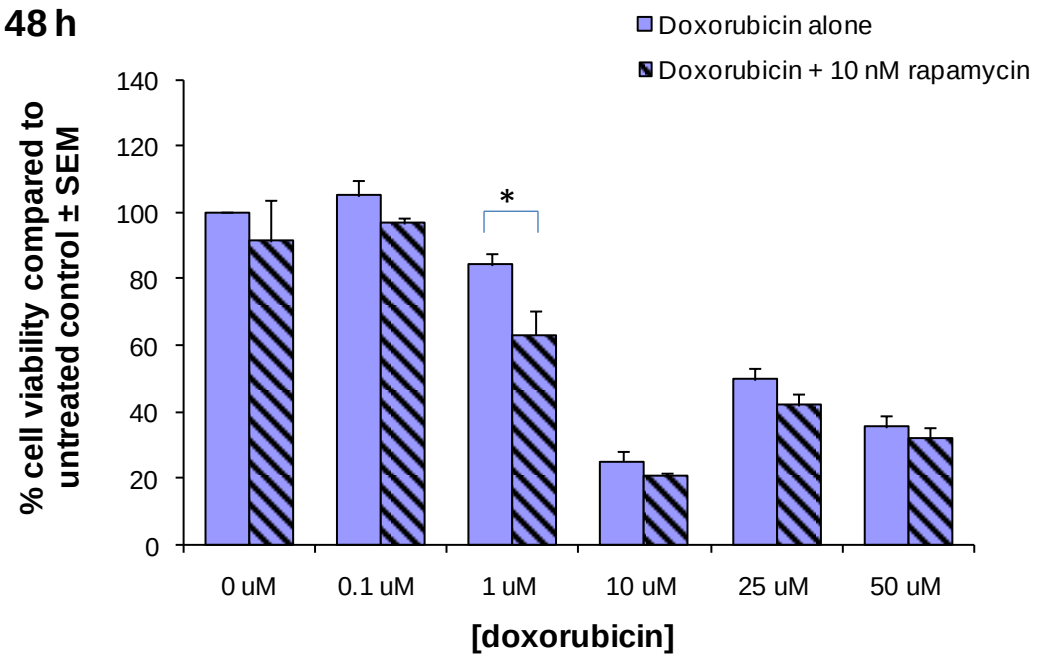

Figure 5.2 The Effects of 48 Hours Exposure to Varying Concentrations of Doxorubicin + 10 nM Rapamycin on the Viability of HepG2 Cells Cultured under Normoxic Conditions.

$1x10^4$ cells/200 µl were added to each well of a 96-well plate and incubated overnight at 37°C under normoxic conditions. The media was removed and replaced with a range of doxorubicin concentrations + 10 nM rapamycin. 6 replicate wells for each concentration. The plates were incubated under normoxic conditions for 48 hours. Cell viability was measured using MTS assay and normalised to untreated control. Data points represent mean of 3 separate experiments ± standard error of the mean. Statistical analysis was carried out using a one tailed paired t test. * denotes a significant difference, $p = < 0.05$.

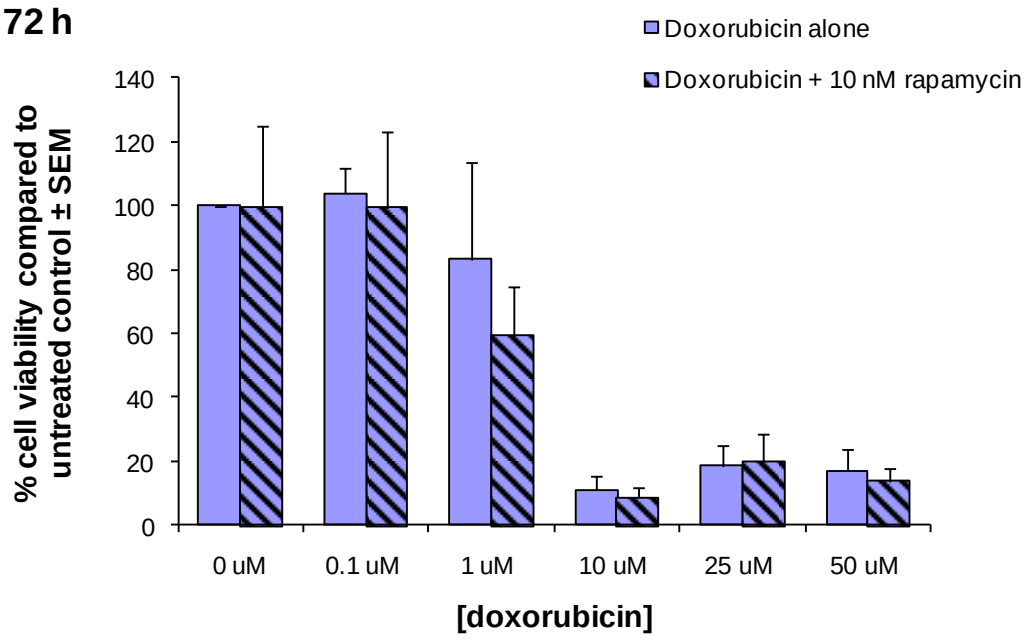

Figure 5.3 The Effects of 72 Hours Exposure to Varying Concentrations of Doxorubicin + 10 nM Rapamycin on the Viability of HepG2 Cells Cultured under Normoxic Conditions.

$1x10^4$ cells/200 µl were added to each well of a 96-well plate and incubated overnight at 37°C under normoxic conditions. The media was removed and replaced with a range of doxorubicin concentrations + 10 nM rapamycin. 6 replicate wells for each concentration. The plates were incubated under normoxic conditions for 72 hours. Cell viability was measured using MTS assay and normalised to untreated control. Data points represent mean of 3 separate experiments ± standard error of the mean.

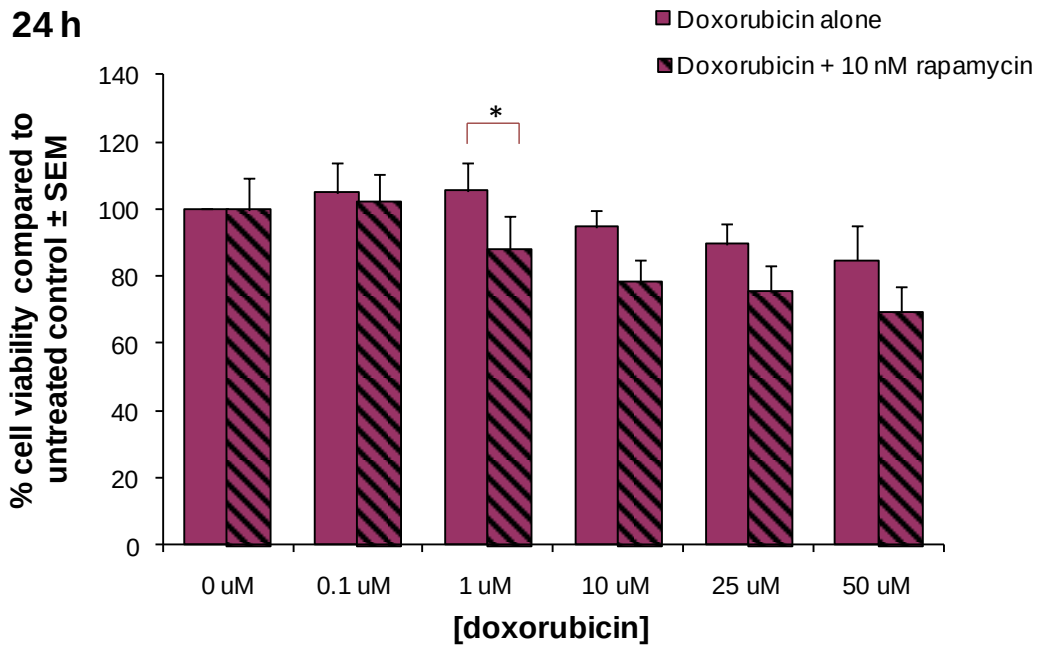

Figure 5.4 The Effects of 24 Hours Exposure to Varying Concentrations of Doxorubicin + 10 nM Rapamycin on the Viability of HepG2 Cells Cultured under Hypoxic Conditions.

$1x10^4$ cells/200 µl were added to each well of a 96-well plate and incubated overnight at 37°C under normoxic conditions. The plates were removed to hypoxic conditions and the media was removed and replaced with a range of doxorubicin concentrations + 10 nM rapamycin. 6 replicate wells for each concentration. The plates were incubated under hypoxic conditions for 24 hours. Cell viability was measured using MTS assay and normalised to untreated control. Data points represent mean of 3 separate experiments ± standard error of the mean. Statistical analysis was carried out using a one tailed paired t test. * denotes a significant difference, $p = < 0.05$.

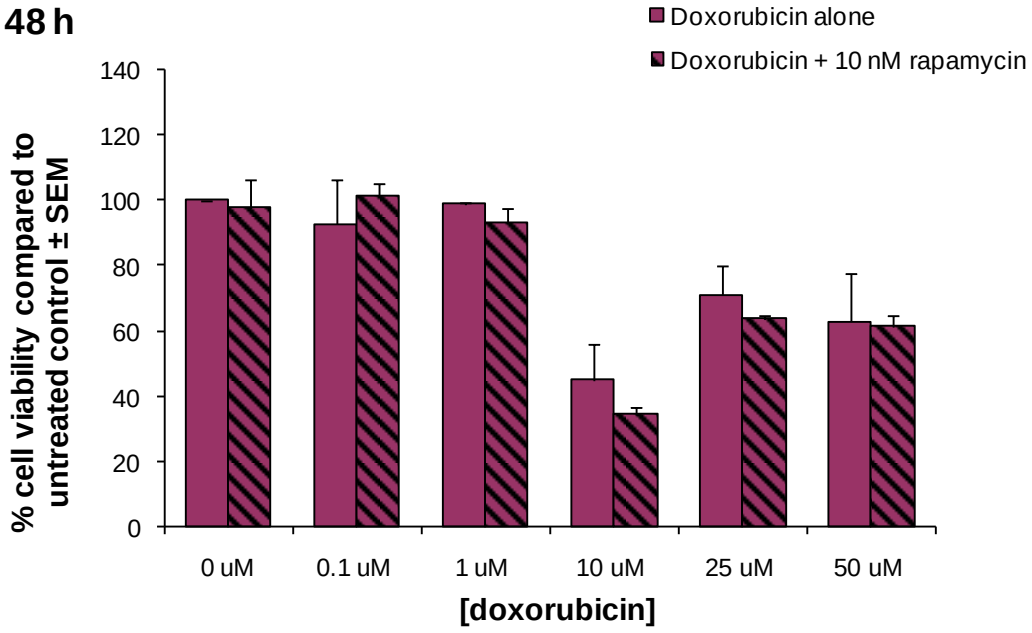

Figure 5.5 The Effects of 48 Hours Exposure to Varying Concentrations of Doxorubicin + 10 nM Rapamycin on the Viability of HepG2 Cells Cultured under Hypoxic Conditions.

$1x10^4$ cells/200 µl were added to each well of a 96-well plate and incubated overnight at 37°C under normoxic conditions. The plates were removed to hypoxic conditions and the media was removed and replaced with a range of doxorubicin concentrations + 10 nM rapamycin. 6 replicate wells for each concentration. The plates were incubated under hypoxic conditions for 48 hours. Cell viability was measured using MTS assay and normalised to untreated control. Data points represent mean of 3 separate experiments ± standard error of the mean.

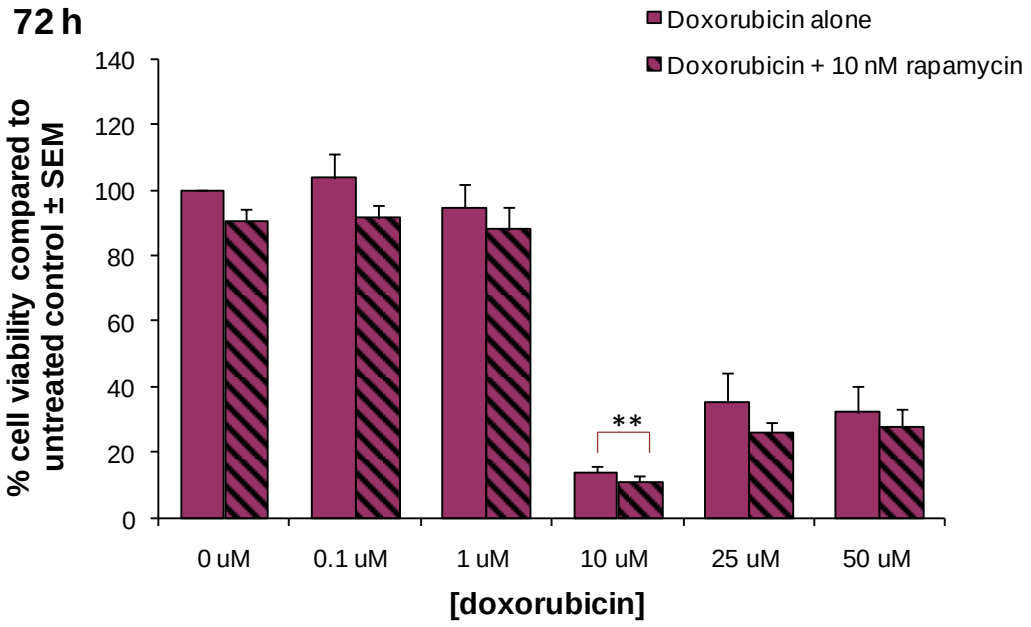

Figure 5.6 The Effects of 72 Hours Exposure to Varying Concentrations of Doxorubicin + 10 nM Rapamycin on the Viability of HepG2 Cells Cultured under Hypoxic Conditions.
$1x10^4$ cells/200 µl were added to each well of a 96-well plate and incubated overnight at 37°C under normoxic conditions. The plates were removed to hypoxic conditions and the media was removed and replaced with a range of doxorubicin concentrations + 10 nM rapamycin. 6 replicate wells for each concentration. The plates were incubated under hypoxic conditions for 72 hours. Cell viability was measured using MTS assay and normalised to untreated control. Data points represent mean of 3 separate experiments ± standard error of the mean. Statistical analysis was carried out using a one tailed paired t test. * denotes a significant difference, $p = < 0.05$.

5.3.2 There is No Additive Effect on the Attenuation of Hypoxia Stimulated HIF-1α Nuclear Accumulation after Combination Treatments.

To determine the effect of rapamycin and doxorubicin combination treatments on hypoxia stimulated nuclear accumulation of HIF-1α, SDS-PAGE and Western Blotting was carried out on nuclear extracts from HepG2 cells cultured under hypoxic conditions, and exposed to drug concentrations as shown, see Figure 5.7. Whilst the application of 10 nM rapamycin alone reduced the amount of nuclear HIF-1α ($p = 0.060$) (Lanes 1 and 2), the addition of either 10 nM rapamycin or 100 nM rapamycin to 10 µM doxorubicin did not result in increased reduction of HIF-1α when compared to 10 µM doxorubicin alone (Lanes 3, 4, and 5). The application of 50 µM doxorubicin alone caused a reduction in HIF-1α, although the small sample size precluded statistical analysis (Lane 6). Again, the addition of either 10 nM rapamycin or 100 nM rapamycin to 50 µM doxorubicin did not result in increased reduction of HIF-1α when compared to 50 µM doxorubicin alone (Lanes 7 and 8).

5.3.3 Nuclear Accumulation of NFkB p50 after Combination Treatments of Hypoxic Cells.

To determine the effect of rapamycin alone, and rapamycin and doxorubicin combinations on hypoxia stimulated nuclear accumulation of NFkB p50, SDS-PAGE and Western Blotting was carried out on nuclear extracts from HepG2 cells cultured under hypoxic conditions, see Figure 5.8. Although there appeared to be some reduction in the amount of nuclear NFkB p50 after rapamycin treatment, no significant effect was observed (Lanes 1, 2 and 3). No other significant effects were observed, although the addition of rapamycin to doxorubicin treatments suggested increased NFkB activity compared to doxorubicin alone.

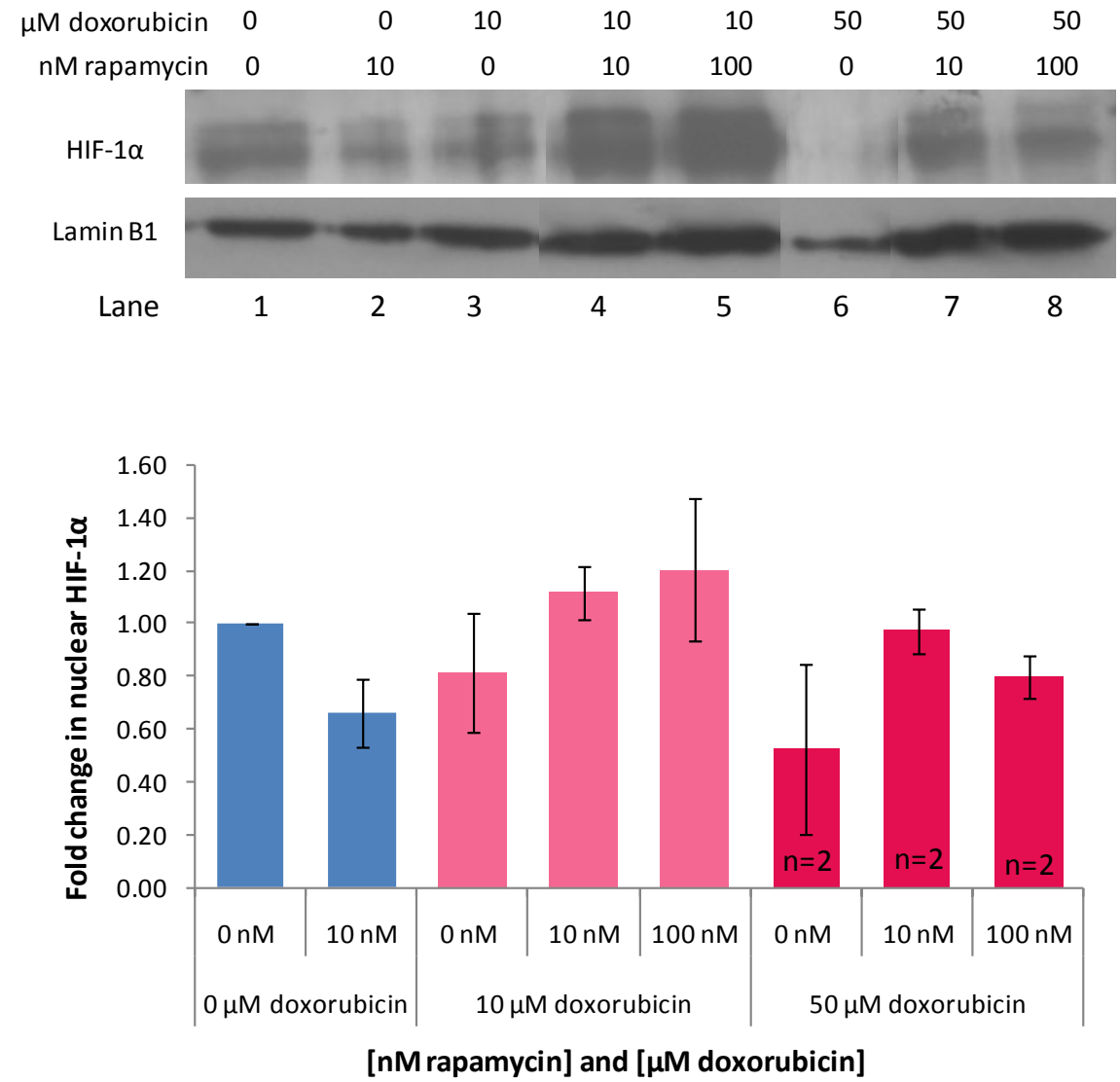

Figure 5.7 Nuclear Accumulation of HIF-1α after Rapamycin and Doxorubicin Combination Treatments.
HepG2 cells were seeded into T75 tissue culture flasks and incubated under normoxic conditions until the cells reached 60% confluence. The flasks were removed to hypoxic conditions and the cells exposed to different concentrations of rapamycin, doxorubicin and both in combination in growth medium. The flasks were incubated under hypoxic conditions for 24 hours, and the cells were harvested. Nuclear extracts were prepared and equal quantities of protein were fractionated on a 10% SDS-PAGE gel. The proteins were transferred to a PVDF membrane and probed with anti-HIF-1α antibodies. Proteins were visualised using chemiluminescent reagents. The membrane was stripped and reprobed using antibodies against the nuclear house-keeping protein Lamin B1. Protein levels were quantified using densitometry analysis. The amount of HIF-1α was normalised to Lamin. Fold change compared to untreated hypoxic cells was calculated. Data shown represents mean of 3 independent experiments ± standard error of the mean, unless indicated otherwise.

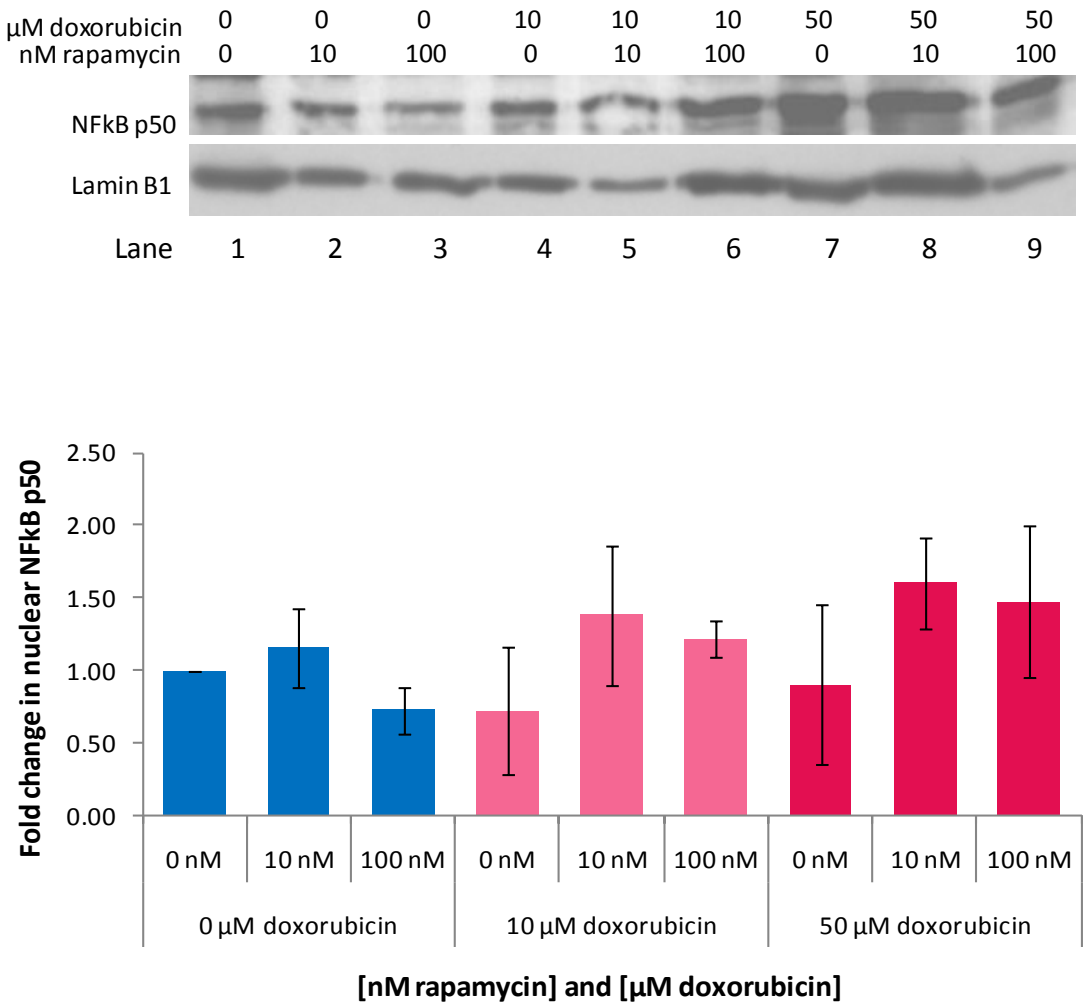

Figure 5.8 Nuclear Accumulation of NFkB p50 after Combination Treatments of Hypoxic Cells.
HepG2 cells were seeded into T75 tissue culture flasks and incubated under normoxic conditions until the cells reached 60% confluence. The flasks were removed to hypoxic conditions and the cells exposed to different concentrations of rapamycin, doxorubicin and both in combination in growth medium. The flasks were incubated under hypoxic conditions for 24 hours, and the cells were harvested. Nuclear extracts were prepared and equal quantities of protein were fractionated on a 10% SDS-PAGE gel. The proteins were transferred to a PVDF membrane and probed with anti-NFkB p50 antibodies. Proteins were visualised using chemiluminescent reagents. The membrane was stripped and reprobed using antibodies against the nuclear house-keeping protein Lamin B1. Protein levels were quantified using densitometry analysis. The amount of NFkB p50 was normalised to Lamin. Fold change compared to untreated hypoxic cells was calculated. Data shown represents mean of 3 separate experiments ± standard error of the mean.

5.4 Discussion.

5.4.1 Combination Treatments and Cell Viability.

This study has shown that the addition of the mTOR inhibitor rapamycin to the standard chemotherapeutic agent doxorubicin significantly decreases cell viability compared to doxorubicin treatment alone in both normoxic and hypoxic cells. The effects of rapamycin were more pronounced at 24 hours than at later time points and this is consistent with reports from *in vitro* and *in vivo* studies that metronomic applications of rapamycin appear to more effective than single applications (Guba *et al*., 2005, Tabernero *et al*., 2008).

It has been suggested that pre-incubating cells with rapamycin before the addition of doxorubicin may be more effective than adding both the drugs at the same time. Semela and co-workers (2008) investigated doxorubicin and temsirolimus combinations on the viability of Morris Hepatoma (MH) cells (isogenic rat liver cancer cells) and rat endothelial cells. They used 1 nM and 10 nM temsirolimus in combination with 15 nM or 150 nM doxorubicin. In concordance with the data shown here, 150 nM doxorubicin monotherapy had only a weak effect on cell proliferation, and the addition of temsirolimus had no further effect. However, when the same regimen was tested on rat endothelial cells the minimum effective dose of doxorubicin as a monotherapy was found to be 15 nM, and the addition of rapamycin at both 1 nM and 10 nM increased the cytotoxic effects. Interestingly, the addition of temsirolimus to the higher dose of doxorubicin had no additive effect.

As mentioned previously, one of the mechanisms contributing to drug resistance is the upregulation of P-glycoprotein MDR1 (Roninson, 1992). Rapamycin has been reported to improve the uptake of chemotherapeutics in multidrug-resistant cell lines due to competitive inhibition because of a direct interaction of rapamycin with Pgp

(Hoof *et al*., 1993, Arceci *et al*., 1992, Pawarode *et al*., 2007). In one study, rapamycin bound with high affinity to Pgp and enhanced growth inhibitory effects of doxorubicin in Chinese hamster ovary cells (Hoof *et al*., 1993). 1 uM rapamycin reduced the IC50 of doxorubicin from 18 ng/ml to 9 ng/ml in the parent cell line, and from 280 ng/ml to 200 ng/ml in a multi-drug resistant mutant (Hoof *et al*., 1993). Another study demonstrated a similar reversal of multi drug resistance by rapamycin, but only at μM concentrations that would not therefore be suitable *in vivo* (Arceci *et al*., 1992). Pawarode *et al* (2007) showed that rapamycin enhanced the cellular uptake of drugs in cells overexpressing Pgp and MDR-1. The optimal rapamycin concentration was 2.5 μM, but they showed an effect with 250 nM rapamycin if the cells were pre-incubated for 30 minutes prior to drug exposure, where the rapamycin saturated the MDR-1 binding sites before the application of doxorubicin (Pawarode *et al*., 2007). In this study there was less of an additive effect with rapamycin in hypoxic cells compared to normoxic cells. Hypoxic cells are likely to have upregulated drug resistance mechanisms as a consequence of HIF activation, and if rapamycin prevents some of the Pgp regulated doxorubicin resistance and therefore increases its cytotoxicity, would that be more apparent in hypoxic than in normoxic cells? Pre-incubation of the cells with rapamycin before the addition of doxorubicin may increase the additive effects, and this should be explored further.

As discussed previously, the PI3K/Akt/mTOR pathway is constitutively active in many cancers, and this is often due to mutations or deletions in the tumour suppressor phosphatase protein PTEN. A 10 nM dose of rapamycin was shown to increase the sensitivity of the PTEN deleted cell line PC-3 to doxorubicin, as did transfection with a PTEN construct (Grunwald *et al*., 2002). Akt activation confers resistance to doxorubicin treatment (Tanaka *et al*., 2000, Tanaka *et al*., 2005), and

this may be due to protection from apoptosis (Huang *et al*., 2001). One study looked at the rapalog everolimus in combination with cisplatin in HCC cell lines with different p53 status (HepG2, He3p3B and PLC) and found that everolimus sensitised all the cell lines to cisplatin cytotoxicity. Whilst this was independent of p53, it appeared to be related to p21-induced apoptosis in response to DNA damage (Tam *et al*., 2009). This then raises the question of whether inhibition of mTOR using rapamycin sensitises PTEN deficient cells to doxorubicin induced apoptosis.

5.4.2 Combination Treatments.

There was no evidence of any complimentary inhibition of HIF-1α after combination treatments. Indeed, the results suggested that the addition of rapamycin led to an attenuation of the effect on HIF-1α of either drug alone.

5.4.3 Activation of the Transcription Factor NFkB.

There was a suggestion that 100 nM rapamycin inhibited the hypoxia stimulated activation of NFkB, although the result was not statistically significant (Figure 5.8, Lanes 1 and 3). It has been reported that rapamycin can prevent the translocation of NFkB to the nucleus. Rapamycin binds to FKBP51, which is an important co-factor of the IKK complex, inhibits IKK kinase activity and prevents degradation of IkB (Giordano *et al*., 2006, Romano *et al*., 2004). Furthermore, rapamycin has been shown to inhibit doxorubicin-induced NFkB activation and enhance apoptosis in melanoma cells (Romano *et al*., 2004). However, in this study rapamycin failed to inhibit p50 NFkB in doxorubicin-treated hypoxic cells (Figure 5.8, Lanes 4 – 9). This study did not investigate the effect of rapamycin on p50 NFkB in doxorubicin-treated normoxic cells, and this is work that clearly needs to be done.

5.5 Conclusions.

A combination of low dose rapamycin and doxorubicin appears to have improved cytotoxicity towards both normoxic and hypoxic HepG2 cells than either treatment alone.

Whilst 50 μM doxorubicin and 10 nM and 100 nM rapamycin attenuated the stabilisation of HIF-1α under hypoxic conditions, doxorubicin and rapamycin combinations showed no evidence of complimentary effects. Doxorubicin induced nuclear localisation of NFkB in normoxic cells. Hypoxia alone also induced nuclear localisation of NFkB, with no further localisation observed after application of doxorubicin. The results presented here suggest that rapamycin may inhibit the extent of NFkB activation.

Consequent to the findings described above, the anti-tumour effects of doxorubicin and rapamycin both as monotherapies and in combination *in vivo*, were evaluated in a murine model of HCC.

Chapter 6

In Vivo Investigations into the Effects of Doxorubicin-eluting Beads and Rapamycin as Monotherapies and in Combination on Tumour Burden in an Ectopic Xenograft Mouse Model of Hepatocellular Carcinoma.

6.1 Introduction

Hepatocellular carcinoma (HCC) is a leading cause of cancer-related death worldwide (Parkin *et al*., 2005). Treatment options for HCC are limited due to tumour stage at diagnosis, and treatment outcomes are often poor (Colombo and Sangiovanni, 2003, Raoul, 2008). The standard of care for patients unsuitable for the potentially curative therapies of ablation, resection or transplantation is TACE (Lencioni, 2010). DEB-TACE using doxorubicin-loaded microspheres is a treatment regime which has been shown to have improved response rates when compared with conventional TACE (Dhanasekaran *et al*., 2010, Lammer *et al*., 2010). For patients with more advanced disease, sorafenib is the standard of care (Lencioni, 2010).

Targeting signalling pathways that are aberrantly activated in HCC can potentially inhibit tumour growth (Whittaker *et al*., 2010). mTOR has a critical role in the pathogenesis of HCC and is associated with a poor prognosis (Villanueva *et al*., 2008, Chen *et al*., 2009a, Whittaker *et al*., 2010, Zhou *et al*., 2010b). Activated mTOR has been reported in 40% of explanted HCCs (Sieghart *et al*., 2007). Pre-clinical investigations of rapamycin and its analogues have shown anti-tumoural effects in mouse models of HCC (Guba *et al*., 2002, Huynh *et al*., 2008a, Huynh *et al*., 2008b, Ong *et al*., 2009, Wang *et al*., 2008b, Wang *et al*., 2008c, Semela *et al*., 2007, Piguet *et al*., 2011, O'Reilly *et al*., 2011).

Since rapamycin demonstrates both immunosuppressive and anti-cancer effects, it is increasingly being utilised as the immunosuppressant of choice for HCC patients undergoing liver transplantation (Castroagudin *et al*., 2011, Sanchez Antolin *et al*.,

2011). Fourteen clinical studies have been published which suggest improved survival times and anti-tumour effects of mTOR inhibition after liver transplantation for HCC (Schnitzbauer *et al*., 2011). However, no randomized trials evaluating immunosuppressive drugs and HCC recurrence after liver transplantation have so far been published, although a prospective randomised clinical trial is now underway (Schnitzbauer *et al*., 2010). One pilot study assessing rapamycin as a single agent for the treatment of advanced HCC found that, although the drug was well tolerated, it was only minimally effective (Schoniger-Hekele and Muller, 2010). However, another pilot study showed that the drug was well tolerated in cirrhotic patients with advanced HCC, and had a significant impact on tumour growth in 40% of the cohort (Decaens, 2009). A phase 1/2 study of everolimus for advanced HCC has shown preliminary evidence of anti-tumour activity (Zhu *et al*., 2011).

In vivo animal research indicates that rapamycin may have additive or synergistic effects when used in combination with other chemotherapeutics or other molecular inhibitors (Huynh *et al*., 2008b, LoPiccolo *et al*., 2008, Wang *et al*., 2008c, Piguet *et al*., 2008, Piguet *et al*., 2011, Newell *et al*., 2009, Ong *et al*., 2009, Jasinghe *et al*., 2008, Ribatti *et al*., 2007, Ahn *et al*., 2008). Rapamycin and doxorubicin have been demonstrated to have additive effects *in vivo* in murine models of liver, prostate, cervical and lung cancer (Piguet *et al*., 2008, O'Reilly *et al*., 2011, Grunwald *et al*., 2002).

It has recently been shown that rapamycin can be loaded onto drug-eluting beads either alone or in combination with doxorubicin, without compromising the loading or release kinetics of doxorubicin (Forster 2009). This fact, together with the evidence cited above, warrants further investigations into rapamycin and doxorubicin combinations towards HCC *in vivo*.

6.2 Aims.

To evaluate the anti-cancer effects of rapamycin and doxorubicin monotherapies and combinations in HepG2 tumour-bearing mice treated with doxorubicin-loaded beads (DOXDEB); rapamycin-loaded beads (RAPADEB); rapamycin and doxorubicin co-loaded beads (RAPADOXDEB); oral rapamycin (rapa p.o.); and DOXDEB in combination with oral rapamycin.

6.3 Results.

Using a mouse model of HCC we investigated the effects of DOXDEB; RAPADEB; RAPADOXDEB; rapamycin p.o.; and DOXDEB in combination with rapamycin p.o. HepG2 cells were implanted subcutaneously and tumour growth was monitored regularly. When tumours reached palpable size, at day 23, treatment regimes commenced. Tumour burden was evaluated by measuring tumour volume (length x width x width x $\pi/6$) at days 23, 25, 28, 30, 32, 35, 42 and 45. Anti-tumour activity was assessed by comparing tumour volumes, comparing final tumour volume/control and comparing tumour weight *post mortem*. Toxicity was assessed using mouse body weight and behavioural and physiological observations. The sample size for each treatment was n = 3.

6.3.1 Untreated Control.

Unfortunately, the tumour transplantation was unsuccessful in one of the control animals, thus reducing the sample size of the control group to n = 2. The mean increase in tumour size in the successful transplants was > 700% between day 23 and day 45.

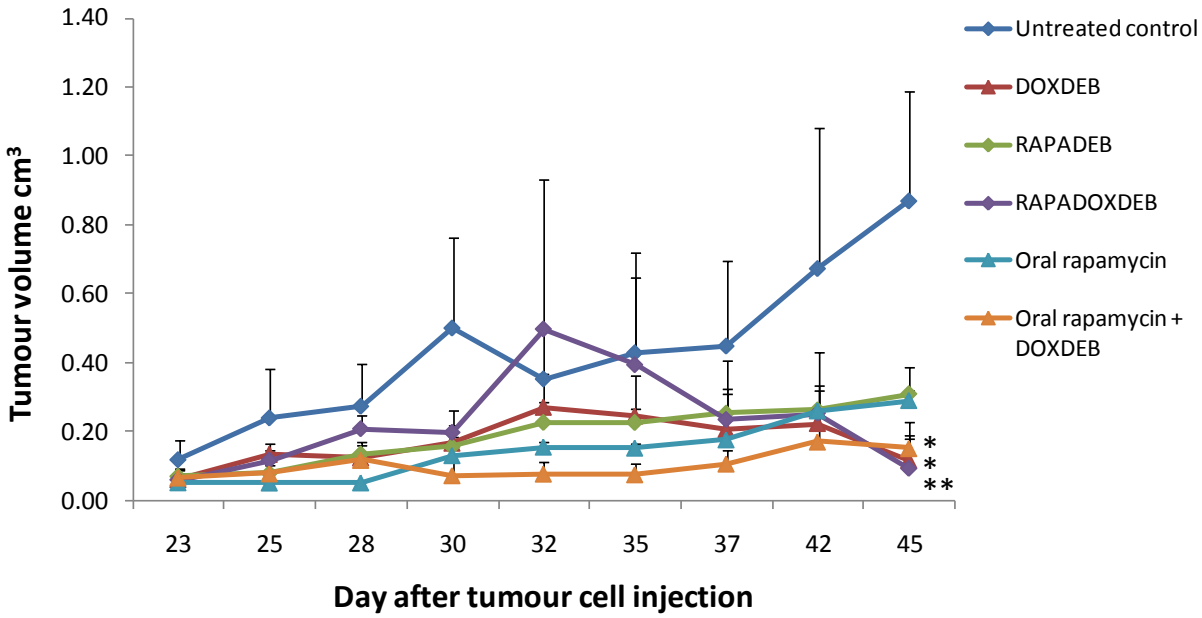

Figure 6.1 Anti-tumoural Activity of Doxorubicin and Rapamycin Treatments in a Mouse Model of HCC.
5 x 10^6 HepG2 cells were subcutaneously implanted in NMRI: nu/nu mice at day 0. Tumour volume was palpable at day 23 after implantation and treatment was initiated. Rapamycin was administered by gavage at a dose of 1 mg/kg/day. 100 ul of beads loaded as specified was injected adjacent to the tumour at day 23. Tumour volume was measured at days 23, 25, 28, 30, 32, 35, 37, 42 and 45. Data shown represents the mean value of 3 replicates per group ± standard error of the mean, apart from the control group where data represents mean of 2 replicates ± standard error of the mean. Data was found to be normally distributed with equal variance. Multivariate ANOVA (general linear model) data analysis showed a significant difference between the groups at day 45, $p = < 0.01$. Post hoc Bonferroni pairwise comparisons at day 45 identified significant differences between control *vs.* DOXDEB, $p = < 0.05$; control *vs.* RAPADOXDEB, $p = < 0.01$; and control *vs.* rapamycin p.o. + DOXDEB, $p = < 0.05$. * denotes a significant difference, $p = < 0.05$; ** denotes a significant difference, $p = < 0.01$.

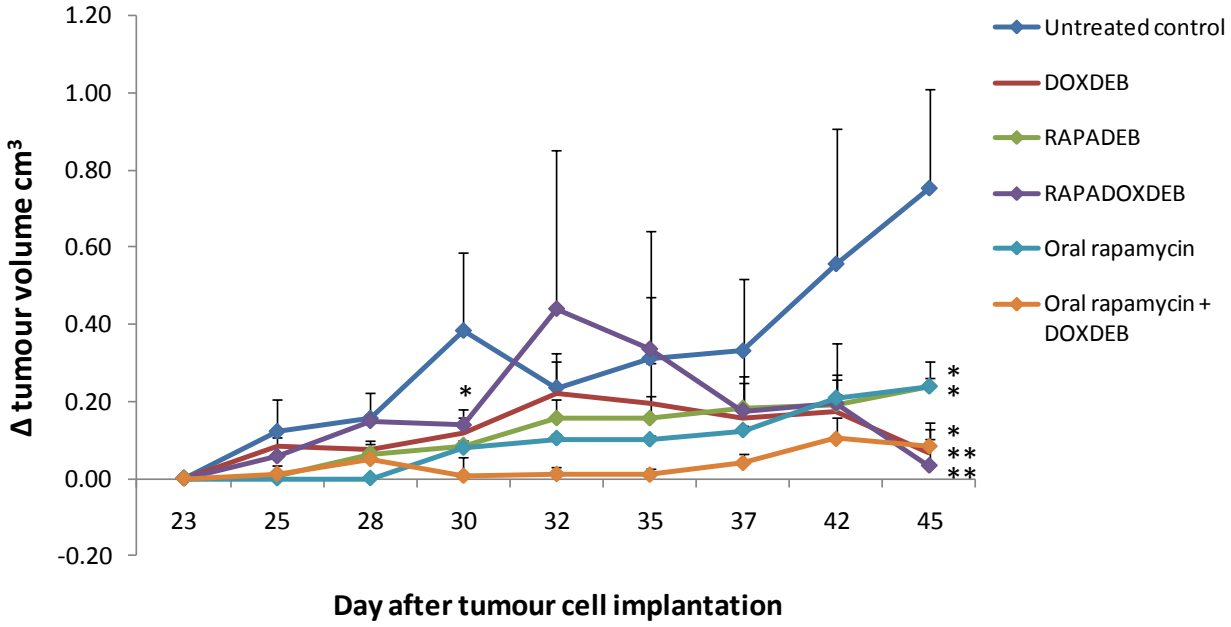

Figure 6.2 Anti-tumoural Activity of Doxorubicin and Rapamycin Treatments in a Mouse Model of HCC.

5 x 10^6 HepG2 cells were subcutaneously implanted in NMRI: nu/nu mice at day 0. Tumour volume was palpable at day 23 after implantation and treatment was initiated. Rapamycin was administered by gavage at a dose of 1 mg/kg/day. 100 ul of beads loaded as specified was injected adjacent to the tumour at day 23. Tumour volume was measured at days 23, 25, 28, 30, 32, 35, 37, 42 and 45. The difference (Δ) in tumour volume compared to day 23 was calculated for each treatment at each time point by subtraction. Data shown represents the mean value of 3 replicates per group ± standard error of the mean, apart from the control group where data represents mean of 2 replicates ± standard error of the mean. Data was found to be normally distributed with equal variance. Multivariate ANOVA (general linear model) data analysis showed a significant difference between the groups at day 28, $p = < 0.05$; day 30, $p = < 0.05$; and day 45, $p = < 0.01$. Post hoc Bonferroni pairwise comparisons at day 28 identified significant differences between rapamycin p.o. *vs.* RAPADOXDEB, $p = < 0.05$. Post hoc Bonferroni pairwise comparisons at day 30 identified significant differences between control *vs.* rapamycin p.o. + DOXDEB, $p = < 0.05$. Post hoc Bonferroni pairwise comparisons at day 45 identified significant differences between control *vs.* DOXDEB, $p = < 0.05$; control *vs.* RAPADEB, $p = < 0.05$; control *vs.* RAPADOXDEB, $p = < 0.01$; control *vs.* rapamycin p.o., $p = < 0.05$; and control *vs.* rapamycin p.o. + DOXDEB, $p = < 0.01$. * denotes a significant difference, $p = < 0.05$; ** denotes a significant difference, $p = < 0.01$.

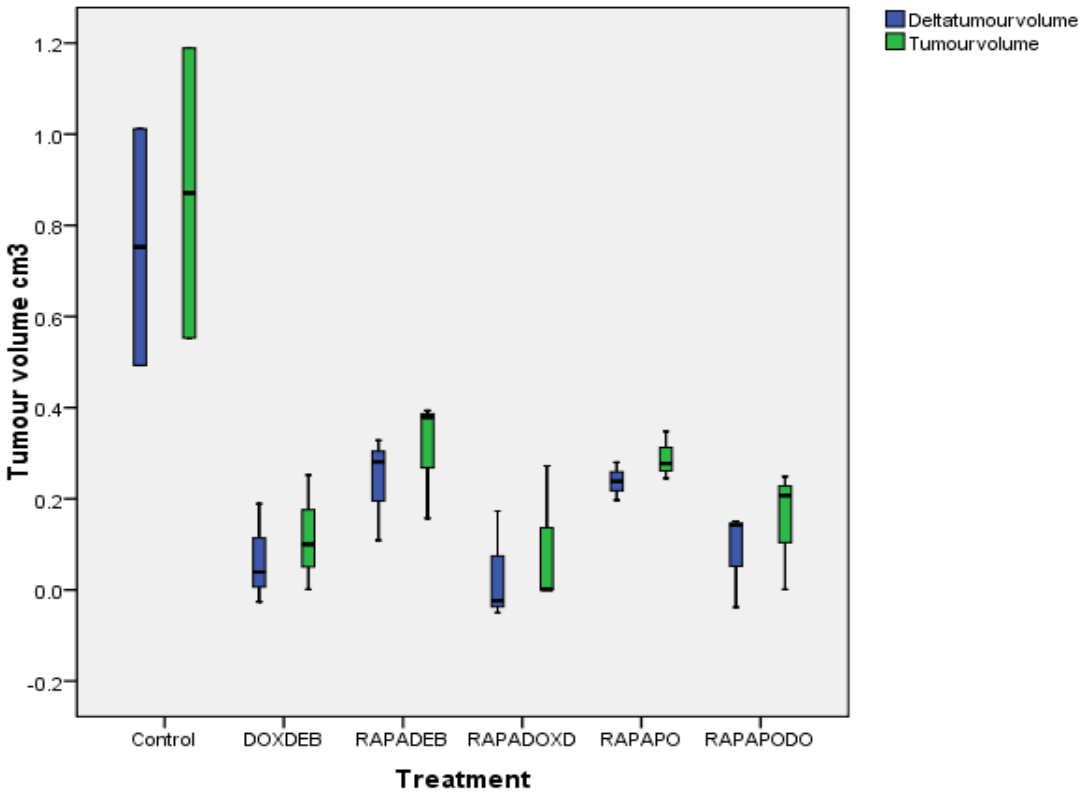

Figure 6.3 Box Plots of Tumour Volumes and delta Tumour Volumes at Day 45. HepG2 cells were subcutaneously implanted in NMRI: nu/nu mice at day 0. Tumour volume was palpable at day 23 after implantation and treatment was initiated. Rapamycin was administered by gavage at a dose of 1 mg/kg/day. 100 ul of beads loaded as specified was injected adjacent to the tumour at day 23. Tumour volume was measured at day 45. Delta tumour volume was calculated by subtracting volume at day 23 from volume at day 45. Data shown represents 3 replicates per group ± standard error of the mean, apart from the control group where data represents 2 replicates.

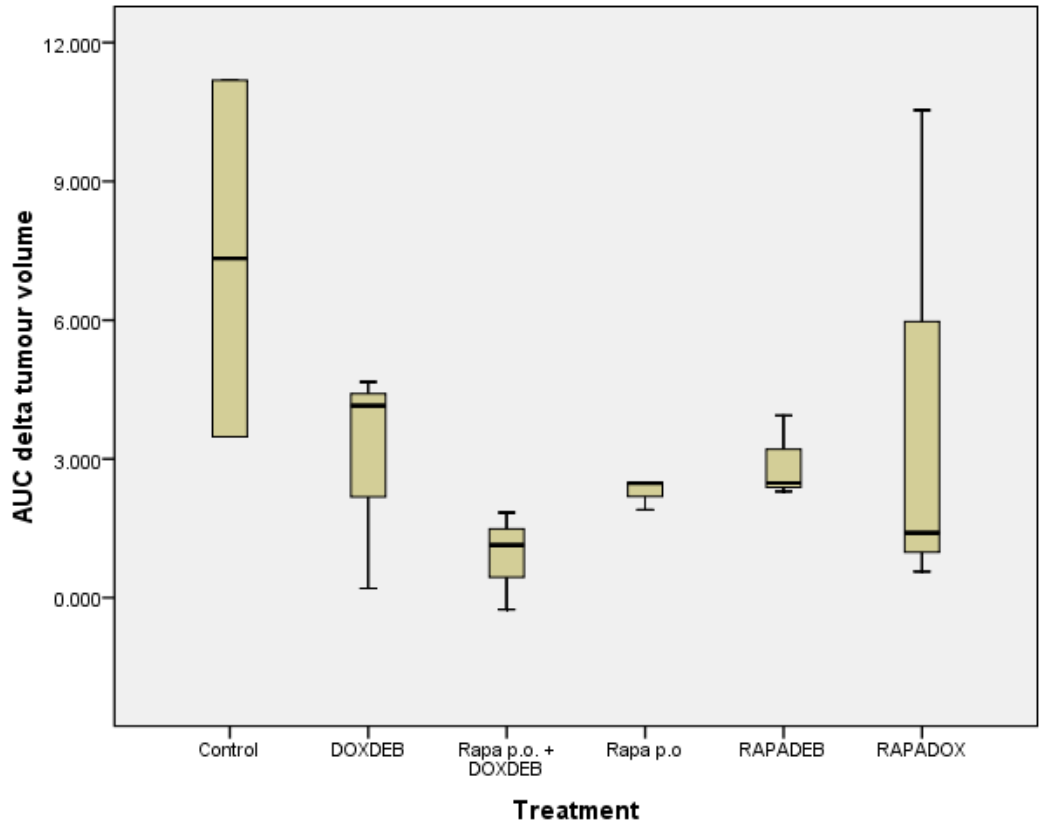

Figure 6.4 Box Plots of AUC Day 23 – 45 for Tumour Volumes and delta Tumour Volumes.
HepG2 cells were subcutaneously implanted in NMRI: nu/nu mice at day 0. Tumour volume was palpable at day 23 after implantation and treatment was initiated. Rapamycin was administered by gavage at a dose of 1 mg/kg/day. 100 ul of beads loaded as specified was injected adjacent to the tumour at day 23. Tumour volume was measured at day 45. Delta tumour volume was calculated by subtracting volume at day 23 from volume at day 45. AUC between day 23 and day 45 was calculated for tumour volume and delta tumour volume. Data shown represents 3 replicates per group ± standard error of the mean, apart from the control group where data represents 2 replicates.

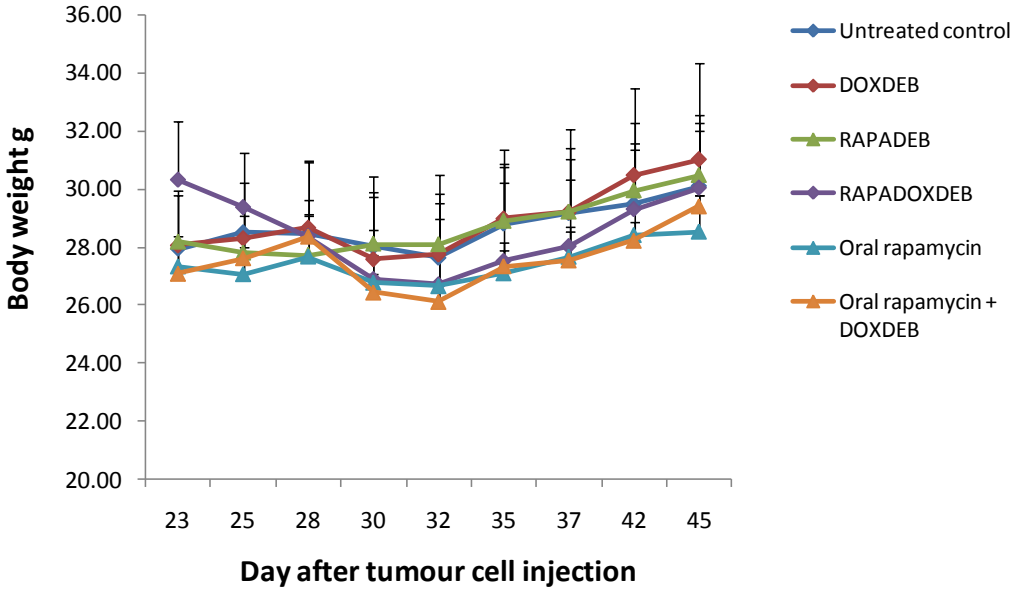

Figure 6.5 Effects of Doxorubicin and Rapamycin Treatments on Body Weight between Day 23 and Day 45 in a Mouse Model of HCC.
Mice were weighed at days 23, 25, 28, 30, 32, 35, 37, 42 and 45. Data shown represents the mean value of 3 replicates per group ± standard error of the mean, apart from the control group where data represents mean of 2 replicates. Data was found to be normally distributed with equal variance. Multivariate ANOVA (general linear model) data analysis showed no significant differences in body weight between treatment groups, and no significant differences in body weight between days within each treatment group.

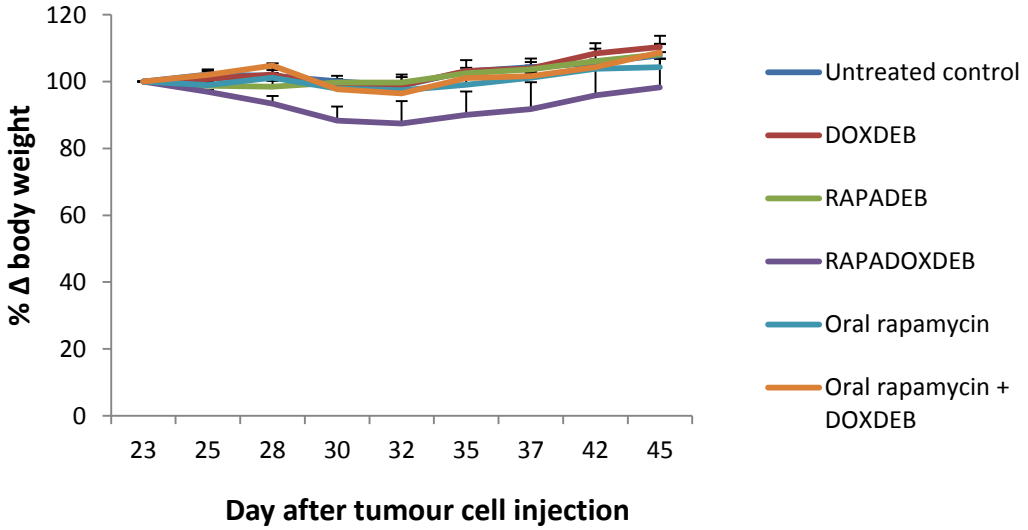

Figure 6.6 % Change in Body Weight after Doxorubicin and Rapamycin Treatments in a Mouse Model of HCC.
Data was found to be normally distributed with equal variance. Multivariate ANOVA (general linear model) data analysis showed a significant difference between the treatments at day 28 ($p = 0.016$). Post hoc Bonferroni pairwise comparisons identified this as a significant difference between the RAPADOX DEB *vs*. oral rapamycin + DOXDEB treated animals ($p = 0.017$). No significant differences were found between days within each treatment group.

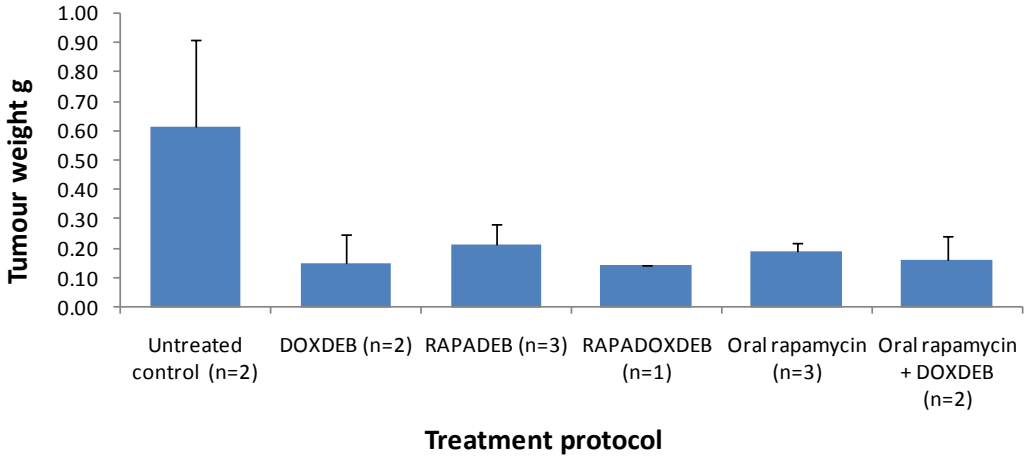

Figure 6.7 Effects of Doxorubicin and Rapamycin Treatments on Tumour Weight at Day 45 in a Mouse Model of HCC.
Mice were euthanized at day 45, and the tumours excised and weighed. Data represents mean ± standard error of the mean. Because of the small sample sizes, statistical analysis was not carried out.

Treatment	**Observations**
Control 1	No tumour growth
Control 2	OK
Control 3	OK
DOXDEB 1	From day 42 ulceration
DOXDEB 2	From day 37 ulceration
DOXDEB 3	OK
RAPADEB 1	OK
RAPADEB 2	OK
RAPADEB 3	OK
RAPADOXDEB 1	From day 30 ulceration
RAPADOXDEB 2	From day 35 ulceration
RAPADOXDEB 3	From day 37 ulceration
Rapamycin p.o. 1	OK
Rapamycin p.o. 2	OK
Rapamycin p.o. 3	OK
Rapamycin p.o. + DOXDEB 1	OK
Rapamycin p.o. + DOXDEB 2	From day 28 ulceration
Rapamycin p.o. + DOXDEB 3	From day 28 ulceration

Table 6. 1 Physiological Examination of Tumour-bearing Animals.
HepG2 cells were subcutaneously implanted in NMRI: nu/nu mice at day 0. Tumour volume was palpable at day 23 when treatment was initiated. Rapamycin was administered by gavage at a dose of 1 mg/kg/day. 100 ul of beads loaded as specified was injected adjacent to the tumour at day 23. Gross physiological examination was made at days 23, 25, 28, 30, 32, 35, 37, 42 and 45. No behavioural changes were reported, and no mice were euthanized due to toxic effects or to tumour load being ≥ 10% of body size.

Treatment	Tumour volume (cm^3) ± SEM	Δ tumour volume (cm^3) ± SEM	Tumour volume T/C (95% CI)	Δ tumour volume T/C (95% CI)	Tumour weight T/C	Body weight T/C (95% CI)	AUC Δ tumour volume T/C (95% CI)
Control	0.871 ± 0.318	0.753 ± 0.080	1.00 (0.72)	1.00 (0.21)	1.00 (0.68)	1.00 (0.02)	1.00 (1.03)
DOXDEB	0.118 ± 0.073 (p = 0.012)	0.067 ± 0.070 (p = 0.005)	0.14 (0.16)	0.09 (0.18)	0.25 (0.22)	1.03 (0.07)	0.41 (0.38)
RAPADEB	0.310 ± 0.077 (p = 0.089)	0.239 ± 0.038 (p = 0.045)	0.36 (0.17)	0.32 (0.10)	0.35 (0.16)	1.01 (0.06)	0.40 (0.14)
RAPADOXDEB	0.091 ± 0.090 (p = 0.009)	0.033 ± 0.073 (p = 0.004)	0.10 (0.20)	0.04 (0.19)	0.24 (-)	1.00 (0.17)	0.57 (0.85)
Rapamycin p.o.	0.290 ± 0.030 (p = 0.072)	0.238 ± 0.280 (p = 0.044)	0.33 (0.07)	0.32 (0.73)	0.31 (0.07)	0.95 (0.05)	0.31 (0.05)
Rapamycin p.o. + DOXDEB	0.152 ± 0.077 (p = 0.017)	0.085 ± 0.069 (p = 0.007)	0.17 (0.17)	0.11 (0.18)	0.26 (0.18)	0.98 (0.05)	0.12 (0.16)

Table 6.2 Anti-tumour Effects of Doxorubicin and Rapamycin Treatments in a Mouse Model of HCC at Day 45.
HepG2 cells were subcutaneously implanted in NMRI: nu/nu mice at day 0. Tumour volume was palpable at day 23 after implantation and treatment was initiated. Rapamycin was administered by gavage at a dose of 1 mg/kg/day. 100 ul of beads loaded as specified was injected adjacent to the tumour at day 23. Tumour volume, mouse body weight and tumour weight of excised tumour were measured at day 45. Tumour volume and body weight data shown represents the mean value of 3 replicates per group ± standard error of the mean, apart from the control group where data represents mean of 2 replicates ± standard error of the mean. Statistical analysis of treatment *vs.* control was determined using a multivariate ANOVA with post hoc Bonferroni comparisons. Anti-tumour effect was expressed as T/C. Δ tumour volume = difference in tumour volume between day 23 and day 45 (subtracted). SEM, standard error of the mean; CI, Confidence Interval.

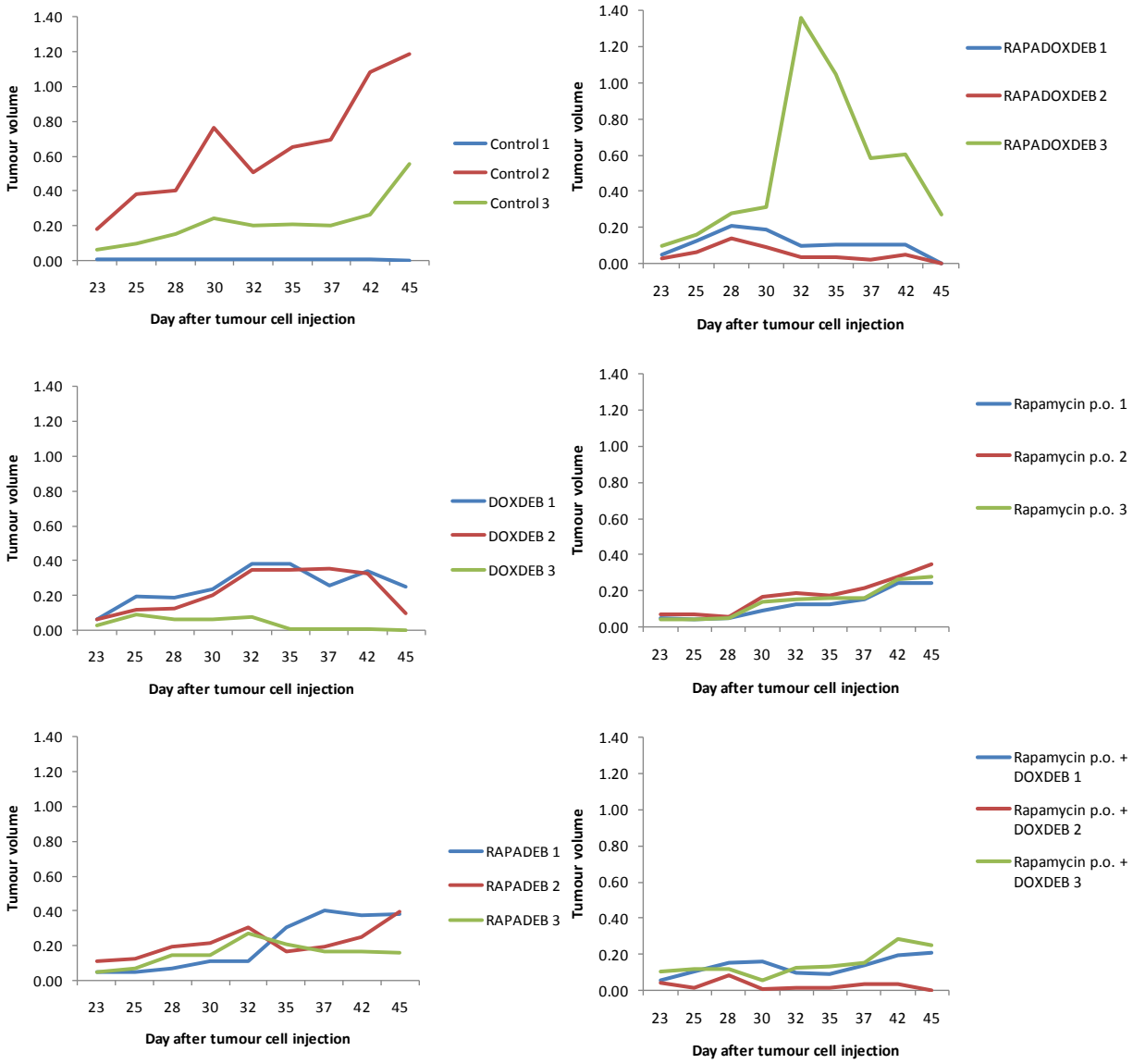

Figure 6.8 Tumour Volumes, Raw Data for each Mouse in a Treatment Group.
NMRI: nu/nu mice were randomly assigned to one of six treatment groups, three mice per group. HepG2 cells were subcutaneously implanted and treatments were initiated at day 23. Tumours were measured at day 23, 25, 28, 30, 32, 35, 38, 42 and 45. Tumour volume was calculated as length x width x width x π/2.

6.3.2 *In Vivo* Activity of DOXDEB.

DOXDEB demonstrated sustained inhibition of tumour growth compared to control, with tumour regression from day 32. Tumour regression was more pronounced from day 42. At day 45, DOXDEB showed significant anti-tumour activity compared to untreated control ($p = 0.12$ for tumour volume, $p = 0.05$ for Δ tumour volume). The mean tumour weight at day 45 was 25% that of control (95% CI, 22) (Table 6.2). Final tumour volume was 14% of control (95% CI, 16); final Δ tumour volume was 9% of control (95% CI, 18). Δ tumour volume over the time course of the experiment (as calculated using AUC day 23 - 45) was 41% that of control. There was no significant body weight loss compared to any of the other groups and no significant differences in body weight over time (Figure 6.5 and 6.6). Two of the mice in this group suffered ulceration at the tumour injection site; one from day 37 and one from day 42 (Table 6.1).

6.3.3 *In Vivo* Activity of RAPADEB.

RAPADEB demonstrated sustained inhibition of tumour growth compared to control, although no tumour regression was apparent. At day 45, RAPADEB showed significant anti-tumour activity compared to untreated control ($p = 0.045$ for Δ tumour volume). The mean tumour weight at day 45 was 35% (95% CI, 16) that of control (Table 6.2). Mean tumour volume at day 45 was 36% of control (95% CI, 17), and mean Δ tumour volume at day 45 was 32% of control (95% CI, 10) (Figures 6.1 and 6.2). Δ tumour volume over the time course of the experiment (as calculated using AUC day 23 - 45) was 40% that of control. There was no significant body weight loss compared to any of the other groups and no significant difference in

body weight between days of treatment (Figures 6.5 and 6.6). None of the mice in this group suffered ulceration at the tumour injection site (Table 6.1).

6.3.4 *In Vivo* Activity of RAPADOXDEB.

RAPADOXDEB demonstrated inhibition of tumour growth up to day 30, and then tumour regression from day 32. Rapid tumour growth was reported between days 30 and 32. At day 45, RAPADOXDEB showed significant anti-tumour activity compared to untreated control ($p = 0.009$ for tumour volume, $p = 0.004$ for Δ tumour volume). The mean tumour weight at day 45 was 24% that of control (one sample only) (see Table 6.2). Mean tumour volume at day 45 was 10% of control (95% CI, 20), and mean Δ tumour volume at day 45 was 4% of control (95% CI, 19) (Table 6.2). Δ tumour volume over the time course of the experiment (as calculated using AUC day 23 - 45) was 57% that of control. At day 28 the % body weight loss was significantly more in this group compared to the group treated with rapamycin p.o. + DOXDEB ($p = 0.017$). There was no significant difference in body weight between days of treatment (Figures 6.5 and 6.6). Two of the mice in this group suffered ulceration at the tumour injection site; one from day 30, one from day 35 and one from day 37 (Table 6.1).

6.3.5 *In Vivo* Activity of Rapamycin p.o.

Monotherapy with oral rapamycin showed sustained inhibition of tumour growth across the time course of the experiment, with complete inhibition of tumour growth to day 28. At day 28, rapamycin p.o. showed significant anti-tumour activity compared to RAPADOXDEB ($p = 0.033$ for Δ tumour volume). The p value for rapamycin p.o. *vs.* control was 0.051. At day 45, rapamycin p.o. showed significant anti-tumour activity compared to untreated control ($p = 0.044$ for Δ tumour volume).

The mean tumour weight at day 45 was 31% (95% CI, 7) that of control (see Table 6.2). Mean tumour volume at day 45 was 33% of control (95% CI, 7), and mean Δ tumour volume at day 45 was 32% of control (95% CI, 73) (see Table 6.2). Δ tumour volume over the time course of the experiment (as calculated using AUC day 23 - 45) was 31% that of control. There was no significant body weight loss compared to any of the other groups and no significant difference in body weight between days of treatment (Figures 6.5 and 6.6). None of the mice in this group suffered ulceration at the tumour injection site (Table 6.1).

6.3.6 *In Vivo* Activity Rapamycin p.o. in Combination with DOXDEB.

The most effective treatment across the time course of the experiment was the combination of oral rapamycin with DOXDEB (Figure 6.4). Tumour growth was inhibited from day 23 to day 28, with evidence of tumour regression between days 28 and 30, followed by complete inhibition between days 30 to 35. At day 30 rapamycin p.o. + DOXDEB showed significant anti-tumour activity compared to untreated control ($p = 0.035$ for Δ tumour volume). At day 45, rapamycin p.o. + DOXDEB showed significant anti-tumour activity compared to untreated control ($p = 0.017$ for tumour volume, $p = 0.007$ for Δ tumour volume). The mean tumour weight at day 45 was 26% (95% CI, 18) of control (Table 6.2). Mean tumour volume at day 45 was 17% of control (95% CI, 17), and mean Δ tumour volume at day 45 was 11% of control (95% CI, 18) (see Table 6.2). Δ tumour volume over the time course of the experiment (as calculated using AUC day 23 - 45) was 12% that of control. There was a significant difference in % body weight loss at day 28 when compared with RAPADOXDEB, with weight loss being more in the RAPADOXDEB group ($p = 0.017$) (Figure 6.6). There was no significant body weight loss compared to any of

the other groups and no significant difference in body weight between days of treatment (Figure 6.5). Two of the mice in this group suffered ulceration at the tumour injection site. In both cases the ulceration started at day 28 (Table 6.1). At day 45 complete tumour regression was reported in one of the mice. The tumour volume measurements for one of the mice in this group were unusual; with an increase in tumour size > 400% between day 30 and day 32, and this has skewed the data for the group.

6.4 Discussion.

6.4.1 DOXDEB as Monotherapy.

We have shown that monotherapy using DOXDEB is an effective treatment for human HCC tumours growing as subcutaneous xenografts in immunocompromised mice. Tumour regression was observed, with a mean decrease in Δ tumour volume at day 45 of 90% compared to control, with a decrease in AUC for Δ tumour volume of 59%. One of the mice showed tumour shrinkage of > 98% between days 32 and 45, by which point the tumour was barely palpable at 0.001 cm^3. Another tumour from this treatment group weighed only 0.056 g at day 45. The treatment was well tolerated, as assessed using loss of body weight as a parameter for toxicity, although ulceration of the injection site was observed in two out of three animals.

There is no other data on the effect of doxorubicin-eluting microspheres in this type of model with which to compare these results. There have been a few animal studies investigating doxorubicin-eluting beads for liver cancer. Three of these employed the Vx-2 rabbit tumour model. Vx-2 tumours are carcinomas derived from a virus-induced rabbit papilloma, and are characterised by rapid growth (Kidd and Rous, 1940). Vx-2 tumour cells can successfully be implanted into the liver of rabbits, resulting in the growth of a tumour with a hypervascular blood supply, similar to that

of human liver tumours. The size of the animal enables embolisation therapy to the established tumour and so provides a good animal model for investigating the effects of TACE and DEB-TACE (Lee *et al*., 2009b). One study used DOXDEB of 100 – 300 μm diameters, and a doxorubicin dose of 2.6 – 3.2 mg/kg. Intratumoural doxorubicin concentration was 414 nM/g, 116 nM/g and 42 nM/g at 3, 7 and 14 days after treatment respectively. Necrosis was greatest at 7 days after treatment (Hong *et al*., 2006). Another study used Contour SE (Contour SE, Boston Scientific, Natick, Massachusetts) and two different prototype PVA microspheres (diameters 100 – 300 μm) and a doxorubicin dose of 1 mg/kg. Two days after treatment the intratumoural concentration of doxorubicin was 160 nM/g (Lee *et al*., 2008). More recently, a study using doxorubicin-loaded Quadraspheres (QuadraSphere^{s} microspheres; BioSphere Medical, Inc., Rockland, MA, USA) resulted in intratumoural concentrations of 50 nM/g at day 3 and 23 nM/g at day 7; in accordance with the DOXDEB study, necrosis was greatest 7 days after treatment (Lee *et al*., 2010).

Here tumour regression was observed from 9 days after treatment in the DOXDEB and RAPADOXDEB groups, which continued out to day 45. The observations from this thesis and the other studies mentioned suggest that it takes some days for doxorubicin to elute from the beads and concentrate in sufficient amounts for necrosis to occur. It is interesting to note that at day 37 there is increased cell proliferation in the untreated control group, and that this occurs 5 days prior to increased tumour regression in the doxorubicin-treated groups. Several of the mechanisms of cytotoxicity of doxorubicin are known to be dependent on cell division (Aubel-Sadron and Londos-Gagliardi, 1984), perhaps explaining the connection between these two events.

6.4.2 Rapamycin Monotherapies.

Monotherapy using RAPADEB was also shown to be an effective treatment using this model. Here, the observation was of a pattern of sustained inhibition of tumour growth, rather than tumour regression, with a mean decreases in tumour volume and tumour weight at day 45 of > 60% when compared to control; and a decrease in AUC for Δ tumour volume of 60%. The treatment was well tolerated and no ulceration was observed. Again, there is no comparable data from other studies available.

Monotherapy using low dose metronomic orally administered rapamycin demonstrated anti-tumoural activity across the time course of the experiment, and complete inhibition of tumour growth to day 28. As was the case with RAPADEB we observed a pattern of sustained inhibition of tumour growth rather than tumour regression, with a mean decrease in tumour volume and tumour weight at day 45 of almost 70% when compared to control, and a decrease in AUC for Δ tumour volume of 69%. The treatment was well tolerated. These findings are in accordance with several other published studies on mTOR inhibition for HCC. 2 mg/kg/day of oral rapamycin for 4 weeks was found to significantly reduce HCC growth and improve survival in an orthotopic allograft rat model, primarily *via* antiangiogenesis (Semela *et al*., 2007). 1 mg/kg/day oral rapamycin inhibited tumour growth in an orthotopic intraportal HepG2 mouse model in mice (Ong *et al*., 2009). This group used Micro-PET imaging and histological analysis to assess HCC inhibition, and concluded that rapamycin has anti-angiogenic activity towards both tumour and normal hepatocytes. Other studies using orthotopic highly metastatic mouse models of HCC found that 2 mg/kg/day of oral rapamycin for five weeks prevented growth and metastatic progression and downregulated the expression of HIF-1α (Wang *et al*., 2009c). Another group used a chemically-induced HCC model in rats, and found that

rapamycin at doses 1.5 mg/kg/day and 4.5 mg/kg/day "repressed the expression of HIF-1α and VEGF…. and significantly inhibited the growth and metastasis of HCC" and that there was no significant difference between these two doses (Wang *et al*., 2008b). Everolimus is a derivative of rapamycin which has improved aqueous solubility and bioavailability (Schuler *et al*., 1997), and suppresses tumour growth in subcutaneous HCC xenografts in mice (Tam *et al*., 2009, Huynh *et al*., 2008a).

In this experiment oral rapamycin inhibited the growth of HCC more effectively than RAPADOX. The elution kinetics of rapamycin from the microspheres has not been extensively investigated, although we know that the theoretical maximum possible eluted dose is 0.67 mg in total. Several studies have suggested that a continuous low dose rapamycin therapy is the most effective regimen for inhibiting tumour growth (Guba *et al*., 2005, Heuer *et al*., 2009, Wang *et al*., 2008b, O'Reilly *et al*., 2011). It has also been established that the anti-angiogenic activity of rapamycin is due to interference with signalling pathways outside of the tumour itself (Wang *et al*., 2008b, Semela *et al*., 2007). Rapamycin has a relatively long half-life of around 72 hours (Yatscoff *et al*., 1995), and there is some evidence from animal models and phase I clinical trials that weekly doses are as effective as daily doses although daily dosing regimens seem to be the most effective (Boulay *et al*., 2004, Tabernero *et al*., 2008, O'Donnell *et al*., 2008, Guba *et al*., 2005, Rizell *et al*., 2008). The optimal dosing regime is one that results in an effective and sustained inhibition of S6K. Higher doses may be less effective at S6K inhibition than lower doses (Guba *et al*., 2002, Heuer *et al*., 2009). Lower doses of rapamycin are obviously advantageous in terms of minimising adverse side effects associated with rapamycin. Phase I/II clinical trials investigating everolimus for unresectable HCC are underway (NCT00390195, NCT01374750, NCT00516165, NCT01035229), as are Phase II/III

clinical trials investigating sirolimus after liver transplant for HCC (NCT01374750, NCT00328770).

6.4.3 Combination Therapies.

Here we have shown that combination therapy using RAPADOXDEB had anti-tumoural activity against HCC tumours growing as subcutaneous xenografts in immunocompromised mice. Tumour inhibition was apparent from the start of treatment, and tumour regression was observed from day 32, with a mean decrease in Δ tumour volume at day 45 of > 90% compared to control, and a decrease in AUC for Δ tumour volume of 43%. Two of the mice in this group showed tumour reduction of > 99% between days 28 and 45, by which point the tumour was barely palpable at 0.001 cm^3. This treatment had a noticeable, though not significant, impact on mouse body weight. Ulceration of the injection site was observed in all three animals. There is no other data on rapamycin/doxorubicin co-loaded microspheres with which to compare these results.

Interestingly, the data for the individual mice treated with RAPADOXDEB shows wide inter-individual variability, with a noticeable increase in tumour volume between day 30 and day 32 in one animal. This may be due to Akt activation.

Both rapamycin and everolimus inhibit mTORC1 but not mTORC2 (Jacinto *et al.*, 2004), although this is not clear cut and specific effects vary with cell type, mutations to cell signalling pathways, and dosing regimens (Foster and Toschi, 2009, Huang and Manning, 2009, Zhou *et al.*, 2010a, Wander *et al.*, 2011). There is a concern that positive feedback from mTORC2 to Akt may improve tumour cell survival. It has been demonstrated that endothelial cell proliferation in hypoxia depends on both mTORC1 and mTORC2, so that rapamycin does not fully block angiogenesis, although reports are not consensual (Li *et al.*, 2007, Barilli *et al.*,

2008). Akt takes centre stage in the PI3K/Akt/mTOR pathway, with a vast array of effectors under its control (Foster and Fingar, 2010). The outcomes of Akt activation are anti-apoptotic and pro-proliferative cell survival strategies (Jiang and Liu, 2008a). There is some evidence to suggest that activation of Akt only occurs when higher doses of rapamycin/everolimus are used (Tabernero *et al*., 2008). We don't know what the intratumoural concentration of rapamycin is after the administration of rapamycin-loaded beads, but it is likely to be higher than after oral administration, possibly leading to Akt activation in tumour cells. However, whilst we saw increased tumour volume in the RAPADOXDEB group, the same effect was not seen in the RAPADEB group. Akt activation potentially has more than one impact on cell survival in this model, since it protects against doxorubicin-induced apoptosis in HepG2 cells (Alexia *et al*., 2006). Of course, the rapid increase in tumour volume was only observed in one of the mice and more work needs to be done before we can draw any conclusions.

The final combination treatment investigated was oral rapamycin and DOXDEB, which demonstrated the best anti-tumour activity over the time course of the experiment (Figure 6.4), with near-stable disease, and transient tumour regression. Tumour inhibition was apparent from the start of treatment. Tumour regression was observed at day 28, and complete inhibition of tumour growth from day 30 to day 35. However, from day 35 there was an increase in tumour volume. There was a mean decrease in Δ tumour volume at day 30 of > 60% compared to control, and a mean decrease in Δ tumour volume at day 45 of almost 90% compared to control. The decrease in AUC for Δ tumour volume was 88%. Ulceration of the injection site was observed in two animals. There was no significant body weight loss compared to any of the other groups and no significant difference in body weight between days of

treatment (Figure 6.5 and 6.6). At day 45 tumour cure was reported in one of the mice. There is no other data on oral rapamycin combined with doxorubicin-loaded microspheres with which to compare these results.

A few other groups have looked at doxorubicin in combination with mTOR inhibition. In accordance with our findings, combination treatments were found to be more successful at tumour inhibition than monotherapies. Piguet *et al* (2008) reported additive effects in an orthotopic syngeneic rat HCC model. Pegylated liposomal doxorubicin was injected intravenously every four days, with a starting dose of 4.5 mg/kg and subsequent doses of 1 mg/kg. Rapamycin was administered in drinking water at a dose of 2 mg/kg/day. Treatments were well tolerated. T/C after 30 days of treatment was reported as 52%, 56% and 27% for doxorubicin, rapamycin and both in combination respectively. Grunwald and colleagues (2002) reported additive effects in an ectopic xenograft mouse model of prostate cancer. Doxorubicin was administered i.v. as a single dose of 10 mg/kg and the rapamycin analogue CCI-779 was administered i.p. for 5 days at a dose of 10 mg/kg. T/C after 33 days of treatment was reported as 61%, 30% and 23% for doxorubicin, rapamycin and both in combination respectively. Recently, O'Reilly and co-workers (2011) investigated everolimus in combination with doxorubicin for the treatment of ectopic xenograft mouse models of lung and cervical cancers. For the cervical cancer model they reported a synergistic effect when 5 mg/kg/week doxorubicin i.v. was administered alongside 2.5 mg/kg/day everolimus p.o., and for the lung cancer model they reported an additive effect for the same doses. T/C after 16 days of treatment for the cervical cancer model was 6%, 43% and 1% for doxorubicin, rapamycin and both in combination respectively. T/C after 16 days of treatment for the lung cancer model was 31%, 17% and 7% for doxorubicin, rapamycin and both in combination

respectively. Body weight loss was reported after doxorubicin monotherapies, and was more pronounced in the lung cancer model, but was not exacerbated by everolimus – indeed, in the lung cancer model everolimus protected against body weight loss. Continuing everolimus treatment after a one off doxorubicin treatment inhibited tumour outgrowth in the cervical cancer model. The inhibitory effect of DOXDEB in combination with rapamycin p.o. over the 22 day treatment period is striking.

6.4.4 Tolerability.

An important aspect to a pre-clinical study is an initial assessment of drug toxicity. Drug combinations may have additive or synergistic effects with regard to side effects and toxicity, rendering them unsuitable for clinical use. Here we monitored change in mouse body weight as a parameter for toxicity, with measurements taken twice weekly. Regular observations were also made to ascertain any gross physiological or behavioural changes. We used this data to assess the tolerability of the drugs in combination compared to either drug alone.

6.4.4.1 Mouse Body Weight.

Comparisons between the control and treatment showed no significant differences in mouse body weight for any of the treatments at any time point (Figure 6.3), and no significant differences in % change in mouse body weight compared to weight at day 23 (Figure 6.4). Comparisons between the different time points within each treatment also showed no significant differences (multivariate ANOVA analysis, data not shown). Reduction in body weight was most pronounced in the mice treated with RAPADOXDEB. All the mice in this group were observed to have ulceration of the tumour injection site, and the weight loss may be connected to loss of appetite due to

general discomfort. We can conclude that body weight losses for all the treatments are within a tolerable range. However, it should be noted that tolerability data may not be accurate since the metabolism of the drug by the liver is not compromised by the presence of any underlying liver disease.

6.4.4.2 Ulceration.

Gross examination of the tumour injection site showed up localised ulceration, which in some cases was quite extensive. The ulceration was only associated with the application of beads loaded with doxorubicin, and is presumably due to its well recognised activity as a vesicant (causing blistering, ulceration and skin damage) if and when extravasation occurs (Schrijvers, 2003). Rapamycin-loaded microspheres did not cause ulceration, and it is therefore unlikely that either the bead itself or the alginate suspension were the cause. The fact that the beads are positioned subcutaneously and adjacent to the tumour means that extravasation is at least possible, or even likely. Ulceration after application of DOXDEB was reported in two mice, starting at day 37 and day 42 respectively. Ulceration after application of RAPADOXDEB was reported in all three mice starting at day 30, day 35 and day 37 respectively. Ulceration after application of DOXDEB in combination with oral rapamycin was reported in two mice, starting at day 28 and day 28 respectively. The ulceration seems to start earlier and occur more frequently when doxorubicin is used in combination with rapamycin. The ulceration amongst the mice in the RAPADOXDEB group was reported as being the most severe. The local concentration of rapamycin as eluted from the microsphere is likely to be much higher than from an oral dose. Rapamycin is known to impair wound healing by a number of different mechanisms (Ekici *et al*., 2007, Weinreich *et al*., 2011), and may well be exacerbating the effects of the vesicant activity of the doxorubicin.

6.4.5 Limitations of the Mouse Model.

There a several limitations regarding the use of this mouse model. Firstly, the tumours are implanted ectopically. This facilitates tumour measurement, but the tumour microenvironment is not accurately modelled, since the subcutaneous microenvironment is very different from the liver microenvironment. Interactions between the tumour cells and the graft site will affect the cell phenotype, the availability of growth factors and nutrients, microcirculation, angiogenesis and motility and invasiveness (Kubota, 1994, Fukumura *et al*., 1997, Cespedes *et al*., 2006, Kerbel, 2003). The sensitivity and responses of cancer cells to chemotherapeutics can therefore be altered according to the site of implantation (Fidler *et al*., 1994, Cespedes *et al*., 2006). However, for early pre-clinical studies where budgets are limited, ectopic mouse models are useful predictors of outcome. Interesting or promising results can then be investigated further using a more suitable animal model.

Secondly, the dose of doxorubicin delivered does not reflect the dose used in clinic. Here we used DEBs loaded with 25 mg/ml doxorubicin. 1 ml of DEB was then mixed with 3 ml of alginate solution, giving a final doxorubicin concentration of 6.25 mg/ml. 100 µl of DEB was injected for each treatment, equivalent to 0.625 mg doxorubicin/mouse. This represents a theoretical maximum dose of 30 mg/kg. The maximum recommended clinical dosage of doxorubicin in one procedure is 150 mg. For DEB-TACE 4 ml of 37.5 mg/ml doxorubicin DOXDEB are injected per embolisation. This represents a dose of 2 – 3 mg/kg, and no systemic doxorubicin-related toxicities at this dosage of DEB-TACE have been reported (Malagari, 2008). Animal studies have found that hepatic intra-arterial delivery of 3-4 mg doxorubicin/kg loaded into DEBs proves cytotoxic to cells at a locoregional site, and

is well tolerated by the animal (Lewis *et al*., 2006, Hong *et al*., 2006, Eyol *et al*., 2008). However, doses in the range 15 – 60 mg/kg 'were efficacious…..but induced significant hepato-toxicity, often leading to the death of the animal' (Eyol *et al*., 2008). We have delivered a theoretical maximum dose of 30 mg/kg. *In vivo* studies estimate that 43% of the drug is eluted from the bead 28 days after embolisation (Namur *et al*., 2010). The time course of our model ran out to 22 days, at which point we could expect < 50% of the drug, equivalent to < 15 mg/kg, to have eluted from the bead. Note that delivery was subcutaneous, so that the concentrations within the liver would not be as high as in the Eyol *et al* (2008) experiment; and that liver function in our experiment was not compromised by the presence of disease. So, whilst the delivered dose exceeds that used in the clinic, there is no evidence from the body weight data that it impacts on the general well-being of the mouse.

Thirdly, and perhaps most importantly, the delivery of DOXDEB is not intra-arterial or embolic. DEBs were injected as close to the tumour as possible, and delivered in an alginate solution in an attempt to stop the DEBS drifting away from the tumour. Regions of hypoxia will be present in the subcutaneous tumours once they reach a palpable size, and the presence of the beads may well disrupt the supply of blood to the tumour, but the mode of delivery does not model DEB-TACE and the resulting intra-tumoural anoxia or hypoxia. Since we are interested in the effects of chemotherapeutics on hypoxia-induced survival pathways, we would ideally use an animal model which allows DEB-TACE. As discussed above, the rabbit Vx-2 tumour model enables embolisation therapy to the established tumour. Previous experiments using this model demonstrate the existence of intrinsic intratumoural hypoxia (Rhee *et al*., 2007, Virmani *et al*., 2008), and show that TAE results in further increases in HIF-1α expression compared to control (Rhee *et al*., 2007), and

that post-TAE biopsy specimens have significantly higher HIF-1α levels than pre-TAE specimens from the same rabbit (Virmani *et al*., 2008). This model has been used to study DEB-TACE using doxorubicin-eluting microspheres (Hong *et al*., 2006, Lee *et al*., 2008, Lee *et al*., 2010). However, no investigations into mTOR inhibition in combination with DEB-TACE have yet been carried out using this model.

6.5 Conclusions.

In this study we evaluated tumour burden in a mouse model of HCC. Rapamycin monotherapies inhibited tumour growth for the duration of the experiment, and oral rapamycin inhibited tumour growth more effectively than RAPADEB, although the pattern of growth inhibition was the same for both treatments. DOXDEB inhibited tumour growth in a similar manner to RAPADEB up to day 32. We found that doxorubicin was necessary and sufficient for tumour regression, which occurred from day 32 in the DOXDEB and RAPADOXDEB groups. The most effective treatment overall was the combination of DOXDEB and oral rapamycin, which resulted in almost total inhibition of tumour growth to day 35; tumour regression day 28 to 30 and day 42 to 45; and complete tumour destruction reported in one animal by day 45. There was evidence of increased anti-tumoural activity with combination therapies compared to either treatment alone, and all treatments were well tolerated.

Chapter 7

Discussion.

Molecular oxygen is an essential substrate for eukaryotic cell respiration, and organisms have evolved a range of adaptive and protective mechanisms to survive episodes of decreased oxygen supply. The transcription factor HIF-1 regulates the expression of most of the genes involved in adaptations to hypoxia. The protein products of genes regulated by HIF-1 are involved in increasing oxygen availability and in regulating essential metabolic alterations that allow the cell and the organism to survive hypoxic conditions (Semenza, 2000a).

Intratumoural hypoxia is a feature of solid tumours, and hypoxia-derived angiogenesis is a requirement for tumour growth (Harris, 2002). Cellular adaptations to hypoxia potentially increases the malignancy of the cancer, since HIF-1 upregulates genes associated with increased survival, invasiveness, metastases and tumour growth; and radio- and chemo-therapy resistance (Huynh *et al*., 2009a, Maxwell *et al*., 2001; Unruh *et al*., 2003).

Hepatocellular carcinoma is a major cause of cancer-related mortality. Treatment options are limited by disease stage at diagnosis, and overall survival rates for inoperable HCC are poor (Sapra *et al*., 2011b). The current standard of care for intermediate HCC combines locoregional delivery of the chemotherapeutic doxorubicin with trans-arterial embolisation. Embolisation therapies result in the necrosis of cells exposed to severe hypoxia or anoxia, but also result in the escape and proliferation of those cells which adapt to hypoxia and display a hypoxia-resistant phenotype. Targeting HIF-1 presents an opportunity to improve treatment outcome for patients with HCC.

The majority of *in vitro* investigations are carried out at ambient (21%) oxygen, and do not properly model *in vivo* intratumoural physiology, wherein oxygen concentrations are likely to be much lower. The phenotypic alterations which occur as a result of hypoxia reduces the chemosensitivity of cancer cells via a number of different mechanisms (Dong *et al*., 2003, Tak *et al*., 2011, Erler *et al*., 2004, Baek *et al*., 2000; Comerford *et al*., 2002, Ding *et al*., 2010, Zhu *et al*., 2005). Toxic effects which are oxygen-dependent, as is the case with some of the anthracyclines, are also reduced in hypoxia (Gewirtz, 1999).

In this thesis *in vitro* investigations were carried out under both normoxic and hypoxic culture conditions. The HepG2 cell line was used as a model for HCC. Two drugs – doxorubicin and rapamycin - were investigated, both as monotherapies and in combination. Doxorubicin is the current standard of care for TACE and there is some evidence that doxorubicin inhibits the activity of HIF-1 in cancer cells. Rapamycin is currently under investigation as a treatment for HCC, and downregulates HIF-1α expression *via* suppression of mTOR (Land and Tee, 2007).

In addition to the potential for either one of these drugs to be used against HCC, there is also potential for using both in combination. The use of traditional chemotherapeutics in combination with therapies that target signalling pathways has been the subject of much recent investigation, and results from pre-clinical and clinical trials are encouraging. Whilst the cytotoxicity of the more traditional chemotherapeutic drugs depends on cell division, which has implications for other non-cancerous dividing cells in the body, drugs which target molecular pathways exert their effects on stromal tissues and cells and the processes which support tumour growth, as well as on tumour cells themselves. Rapamycin interferes with the PI3K/Akt/mTOR signalling pathway, a pathway that is known to play an important

role in cancer progression and is known to be dysregulated in around half of all HCCs (Sokolosky *et al*., 2011b). Rapamycin and doxorubicin have been demonstrated to have additive effects *in vivo* in murine models of liver, prostate, cervical and lung cancer (Piguet *et al*., 2008, O'Reilly *et al*., 2011, Grunwald *et al*., 2002).

The results from Chapter 3 demonstrate two important findings – that hypoxia protects cells from the cytotoxic effects of doxorubicin at doses of 5 μM and above; and that there is a biphasic effect where higher doses are significantly less effective against hypoxic HepG2 cells than the 10 μM treatment. 10 μM is as effective as higher doses in normoxic cells and so this study has identified a therapeutic window of 10 μM where doxorubicin inhibits cell proliferation of normoxic cells by ≈ 70% at 48 hours and ≈ 90% at 72 hours, and hypoxic cells by ≈ 60% at 48 hours and ≈ 80% at 72 hours (Figures 3.2 and 3.3). The differences in cell viability between normoxic and hypoxic cells are significant for 10 μM treatment at both these time points.

The results from Chapter 3 (Figure 3.5) clearly demonstrate that only the 50 μM dose of doxorubicin inhibits the hypoxia stimulated nuclear accumulation of HIF-1α. There are important experiments that need to be carried out for further elucidation of doxorubicin activity in hypoxic conditions. The first is to block the VHL pathway using the proteasome inhibitor MG132. The accumulation of HIF-1α after proteosome inhibition reflects the rate of synthesis of the protein and so it is possible to determine whether the abrogation of HIF-1α following 50 μM treatment is due to a reduction in the expression of the protein itself at the transcriptional or translational level, or if this concentration of doxorubicin stimulates the degradation of HIF-1α even in the absence of oxygen. It would also be interesting to observe the effects of doxorubicin on HIF-1α that has been stabilised in normoxia using a hypoxia mimetic

such as cobalt chloride or desferrioxamine. Experiments could then be carried out to determine the effects of doxorubicin on the expression of HIF-1α mRNA, and the effects of inhibiting translation using actinomycin D, a compound that inhibits protein synthesis (Wang *et al.,* 2009a). The data presented here indicates that the mechanism by which doxorubicin exerts its cytotoxic effect is distinct from the mechanism by which it inhibits HIF-1α.

An important next step will be to determine what effect 10 μM doxorubicin has on the expression of genes downstream of HIF-1, and whether doxorubicin interferes with the transcriptional activity of HIF-1, as has been reported in Hep3B cells (Lee *et al*., 2009a).

Hypoxia-induced mechanisms of resistance to doxorubicin include reduced drug accumulation and increased drug efflux (Comerford *et al*., 2002, Ding *et al*., 2010, Zhu *et al*., 2005); resistance to apoptosis (Dong *et al*., 2003, Erler *et al*., 2004, Lechanteur *et al*., 2005, Piret *et al*., 2002a); decreased levels of topoisomerase II (Tomida and Tsuruo, 1999, Ogiso *et al*., 2000); and a reduction in free radical-dependant DNA damage (Potmesil *et al*., 1983, Smith *et al*., 1980, Tannock, 1982, Rharass *et al*., 2008).

NFkB activation and post-translational modification and the consequent effects of NFkB activation on apoptosis, seems to vary with cell type and with the NFkB inducer (Cho *et al*., 2008, Perkins, 2006). Looking at Figure 3.6, there would appear to be a difference in post translational modification of NFkB under hypoxia when compared to doxorubicin treatment. Doxorubicin-activated NFkB has been reported to be both anti-apoptotic (Bednarski *et al*., 2008, Chiao *et al*., 2002) and pro-apoptotic (Wang *et al*., 2011). Basal levels of NFkB have been reported to increase resistance to doxorubicin (Gangadharan *et al*., 2009) and overexpression of VHL

protein increased the sensitivity of cells to doxorubicin in a mouse model of HCC (Wang *et al*., 2010). In this study doxorubicin was found to activate NFkB in normoxic cells. However, hypoxia was also observed to activate NFkB, and after doxorubicin treatment of hypoxic cells no further activation was observed (Figure 3.6). It would be interesting to explore whether activation of NFkB by doxorubicin has pro-apoptotic consequences, and activation of NFkB by hypoxia has anti-apoptotic consequences in HepG2 cells.

However, the key finding from these investigations into doxorubicin and cell viability is the identification of 10 µM as a dose which is efficacious against both normoxic and hypoxic cells. This 10 µM dose is commensurate with concentrations of doxorubicin that are eluted from DC Beads at distances of up to 350 µm and 600 µm in animal models, and where tissue necrosis was associated with penetration and concentration of doxorubicin (Reddy *et al*., 2010, Namur *et al*., 2008a). Evidence from the clinic suggests that effective concentrations of doxorubicin are eluted for up to 40 days post DEB-TACE (Moschouris *et al*., 2010). This is in accordance with the findings from the *in vivo* study presented in this thesis, where the application of doxorubicin-eluting microspheres significantly inhibited the growth of an ectopic xenograft tumour in a mouse model of HCC (Figure 6.1 and 6.2). It should be noted, however, that in this animal study, the tumour xenografts are subcutaneous and ectopic, so embolisation is not accurately modelled, and this will have an impact on intratumoural hypoxia.

Following on from investigations into the effects of doxorubicin on normoxic and hypoxic HepG2 cells, the next stage of this thesis was concerned with the impact of rapamycin treatment. The effect of rapamycin on cell viability in normoxic and hypoxic cells was most noticeable after 48 hours (Figure 4.2). The minimum

concentration of rapamycin effective against normoxic cells was 10 nM, whilst for hypoxic cells the minimum effective concentration was 100 nM (Figure 4.2). After 72 hours, the single dose of rapamycin had ceased to have an effect (Figure 4.3). Again, hypoxia protected the cells against the effects of rapamycin on cell viability. Both 10 nM and 100 nM rapamycin inhibited the hypoxia stimulated nuclear accumulation of HIF-1α, although 100 nM was more effective (Figure 4.5). Hypoxia did not result in a reduction in phosphorylation of p70 S6K, but rapamycin inhibited phosphorylation of p70 S6K in both normoxic and hypoxic cells. This suggests that the mechanism by which rapamycin inhibits cell viability is due to a reduction in cell growth and proliferation, being cytostatic rather than cytotoxic. This is supported by the fact that at 72 hours, the inhibitory effects of rapamycin were abolished.

The effects of rapamycin as a monotherapy in the *in vivo* studies presented here are quite striking. Oral rapamycin appears to be more effective than rapamycin delivered loco-regionally and this may reflect the effects of rapamycin on inhibition of angiogenic signalling pathways in stromal cells (Figure 6.1 and 6.2).

Finally, the effects of combined doxorubicin and rapamycin treatments were investigated. The addition of rapamycin to doxorubicin consistently led to a further decrease in cell viability (Figures 5.1 – 5.6). Spiking the cells with rapamycin every 24 hours, or pre-treatment with rapamycin before the addition of doxorubicin should be investigated, as this may increase the additive effects that were observed after a single application of rapamycin.

Paradoxically, the addition of rapamycin to doxorubicin treated cells appeared to abrogate any inhibitory effects of either drug as monotherapy on the nuclear accumulation of hypoxia stimulated HIF-1α, although these results were not statistically significant (Figure 5.7). Doxorubicin had no effect on the

phosphorylation of p70 S6K, which suggests that the inhibition of HIF-1α occurs by a different pathway or mechanism than inhibition of HIF-1α by rapamycin (Figure 3.7).

In vivo, the combination of oral rapamycin and loco-regional delivery of doxorubicin was the most effective of all the treatment regimens investigated. The combined loco-regional delivery was as effective at day 45, but the disease control across the time course of the experiment was not seen Figure 6.1).

Little is yet know about the effect of doxorubicin/rapamycin combinations on the health of cardiomyocytes. The role of mTOR signalling in the survival of both cancer cells and cardiomyocytes could lead to off-target effects which potentially increase doxorubicin-induced cardiotoxicity (Xiang *et al*., 2011), or inhibit wound healing (Ekici *et al*., 2007, Weinreich *et al*., 2011).

Further studies are needed on the anti-tumoural activity of combinations of doxorubicin DEB-TACE and low dose oral rapamycin, preferably using an animal model that allows true embolisation of an orthotopic HCC. Immunohistochemical analysis of post mortem tumour samples could improve the understanding of the molecular mechanisms involved.

Clinical trials using DEBDOX in combination with oral administration of everolimus have recently begun. In Switzerland, the 'Phase I Open Label/Phase II Randomized, Double Blind, Multicentre Trial investigating the combination of Everolimus and Transarterial Chemoembolization with Doxorubicin Versus Transarterial Chemoembolization with Doxorubicin Alone in Patients With Hepatocellular Carcinoma' (NCT01009801) is currently recruiting participants. This study is chaired by Jean-Francois Dufour, MD (University Hospital Inselspital, Berne), for the Swiss

Group for Clinical Cancer Research. Phase I will determine the recommended dose of everolimus in patients with HCC treated with DEBDOX TACE, and Phase II will determine the efficacy and tolerability of everolimus in patients with HCC treated with TACE as compared to TACE alone. Entry criteria include confirmed HCC at Intermediate stage B (according to BCLC classification), a Child Pugh score < 8, and no tumour involvement in > 50% of the liver. Patients with advanced disease, presence or history of metastatic spread, or those awaiting OLT will not be included. The expected enrolment is 98 patients, from eight clinics in Switzerland. Phase I is a dose escalation study, where patients receive oral everolimus once daily, followed by DEBDOX TACE seven days later. After one month an MRI scan will be carried out. If a viable tumour is detected then patients will undergo TACE treatment monthly for up to five treatments. Phase II is a randomised two arm study. Arm I patients will receive an oral placebo once daily for up to 12 months, and undergo DEBDOX TACE as in phase I at the maximum tolerated dose (MTD). Arm II patients will receive oral everolimus once daily for up to 12 months, and undergo DEBDOX TACE as in phase I at the maximum tolerated dose (MTD). Primary Outcomes are dose limiting toxicity (Phase I), and time to progression (Phase II). Secondary Outcomes include adverse events, tumour response, progression-free survival at 12 months and overall survival. The start date was February 2010, and the estimated primary completion date is September 2012.

The second clinical trial is based in Asia. The 'Phase II Randomized, Double-blind, Multicenter Asian Study Investigating the Combination of Transcatheter Arterial Chemoembolization (TACE) and Oral Everolimus (RAD001, Afinitor®) in Localised Unresectable Hepatocellular Carcinoma (HCC) - The TRACER Study' (NCT01379521), chaired by Professor Ronnie Poon and Novartis Pharmaceuticals,

started in June 2011 and is not yet recruiting participants. The Primary Outcome is time to progression, and Secondary Outcomes include overall response rate, disease control rate, overall survival, tumour response and adverse events. The estimated enrolment is 80 patients, recruited from Hong Kong, Taiwan, Thailand and the Republic of Korea. This is a two arm study, where one arm will receive everolimus with DEBDOX TACE, and the other will receive everolimus placebo with DEBDOX TACE. Entry criteria, as in the Swiss study, include confirmed HCC at Intermediate stage B. The estimated primary completion date is January 2013.

If cancer cells with a hypoxic phenotype, as well as cancer cells with a normoxic phenotype, can be successfully targeted by specific drug regimens, as has been indicated by the data presented in this thesis, there is the possibility of improving the outcome of patients suffering from primary liver cancer, a disease which at present has a dismal prognosis.

References.

ACKERMAN, N. B. 1972. Experimental studies on the circulation dynamics of intrahepatic tumor blood supply. *Cancer,* 29**,** 435-9.

AHN, K. S., SETHI, G. & AGGARWAL, B. B. 2008. Reversal of chemoresistance and enhancement of apoptosis by statins through down-regulation of the NF-kappaB pathway. *Biochem Pharmacol,* 75**,** 907-13.

AL-RAWASHDEH, F. Y., SCRIVEN, P., CAMERON, I. C., VERGANI, P. V. & WYLD, L. 2010. Unfolded protein response activation contributes to chemoresistance in hepatocellular carcinoma. *Eur J Gastroenterol Hepatol,* 22**,** 1099-105.

ALEXIA, C., BRAS, M., FALLOT, G., VADROT, N., DANIEL, F., LASFER, M., TAMOUZA, H. & GROYER, A. 2006. Pleiotropic effects of PI-3' kinase/Akt signaling in human hepatoma cell proliferation and drug-induced apoptosis. *Ann N Y Acad Sci,* 1090**,** 1-17.

APRELIKOVA, O., CHANDRAMOULI, G. V., WOOD, M., VASSELLI, J. R., RISS, J., MARANCHIE, J. K., LINEHAN, W. M. & BARRETT, J. C. 2004. Regulation of HIF prolyl hydroxylases by hypoxia-inducible factors. *J Cell Biochem,* 92**,** 491-501.

ARATANI, Y., ANDOH, T. & KOYAMA, H. 1996. Effects of DNA topoisomerase inhibitors on nonhomologous and homologous recombination in mammalian cells. *Mutat Res,* 362**,** 181-91.

ARCECI, R. J., STIEGLITZ, K. & BIERER, B. E. 1992. Immunosuppressants FK506 and rapamycin function as reversal agents of the multidrug resistance phenotype. *Blood,* 80**,** 1528-36.

ARSHAM, A. M., HOWELL, J. J. & SIMON, M. C. 2003. A novel hypoxia-inducible factor-independent hypoxic response regulating mammalian target of rapamycin and its targets. *J Biol Chem,* 278**,** 29655-60.

ARSURA, M. & CAVIN, L. G. 2005. Nuclear factor-kappaB and liver carcinogenesis. *Cancer Lett,* 229**,** 157-69.

AUBEL-SADRON, G. & LONDOS-GAGLIARDI, D. 1984. Daunorubicin and doxorubicin, anthracycline antibiotics, a physicochemical and biological review. *Biochimie,* 66**,** 333-52.

AVELLINO, R., ROMANO, S., PARASOLE, R., BISOGNI, R., LAMBERTI, A., POGGI, V., VENUTA, S. & ROMANO, M. F. 2005. Rapamycin stimulates apoptosis of childhood acute lymphoblastic leukemia cells. *Blood,* 106**,** 1400-6.

AVERBUCH, S. D., GAUDIANO, G., KOCH, T. H. & BACHUR, N. R. 1985. Radical dimer rescue of toxicity and improved therapeutic index of adriamycin in tumor-bearing mice. *Cancer Res,* 45**,** 6200-4.

BAEK, J. H., JANG, J. E., KANG, C. M., CHUNG, H. Y., KIM, N. D. & KIM, K. W. 2000. Hypoxia-induced VEGF enhances tumor survivability via suppression of serum deprivation-induced apoptosis. *Oncogene,* 19**,** 4621-31.

BARILLI, A., VISIGALLI, R., SALA, R., GAZZOLA, G. C., PAROLARI, A., TREMOLI, E., BONOMINI, S., SIMON, A., CLOSS, E. I., DALL'ASTA, V. & BUSSOLATI, O. 2008. In human endothelial cells rapamycin causes mTORC2 inhibition and impairs cell viability and function. *Cardiovasc Res,* 78**,** 563-71.

BATISTA, A., BARATA, J. T., RADERSCHALL, E., SALLAN, S. E., CARLESSO, N., NADLER, L. M. & CARDOSO, A. A. 2011. Targeting of

active mTOR inhibits primary leukemia T cells and synergizes with cytotoxic drugs and signaling inhibitors. *Exp Hematol,* 39**,** 457-472 e3.

BECK, W. T., DANKS, M. K., WOLVERTON, J. S., GRANZEN, B., CHEN, M., SCHMIDT, C. A., BUGG, B. Y., FRICHE, E. & SUTTLE, D. P. 1993. Altered DNA topoisomerase II in multidrug resistance. *Cytotechnology,* 11**,** 115-9.

BEDNARSKI, B. K., DING, X., COOMBE, K., BALDWIN, A. S. & KIM, H. J. 2008. Active roles for inhibitory kappaB kinases alpha and beta in nuclear factor-kappaB-mediated chemoresistance to doxorubicin. *Mol Cancer Ther,* 7**,** 1827-35.

BENCHEKROUN, M. N., POURQUIER, P., SCHOTT, B. & ROBERT, J. 1993a. Doxorubicin-induced lipid peroxidation and glutathione peroxidase activity in tumor cell lines selected for resistance to doxorubicin. *Eur J Biochem,* 211**,** 141-6.

BENCHEKROUN, M. N., SINHA, B. K. & ROBERT, J. 1993b. Doxorubicin-induced oxygen free radical formation in sensitive and doxorubicin-resistant variants of rat glioblastoma cell lines [corrected and republished erratum originally printed in FEBS Lett 1993 May 17;322(3):295-8]. *FEBS Lett,* 326**,** 302-5.

BEPPU, K., NAKAMURA, K., LINEHAN, W. M., RAPISARDA, A. & THIELE, C. J. 2005. Topotecan blocks hypoxia-inducible factor-1alpha and vascular endothelial growth factor expression induced by insulin-like growth factor-I in neuroblastoma cells. *Cancer Res,* 65**,** 4775-81.

BERGER, J. M. & WANG, J. C. 1996. Recent developments in DNA topoisomerase II structure and mechanism. *Curr Opin Struct Biol,* 6**,** 84-90.

BERLIN, V. & HASELTINE, W. A. 1981. Reduction of adriamycin to a semiquinone-free radical by NADPH cytochrome P-450 reductase produces DNA cleavage in a reaction mediated by molecular oxygen. *J Biol Chem,* 256**,** 4747-56.

BERRA, E., BENIZRI, E., GINOUVES, A., VOLMAT, V., ROUX, D. & POUYSSEGUR, J. 2003. HIF prolyl-hydroxylase 2 is the key oxygen sensor setting low steady-state levels of HIF-1alpha in normoxia. *Embo J,* 22**,** 4082-90.

BIOLATO, M., MARRONE, G., RACCO, S., DI STASI, C., MIELE, L., GASBARRINI, G., LANDOLFI, R. & GRIECO, A. 2010. Transarterial chemoembolization (TACE) for unresectable HCC: a new life begins? *Eur Rev Med Pharmacol Sci,* 14**,** 356-62.

BISELLI, M., ANDREONE, P., GRAMENZI, A., TREVISANI, F., CURSARO, C., ROSSI, C., RICCA ROSELLINI, S., CAMMA, C., LORENZINI, S., STEFANINI, G. F., GASBARRINI, G. & BERNARDI, M. 2005. Transcatheter arterial chemoembolization therapy for patients with hepatocellular carcinoma: a case-controlled study. *Clin Gastroenterol Hepatol,* 3**,** 918-25.

BLAGOSKLONNY, M. V., AN, W. G., ROMANOVA, L. Y., TREPEL, J., FOJO, T. & NECKERS, L. 1998. p53 inhibits hypoxia-inducible factor-stimulated transcription. *J Biol Chem,* 273**,** 11995-8.

BOLD, R. J., TERMUHLEN, P. M. & MCCONKEY, D. J. 1997. Apoptosis, cancer and cancer therapy. *Surg Oncol,* 6**,** 133-42.

BOLES, T. C., WHITE, J. H. & COZZARELLI, N. R. 1990. Structure of plectonemically supercoiled DNA. *J Mol Biol,* 213**,** 931-51.

BONADONNA, G., MONFARDINI, S., DE LENA, M. & FOSSATI-BELLANI, F. 1969. Clinical evaluation of adriamycin, a new antitumour antibiotic. *Br Med J,* 3**,** 503-6.

BOS, R., VAN DER GROEP, P., GREIJER, A. E., SHVARTS, A., MEIJER, S., PINEDO, H. M., SEMENZA, G. L., VAN DIEST, P. J. & VAN DER WALL, E. 2003. Levels of hypoxia-inducible factor-1alpha independently predict prognosis in patients with lymph node negative breast carcinoma. *Cancer,* 97**,** 1573-81.

BOULAY, A., ZUMSTEIN-MECKER, S., STEPHAN, C., BEUVINK, I., ZILBERMANN, F., HALLER, R., TOBLER, S., HEUSSER, C., O'REILLY, T., STOLZ, B., MARTI, A., THOMAS, G. & LANE, H. A. 2004. Antitumor efficacy of intermittent treatment schedules with the rapamycin derivative RAD001 correlates with prolonged inactivation of ribosomal protein S6 kinase 1 in peripheral blood mononuclear cells. *Cancer Res,* 64**,** 252-61.

BOULIN, M., GUIU, S., CHAUFFERT, B., AHO, S., CERCUEIL, J. P., GHIRINGHELLI, F., KRAUSE, D., FAGNONI, P., HILLON, P., BEDENNE, L. & GUIU, B. 2011. Screening of anticancer drugs for chemoembolization of hepatocellular carcinoma. *Anticancer Drugs,* 22**,** 741-8.

BRADFORD, M. M. 1976. A rapid and sensitive method for the quantitation of microgram quantities of protein utilizing the principle of protein-dye binding. *Anal Biochem,* 72**,** 248-54.

BRAHIMI-HORN, C. & POUYSSEGUR, J. 2006. The role of the hypoxia-inducible factor in tumor metabolism growth and invasion. *Bull Cancer,* 93**,** E73-80.

BREEDIS, C. & YOUNG, G. 1954. The blood supply of neoplasms in the liver. *Am J Pathol,* 30**,** 969-77.

BRUGAROLAS, J., LEI, K., HURLEY, R. L., MANNING, B. D., REILING, J. H., HAFEN, E., WITTERS, L. A., ELLISEN, L. W. & KAELIN, W. G., JR. 2004. Regulation of mTOR function in response to hypoxia by REDD1 and the TSC1/TSC2 tumor suppressor complex. *Genes Dev,* 18**,** 2893-904.

BRUICK, R. K. & MCKNIGHT, S. L. 2001. A conserved family of prolyl-4-hydroxylases that modify HIF. *Science,* 294**,** 1337-40.

BRUIX, J., HESSHEIMER, A. J., FORNER, A., BOIX, L., VILANA, R. & LLOVET, J. M. 2006. New aspects of diagnosis and therapy of hepatocellular carcinoma. *Oncogene,* 25**,** 3848-56.

BRUIX, J., SALA, M. & LLOVET, J. M. 2004. Chemoembolization for hepatocellular carcinoma. *Gastroenterology,* 127**,** S179-88.

BURGESS, D. J., DOLES, J., ZENDER, L., XUE, W., MA, B., MCCOMBIE, W. R., HANNON, G. J., LOWE, S. W. & HEMANN, M. T. 2008. Topoisomerase levels determine chemotherapy response in vitro and in vivo. *Proc Natl Acad Sci U S A,* 105**,** 9053-8.

CARMELIET, P., DOR, Y., HERBERT, J. M., FUKUMURA, D., BRUSSELMANS, K., DEWERCHIN, M., NEEMAN, M., BONO, F., ABRAMOVITCH, R., MAXWELL, P., KOCH, C. J., RATCLIFFE, P., MOONS, L., JAIN, R. K., COLLEN, D. & KESHERT, E. 1998. Role of HIF-1alpha in hypoxia-mediated apoptosis, cell proliferation and tumour angiogenesis. *Nature,* 394**,** 485-90.

CARTER, S. & MARTIN II, R. C. 2009. Drug-eluting bead therapy in primary and metastatic disease of the liver. *HPB (Oxford),* 11**,** 541-50.

CASTROAGUDIN, J. F., MOLINA-PEREZ, E., FERREIRO-IGLESIAS, R. & VARO-PEREZ, E. 2011. Strategies of immunosuppression for liver transplant recipients with hepatocellular carcinoma. *Transplant Proc,* 43**,** 711-3.

CESPEDES, M. V., CASANOVA, I., PARRENO, M. & MANGUES, R. 2006. Mouse models in oncogenesis and cancer therapy. *Clin Transl Oncol,* 8**,** 318-29.

CHANG, H., SHYU, K. G., LEE, C. C., TSAI, S. C., WANG, B. W., HSIEN LEE, Y. & LIN, S. 2003. GL331 inhibits HIF-1alpha expression in a lung cancer model. *Biochem Biophys Res Commun,* 302**,** 95-100.

CHANG, Q., QIN, R. Y., HUANG, T., GAO, J. & FENG, Y. P. 2006. Effect of antisense hypoxia-inducible factor 1 alpha on progression, metastasis, and chemosensitivity of pancreatic cancer. *Pancreas,* 32**,** 297-305.

CHAPMAN-SMITH, A., LUTWYCHE, J. K. & WHITELAW, M. L. 2004. Contribution of the Per/Arnt/Sim (PAS) domains to DNA binding by the basic helix-loop-helix PAS transcriptional regulators. *J Biol Chem,* 279**,** 5353-62.

CHEN, D., LI, M., LUO, J. & GU, W. 2003. Direct interactions between HIF-1 alpha and Mdm2 modulate p53 function. *J Biol Chem,* 278**,** 13595-8.

CHEN, J. & FANG, Y. 2002. A novel pathway regulating the mammalian target of rapamycin (mTOR) signaling. *Biochem Pharmacol,* 64**,** 1071-7.

CHEN, J. S., WANG, Q., FU, X. H., HUANG, X. H., CHEN, X. L., CAO, L. Q., CHEN, L. Z., TAN, H. X., LI, W., BI, J. & ZHANG, L. J. 2009a. Involvement of PI3K/PTEN/AKT/mTOR pathway in invasion and metastasis in hepatocellular carcinoma: Association with MMP-9. *Hepatol Res,* 39**,** 177-86.

CHEN, L., FENG, P., LI, S., LONG, D., CHENG, J., LU, Y. & ZHOU, D. 2009b. Effect of hypoxia-inducible factor-1alpha silencing on the sensitivity of human brain glioma cells to doxorubicin and etoposide. *Neurochem Res,* 34**,** 984-90.

CHENG, A. L., KANG, Y. K., CHEN, Z., TSAO, C. J., QIN, S., KIM, J. S., LUO, R., FENG, J., YE, S., YANG, T. S., XU, J., SUN, Y., LIANG, H., LIU, J., WANG, J., TAK, W. Y., PAN, H., BUROCK, K., ZOU, J., VOLIOTIS, D. & GUAN, Z. 2009. Efficacy and safety of sorafenib in patients in the Asia-Pacific region with advanced hepatocellular carcinoma: a phase III randomised, double-blind, placebo-controlled trial. *Lancet Oncol,* 10**,** 25-34.

CHENGCHENG HUANG MENGCHAO WU, G. X., DAIZHONG LI, HAN CHENG, ZHENGXING TU, HUIQIU JIANG, JIANREN GU 1992. Overexpression of the MDRl Gene and P-Glycoprotein in Human Hepatocellular Carcinoma. *Journal of the National Cancer Institute,* Vol. 84**,** 262-263.

CHEVROLLIER, A., LOISEAU, D., GAUTIER, F., MALTHIERY, Y. & STEPIEN, G. 2005. ANT2 expression under hypoxic conditions produces opposite cell-cycle behavior in 143B and HepG2 cancer cells. *Mol Carcinog,* 42**,** 1-8.

CHIAO, P. J., NA, R., NIU, J., SCLABAS, G. M., DONG, Q. & CURLEY, S. A. 2002. Role of Rel/NF-kappaB transcription factors in apoptosis of human hepatocellular carcinoma cells. *Cancer,* 95**,** 1696-705.

CHICHE, J., BRAHIMI-HORN, M. C. & POUYSSEGUR, J. 2010. Tumour hypoxia induces a metabolic shift causing acidosis: a common feature in cancer. *J Cell Mol Med,* 14**,** 771-94.

CHOI, J., CHEN, J., SCHREIBER, S. L. & CLARDY, J. 1996. Structure of the FKBP12-rapamycin complex interacting with the binding domain of human FRAP. *Science,* 273**,** 239-42.

CHOI, K. O., LEE, T., LEE, N., KIM, J. H., YANG, E. G., YOON, J. M., KIM, J. H., LEE, T. G. & PARK, H. 2005. Inhibition of the catalytic activity of hypoxia-inducible factor-1alpha-prolyl-hydroxylase 2 by a MYND-type zinc finger. *Mol Pharmacol,* 68**,** 1803-9.

CHOI, Y. J., RHO, J. K., LEE, S. J., JANG, W. S., LEE, S. S., KIM, C. H. & LEE, J. C. 2009. HIF-1alpha modulation by topoisomerase inhibitors in non-small cell lung cancer cell lines. *J Cancer Res Clin Oncol,* 135**,** 1047-53.

CHRESTA, C. M., ARRIOLA, E. L. & HICKMAN, J. A. 1996. Apoptosis and cancer chemotherapy. *Behring Inst Mitt***,** 232-40.

CHU, E. C. & TARNAWSKI, A. S. 2004. PTEN regulatory functions in tumor suppression and cell biology. *Med Sci Monit,* 10**,** RA235-41.

CITRON, S., DUPUIS, M., GALLARDO, E. & WHEELER, S. 2008. Doxorubicin-loaded LC Bead chemoembolisation for HCC (Precision Tace): Assessment of tumour necrosis with imaging and histological follow-up. *International Liver CancerAssociation 2008.* Chicago USA.

COLEMAN, C. N., MITCHELL, J. B. & CAMPHAUSEN, K. 2002. Tumor hypoxia: chicken, egg, or a piece of the farm? *J Clin Oncol,* 20**,** 610-5.

COLOMBO, M. & SANGIOVANNI, A. 2003. Etiology, natural history and treatment of hepatocellular carcinoma. *Antiviral Res,* 60**,** 145-50.

COMERFORD, K. M., WALLACE, T. J., KARHAUSEN, J., LOUIS, N. A., MONTALTO, M. C. & COLGAN, S. P. 2002. Hypoxia-inducible factor-1-dependent regulation of the multidrug resistance (MDR1) gene. *Cancer Res,* 62**,** 3387-94.

CORY, A. H., OWEN, T. C., BARLTROP, J. A. & CORY, J. G. 1991. Use of an aqueous soluble tetrazolium/formazan assay for cell growth assays in culture. *Cancer Commun,* 3**,** 207-12.

CREIGHTON-GUTTERIDGE, M., CARDELLINA, J. H., 2ND, STEPHEN, A. G., RAPISARDA, A., URANCHIMEG, B., HITE, K., DENNY, W. A., SHOEMAKER, R. H. & MELILLO, G. 2007. Cell type-specific, topoisomerase II-dependent inhibition of hypoxia-inducible factor-1alpha protein accumulation by NSC 644221. *Clin Cancer Res,* 13**,** 1010-8.

CULLINANE, C. & PHILLIPS, D. R. 1990. Induction of stable transcriptional blockage sites by adriamycin: GpC specificity of apparent adriamycin-DNA adducts and dependence on iron(III) ions. *Biochemistry,* 29**,** 5638-46.

D'ANGELO, G., DUPLAN, E., BOYER, N., VIGNE, P. & FRELIN, C. 2003. Hypoxia up-regulates prolyl hydroxylase activity: a feedback mechanism that limits HIF-1 responses during reoxygenation. *J Biol Chem,* 278**,** 38183-7.

DAI, M., MIAO, Z. H., REN, X., TONG, L. J., YANG, N., LI, T., LIN, L. P., SHEN, Y. M. & DING, J. 2010. MFTZ-1 reduces constitutive and inducible HIF-1alpha accumulation and VEGF secretion independent of its topoisomerase II inhibition. *J Cell Mol Med,* 14**,** 2281-91.

DANCEY, J. E. 2006. Therapeutic targets: MTOR and related pathways. *Cancer Biol Ther,* 5**,** 1065-73.

DASKALOW, K., ROHWER, N., RASKOPF, E., DUPUY, E., KUHL, A., LODDENKEMPER, C., WIEDENMANN, B., SCHMITZ, V. & CRAMER, T. 2010. Role of hypoxia-inducible transcription factor 1alpha for progression

and chemosensitivity of murine hepatocellular carcinoma. *J Mol Med,* 88**,** 817-27.

DE MILITO, A. & FAIS, S. 2005. Tumor acidity, chemoresistance and proton pump inhibitors. *Future Oncol,* 1**,** 779-86.

DECAENS, T. A. L., E. ITTI, A. HULIN, M. HURTOVA, A. LAURENT, D. CHERQUI, A. MALLAT, C. DUVOUX. Year. Pilot study of sirolimus in cirrhotic patients with advanced hepatocellular carcinoma. In: *Gastrointestinal Cancers Symposium, 2009* San Francisco, USA.

DEYOUNG, M. P., HORAK, P., SOFER, A., SGROI, D. & ELLISEN, L. W. 2008. Hypoxia regulates TSC1/2-mTOR signaling and tumor suppression through REDD1-mediated 14-3-3 shuttling. *Genes Dev,* 22**,** 239-51.

DHANASEKARAN, R., KOOBY, D. A., STALEY, C. A., KAUH, J. S., KHANNA, V. & KIM, H. S. 2010. Comparison of conventional transarterial chemoembolization (TACE) and chemoembolization with doxorubicin drug eluting beads (DEB) for unresectable hepatocelluar carcinoma (HCC). *J Surg Oncol,* 101**,** 476-80.

DI BISCEGLIE, A. M. 1995. Hepatitis C and hepatocellular carcinoma. *Semin Liver Dis,* 15**,** 64-9.

DILLS, W. L., JR. 1993. Nutritional and physiological consequences of tumour glycolysis. *Parasitology,* 107 Suppl**,** S177-86.

DING, J., GAO, Y., LIU, R., XU, F. & LIU, H. 2011. Association of PTEN polymorphisms with susceptibility to hepatocellular carcinoma in a Han Chinese population. *DNA Cell Biol,* 30**,** 229-34.

DING, Z., YANG, L., XIE, X., XIE, F., PAN, F., LI, J., HE, J. & LIANG, H. 2010. Expression and significance of hypoxia-inducible factor-1 alpha and MDR1/P-glycoprotein in human colon carcinoma tissue and cells. *J Cancer Res Clin Oncol,* 136**,** 1697-707.

DONG-DONG, L., XI-RAN, Z. & XIANG-RONG, C. 2003. Expression and significance of new tumor suppressor gene PTEN in primary liver cancer. *J Cell Mol Med,* 7**,** 67-71.

DONG, Z., WANG, J. Z., YU, F. & VENKATACHALAM, M. A. 2003. Apoptosis-resistance of hypoxic cells: multiple factors involved and a role for IAP-2. *Am J Pathol,* 163**,** 663-71.

DOROSHOW, J. H. 1983. Anthracycline antibiotic-stimulated superoxide, hydrogen peroxide, and hydroxyl radical production by NADH dehydrogenase. *Cancer Res,* 43**,** 4543-51.

DREHER, M., SHARMER, K., ORANDI, B., DONAHUE, D., TANG, Y., LEWIS, A., KARANIAN, J., CHIESAS, O., PRITCHARD, W. & WOOD, B. 2009. Distribution of Image-Able Beads and Doxorubicin Following Transcatheter Arterial Chemoembolisation. *Journal of Vascular and Interventional Radiology.,* Volume 20**,** S104.

DREVS, J., FAKLER, J., EISELE, S., MEDINGER, M., BING, G., ESSER, N., MARME, D. & UNGER, C. 2004. Antiangiogenic potency of various chemotherapeutic drugs for metronomic chemotherapy. *Anticancer Res,* 24**,** 1759-63.

DU, G., LIN, H., WANG, M., ZHANG, S., WU, X., LU, L., JI, L. & YU, L. 2010. Quercetin greatly improved therapeutic index of doxorubicin against 4T1 breast cancer by its opposing effects on HIF-1alpha in tumor and normal cells. *Cancer Chemother Pharmacol,* 65**,** 277-87.

DUFNER, A., ANDJELKOVIC, M., BURGERING, B. M., HEMMINGS, B. A. & THOMAS, G. 1999. Protein kinase B localization and activation differentially affect S6 kinase 1 activity and eukaryotic translation initiation factor 4E-binding protein 1 phosphorylation. *Mol Cell Biol,* 19**,** 4525-34.

DUFNER, A. & THOMAS, G. 1999. Ribosomal S6 kinase signaling and the control of translation. *Exp Cell Res,* 253**,** 100-9.

DUYNDAM, M. C., VAN BERKEL, M. P., DORSMAN, J. C., ROCKX, D. A., PINEDO, H. M. & BOVEN, E. 2007. Cisplatin and doxorubicin repress Vascular Endothelial Growth Factor expression and differentially down-regulate Hypoxia-inducible Factor I activity in human ovarian cancer cells. *Biochem Pharmacol,* 74**,** 191-201.

EKICI, Y., EMIROGLU, R., OZDEMIR, H., ALDEMIR, D., KARAKAYALI, H. & HABERAL, M. 2007. Effect of rapamycin on wound healing: an experimental study. *Transplant Proc,* 39**,** 1201-3.

ELLISEN, L. W. 2005. Growth control under stress: mTOR regulation through the REDD1-TSC pathway. *Cell Cycle,* 4**,** 1500-02.

ELVIDGE, G. P., GLENNY, L., APPELHOFF, R. J., RATCLIFFE, P. J., RAGOUSSIS, J. & GLEADLE, J. M. 2006. Concordant regulation of gene expression by hypoxia and 2-oxoglutarate-dependent dioxygenase inhibition: the role of HIF-1alpha, HIF-2alpha, and other pathways. *J Biol Chem,* 281**,** 15215-26.

EMERLING, B. M., WEINBERG, F., LIU, J. L., MAK, T. W. & CHANDEL, N. S. 2008. PTEN regulates p300-dependent hypoxia-inducible factor 1 transcriptional activity through Forkhead transcription factor 3a (FOXO3a). *Proc Natl Acad Sci U S A,* 105**,** 2622-7.

EPSTEIN, A. C., GLEADLE, J. M., MCNEILL, L. A., HEWITSON, K. S., O'ROURKE, J., MOLE, D. R., MUKHERJI, M., METZEN, E., WILSON, M. I., DHANDA, A., TIAN, Y. M., MASSON, N., HAMILTON, D. L., JAAKKOLA, P., BARSTEAD, R., HODGKIN, J., MAXWELL, P. H., PUGH, C. W., SCHOFIELD, C. J. & RATCLIFFE, P. J. 2001. C. elegans EGL-9 and mammalian homologs define a family of dioxygenases that regulate HIF by prolyl hydroxylation. *Cell,* 107**,** 43-54.

ERLER, J. T., CAWTHORNE, C. J., WILLIAMS, K. J., KORITZINSKY, M., WOUTERS, B. G., WILSON, C., MILLER, C., DEMONACOS, C., STRATFORD, I. J. & DIVE, C. 2004. Hypoxia-mediated down-regulation of Bid and Bax in tumors occurs via hypoxia-inducible factor 1-dependent and -independent mechanisms and contributes to drug resistance. *Mol Cell Biol,* 24**,** 2875-89.

EYOL, E., BOLEIJ, A., TAYLOR, R. R., LEWIS, A. L. & BERGER, M. R. 2008. Chemoembolisation of rat colorectal liver metastases with drug eluting beads loaded with irinotecan or doxorubicin. *Clin Exp Metastasis,* 25**,** 273-82.

FELIX, C. A. 1998. Secondary leukemias induced by topoisomerase-targeted drugs. *Biochim Biophys Acta,* 1400**,** 233-55.

FERRER PUCHOL, M. D., LA PARRA, C., ESTEBAN, E., VANO, M., FORMENT, M., VERA, A. & COSIN, O. 2011. [Comparison of doxorubicin-eluting bead transarterial chemoembolization (DEB-TACE) with conventional transarterial chemoembolization (TACE) for the treatment of hepatocellular carcinoma]. *Radiologia,* 53**,** 246-53.

FIDLER, I. J., WILMANNS, C., STAROSELSKY, A., RADINSKY, R., DONG, Z. & FAN, D. 1994. Modulation of tumor cell response to chemotherapy by the organ environment. *Cancer Metastasis Rev,* 13**,** 209-22.

FORNARI, F. A., RANDOLPH, J. K., YALOWICH, J. C., RITKE, M. K. & GEWIRTZ, D. A. 1994. Interference by doxorubicin with DNA unwinding in MCF-7 breast tumor cells. *Mol Pharmacol,* 45**,** 649-56.

FORSTER, R. 2009. Hydrogel Microspheres for the Treatment of Tumours. *PhD Thesis, University of Brighton*.

FORTUNE, J. M. & OSHEROFF, N. 2000. Topoisomerase II as a target for anticancer drugs: when enzymes stop being nice. *Prog Nucleic Acid Res Mol Biol,* 64**,** 221-53.

FOSTER, D. A. & TOSCHI, A. 2009. Targeting mTOR with rapamycin: one dose does not fit all. *Cell Cycle,* 8**,** 1026-9.

FOSTER, K. G. & FINGAR, D. C. 2010. Mammalian target of rapamycin (mTOR): conducting the cellular signaling symphony. *J Biol Chem,* 285**,** 14071-7.

FUKUMURA, D., YUAN, F., MONSKY, W. L., CHEN, Y. & JAIN, R. K. 1997. Effect of host microenvironment on the microcirculation of human colon adenocarcinoma. *Am J Pathol,* 151**,** 679-88.

GANGADHARAN, C., THOH, M. & MANNA, S. K. 2009. Inhibition of constitutive activity of nuclear transcription factor kappaB sensitizes doxorubicin-resistant cells to apoptosis. *J Cell Biochem,* 107**,** 203-13.

GERWECK, L. E., KOZIN, S. V. & STOCKS, S. J. 1999. The pH partition theory predicts the accumulation and toxicity of doxorubicin in normal and low-pH-adapted cells. *Br J Cancer,* 79**,** 838-42.

GEWIRTZ, D. A. 1999. A critical evaluation of the mechanisms of action proposed for the antitumor effects of the anthracycline antibiotics adriamycin and daunorubicin. *Biochem Pharmacol,* 57**,** 727-41.

GILMORE, T. D. 2006. Introduction to NF-kappaB: players, pathways, perspectives. *Oncogene,* 25**,** 6680-4.

GIORDANO, A., AVELLINO, R., FERRARO, P., ROMANO, S., CORCIONE, N. & ROMANO, M. F. 2006. Rapamycin antagonizes NF-kappaB nuclear translocation activated by TNF-alpha in primary vascular smooth muscle cells and enhances apoptosis. *Am J Physiol Heart Circ Physiol,* 290**,** H2459-65.

GODA, N., DOZIER, S. J. & JOHNSON, R. S. 2003. HIF-1 in cell cycle regulation, apoptosis, and tumor progression. *Antioxid Redox Signal,* 5**,** 467-73.

GOODMAN, J. & HOCHSTEIN, P. 1977. Generation of free radicals and lipid peroxidation by redox cycling of adriamycin and daunomycin. *Biochem Biophys Res Commun,* 77**,** 797-803.

GRANITO, A. & BOLONDI, L. 2009. Medical treatment of hepatocellular carcinoma. *Mediterr J Hematol Infect Dis,* 1**,** e2009021.

GREIJER, A. E., VAN DER GROEP, P., KEMMING, D., SHVARTS, A., SEMENZA, G. L., MEIJER, G. A., VAN DE WIEL, M. A., BELIEN, J. A., VAN DIEST, P. J. & VAN DER WALL, E. 2005. Up-regulation of gene expression by hypoxia is mediated predominantly by hypoxia-inducible factor 1 (HIF-1). *J Pathol,* 206**,** 291-304.

GREIJER, A. E. & VAN DER WALL, E. 2004. The role of hypoxia inducible factor 1 (HIF-1) in hypoxia induced apoptosis. *J Clin Pathol,* 57**,** 1009-14.

GRUBER, B. M., ANUSZEWSKA, E. L., BUBKO, I., KASPRZYCKA-GUTTMAN, T., MISIEWICZ, I., SKUPINSKA, K., FOKT, I. & PIEBE, W.

2008. NFkappaB activation and drug sensitivity in human neoplastic cells treated with anthracyclines. *Acta Pol Pharm,* 65**,** 267-71.

GRUNWALD, V., DEGRAFFENRIED, L., RUSSEL, D., FRIEDRICHS, W. E., RAY, R. B. & HIDALGO, M. 2002. Inhibitors of mTOR reverse doxorubicin resistance conferred by PTEN status in prostate cancer cells. *Cancer Res,* 62**,** 6141-5.

GUBA, M., KOEHL, G. E., NEPPL, E., DOENECKE, A., STEINBAUER, M., SCHLITT, H. J., JAUCH, K. W. & GEISSLER, E. K. 2005. Dosing of rapamycin is critical to achieve an optimal antiangiogenic effect against cancer. *Transpl Int,* 18**,** 89-94.

GUBA, M., VON BREITENBUCH, P., STEINBAUER, M., KOEHL, G., FLEGEL, S., HORNUNG, M., BRUNS, C. J., ZUELKE, C., FARKAS, S., ANTHUBER, M., JAUCH, K. W. & GEISSLER, E. K. 2002. Rapamycin inhibits primary and metastatic tumor growth by antiangiogenesis: involvement of vascular endothelial growth factor. *Nat Med,* 8**,** 128-35.

GUO, W. J., LI, J., CHEN, Z., ZHUANG, J. Y., GU, W. H., ZHANG, L., PANG, J., LU, C. H., ZHANG, W. Z. & CHENG, Y. F. 2004. Transient increased expression of VEGF and MMP-1 in a rat liver tumor model after hepatic arterial occlusion. *Hepatogastroenterology,* 51**,** 381-6.

GUO, W. J., LI, J., LING, W. L., BAI, Y. R., ZHANG, W. Z., CHENG, Y. F., GU, W. H. & ZHUANG, J. Y. 2002. Influence of hepatic arterial blockage on blood perfusion and VEGF, MMP-1 expression of implanted liver cancer in rats. *World J Gastroenterol,* 8**,** 476-9.

GUPTA, S., KOBAYASHI, S., PHONGKITKARUN, S., BROEMELING, L. D. & KAN, Z. 2006. Effect of transcatheter hepatic arterial embolization on angiogenesis in an animal model. *Invest Radiol,* 41**,** 516-21.

GUPTA, V. & COSTANZI, J. J. 1987. Role of hypoxia in anticancer drug-induced cytotoxicity for Ehrlich ascites cells. *Cancer Res,* 47**,** 2407-12.

HAMMOND, E. M. & GIACCIA, A. J. 2002. Antiangiogenic therapy and p53. *Science,* 297**,** 471; discussion 471.

HARITUNIANS, T., MORI, A., O'KELLY, J., LUONG, Q. T., GILES, F. J. & KOEFFLER, H. P. 2007. Antiproliferative activity of RAD001 (everolimus) as a single agent and combined with other agents in mantle cell lymphoma. *Leukemia,* 21**,** 333-9.

HARRIS, A. L. 2002. Hypoxia - A key regulatory factor in tumour growth. *Nature Reviews Cancer,* 2**,** 38-47.

HE, G. & KARIN, M. 2011. NF-kappaB and STAT3 - key players in liver inflammation and cancer. *Cell Res,* 21**,** 159-68.

HEIDBREDER, M., FROHLICH, F., JOHREN, O., DENDORFER, A., QADRI, F. & DOMINIAK, P. 2003. Hypoxia rapidly activates HIF-3alpha mRNA expression. *Faseb J,* 17**,** 1541-3.

HESS, G. 2009. Temsirolimus for the treatment of mantle cell lymphoma. *Expert Rev Hematol,* 2**,** 631-40.

HEUER, M., BENKO, T., CICINNATI, V. R., KAISER, G. M., SOTIROPOULOS, G. C., BABA, H. A., TRECKMANN, J. W., BROELSCH, C. E. & PAUL, A. 2009. Effect of low-dose rapamycin on tumor growth in two human hepatocellular cancer cell lines. *Transplant Proc,* 41**,** 359-65.

HIROTA, K. & SEMENZA, G. L. 2006. Regulation of angiogenesis by hypoxia-inducible factor 1. *Crit Rev Oncol Hematol,* 59**,** 15-26.

HOCKEL, M. & VAUPEL, P. 2001. Tumor hypoxia: definitions and current clinical, biologic, and molecular aspects. *J Natl Cancer Inst,* 93**,** 266-76.

HOFFMAN, D. M., GROSSANO, D. D., DAMIN, L. & WOODCOCK, T. M. 1979. Stability of refrigerated and frozen solutions of doxorubicin hydrochloride. *Am J Hosp Pharm,* 36**,** 1536-8.

HOFMANN, G. A. & MATTERN, M. R. 1993. Topoisomerase II in multiple drug resistance. *Cytotechnology,* 12**,** 137-54.

HONG, K., KHWAJA, A., LIAPI, E., TORBENSON, M. S., GEORGIADES, C. S. & GESCHWIND, J. F. 2006. New intra-arterial drug delivery system for the treatment of liver cancer: preclinical assessment in a rabbit model of liver cancer. *Clin Cancer Res,* 12**,** 2563-7.

HOOF, T., DEMMER, A., CHRISTIANS, U. & TUMMLER, B. 1993. Reversal of multidrug resistance in Chinese hamster ovary cells by the immunosuppressive agent rapamycin. *Eur J Pharmacol,* 246**,** 53-8.

HOUGHTON, P. J. & HUANG, S. 2004. mTOR as a target for cancer therapy. *Curr Top Microbiol Immunol,* 279**,** 339-59.

HU, T. H., HUANG, C. C., LIN, P. R., CHANG, H. W., GER, L. P., LIN, Y. W., CHANGCHIEN, C. S., LEE, C. M. & TAI, M. H. 2003. Expression and prognostic role of tumor suppressor gene PTEN/MMAC1/TEP1 in hepatocellular carcinoma. *Cancer,* 97**,** 1929-40.

HUANG, H., CHEVILLE, J. C., PAN, Y., ROCHE, P. C., SCHMIDT, L. J. & TINDALL, D. J. 2001. PTEN induces chemosensitivity in PTEN-mutated prostate cancer cells by suppression of Bcl-2 expression. *J Biol Chem,* 276**,** 38830-6.

HUANG, J. & MANNING, B. D. 2009. A complex interplay between Akt, TSC2 and the two mTOR complexes. *Biochem Soc Trans,* 37**,** 217-22.

HUANG, J. J., LI, Z. M., HUANG, Y., TIAN, Y., HE, X. X., XIAO, J. & LIN, T. Y. 2010. Schedule-dependent inhibition of T-cell lymphoma cells by cotreatment with the mTOR inhibitor everolimus and anticancer drugs. *Invest New Drugs,* Oct. Epub ahead of print.

HUANG, L. E., GU, J., SCHAU, M. & BUNN, H. F. 1998. Regulation of hypoxia-inducible factor 1alpha is mediated by an O2-dependent degradation domain via the ubiquitin-proteasome pathway. *Proc Natl Acad Sci U S A,* 95**,** 7987-92.

HUANG, S., BJORNSTI, M. A. & HOUGHTON, P. J. 2003. Rapamycins: mechanism of action and cellular resistance. *Cancer Biol Ther,* 2**,** 222-32.

HUANG, S. & HOUGHTON, P. J. 2003. Targeting mTOR signaling for cancer therapy. *Curr Opin Pharmacol,* 3**,** 371-7.

HUDES, G. R., BERKENBLIT, A., FEINGOLD, J., ATKINS, M. B., RINI, B. I. & DUTCHER, J. 2009. Clinical trial experience with temsirolimus in patients with advanced renal cell carcinoma. *Semin Oncol,* 36 Suppl 3**,** S26-36.

HUDSON, C. C., LIU, M., CHIANG, G. G., OTTERNESS, D. M., LOOMIS, D. C., KAPER, F., GIACCIA, A. J. & ABRAHAM, R. T. 2002. Regulation of hypoxia-inducible factor 1alpha expression and function by the mammalian target of rapamycin. *Mol Cell Biol,* 22**,** 7004-14.

HUI, I. C., TUNG, E. K., SZE, K. M., CHING, Y. P. & NG, I. O. 2010. Rapamycin and CCI-779 inhibit the mammalian target of rapamycin signalling in hepatocellular carcinoma. *Liver Int,* 30**,** 65-75.

HUYNH, H., CHOW, K. H., SOO, K. C., TOH, H. C., CHOO, S. P., FOO, K. F., POON, D., NGO, V. C. & TRAN, E. 2009a. RAD001 (everolimus) inhibits

tumour growth in xenograft models of human hepatocellular carcinoma. *J Cell Mol Med,* 13**,** 1371-80.

HUYNH, H., CHOW, P. K., PALANISAMY, N., SALTO-TELLEZ, M., GOH, B. C., LEE, C. K., SOMANI, A., LEE, H. S., KALPANA, R., YU, K., TAN, P. H., WU, J., SOONG, R., LEE, M. H., HOR, H., SOO, K. C., TOH, H. C. & TAN, P. 2008b. Bevacizumab and rapamycin induce growth suppression in mouse models of hepatocellular carcinoma. *J Hepatol,* 49**,** 52-60.

HUYNH, H., NGO, V. C., KOONG, H. N., POON, D., CHOO, S. P., THNG, C. H., CHOW, P., ONG, H. S., CHUNG, A. & SOO, K. C. 2009b. Sorafenib and Rapamycin Induce Growth Suppression in Mouse Models of Hepatocellular Carcinoma. *J Cell Mol Med*.

IVAN, M., KONDO, K., YANG, H., KIM, W., VALIANDO, J., OHH, M., SALIC, A., ASARA, J. M., LANE, W. S. & KAELIN, W. G., JR. 2001. HIFalpha targeted for VHL-mediated destruction by proline hydroxylation: implications for O2 sensing. *Science,* 292**,** 464-8.

IWAI, K., YAMANAKA, K., KAMURA, T., MINATO, N., CONAWAY, R. C., CONAWAY, J. W., KLAUSNER, R. D. & PAUSE, A. 1999. Identification of the von Hippel-lindau tumor-suppressor protein as part of an active E3 ubiquitin ligase complex. *Proc Natl Acad Sci U S A,* 96**,** 12436-41.

IYER, N. V., LEUNG, S. W. & SEMENZA, G. L. 1998. The human hypoxia-inducible factor 1alpha gene: HIF1A structure and evolutionary conservation. *Genomics,* 52**,** 159-65.

JAAKKOLA, P., MOLE, D. R., TIAN, Y. M., WILSON, M. I., GIELBERT, J., GASKELL, S. J., KRIEGSHEIM, A., HEBESTREIT, H. F., MUKHERJI, M., SCHOFIELD, C. J., MAXWELL, P. H., PUGH, C. W. & RATCLIFFE, P. J. 2001. Targeting of HIF-alpha to the von Hippel-Lindau ubiquitylation complex by O2-regulated prolyl hydroxylation. *Science,* 292**,** 468-72.

JACINTO, E., LOEWITH, R., SCHMIDT, A., LIN, S., RUEGG, M. A., HALL, A. & HALL, M. N. 2004. Mammalian TOR complex 2 controls the actin cytoskeleton and is rapamycin insensitive. *Nat Cell Biol,* 6**,** 1122-8.

JASINGHE, V. J., XIE, Z., ZHOU, J., KHNG, J., POON, L. F., SENTHILNATHAN, P., GLASER, K. B., ALBERT, D. H., DAVIDSEN, S. K. & CHEN, C. S. 2008. ABT-869, a multi-targeted tyrosine kinase inhibitor, in combination with rapamycin is effective for subcutaneous hepatocellular carcinoma xenograft. *J Hepatol,* 49**,** 985-97.

JIANG, B. H. & LIU, L. Z. 2008a. PI3K/PTEN signaling in tumorigenesis and angiogenesis. *Biochim Biophys Acta,* 1784**,** 150-8.

JIANG, B. H. & LIU, L. Z. 2008b. Role of mTOR in anticancer drug resistance: perspectives for improved drug treatment. *Drug Resist Updat,* 11**,** 63-76.

JIANG, B. H., SEMENZA, G. L., BAUER, C. & MARTI, H. H. 1996. Hypoxia-inducible factor 1 levels vary exponentially over a physiologically relevant range of O2 tension. *Am J Physiol,* 271**,** C1172-80.

JIANG, H. Y. & FENG, Y. J. 2004. [Inhibition of hypoxia-inducible factor 1alpha expression and tumor growth in SKOV3 ovarian cancer model by sirolimus]. *Zhonghua Fu Chan Ke Za Zhi,* 39**,** 474-7.

JIMENEZ, R. H., BOYLAN, J. M., LEE, J. S., FRANCESCONI, M., CASTELLANI, G., SANDERS, J. A. & GRUPPUSO, P. A. 2009. Rapamycin response in tumorigenic and non-tumorigenic hepatic cell lines. *PLoS One,* 4**,** e7373.

JUNG, E. U., YOON, J. H., LEE, Y. J., LEE, J. H., KIM, B. H., YU, S. J., MYUNG, S. J., KIM, Y. J. & LEE, H. S. 2010. Hypoxia and retinoic acid-inducible NDRG1 expression is responsible for doxorubicin and retinoic acid resistance in hepatocellular carcinoma cells. *Cancer Lett,* 298**,** 9-15.

KAELIN, W. G., JR. & RATCLIFFE, P. J. 2008. Oxygen sensing by metazoans: the central role of the HIF hydroxylase pathway. *Mol Cell,* 30**,** 393-402.

KAIBORI, M., TANIGAWA, N., MATSUI, Y., SAITO, T., UCHIDA, Y., ISHIZAKI, M., TANAKA, H. & KAMIYAMA, Y. 2006. Influence of transcatheter arterial chemoembolization on the prognosis after hepatectomy for hepatocellular carcinoma in patients with severe liver dysfunction. *Anticancer Res,* 26**,** 3685-92.

KALRA, R., JONES, A. M., KIRK, J., ADAMS, G. E. & STRATFORD, I. J. 1993. The effect of hypoxia on acquired drug resistance and response to epidermal growth factor in Chinese hamster lung fibroblasts and human breast-cancer cells in vitro. *Int J Cancer,* 54**,** 650-5.

KALUZOVA, M., KALUZ, S., LERMAN, M. I. & STANBRIDGE, E. J. 2004. DNA damage is a prerequisite for p53-mediated proteasomal degradation of HIF-1alpha in hypoxic cells and downregulation of the hypoxia marker carbonic anhydrase IX. *Mol Cell Biol,* 24**,** 5757-66.

KAMURA, T., SATO, S., IWAI, K., CZYZYK-KRZESKA, M., CONAWAY, R. C. & CONAWAY, J. W. 2000. Activation of HIF1alpha ubiquitination by a reconstituted von Hippel-Lindau (VHL) tumor suppressor complex. *Proc Natl Acad Sci U S A,* 97**,** 10430-5.

KANTIDZE, O. L. & RAZIN, S. V. 2007. Chemotherapy-related secondary leukemias: A role for DNA repair by error-prone non-homologous end joining in topoisomerase II - Induced chromosomal rearrangements. *Gene,* 391**,** 76-9.

KAPER, F., DORNHOEFER, N. & GIACCIA, A. J. 2006. Mutations in the PI3K/PTEN/TSC2 pathway contribute to mammalian target of rapamycin activity and increased translation under hypoxic conditions. *Cancer Res,* 66**,** 1561-9.

KEATING, G. M. & SANTORO, A. 2009. Sorafenib: a review of its use in advanced hepatocellular carcinoma. *Drugs,* 69**,** 223-40.

KEIZER, H. G., PINEDO, H. M., SCHUURHUIS, G. J. & JOENJE, H. 1990. Doxorubicin (adriamycin): a critical review of free radical-dependent mechanisms of cytotoxicity. *Pharmacol Ther,* 47**,** 219-31.

KENNEDY, K. A., SIEGFRIED, J. M., SARTORELLI, A. C. & TRITTON, T. R. 1983. Effects of anthracyclines on oxygenated and hypoxic tumor cells. *Cancer Res,* 43**,** 54-9.

KERBEL, R. S. 2000. Tumor angiogenesis: past, present and the near future. *Carcinogenesis,* 21**,** 505-15.

KERBEL, R. S. 2003. Human tumor xenografts as predictive preclinical models for anticancer drug activity in humans: better than commonly perceived-but they can be improved. *Cancer Biol Ther,* 2**,** S134-9.

KIDD, J. G. & ROUS, P. 1940. A transplantable rabbit carcinoma originating in a virus-induced papilloma and containing the virus in masked or altered form. *J Exp Med,* 71**,** 813-38.

KIM, J. W. & DANG, C. V. 2006. Cancer's molecular sweet tooth and the Warburg effect. *Cancer Res,* 66**,** 8927-30.

KIM, J. Y. & PARK, J. H. 2003. ROS-dependent caspase-9 activation in hypoxic cell death. *FEBS Lett,* 549**,** 94-8.

KIM, Y. B., PARK, Y. N. & PARK, C. 2001. Increased proliferation activities of vascular endothelial cells and tumour cells in residual hepatocellular carcinoma following transcatheter arterial embolization. *Histopathology,* 38**,** 160-6.

KNETEMAN, N. M., OBERHOLZER, J., AL SAGHIER, M., MEEBERG, G. A., BLITZ, M., MA, M. M., WONG, W. W., GUTFREUND, K., MASON, A. L., JEWELL, L. D., SHAPIRO, A. M., BAIN, V. G. & BIGAM, D. L. 2004. Sirolimus-based immunosuppression for liver transplantation in the presence of extended criteria for hepatocellular carcinoma. *Liver Transpl,* 10**,** 1301-11.

KONNO, T. 1990. Targeting cancer chemotherapeutic agents by use of lipiodol contrast medium. *Cancer,* 66**,** 1897-903.

KOONG, A. C., CHEN, E. Y. & GIACCIA, A. J. 1994a. Hypoxia causes the activation of nuclear factor kappa B through the phosphorylation of I kappa B alpha on tyrosine residues. *Cancer Res,* 54**,** 1425-30.

KOONG, A. C., CHEN, E. Y., MIVECHI, N. F., DENKO, N. C., STAMBROOK, P. & GIACCIA, A. J. 1994b. Hypoxic activation of nuclear factor-kappa B is mediated by a Ras and Raf signaling pathway and does not involve MAP kinase (ERK1 or ERK2). *Cancer Res,* 54**,** 5273-9.

KOSHIJI, M. & HUANG, L. E. 2004. Dynamic balancing of the dual nature of HIF-1alpha for cell survival. *Cell Cycle,* 3**,** 853-4.

KOUMENIS, C., ALARCON, R., HAMMOND, E., SUTPHIN, P., HOFFMAN, W., MURPHY, M., DERR, J., TAYA, Y., LOWE, S. W., KASTAN, M. & GIACCIA, A. 2001. Regulation of p53 by hypoxia: dissociation of transcriptional repression and apoptosis from p53-dependent transactivation. *Mol Cell Biol,* 21**,** 1297-310.

KREBS, H. A. 1972. The Pasteur effect and the relations between respiration and fermentation. *Essays Biochem,* 8**,** 1-34.

KUBOTA, T. 1994. Metastatic models of human cancer xenografted in the nude mouse: the importance of orthotopic transplantation. *J Cell Biochem,* 56**,** 4-8.

LAMMER, J., MALAGARI, K., VOGL, T., PILLEUL, F., DENYS, A., WATKINSON, A., PITTON, M., SERGENT, G., PFAMMATTER, T., TERRAZ, S., BENHAMOU, Y., AVAJON, Y., GRUENBERGER, T., POMONI, M., LANGENBERGER, H., SCHUCHMANN, M., DUMORTIER, J., MUELLER, C., CHEVALLIER, P. & LENCIONI, R. 2010. Prospective randomized study of doxorubicin-eluting-bead embolization in the treatment of hepatocellular carcinoma: results of the PRECISION V study. *Cardiovasc Intervent Radiol,* 33**,** 41-52.

LAND, S. C. & TEE, A. R. 2007. Hypoxia-inducible factor 1alpha is regulated by the mammalian target of rapamycin (mTOR) via an mTOR signaling motif. *J Biol Chem,* 282**,** 20534-43.

LANDO, D., PEET, D. J., GORMAN, J. J., WHELAN, D. A., WHITELAW, M. L. & BRUICK, R. K. 2002. FIH-1 is an asparaginyl hydroxylase enzyme that regulates the transcriptional activity of hypoxia-inducible factor. *Genes Dev,* 16**,** 1466-71.

LANG, K. J., KAPPEL, A. & GOODALL, G. J. 2002. Hypoxia-inducible factor-1alpha mRNA contains an internal ribosome entry site that allows efficient translation during normoxia and hypoxia. *Mol Biol Cell,* 13**,** 1792-801.

LECHANTEUR, C., JACOBS, N., GREIMERS, R., BENOIT, V., DEREGOWSKI, V., CHARIOT, A., MERVILLE, M. P. & BOURS, V. 2005. Low daunomycin concentrations protect colorectal cancer cells from hypoxia-induced apoptosis. *Oncogene,* 24**,** 1788-1793.

LEE, K., QIAN, D. Z., REY, S., WEI, H., LIU, J. O. & SEMENZA, G. L. 2009a. Anthracycline chemotherapy inhibits HIF-1 transcriptional activity and tumor-induced mobilization of circulating angiogenic cells. *Proc Natl Acad Sci U S A,* 106**,** 2353-8.

LEE, K., ROTH, R. A. & LAPRES, J. J. 2007. Hypoxia, drug therapy and toxicity. *Pharmacol Ther,* 113**,** 229-46.

LEE, K. H., LIAPI, E., BUIJS, M., VOSSEN, J., HONG, K., GEORGIADES, C. & GESCHWIND, J. F. 2009b. Considerations for implantation site of VX2 carcinoma into rabbit liver. *J Vasc Interv Radiol,* 20**,** 113-7.

LEE, K. H., LIAPI, E., VENTURA, V. P., BUIJS, M., VOSSEN, J. A., VALI, M. & GESCHWIND, J. F. 2008. Evaluation of different calibrated spherical polyvinyl alcohol microspheres in transcatheter arterial chemoembolization: VX2 tumor model in rabbit liver. *J Vasc Interv Radiol,* 19**,** 1065-9.

LEE, K. H., LIAPI, E. A., CORNELL, C., REB, P., BUIJS, M., VOSSEN, J. A., VENTURA, V. P. & GESCHWIND, J. F. 2010. Doxorubicin-loaded QuadraSphere microspheres: plasma pharmacokinetics and intratumoral drug concentration in an animal model of liver cancer. *Cardiovasc Intervent Radiol,* 33**,** 576-82.

LEE, T. K., LAU, T. C. & NG, I. O. 2002. Doxorubicin-induced apoptosis and chemosensitivity in hepatoma cell lines. *Cancer Chemother Pharmacol,* 49**,** 78-86.

LEE, T. K., POON, R. T., YUEN, A. P., MAN, K., YANG, Z. F., GUAN, X. Y. & FAN, S. T. 2006. Rac activation is associated with hepatocellular carcinoma metastasis by up-regulation of vascular endothelial growth factor expression. *Clin Cancer Res,* 12**,** 5082-9.

LENCIONI, R. 2010. Loco-regional treatment of hepatocellular carcinoma. *Hepatology,* 52**,** 762-73.

LEWIS, A. L., GONZALEZ, M. V., LEPPARD, S. W., BROWN, J. E., STRATFORD, P. W., PHILLIPS, G. J. & LLOYD, A. W. 2007. Doxorubicin eluting beads - 1: effects of drug loading on bead characteristics and drug distribution. *J Mater Sci Mater Med,* 18**,** 1691-9.

LEWIS, A. L. & HOLDEN, R. R. 2011. DC Bead embolic drug-eluting bead: clinical application in the locoregional treatment of tumours. *Expert Opin Drug Deliv,* 8**,** 153-69.

LEWIS, A. L., TAYLOR, R. R., HALL, B., GONZALEZ, M. V., WILLIS, S. L. & STRATFORD, P. W. 2006. Pharmacokinetic and safety study of doxorubicin-eluting beads in a porcine model of hepatic arterial embolization. *J Vasc Interv Radiol,* 17**,** 1335-43.

LEWIS, S. A. 2002. Assessing Epithelial Cell Confluence by Spectroscopy. *In:* WISE, C. (ed.) *Epithelial Cell Culture Protocols.* Humana Press.

LI, L., LIN, X., SHOEMAKER, A. R., ALBERT, D. H., FESIK, S. W. & SHEN, Y. 2006. Hypoxia-inducible factor-1 inhibition in combination with temozolomide treatment exhibits robust antitumor efficacy in vivo. *Clin Cancer Res,* 12**,** 4747-54.

LI, W., PETRIMPOL, M., MOLLE, K. D., HALL, M. N., BATTEGAY, E. J. & HUMAR, R. 2007. Hypoxia-induced endothelial proliferation requires both mTORC1 and mTORC2. *Circ Res,* 100**,** 79-87.

LI, X., FENG, G. S., ZHENG, C. S., ZHUO, C. K. & LIU, X. 2003. Influence of transarterial chemoembolization on angiogenesis and expression of vascular endothelial growth factor and basic fibroblast growth factor in rat with Walker-256 transplanted hepatoma: an experimental study. *World J Gastroenterol,* 9**,** 2445-9.

LI, X., FENG, G. S., ZHENG, C. S., ZHUO, C. K. & LIU, X. 2004. Expression of plasma vascular endothelial growth factor in patients with hepatocellular carcinoma and effect of transcatheter arterial chemoembolization therapy on plasma vascular endothelial growth factor level. *World J Gastroenterol,* 10**,** 2878-82.

LIANG, B., ZHENG, C., FENG, G., WANG, Y., ZHAO, H., LIANG, H. & XIAO, E. 2009. Expression of hypoxia-inducible factor-1alpha in liver tumors after transcatheter arterial embolization in an animal model. *J Huazhong Univ Sci Technolog Med Sci,* 29**,** 776-81.

LIANG, B., ZHENG, C., FENG, G., WU, H., WANG, Y., ZHAO, H., LI, X., QIAN, J. & LIANG, H. 2010a. Experimental evaluation of inhibitory effect of 10-hydroxycamptothecin on hypoxia-inducible factor-1alpha expression and angiogenesis in liver tumors after transcatheter arterial embolization. *J Vasc Interv Radiol,* 21**,** 1565-72.

LIANG, B., ZHENG, C. S., FENG, G. S., WU, H. P., WANG, Y., ZHAO, H., QIAN, J. & LIANG, H. M. 2010b. Correlation of hypoxia-inducible factor 1alpha with angiogenesis in liver tumors after transcatheter arterial embolization in an animal model. *Cardiovasc Intervent Radiol,* 33**,** 806-12.

LIANG, G., TANG, A., LIN, X., LI, L., ZHANG, S., HUANG, Z., TANG, H. & LI, Q. Q. 2010c. Green tea catechins augment the antitumor activity of doxorubicin in an in vivo mouse model for chemoresistant liver cancer. *Int J Oncol,* 37**,** 111-23.

LIAO, X., YI, J., LI, X., YANG, Z., DENG, W. & TIAN, G. 2003. Expression of angiogenic factors in hepatocellular carcinoma after transcatheter arterial chemoembolization. *J Huazhong Univ Sci Technolog Med Sci,* 23**,** 280-2.

LIAO, X. F., YI, J. L., LI, X. R., DENG, W., YANG, Z. F. & TIAN, G. 2004. Angiogenesis in rabbit hepatic tumor after transcatheter arterial embolization. *World J Gastroenterol,* 10**,** 1885-9.

LIAPI, E. & GESCHWIND, J. F. 2010. Chemoembolization for primary and metastatic liver cancer. *Cancer J,* 16**,** 156-62.

LIAPI, E. & GESCHWIND, J. F. 2011. Transcatheter arterial chemoembolization for liver cancer: is it time to distinguish conventional from drug-eluting chemoembolization? *Cardiovasc Intervent Radiol,* 34**,** 37-49.

LIEB, M. E., MENZIES, K., MOSCHELLA, M. C., NI, R. & TAUBMAN, M. B. 2002. Mammalian EGLN genes have distinct patterns of mRNA expression and regulation. *Biochem Cell Biol,* 80**,** 421-6.

LIN, C. I., WHANG, E. E., DONNER, D. B., DU, J., LORCH, J., HE, F., JIANG, X., PRICE, B. D., MOORE, F. D., JR. & RUAN, D. T. 2010. Autophagy induction with RAD001 enhances chemosensitivity and radiosensitivity through Met inhibition in papillary thyroid cancer. *Mol Cancer Res,* 8**,** 1217-26.

LINDSLEY, J. E. & WANG, J. C. 1991. Proteolysis patterns of epitopically labeled yeast DNA topoisomerase II suggest an allosteric transition in the enzyme induced by ATP binding. *Proc Natl Acad Sci U S A,* 88**,** 10485-9.

LINDSLEY, J. E. & WANG, J. C. 1993. On the coupling between ATP usage and DNA transport by yeast DNA topoisomerase II. *J Biol Chem,* 268**,** 8096-104.

LIU, F., WANG, P., JIANG, X., TAN, G., QIAO, H., JIANG, H., KRISSANSEN, G. W. & SUN, X. 2008a. Antisense hypoxia-inducible factor 1alpha gene therapy enhances the therapeutic efficacy of doxorubicin to combat hepatocellular carcinoma. *Cancer Sci,* 99**,** 2055-61.

LIU, L., NING, X., SUN, L., ZHANG, H., SHI, Y., GUO, C., HAN, S., LIU, J., SUN, S., HAN, Z., WU, K. & FAN, D. 2008b. Hypoxia-inducible factor-1 alpha contributes to hypoxia-induced chemoresistance in gastric cancer. *Cancer Sci,* 99**,** 121-8.

LIU, Q., THOREEN, C., WANG, J., SABATINI, D. & GRAY, N. S. 2009. mTOR Mediated Anti-Cancer Drug Discovery. *Drug Discov Today Ther Strateg,* 6**,** 47-55.

LIU, Y. & WU, F. 2010. Global burden of aflatoxin-induced hepatocellular carcinoma: a risk assessment. *Environ Health Perspect,* 118**,** 818-24.

LLOVET, J. M. & BRUIX, J. 2003. Systematic review of randomized trials for unresectable hepatocellular carcinoma: Chemoembolization improves survival. *Hepatology,* 37**,** 429-42.

LLOVET, J. M., RICCI, S., MAZZAFERRO, V., HILGARD, P., GANE, E., BLANC, J. F., DE OLIVEIRA, A. C., SANTORO, A., RAOUL, J. L., FORNER, A., SCHWARTZ, M., PORTA, C., ZEUZEM, S., BOLONDI, L., GRETEN, T. F., GALLE, P. R., SEITZ, J. F., BORBATH, I., HAUSSINGER, D., GIANNARIS, T., SHAN, M., MOSCOVICI, M., VOLIOTIS, D. & BRUIX, J. 2008. Sorafenib in advanced hepatocellular carcinoma. *N Engl J Med,* 359**,** 378-90.

LOBODA, A., JOZKOWICZ, A. & DULAK, J. 2010. HIF-1 and HIF-2 transcription factors--similar but not identical. *Mol Cells,* 29**,** 435-42.

LOPICCOLO, J., BLUMENTHAL, G. M., BERNSTEIN, W. B. & DENNIS, P. A. 2008. Targeting the PI3K/Akt/mTOR pathway: effective combinations and clinical considerations. *Drug Resist Updat,* 11**,** 32-50.

LU, K. H., WU, W., DAVE, B., SLOMOVITZ, B. M., BURKE, T. W., MUNSELL, M. F., BROADDUS, R. R. & WALKER, C. L. 2008. Loss of tuberous sclerosis complex-2 function and activation of mammalian target of rapamycin signaling in endometrial carcinoma. *Clin Cancer Res,* 14**,** 2543-50.

LUEDDE, T. & SCHWABE, R. F. 2011. NF-kappaB in the liver--linking injury, fibrosis and hepatocellular carcinoma. *Nat Rev Gastroenterol Hepatol,* 8**,** 108-18.

LUK, C. K., VEINOT-DREBOT, L., TJAN, E. & TANNOCK, I. F. 1990. Effect of transient hypoxia on sensitivity to doxorubicin in human and murine cell lines. *J Natl Cancer Inst,* 82**,** 684-92.

LUKASHEV, D., KLEBANOV, B., KOJIMA, H., GRINBERG, A., OHTA, A., BERENFELD, L., WENGER, R. H., OHTA, A. & SITKOVSKY, M. 2006. Cutting edge: hypoxia-inducible factor 1alpha and its activation-inducible short isoform I.1 negatively regulate functions of CD4+ and CD8+ T lymphocytes. *J Immunol,* 177**,** 4962-5.

MA, D. Z., XU, Z., LIANG, Y. L., SU, J. M., LI, Z. X., ZHANG, W., WANG, L. Y. & ZHA, X. L. 2005. Down-regulation of PTEN expression due to loss of promoter activity in human hepatocellular carcinoma cell lines. *World J Gastroenterol,* 11**,** 4472-7.

MAEHAMA, T. & DIXON, J. E. 1998. The tumor suppressor, PTEN/MMAC1, dephosphorylates the lipid second messenger, phosphatidylinositol 3,4,5-trisphosphate. *J Biol Chem,* 273**,** 13375-8.

MAEHAMA, T. & DIXON, J. E. 1999. PTEN: a tumour suppressor that functions as a phospholipid phosphatase. *Trends Cell Biol,* 9**,** 125-8.

MAHON, P. C., HIROTA, K. & SEMENZA, G. L. 2001. FIH-1: a novel protein that interacts with HIF-1alpha and VHL to mediate repression of HIF-1 transcriptional activity. *Genes Dev,* 15**,** 2675-86.

MALAGARI, K. 2008. Drug-eluting particles in the treatment of HCC: chemoembolization with doxorubicin-loaded DC Bead. *Expert Rev Anticancer Ther,* 8**,** 1643-50.

MALAGARI, K., POMONI, M., KELEKIS, A., POMONI, A., DOURAKIS, S., SPYRIDOPOULOS, T., MOSCHOURIS, H., EMMANOUIL, E., RIZOS, S. & KELEKIS, D. 2010. Prospective randomized comparison of chemoembolization with doxorubicin-eluting beads and bland embolization with BeadBlock for hepatocellular carcinoma. *Cardiovasc Intervent Radiol,* 33**,** 541-51.

MARTIN, W. M. & MCNALLY, N. J. 1980. Cytotoxicity of adriamycin to tumour cells in vivo and in vitro. *Br J Cancer,* 42**,** 881-9.

MASSON, N., WILLAM, C., MAXWELL, P. H., PUGH, C. W. & RATCLIFFE, P. J. 2001. Independent function of two destruction domains in hypoxia-inducible factor-alpha chains activated by prolyl hydroxylation. *Embo J,* 20**,** 5197-206.

MAXWELL, P. H., PUGH, C. W. & RATCLIFFE, P. J. 2001. Activation of the HIF pathway in cancer. *Curr Opin Genet Dev,* 11**,** 293-9.

MAXWELL, P. H., WIESENER, M. S., CHANG, G. W., CLIFFORD, S. C., VAUX, E. C., COCKMAN, M. E., WYKOFF, C. C., PUGH, C. W., MAHER, E. R. & RATCLIFFE, P. J. 1999. The tumour suppressor protein VHL targets hypoxia-inducible factors for oxygen-dependent proteolysis. *Nature,* 399**,** 271-5.

MCALISTER, V. C., GAO, Z., PELTEKIAN, K., DOMINGUES, J., MAHALATI, K. & MACDONALD, A. S. 2000. Sirolimus-tacrolimus combination immunosuppression. *Lancet,* 355**,** 376-7.

MCCLENDON, A. K. & OSHEROFF, N. 2007. DNA topoisomerase II, genotoxicity, and cancer. *Mutat Res,* 623**,** 83-97.

MCNEILL, L. A., HEWITSON, K. S., CLARIDGE, T. D., SEIBEL, J. F., HORSFALL, L. E. & SCHOFIELD, C. J. 2002. Hypoxia-inducible factor asparaginyl hydroxylase (FIH-1) catalyses hydroxylation at the beta-carbon of asparagine-803. *Biochem J,* 367**,** 571-5.

MELLOR, H. R. & CALLAGHAN, R. 2011. Accumulation and distribution of doxorubicin in tumour spheroids: the influence of acidity and expression of P-glycoprotein. *Cancer Chemother Pharmacol,* Mar 15. Epub ahead of print.

MI, D., YI, J., LIU, E. & LI, X. 2006. Relationsip between PTEN and VEGF expression and clinicopathological characteristics in HCC. *J Huazhong Univ Sci Technolog Med Sci,* 26**,** 682-5.

MI, J., ZHANG, X., RABBANI, Z. N., LIU, Y., REDDY, S. K., SU, Z., SALAHUDDIN, F. K., VILES, K., GIANGRANDE, P. H., DEWHIRST, M. W., SULLENGER, B. A., KONTOS, C. D. & CLARY, B. M. 2008. RNA aptamer-targeted inhibition of NF-kappa B suppresses non-small cell lung cancer resistance to doxorubicin. *Mol Ther,* 16**,** 66-73.

MIMNAUGH, E. G., KENNEDY, K. A., TRUSH, M. A. & SINHA, B. K. 1985a. Adriamycin-enhanced membrane lipid peroxidation in isolated rat nuclei. *Cancer Res,* 45**,** 3296-304.

MIMNAUGH, E. G., TRUSH, M. A., BHATNAGAR, M. & GRAM, T. E. 1985b. Enhancement of reactive oxygen-dependent mitochondrial membrane lipid peroxidation by the anticancer drug adriamycin. *Biochem Pharmacol,* 34**,** 847-56.

MITA, M. M., MITA, A. & ROWINSKY, E. K. 2003. The molecular target of rapamycin (mTOR) as a therapeutic target against cancer. *Cancer Biol Ther,* 2**,** S169-77.

MOK, T. S., YEO, W., YU, S., LAI, P., CHAN, H. L., CHAN, A. T., LAU, J. W., WONG, H., LEUNG, N., HUI, E. P., SUNG, J., KOH, J., MO, F., ZEE, B. & JOHNSON, P. J. 2005. An intensive surveillance program detected a high incidence of hepatocellular carcinoma among hepatitis B virus carriers with abnormal alpha-fetoprotein levels or abdominal ultrasonography results. *J Clin Oncol,* 23**,** 8041-7.

MOLINARI, M., KACHURA, J. R., DIXON, E., RAJAN, D. K., HAYEEMS, E. B., ASCH, M. R., BENJAMIN, M. S., SHERMAN, M., GALLINGER, S., BURNETT, B., FELD, R., CHEN, E., GREIG, P. D., GRANT, D. R. & KNOX, J. J. 2006. Transarterial chemoembolisation for advanced hepatocellular carcinoma: results from a North American cancer centre. *Clin Oncol (R Coll Radiol),* 18**,** 684-92.

MONDESIRE, W. H., JIAN, W., ZHANG, H., ENSOR, J., HUNG, M. C., MILLS, G. B. & MERIC-BERNSTAM, F. 2004. Targeting mammalian target of rapamycin synergistically enhances chemotherapy-induced cytotoxicity in breast cancer cells. *Clin Cancer Res,* 10**,** 7031-42.

MOSCHOURIS, H., MALAGARI, K., PAPADAKI, M. G., KORNEZOS, I. & MATSAIDONIS, D. 2010. Contrast-enhanced ultrasonography of hepatocellular carcinoma after chemoembolisation using drug-eluting beads: a pilot study focused on sustained tumor necrosis. *Cardiovasc Intervent Radiol,* 33**,** 1022-7.

MOTZER, R. J., ESCUDIER, B., OUDARD, S., HUTSON, T. E., PORTA, C., BRACARDA, S., GRUNWALD, V., THOMPSON, J. A., FIGLIN, R. A., HOLLAENDER, N., KAY, A. & RAVAUD, A. 2010. Phase 3 trial of everolimus for metastatic renal cell carcinoma : final results and analysis of prognostic factors. *Cancer,* 116**,** 4256-65.

NAKAYAMA, K. & RONAI, Z. 2004. Siah: new players in the cellular response to hypoxia. *Cell Cycle,* 3**,** 1345-7.

NAMUR, J., CITRON, S., DUPUIS, M., SELLERS, M., WASSEL, M., MANFAIT, M. & LAURENT, A. 2008a. Doxorubicin Eluting Beads in a Pig Liver Embolisation Model: Drug Distribution and Pathological Findings. *International Liver Cancer Association.* Chicago USA.

NAMUR, J., CITRON, S., DUPUIS, M., SELLERS, M., WASSEL, M., MANFAIT, M. & LAURENT, A. 2008b. Doxorubicin Tissue Release from Drug Eluting

Beads in Hepatocellular Carcinoma. *International Liver Cancer Association.* Chicago USA.

NAMUR, J., CITRON, S. J., SELLERS, M. T., DUPUIS, M. H., WASSEF, M., MANFAIT, M. & LAURENT, A. 2011. Embolization of hepatocellular carcinoma with drug-eluting beads: Doxorubicin tissue concentration and distribution in patient liver explants. *J Hepatol*.

NAMUR, J., WASSEF, M., MILLOT, J. M., LEWIS, A. L., MANFAIT, M. & LAURENT, A. 2010. Drug-eluting beads for liver embolization: concentration of doxorubicin in tissue and in beads in a pig model. *J Vasc Interv Radiol,* 21**,** 259-67.

NARDINOCCHI, L., PUCA, R., SACCHI, A. & D'ORAZI, G. 2009a. Inhibition of HIF-1alpha activity by homeodomain-interacting protein kinase-2 correlates with sensitization of chemoresistant cells to undergo apoptosis. *Mol Cancer,* 8**,** 1.

NARDINOCCHI, L., PUCA, R., SACCHI, A., RECHAVI, G., GIVOL, D. & D'ORAZI, G. 2009b. Targeting hypoxia in cancer cells by restoring homeodomain interacting protein-kinase 2 and p53 activity and suppressing HIF-1alpha. *PLoS One,* 4**,** e6819.

NASS, R. & CRINO, P. B. 2008. Tuberous sclerosis complex: a tale of two genes. *Neurology,* 70**,** 904-5.

NEIDLE, S. 1979. The molecular basis for the action of some DNA-binding drugs. *Prog Med Chem,* 16**,** 151-221.

NEUHAUS, P., KLUPP, J. & LANGREHR, J. M. 2001. mTOR inhibitors: an overview. *Liver Transpl,* 7**,** 473-84.

NEWELL, P., TOFFANIN, S., VILLANUEVA, A., CHIANG, D. Y., MINGUEZ, B., CABELLOS, L., SAVIC, R., HOSHIDA, Y., LIM, K. H., MELGAR-LESMES, P., YEA, S., PEIX, J., DENIZ, K., FIEL, M. I., THUNG, S., ALSINET, C., TOVAR, V., MAZZAFERRO, V., BRUIX, J., ROAYAIE, S., SCHWARTZ, M., FRIEDMAN, S. L. & LLOVET, J. M. 2009. Ras pathway activation in hepatocellular carcinoma and anti-tumoral effect of combined sorafenib and rapamycin in vivo. *J Hepatol,* 51**,** 725-33.

NITISS, J. L. 2009. DNA topoisomerase II and its growing repertoire of biological functions. *Nat Rev Cancer,* 9**,** 327-37.

O'DONNELL, A., FAIVRE, S., BURRIS, H. A., 3RD, REA, D., PAPADIMITRAKOPOULOU, V., SHAND, N., LANE, H. A., HAZELL, K., ZOELLNER, U., KOVARIK, J. M., BROCK, C., JONES, S., RAYMOND, E. & JUDSON, I. 2008. Phase I pharmacokinetic and pharmacodynamic study of the oral mammalian target of rapamycin inhibitor everolimus in patients with advanced solid tumors. *J Clin Oncol,* 26**,** 1588-95.

O'REILLY, T., MCSHEEHY, P. M., WARTMANN, M., LASSOTA, P., BRANDT, R. & LANE, H. A. 2011. Evaluation of the mTOR inhibitor, everolimus, in combination with cytotoxic antitumor agents using human tumor models in vitro and in vivo. *Anticancer Drugs,* 22**,** 58-78.

O'ROURKE, J. F., TIAN, Y. M., RATCLIFFE, P. J. & PUGH, C. W. 1999. Oxygen-regulated and transactivating domains in endothelial PAS protein 1: comparison with hypoxia-inducible factor-1alpha. *J Biol Chem,* 274**,** 2060-71.

OGISO, Y., TOMIDA, A., LEI, S., OMURA, S. & TSURUO, T. 2000. Proteasome inhibition circumvents solid tumor resistance to topoisomerase II-directed drugs. *Cancer Res,* 60**,** 2429-34.

OKAMOTO, I., DOI, T., OHTSU, A., MIYAZAKI, M., TSUYA, A., KUREI, K., KOBAYASHI, K. & NAKAGAWA, K. 2010. Phase I clinical and pharmacokinetic study of RAD001 (everolimus) administered daily to Japanese patients with advanced solid tumors. *Jpn J Clin Oncol,* 40**,** 17-23.

ONG, L. C., SONG, I. C., JIN, Y., KEE, I. H., SIEW, E., YU, S., THNG, C. H., HUYNH, H. & CHOW, P. K. 2009. Effective inhibition of xenografts of hepatocellular carcinoma (HepG2) by rapamycin and bevacizumab in an intrahepatic model. *Mol Imaging Biol,* 11**,** 334-42.

OSHEROFF, N. 1989. Biochemical basis for the interactions of type I and type II topoisomerases with DNA. *Pharmacol Ther,* 41**,** 223-41.

OSHEROFF, N., ZECHIEDRICH, E. L. & GALE, K. C. 1991. Catalytic function of DNA topoisomerase II. *Bioessays,* 13**,** 269-73.

PAPANDREOU, I., CAIRNS, R. A., FONTANA, L., LIM, A. L. & DENKO, N. C. 2006. HIF-1 mediates adaptation to hypoxia by actively downregulating mitochondrial oxygen consumption. *Cell Metab,* 3**,** 187-97.

PARKIN, D. M., BRAY, F., FERLAY, J. & PISANI, P. 2005. Global cancer statistics, 2002. *CA Cancer J Clin,* 55**,** 74-108.

PATEL, D. J., KOZLOWSKI, S. A. & RICE, J. A. 1981. Hydrogen bonding, overlap geometry, and sequence specificity in anthracycline antitumor antibiotic.DNA complexes in solution. *Proc Natl Acad Sci U S A,* 78**,** 3333-7.

PAWARODE, A., SHUKLA, S., MINDERMAN, H., FRICKE, S. M., PINDER, E. M., O'LOUGHLIN, K. L., AMBUDKAR, S. V. & BAER, M. R. 2007. Differential effects of the immunosuppressive agents cyclosporin A, tacrolimus and sirolimus on drug transport by multidrug resistance proteins. *Cancer Chemother Pharmacol,* 60**,** 179-88.

PERKINS, N. D. 2006. Post-translational modifications regulating the activity and function of the nuclear factor kappa B pathway. *Oncogene,* 25**,** 6717-30.

PEYROU, M., BOURGOIN, L. & FOTI, M. 2010. PTEN in liver diseases and cancer. *World J Gastroenterol,* 16**,** 4627-33.

PIGRAM, W. J., FULLER, W. & HAMILTON, L. D. 1972. Stereochemistry of intercalation: interaction of daunomycin with DNA. *Nat New Biol,* 235**,** 17-9.

PIGUET, A. C., SAAR, B., HLUSHCHUK, R., ST-PIERRE, M. V., MCSHEEHY, P. M., RADOJEVIC, V., AFTHINOS, M., TERRACCIANO, L., DJONOV, V. & DUFOUR, J. F. 2011. Everolimus augments the effects of sorafenib in a syngeneic orthotopic model of hepatocellular carcinoma. *Mol Cancer Ther,* 10**,** 1007-17.

PIGUET, A. C., SEMELA, D., KEOGH, A., WILKENS, L., STROKA, D., STOUPIS, C., ST-PIERRE, M. V. & DUFOUR, J. F. 2008. Inhibition of mTOR in combination with doxorubicin in an experimental model of hepatocellular carcinoma. *J Hepatol,* 49**,** 78-87.

PIRET, J. P., MINET, E., COSSE, J. P., NINANE, N., DEBACQ, C., RAES, M. & MICHIELS, C. 2005. Hypoxia-inducible factor-1-dependent overexpression of myeloid cell factor-1 protects hypoxic cells against tert-butyl hydroperoxide-induced apoptosis. *J Biol Chem,* 280**,** 9336-44.

PIRET, J. P., MOTTET, D., RAES, M. & MICHIELS, C. 2002a. CoCl2, a chemical inducer of hypoxia-inducible factor-1, and hypoxia reduce apoptotic cell death in hepatoma cell line HepG2. *Ann N Y Acad Sci,* 973**,** 443-7.

PIRET, J. P., MOTTET, D., RAES, M. & MICHIELS, C. 2002b. Is HIF-1alpha a pro- or an anti-apoptotic protein? *Biochem Pharmacol,* 64**,** 889-92.

POMMIER, Y., LEO, E., ZHANG, H. & MARCHAND, C. 2010. DNA topoisomerases and their poisoning by anticancer and antibacterial drugs. *Chem Biol,* 17**,** 421-33.

PONS, F., VARELA, M. & LLOVET, J. M. 2005. Staging systems in hepatocellular carcinoma. *HPB (Oxford),* 7**,** 35-41.

POON, R. T., LAU, C., YU, W. C., FAN, S. T. & WONG, J. 2004. High serum levels of vascular endothelial growth factor predict poor response to transarterial chemoembolization in hepatocellular carcinoma: a prospective study. *Oncol Rep,* 11**,** 1077-84.

POTMESIL, M., KIRSCHENBAUM, S., ISRAEL, M., LEVIN, M., KHETARPAL, V. K. & SILBER, R. 1983. Relationship of adriamycin concentrations to the DNA lesions induced in hypoxic and euoxic L1210 cells. *Cancer Res,* 43**,** 3528-33.

PRIMEAU, A. J., RENDON, A., HEDLEY, D., LILGE, L. & TANNOCK, I. F. 2005. The distribution of the anticancer drug Doxorubicin in relation to blood vessels in solid tumors. *Clin Cancer Res,* 11**,** 8782-8.

PUPPO, M., BATTAGLIA, F., OTTAVIANO, C., DELFINO, S., RIBATTI, D., VARESIO, L. & BOSCO, M. C. 2008. Topotecan inhibits vascular endothelial growth factor production and angiogenic activity induced by hypoxia in human neuroblastoma by targeting hypoxia-inducible factor-1alpha and -2alpha. *Mol Cancer Ther,* 7**,** 1974-84.

QUESADA, A. J., NELIUS, T., YAP, R., ZAICHUK, T. A., ALFRANCA, A., FILLEUR, S., VOLPERT, O. V. & REDONDO, J. M. 2005. In vivo upregulation of CD95 and CD95L causes synergistic inhibition of angiogenesis by TSP1 peptide and metronomic doxorubicin treatment. *Cell Death Differ,* 12**,** 649-58.

QUIGLEY, G. J., WANG, A. H., UGHETTO, G., VAN DER MAREL, G., VAN BOOM, J. H. & RICH, A. 1980. Molecular structure of an anticancer drug-DNA complex: daunomycin plus d(CpGpTpApCpG). *Proc Natl Acad Sci U S A,* 77**,** 7204-8.

RAGHUNAND, N., HE, X., VAN SLUIS, R., MAHONEY, B., BAGGETT, B., TAYLOR, C. W., PAINE-MURRIETA, G., ROE, D., BHUJWALLA, Z. M. & GILLIES, R. J. 1999. Enhancement of chemotherapy by manipulation of tumour pH. *Br J Cancer,* 80**,** 1005-11.

RAMPONE, B., SCHIAVONE, B., MARTINO, A., VIVIANO, C. & CONFUORTO, G. 2009. Current management strategy of hepatocellular carcinoma. *World J Gastroenterol,* 15**,** 3210-6.

RAOUL, J. L. 2008. Natural history of hepatocellular carcinoma and current treatment options. *Semin Nucl Med,* 38**,** S13-8.

RAOUL, J. L., HERESBACH, D., BRETAGNE, J. F., FERRER, D. B., DUVAUFERRIER, R., BOURGUET, P., MESSNER, M. & GOSSELIN, M. 1992. Chemoembolization of hepatocellular carcinomas. A study of the biodistribution and pharmacokinetics of doxorubicin. *Cancer,* 70**,** 585-90.

RAOUL, J. L., SANGRO, B., FORNER, A., MAZZAFERRO, V., PISCAGLIA, F., BOLONDI, L. & LENCIONI, R. 2011. Evolving strategies for the management of intermediate-stage hepatocellular carcinoma: available evidence and expert opinion on the use of transarterial chemoembolization. *Cancer Treat Rev,* 37**,** 212-20.

RAPISARDA, A., URANCHIMEG, B., SORDET, O., POMMIER, Y., SHOEMAKER, R. H. & MELILLO, G. 2004a. Topoisomerase I-mediated

inhibition of hypoxia-inducible factor 1: mechanism and therapeutic implications. *Cancer Res,* 64**,** 1475-82.

RAPISARDA, A., ZALEK, J., HOLLINGSHEAD, M., BRAUNSCHWEIG, T., URANCHIMEG, B., BONOMI, C. A., BORGEL, S. D., CARTER, J. P., HEWITT, S. M., SHOEMAKER, R. H. & MELILLO, G. 2004b. Schedule-dependent inhibition of hypoxia-inducible factor-1alpha protein accumulation, angiogenesis, and tumor growth by topotecan in U251-HRE glioblastoma xenografts. *Cancer Res,* 64**,** 6845-8.

REDDY, G., SHARMA, K. V., DREHER, M., WOODS, D. L. & WOOD, B. J. 2010. Tissue Penetration of Drug from Doxorubicin Eluting Radiopaque Embolization Beads;. *SIR (Society of Interventional Radiology) Conference.* Tampa, Florida, USA.

REYES, D. K., VOSSEN, J. A., KAMEL, I. R., AZAD, N. S., WAHLIN, T. A., TORBENSON, M. S., CHOTI, M. A. & GESCHWIND, J. F. 2009. Single-center phase II trial of transarterial chemoembolization with drug-eluting beads for patients with unresectable hepatocellular carcinoma: initial experience in the United States. *Cancer J,* 15**,** 526-32.

REYNOLDS, T. Y., ROCKWELL, S. & GLAZER, P. M. 1996. Genetic instability induced by the tumor microenvironment. *Cancer Res,* 56**,** 5754-7.

RHARASS, T., VIGO, J., SALMON, J. M. & RIBOU, A. C. 2008. New method for the detection of reactive oxygen species in anti-tumoural activity of adriamycin: a comparison between hypoxic and normoxic cells. *Free Radic Res,* 42**,** 124-34.

RHEE, T. K., YOUNG, J. Y., LARSON, A. C., HAINES, G. K., 3RD, SATO, K. T., SALEM, R., MULCAHY, M. F., KULIK, L. M., PAUNESKU, T., WOLOSCHAK, G. E. & OMARY, R. A. 2007. Effect of transcatheter arterial embolization on levels of hypoxia-inducible factor-1alpha in rabbit VX2 liver tumors. *J Vasc Interv Radiol,* 18**,** 639-45.

RIBATTI, D., NICO, B., MANGIERI, D., LONGO, V., SANSONNO, D., VACCA, A. & DAMMACCO, F. 2007. In vivo inhibition of human hepatocellular carcinoma related angiogenesis by vinblastine and rapamycin. *Histol Histopathol,* 22**,** 285-9.

RIZELL, M., ANDERSSON, M., CAHLIN, C., HAFSTROM, L., OLAUSSON, M. & LINDNER, P. 2008. Effects of the mTOR inhibitor sirolimus in patients with hepatocellular and cholangiocellular cancer. *Int J Clin Oncol,* 13**,** 66-70.

ROHWER, N., DAME, C., HAUGSTETTER, A., WIEDENMANN, B., DETJEN, K., SCHMITT, C. A. & CRAMER, T. 2010. Hypoxia-inducible factor 1alpha determines gastric cancer chemosensitivity via modulation of p53 and NF-kappaB. *PLoS One,* 5**,** e12038.

ROMANO, M. F., AVELLINO, R., PETRELLA, A., BISOGNI, R., ROMANO, S. & VENUTA, S. 2004. Rapamycin inhibits doxorubicin-induced NF-kappaB/Rel nuclear activity and enhances the apoptosis of melanoma cells. *Eur J Cancer,* 40**,** 2829-36.

RONINSON, I. B. 1992. The role of the MDR1 (P-glycoprotein) gene in multidrug resistance in vitro and in vivo. *Biochem Pharmacol,* 43**,** 95-102.

ROWLEY, D. A. & HALLIWELL, B. 1983. DNA damage by superoxide-generating systems in relation to the mechanism of action of the anti-tumour antibiotic adriamycin. *Biochim Biophys Acta,* 761**,** 86-93.

SAHIN, F., KANNANGAI, R., ADEGBOLA, O., WANG, J., SU, G. & TORBENSON, M. 2004. mTOR and P70 S6 kinase expression in primary liver neoplasms. *Clin Cancer Res,* 10**,** 8421-5.

SAIKUMAR, P., DONG, Z., PATEL, Y., HALL, K., HOPFER, U., WEINBERG, J. M. & VENKATACHALAM, M. A. 1998. Role of hypoxia-induced Bax translocation and cytochrome c release in reoxygenation injury. *Oncogene,* 17**,** 3401-15.

SAKATA, K., KWOK, T. T., MURPHY, B. J., LADEROUTE, K. R., GORDON, G. R. & SUTHERLAND, R. M. 1991. Hypoxia-induced drug resistance: comparison to P-glycoprotein-associated drug resistance. *Br J Cancer,* 64**,** 809-14.

SANCHEZ-PUIG, N., VEPRINTSEV, D. B. & FERSHT, A. R. 2005. Binding of natively unfolded HIF-1alpha ODD domain to p53. *Mol Cell,* 17**,** 11-21.

SANCHEZ ANTOLIN, G., GARCIA PAJARES, F., LORENZO PELAYO, S., HERRANZ BACHILLER, M. T., ALMOHALLA, C., VELICIA, R. & CARO PATON, A. 2011. Indications and effectiveness of the mammalian target of rapamycin in liver transplantation. *Transplant Proc,* 43**,** 714-7.

SANDER, M. & HSIEH, T. 1983. Double strand DNA cleavage by type II DNA topoisomerase from Drosophila melanogaster. *J Biol Chem,* 258**,** 8421-8.

SANGIOVANNI, A., DEL NINNO, E., FASANI, P., DE FAZIO, C., RONCHI, G., ROMEO, R., MORABITO, A., DE FRANCHIS, R. & COLOMBO, M. 2004. Increased survival of cirrhotic patients with a hepatocellular carcinoma detected during surveillance. *Gastroenterology,* 126**,** 1005-14.

SANNA, K. & ROFSTAD, E. K. 1994. Hypoxia-induced resistance to doxorubicin and methotrexate in human melanoma cell lines in vitro. *Int J Cancer,* 58**,** 258-62.

SANTORE, M. T., MCCLINTOCK, D. S., LEE, V. Y., BUDINGER, G. R. & CHANDEL, N. S. 2002. Anoxia-induced apoptosis occurs through a mitochondria-dependent pathway in lung epithelial cells. *Am J Physiol Lung Cell Mol Physiol,* 282**,** L727-34.

SANYAL, A. J., YOON, S. K. & LENCIONI, R. 2010. The etiology of hepatocellular carcinoma and consequences for treatment. *Oncologist,* 15 Suppl 4**,** 14-22.

SAPRA, P., KRAFT, P., PASTORINO, F., RIBATTI, D., DUMBLE, M., MEHLIG, M., WANG, M., PONZONI, M., GREENBERGER, L. M. & HORAK, I. D. 2011a. Potent and sustained inhibition of HIF-1alpha and downstream genes by a polyethyleneglycol-SN38 conjugate, EZN-2208, results in anti-angiogenic effects. *Angiogenesis,* 14(3), 245-53.

SAPRA, P., KRAFT, P., PASTORINO, F., RIBATTI, D., DUMBLE, M., MEHLIG, M., WANG, M., PONZONI, M., GREENBERGER, L. M. & HORAK, I. D. 2011b. Potent and sustained inhibition of HIF-1alpha and downstream genes by a polyethyleneglycol-SN38 conjugate, EZN-2208, results in anti-angiogenic effects. *Angiogenesis,* 14**,** 245-53.

SARBASSOV, D. D., ALI, S. M., SENGUPTA, S., SHEEN, J. H., HSU, P. P., BAGLEY, A. F., MARKHARD, A. L. & SABATINI, D. M. 2006. Prolonged rapamycin treatment inhibits mTORC2 assembly and Akt/PKB. *Mol Cell,* 22**,** 159-68.

SARBASSOV, D. D., GUERTIN, D. A., ALI, S. M. & SABATINI, D. M. 2005. Phosphorylation and regulation of Akt/PKB by the rictor-mTOR complex. *Science,* 307**,** 1098-101.

SCHNITZBAUER, A. A., SCHLITT, H. J. & GEISSLER, E. K. 2011. Influence of immunosuppressive drugs on the recurrence of hepatocellular carcinoma after liver transplantation: a gap between basic science and clinical evidence. *Transplantation,* 91**,** 1173-6.

SCHNITZBAUER, A. A., ZUELKE, C., GRAEB, C., ROCHON, J., BILBAO, I., BURRA, P., DE JONG, K. P., DUVOUX, C., KNETEMAN, N. M., ADAM, R., BECHSTEIN, W. O., BECKER, T., BECKEBAUM, S., CHAZOUILLERES, O., CILLO, U., COLLEDAN, M., FANDRICH, F., GUGENHEIM, J., HAUSS, J. P., HEISE, M., HIDALGO, E., JAMIESON, N., KONIGSRAINER, A., LAMBY, P. E., LERUT, J. P., MAKISALO, H., MARGREITER, R., MAZZAFERRO, V., MUTZBAUER, I., OTTO, G., PAGEAUX, G. P., PINNA, A. D., PIRENNE, J., RIZELL, M., ROSSI, G., ROSTAING, L., ROY, A., TURRION, V. S., SCHMIDT, J., TROISI, R. I., VAN HOEK, B., VALENTE, U., WOLF, P., WOLTERS, H., MIRZA, D. F., SCHOLZ, T., STEININGER, R., SODERDAHL, G., STRASSER, S. I., JAUCH, K. W., NEUHAUS, P., SCHLITT, H. J. & GEISSLER, E. K. 2010. A prospective randomised, open-labeled, trial comparing sirolimus-containing versus mTOR-inhibitor-free immunosuppression in patients undergoing liver transplantation for hepatocellular carcinoma. *BMC Cancer,* 10**,** 190.

SCHONIGER-HEKELE, M. & MULLER, C. 2010. Pilot study: rapamycin in advanced hepatocellular carcinoma. *Aliment Pharmacol Ther,* 32**,** 763-8.

SCHRIJVERS, D. L. 2003. Extravasation: a dreaded complication of chemotherapy. *Ann Oncol,* 14 Suppl 3**,** iii26-30.

SCHULER, W., SEDRANI, R., COTTENS, S., HABERLIN, B., SCHULZ, M., SCHUURMAN, H. J., ZENKE, G., ZERWES, H. G. & SCHREIER, M. H. 1997. SDZ RAD, a new rapamycin derivative: pharmacological properties in vitro and in vivo. *Transplantation,* 64**,** 36-42.

SCHUMACHER, G., OIDTMANN, M., ROSEWICZ, S., LANGREHR, J., JONAS, S., MUELLER, A. R., RUEGGEBERG, A., NEUHAUS, R., BAHRA, M., JACOB, D., GERLACH, H. & NEUHAUS, P. 2002. Sirolimus inhibits growth of human hepatoma cells in contrast to tacrolimus which promotes cell growth. *Transplant Proc,* 34**,** 1392-3.

SEMELA, D., PIGUET, A. C., KOLEV, M., SCHMITTER, K., HLUSHCHUK, R., DJONOV, V., STOUPIS, C. & DUFOUR, J. F. 2007. Vascular remodeling and antitumoral effects of mTOR inhibition in a rat model of hepatocellular carcinoma. *J Hepatol,* 46**,** 840-8.

SEMENZA, G. L. 2000a. Expression of hypoxia-inducible factor 1: mechanisms and consequences. *Biochem Pharmacol,* 59**,** 47-53.

SEMENZA, G. L. 2000b. Hypoxia, clonal selection, and the role of HIF-1 in tumor progression. *Crit Rev Biochem Mol Biol,* 35**,** 71-103.

SEMENZA, G. L. 2003. Targeting HIF-1 for cancer therapy. *Nat Rev Cancer,* 3**,** 721-32.

SEMENZA, G. L. 2007b. Hypoxia and cancer. *Cancer Metastasis Rev,* 26**,** 223-4.

SEMENZA, G. L., AGANI, F., BOOTH, G., FORSYTHE, J., IYER, N., JIANG, B. H., LEUNG, S., ROE, R., WIENER, C. & YU, A. 1997. Structural and functional analysis of hypoxia-inducible factor 1. *Kidney Int,* 51**,** 553-5.

SEMENZA, G. L., NEJFELT, M. K., CHI, S. M. & ANTONARAKIS, S. E. 1991. Hypoxia-inducible nuclear factors bind to an enhancer element located 3' to the human erythropoietin gene. *Proc Natl Acad Sci U S A,* 88**,** 5680-4.

SEMENZA, G. L., ROTH, P. H., FANG, H. M. & WANG, G. L. 1994. Transcriptional regulation of genes encoding glycolytic enzymes by hypoxia-inducible factor 1. *J Biol Chem,* 269**,** 23757-63.

SEMENZA, G. L., SHIMODA, L. A. & PRABHAKAR, N. R. 2006. Regulation of gene expression by HIF-1. *Novartis Found Symp,* 272**,** 2-8; discussion 8-14, 33-6.

SEMENZA, G. L. & WANG, G. L. 1992. A nuclear factor induced by hypoxia via de novo protein synthesis binds to the human erythropoietin gene enhancer at a site required for transcriptional activation. *Mol Cell Biol,* 12**,** 5447-54.

SERGIO, A., CRISTOFORI, C., CARDIN, R., PIVETTA, G., RAGAZZI, R., BALDAN, A., GIRARDI, L., CILLO, U., BURRA, P., GIACOMIN, A. & FARINATI, F. 2008. Transcatheter arterial chemoembolization (TACE) in hepatocellular carcinoma (HCC): the role of angiogenesis and invasiveness. *Am J Gastroenterol,* 103**,** 914-21.

SERMEUS, A., COSSE, J. P., CRESPIN, M., MAINFROID, V., DE LONGUEVILLE, F., NINANE, N., RAES, M., REMACLE, J. & MICHIELS, C. 2008. Hypoxia induces protection against etoposide-induced apoptosis: molecular profiling of changes in gene expression and transcription factor activity. *Mol Cancer,* 7**,** 27.

SHAO, G., WANG, J., ZHOU, K. & YAN, Z. 2002. [Intratumoral microvessel density and expression of vascular endothelial growth factor in hepatocellular carcinoma after chemoembolization]. *Zhonghua Gan Zang Bing Za Zhi,* 10**,** 170-3.

SHIM, J. H., PARK, J. W., KIM, J. H., AN, M., KONG, S. Y., NAM, B. H., CHOI, J. I., KIM, H. B., LEE, W. J. & KIM, C. M. 2008. Association between increment of serum VEGF level and prognosis after transcatheter arterial chemoembolization in hepatocellular carcinoma patients. *Cancer Sci,* 99**,** 2037-44.

SHIROUZU, Y., RYSCHICH, E., SALNIKOVA, O., KERKADZE, V., SCHMIDT, J. & ENGELMANN, G. 2010. Rapamycin inhibits proliferation and migration of hepatoma cells in vitro. *J Surg Res,* 159**,** 705-13.

SIEGHART, W., FUEREDER, T., SCHMID, K., CEJKA, D., WERZOWA, J., WRBA, F., WANG, X., GRUBER, D., RASOUL-ROCKENSCHAUB, S., PECK-RADOSAVLJEVIC, M. & WACHECK, V. 2007. Mammalian target of rapamycin pathway activity in hepatocellular carcinomas of patients undergoing liver transplantation. *Transplantation,* 83**,** 425-32.

SINHA, B. K. 1995. Topoisomerase inhibitors. A review of their therapeutic potential in cancer. *Drugs,* 49**,** 11-9.

SINHA, B. K. & CHIGNELL, C. F. 1979. Binding mode of chemically activated semiquinone free radicals from quinone anticancer agents to DNA. *Chem Biol Interact,* 28**,** 301-8.

SLOMOVITZ, B. M., LU, K. H., JOHNSTON, T., COLEMAN, R. L., MUNSELL, M., BROADDUS, R. R., WALKER, C., RAMONDETTA, L. M., BURKE, T. W., GERSHENSON, D. M. & WOLF, J. 2010. A phase 2 study of the oral mammalian target of rapamycin inhibitor, everolimus, in patients with recurrent endometrial carcinoma. *Cancer,* 116**,** 5415-9.

SMITH, E., STRATFORD, I. J. & ADAMS, G. E. 1980. Cytotoxicity of adriamycin on aerobic and hypoxic chinese hamster V79 cells in vitro. *Br J Cancer,* 42**,** 568-73.

SOFER, A., LEI, K., JOHANNESSEN, C. M. & ELLISEN, L. W. 2005. Regulation of mTOR and cell growth in response to energy stress by REDD1. *Mol Cell Biol,* 25**,** 5834-45.

SOKOLOSKY, M. L., STADELMAN, K. M., CHAPPELL, W. H., ABRAMS, S. L., MARTELLI, A. M., STIVALA, F., LIBRA, M., NICOLETTI, F., DROBOT, L. B., FRANKLIN, R. A., STEELMAN, L. S. & MCCUBREY, J. A. 2011a. Involvement of Akt-1 and mTOR in Sensitivity of Breast Cancer to Targeted Therapy. *Oncotarget,* 2(7), 538-50.

SOKOLOSKY, M. L., STADELMAN, K. M., CHAPPELL, W. H., ABRAMS, S. L., MARTELLI, A. M., STIVALA, F., LIBRA, M., NICOLETTI, F., DROBOT, L. B., FRANKLIN, R. A., STEELMAN, L. S. & MCCUBREY, J. A. 2011b. Involvement of Akt-1 and mTOR in sensitivity of breast cancer to targeted therapy. *Oncotarget,* 2**,** 538-50.

SONG, X., LIU, X., CHI, W., LIU, Y., WEI, L., WANG, X. & YU, J. 2006. Hypoxia-induced resistance to cisplatin and doxorubicin in non-small cell lung cancer is inhibited by silencing of HIF-1alpha gene. *Cancer Chemother Pharmacol,* 58**,** 776-84.

SOWTER, H. M., RATCLIFFE, P. J., WATSON, P., GREENBERG, A. H. & HARRIS, A. L. 2001. HIF-1-dependent regulation of hypoxic induction of the cell death factors BNIP3 and NIX in human tumors. *Cancer Res,* 61**,** 6669-73.

STEELMAN, L. S., NAVOLANIC, P. M., SOKOLOSKY, M. L., TAYLOR, J. R., LEHMANN, B. D., CHAPPELL, W. H., ABRAMS, S. L., WONG, E. W., STADELMAN, K. M., TERRIAN, D. M., LESLIE, N. R., MARTELLI, A. M., STIVALA, F., LIBRA, M., FRANKLIN, R. A. & MCCUBREY, J. A. 2008. Suppression of PTEN function increases breast cancer chemotherapeutic drug resistance while conferring sensitivity to mTOR inhibitors. *Oncogene,* 27**,** 4086-95.

STOLZE, I. P., TIAN, Y. M., APPELHOFF, R. J., TURLEY, H., WYKOFF, C. C., GLEADLE, J. M. & RATCLIFFE, P. J. 2004. Genetic analysis of the role of the asparaginyl hydroxylase factor inhibiting hypoxia-inducible factor (HIF) in regulating HIF transcriptional target genes. *J Biol Chem,* 279**,** 42719-25.

SULLIVAN, D. M., CHOW, K. C., GLISSON, B. S. & ROSS, W. E. 1987. Role of proliferation in determining sensitivity to topoisomerase II-active chemotherapy agents. *NCI Monogr***,** 73-8.

SULLIVAN, R. & GRAHAM, C. H. 2009. Hypoxia prevents etoposide-induced DNA damage in cancer cells through a mechanism involving hypoxia-inducible factor 1. *Mol Cancer Ther,* 8**,** 1702-13.

SULLIVAN, R., PARE, G. C., FREDERIKSEN, L. J., SEMENZA, G. L. & GRAHAM, C. H. 2008. Hypoxia-induced resistance to anticancer drugs is associated with decreased senescence and requires hypoxia-inducible factor-1 activity. *Mol Cancer Ther,* 7**,** 1961-73.

SUN, Q., ZHENG, Y., LIU, Q. & CAO, X. 2008. Rapamycin reverses TLR4 signaling-triggered tumor apoptosis resistance by disrupting Akt-mediated Bcl-xL upregulation. *Int Immunopharmacol,* 8**,** 1854-8.

SUN, X., JIANG, H., JIANG, X., TAN, H., MENG, Q., SUN, B., XU, R. & KRISSANSEN, G. W. 2009. Antisense hypoxia-inducible factor-1alpha augments transcatheter arterial embolization in the treatment of hepatocellular carcinomas in rats. *Hum Gene Ther,* 20**,** 314-24.

SUTHERLAND, R. M. 1988. Cell and environment interactions in tumor microregions: the multicell spheroid model. *Science,* 240**,** 177-84.

SWANSON, H. I., CHAN, W. K. & BRADFIELD, C. A. 1995. DNA binding specificities and pairing rules of the Ah receptor, ARNT, and SIM proteins. *J Biol Chem,* 270**,** 26292-302.

SWIFT, L. P., REPHAELI, A., NUDELMAN, A., PHILLIPS, D. R. & CUTTS, S. M. 2006. Doxorubicin-DNA adducts induce a non-topoisomerase II-mediated form of cell death. *Cancer Res,* 66**,** 4863-71.

SZE, K. M., WONG, K. L., CHU, G. K., LEE, J. M., YAU, T. O. & OI-LIN NG, I. 2011. Loss of phosphatase and tensin homolog enhances cell invasion and migration through aKT/Sp-1 transcription factor/matrix metalloproteinase 2 activation in hepatocellular carcinoma and has clinicopathologic significance. *Hepatology,* 53**,** 1558-69.

TABERNERO, J., ROJO, F., CALVO, E., BURRIS, H., JUDSON, I., HAZELL, K., MARTINELLI, E., RAMON Y CAJAL, S., JONES, S., VIDAL, L., SHAND, N., MACARULLA, T., RAMOS, F. J., DIMITRIJEVIC, S., ZOELLNER, U., TANG, P., STUMM, M., LANE, H. A., LEBWOHL, D. & BASELGA, J. 2008. Dose- and schedule-dependent inhibition of the mammalian target of rapamycin pathway with everolimus: a phase I tumor pharmacodynamic study in patients with advanced solid tumors. *J Clin Oncol,* 26**,** 1603-10.

TAK, E., LEE, S., LEE, J., RASHID, M. A., KIM, Y. W., PARK, J. H., PARK, W. S., SHOKAT, K. M., HA, J. & KIM, S. S. 2011. Human carbonyl reductase 1 upregulated by hypoxia renders resistance to apoptosis in hepatocellular carcinoma cells. *J Hepatol,* 54**,** 328-39.

TAKAYASU, K., ARII, S., IKAI, I., OMATA, M., OKITA, K., ICHIDA, T., MATSUYAMA, Y., NAKANUMA, Y., KOJIRO, M., MAKUUCHI, M. & YAMAOKA, Y. 2006. Prospective cohort study of transarterial chemoembolization for unresectable hepatocellular carcinoma in 8510 patients. *Gastroenterology,* 131**,** 461-9.

TAKEDA, K., HO, V. C., TAKEDA, H., DUAN, L. J., NAGY, A. & FONG, G. H. 2006. Placental but not heart defects are associated with elevated hypoxia-inducible factor alpha levels in mice lacking prolyl hydroxylase domain protein 2. *Mol Cell Biol,* 26**,** 8336-46.

TAM, K. H., YANG, Z. F., LAU, C. K., LAM, C. T., PANG, R. W. & POON, R. T. 2009. Inhibition of mTOR enhances chemosensitivity in hepatocellular carcinoma. *Cancer Lett,* 273**,** 201-9.

TAN, C., TASAKA, H., YU, K. P., MURPHY, M. L. & KARNOFSKY, D. A. 1967. Daunomycin, an antitumor antibiotic, in the treatment of neoplastic disease. Clinical evaluation with special reference to childhood leukemia. *Cancer,* 20**,** 333-53.

TANAKA, M., KOUL, D., DAVIES, M. A., LIEBERT, M., STECK, P. A. & GROSSMAN, H. B. 2000. MMAC1/PTEN inhibits cell growth and induces chemosensitivity to doxorubicin in human bladder cancer cells. *Oncogene,* 19**,** 5406-12.

TANAKA, M., ROSSER, C. J. & GROSSMAN, H. B. 2005. PTEN gene therapy induces growth inhibition and increases efficacy of chemotherapy in prostate cancer. *Cancer Detect Prev,* 29**,** 170-4.

TANNOCK, I. 1982. Response of aerobic and hypoxic cells in a solid tumor to adriamycin and cyclophosphamide and interaction of the drugs with radiation. *Cancer Res,* 42**,** 4921-6.

TAPIA, M. A., GONZALEZ-NAVARRETE, I., DALMASES, A., BOSCH, M., RODRIGUEZ-FANJUL, V., ROLFE, M., ROSS, J. S., MEZQUITA, J., MEZQUITA, C., BACHS, O., GASCON, P., ROJO, F., PERONA, R., ROVIRA, A. & ALBANELL, J. 2007. Inhibition of the canonical IKK/NF kappa B pathway sensitizes human cancer cells to doxorubicin. *Cell Cycle,* 6**,** 2284-92.

TEICHER, B. A., LAZO, J. S. & SARTORELLI, A. C. 1981. Classification of antineoplastic agents by their selective toxicities toward oxygenated and hypoxic tumor cells. *Cancer Res,* 41**,** 73-81.

TEWEY, K. M., ROWE, T. C., YANG, L., HALLIGAN, B. D. & LIU, L. F. 1984. Adriamycin-induced DNA damage mediated by mammalian DNA topoisomerase II. *Science,* 226**,** 466-8.

THEWS, O., GASSNER, B., KELLEHER, D. K. & GEKLE, M. 2008. Activity of drug efflux transporters in tumor cells under hypoxic conditions. *Adv Exp Med Biol,* 614**,** 157-64.

THIEBAUT, F., TSURUO, T., HAMADA, H., GOTTESMAN, M. M., PASTAN, I. & WILLINGHAM, M. C. 1987. Cellular localization of the multidrug-resistance gene product P-glycoprotein in normal human tissues. *Proc Natl Acad Sci U S A,* 84**,** 7735-8.

THOMAS, C. E. & AUST, S. D. 1986. Release of iron from ferritin by cardiotoxic anthracycline antibiotics. *Arch Biochem Biophys,* 248**,** 684-9.

TIAN, H., MCKNIGHT, S. L. & RUSSELL, D. W. 1997. Endothelial PAS domain protein 1 (EPAS1), a transcription factor selectively expressed in endothelial cells. *Genes Dev,* 11**,** 72-82.

TIAN, T., NAN, K. J., GUO, H., WANG, W. J., RUAN, Z. P., WANG, S. H., LIANG, X. & LU, C. X. 2010a. PTEN inhibits the migration and invasion of HepG2 cells by coordinately decreasing MMP expression via the PI3K/Akt pathway. *Oncol Rep,* 23**,** 1593-600.

TIAN, T., NAN, K. J., WANG, S. H., LIANG, X., LU, C. X., GUO, H., WANG, W. J. & RUAN, Z. P. 2010b. PTEN regulates angiogenesis and VEGF expression through phosphatase-dependent and -independent mechanisms in HepG2 cells. *Carcinogenesis,* 31**,** 1211-9.

TOMAYKO, M. M. & REYNOLDS, C. P. 1989. Determination of subcutaneous tumor size in athymic (nude) mice. *Cancer Chemother Pharmacol,* 24**,** 148-54.

TOMIDA, A. & TSURUO, T. 1999. Drug resistance mediated by cellular stress response to the microenvironment of solid tumors. *Anticancer Drug Des,* 14**,** 169-77.

TOSO, C., MERANI, S., BIGAM, D. L., SHAPIRO, A. M. & KNETEMAN, N. M. 2010. Sirolimus-based immunosuppression is associated with increased survival after liver transplantation for hepatocellular carcinoma. *Hepatology,* 51**,** 1237-43.

TREIBER, G. 2009. mTOR inhibitors for hepatocellular cancer: a forward-moving target. *Expert Rev Anticancer Ther,* 9**,** 247-61.

TRITTON, T. R. 1991. Cell surface actions of adriamycin. *Pharmacol Ther,* 49**,** 293-309.

TSANG, C. K., QI, H., LIU, L. F. & ZHENG, X. F. 2007. Targeting mammalian target of rapamycin (mTOR) for health and diseases. *Drug Discov Today,* 12**,** 112-24.

UBEZIO, P. & CIVOLI, F. 1994. Flow cytometric detection of hydrogen peroxide production induced by doxorubicin in cancer cells. *Free Radic Biol Med,* 16**,** 509-16.

UNRUH, A., RESSEL, A., MOHAMED, H. G., JOHNSON, R. S., NADROWITZ, R., RICHTER, E., KATSCHINSKI, D. M. & WENGER, R. H. 2003. The hypoxia-inducible factor-1 alpha is a negative factor for tumor therapy. *Oncogene,* 22**,** 3213-20.

VARELA, M., REAL, M. I., BURREL, M., FORNER, A., SALA, M., BRUNET, M., AYUSO, C., CASTELLS, L., MONTANA, X., LLOVET, J. M. & BRUIX, J. 2007. Chemoembolization of hepatocellular carcinoma with drug eluting beads: efficacy and doxorubicin pharmacokinetics. *J Hepatol,* 46**,** 474-81.

VARMA, S. & KHANDELWAL, R. L. 2007. Effects of rapamycin on cell proliferation and phosphorylation of mTOR and p70(S6K) in HepG2 and HepG2 cells overexpressing constitutively active Akt/PKB. *Biochim Biophys Acta,* 1770**,** 71-8.

VAUPEL, P. 2004. The role of hypoxia-induced factors in tumor progression. *Oncologist,* 9 Suppl 5**,** 10-7.

VAUPEL, P. & HARRISON, L. 2004. Tumor hypoxia: causative factors, compensatory mechanisms, and cellular response. *Oncologist,* 9 Suppl 5**,** 4-9.

VAUPEL, P., KALLINOWSKI, F. & OKUNIEFF, P. 1989. Blood flow, oxygen and nutrient supply, and metabolic microenvironment of human tumors: a review. *Cancer Res,* 49**,** 6449-65.

VILLANUEVA, A., CHIANG, D. Y., NEWELL, P., PEIX, J., THUNG, S., ALSINET, C., TOVAR, V., ROAYAIE, S., MINGUEZ, B., SOLE, M., BATTISTON, C., VAN LAARHOVEN, S., FIEL, M. I., DI FEO, A., HOSHIDA, Y., YEA, S., TOFFANIN, S., RAMOS, A., MARTIGNETTI, J. A., MAZZAFERRO, V., BRUIX, J., WAXMAN, S., SCHWARTZ, M., MEYERSON, M., FRIEDMAN, S. L. & LLOVET, J. M. 2008. Pivotal role of mTOR signaling in hepatocellular carcinoma. *Gastroenterology,* 135**,** 1972-83, 1983 e1-11.

VIRMANI, S., RHEE, T. K., RYU, R. K., SATO, K. T., LEWANDOWSKI, R. J., MULCAHY, M. F., KULIK, L. M., SZOLC-KOWALSKA, B., WOLOSCHAK, G. E., YANG, G. Y., SALEM, R., LARSON, A. C. & OMARY, R. A. 2008. Comparison of hypoxia-inducible factor-1alpha expression before and after transcatheter arterial embolization in rabbit VX2 liver tumors. *J Vasc Interv Radiol,* 19**,** 1483-9.

VIVARELLI, M., DAZZI, A., CUCCHETTI, A., GASBARRINI, A., ZANELLO, M., DI GIOIA, P., BIANCHI, G., TAME, M. R., GAUDIO, M. D., RAVAIOLI, M., CESCON, M., GRAZI, G. L. & PINNA, A. D. 2010a. Sirolimus in liver transplant recipients: a large single-center experience. *Transplant Proc,* 42**,** 2579-84.

VIVARELLI, M., DAZZI, A., ZANELLO, M., CUCCHETTI, A., CESCON, M., RAVAIOLI, M., DEL GAUDIO, M., LAURO, A., GRAZI, G. L. & PINNA, A. D. 2010b. Effect of different immunosuppressive schedules on recurrence-free survival after liver transplantation for hepatocellular carcinoma. *Transplantation,* 89**,** 227-31.

VOGL, T. J., NAGUIB, N. N., NOUR-ELDIN, N. E., RAO, P., EMAMI, A. H., ZANGOS, S., NABIL, M. & ABDELKADER, A. 2009. Review on transarterial chemoembolization in hepatocellular carcinoma: palliative, combined, neoadjuvant, bridging, and symptomatic indications. *Eur J Radiol,* 72**,** 505-16.

VOLLMAR, B. & MENGER, M. D. 2009. The hepatic microcirculation: mechanistic contributions and therapeutic targets in liver injury and repair. *Physiol Rev,* 89**,** 1269-339.

WAN, X. W., JIANG, M., CAO, H. F., HE, Y. Q., LIU, S. Q., QIU, X. H., WU, M. C. & WANG, H. Y. 2003. The alteration of PTEN tumor suppressor expression and its association with the histopathological features of human primary hepatocellular carcinoma. *J Cancer Res Clin Oncol,* 129**,** 100-6.

WANDER, S. A., HENNESSY, B. T. & SLINGERLAND, J. M. 2011. Next-generation mTOR inhibitors in clinical oncology: how pathway complexity informs therapeutic strategy. *J Clin Invest,* 121**,** 1231-41.

WANG, B., XU, H., GAO, Z. Q., NING, H. F., SUN, Y. Q. & CAO, G. W. 2008a. Increased expression of vascular endothelial growth factor in hepatocellular carcinoma after transcatheter arterial chemoembolization. *Acta Radiol,* 49**,** 523-9.

WANG, G. L., JIANG, B. H., RUE, E. A. & SEMENZA, G. L. 1995. Hypoxia-inducible factor 1 is a basic-helix-loop-helix-PAS heterodimer regulated by cellular O2 tension. *Proc Natl Acad Sci U S A,* 92**,** 5510-4.

WANG, G. L. & SEMENZA, G. L. 1993. General involvement of hypoxia-inducible factor 1 in transcriptional response to hypoxia. *Proc Natl Acad Sci U S A,* 90**,** 4304-8.

WANG, J., HUANG, Q. & CHEN, M. 2003. The role of NF-kappaB in hepatocellular carcinoma cell. *Chin Med J (Engl),* 116**,** 747-52.

WANG, J., MA, Y., JIANG, H., ZHU, H., LIU, L., SUN, B., PAN, S., KRISSANSEN, G. W. & SUN, X. 2010. Overexpression of von Hippel-Lindau protein synergizes with doxorubicin to suppress hepatocellular carcinoma in mice. *J Hepatol*, 55(2), 359-68.

WANG, J., MA, Y., JIANG, H., ZHU, H., LIU, L., SUN, B., PAN, S., KRISSANSEN, G. W. & SUN, X. 2011. Overexpression of von Hippel-Lindau protein synergizes with doxorubicin to suppress hepatocellular carcinoma in mice. *J Hepatol,* 55**,** 359-68.

WANG, J. C. 2002. Cellular roles of DNA topoisomerases: a molecular perspective. *Nat Rev Mol Cell Biol,* 3**,** 430-40.

WANG, W., JIA, W. D., XU, G. L., WANG, Z. H., LI, J. S., MA, J. L., GE, Y. S., XIE, S. X. & YU, J. H. 2008b. Antitumoral Activity of Rapamycin Mediated Through Inhibition of HIF-1alpha and VEGF in Hepatocellular Carcinoma. *Dig Dis Sci*, 54(10), 2128-36.

WANG, W., JIA, W. D., XU, G. L., WANG, Z. H., LI, J. S., MA, J. L., GE, Y. S., XIE, S. X. & YU, J. H. 2009a. Antitumoral activity of rapamycin mediated through inhibition of HIF-1alpha and VEGF in hepatocellular carcinoma. *Dig Dis Sci*, 54**,** 2128-36.

WANG, W., XU, G. L., JIA, W. D., WANG, Z. H., LI, J. S., MA, J. L. & GE, Y. S. 2009b. [Prevention of hepatic tumor growth and metastasis in rats with rapamycin.]. *Zhonghua Gan Zang Bing Za Zhi,* 17**,** 193-7.

WANG, Y. & MINKO, T. 2004. A novel cancer therapy: combined liposomal hypoxia inducible factor I alpha antisense oligonucleotides and an anticancer drug. *Biochemical Pharmacology,* 68**,** 2031-2042.

WANG, Z., FAN, J., ZHOU, J., WU, Z. Q., QIU, S. J., YU, Y., HUANG, X. W. & TANG, Z. Y. 2006. [Inhibition of growth and metastasis of hepatocellular carcinoma by rapamycin: experiment with mice]. *Zhonghua Yi Xue Za Zhi,* 86**,** 1666-70.

WANG, Z., ZHOU, J., FAN, J., QIU, S. J., YU, Y., HUANG, X. W. & TANG, Z. Y. 2008c. Effect of rapamycin alone and in combination with sorafenib in an orthotopic model of human hepatocellular carcinoma. *Clin Cancer Res,* 14**,** 5124-30.

WANG, Z., ZHOU, J., FAN, J., TAN, C. J., QIU, S. J., YU, Y., HUANG, X. W. & TANG, Z. Y. 2009c. Sirolimus inhibits the growth and metastatic progression of hepatocellular carcinoma. *J Cancer Res Clin Oncol,* 135**,** 715-22.

WARTENBERG, M., LING, F. C., MUSCHEN, M., KLEIN, F., ACKER, H., GASSMANN, M., PETRAT, K., PUTZ, V., HESCHELER, J. & SAUER, H. 2003. Regulation of the multidrug resistance transporter P-glycoprotein in multicellular tumor spheroids by hypoxia-inducible factor (HIF-1) and reactive oxygen species. *FASEB J,* 17**,** 503-5.

WEINREICH, J., LOB, S., LOFFLER, M., KONIGSRAINER, I., ZIEKER, D., KONIGSRAINER, A., COERPER, S. & BECKERT, S. 2011. Rapamycin-induced impaired wound healing is associated with compromised tissue lactate accumulation and extracellular matrix remodeling. *Eur Surg Res,* 47**,** 39-44.

WELFORD, S. M., BEDOGNI, B., GRADIN, K., POELLINGER, L., BROOME POWELL, M. & GIACCIA, A. J. 2006. HIF1alpha delays premature senescence through the activation of MIF. *Genes Dev,* 20**,** 3366-71.

WHITE, S. J., KASMAN, L. M., KELLY, M. M., LU, P., SPRUILL, L., MCDERMOTT, P. J. & VOELKEL-JOHNSON, C. 2007. Doxorubicin generates a proapoptotic phenotype by phosphorylation of elongation factor 2. *Free Radic Biol Med,* 43**,** 1313-21.

WHITTAKER, S., MARAIS, R. & ZHU, A. X. 2010. The role of signaling pathways in the development and treatment of hepatocellular carcinoma. *Oncogene,* 29**,** 4989-5005.

WIESENER, M. S., JURGENSEN, J. S., ROSENBERGER, C., SCHOLZE, C. K., HORSTRUP, J. H., WARNECKE, C., MANDRIOTA, S., BECHMANN, I., FREI, U. A., PUGH, C. W., RATCLIFFE, P. J., BACHMANN, S., MAXWELL, P. H. & ECKARDT, K. U. 2003. Widespread hypoxia-inducible expression of HIF-2alpha in distinct cell populations of different organs. *Faseb J,* 17**,** 271-3.

WIESENER, M. S., TURLEY, H., ALLEN, W. E., WILLAM, C., ECKARDT, K. U., TALKS, K. L., WOOD, S. M., GATTER, K. C., HARRIS, A. L., PUGH, C. W., RATCLIFFE, P. J. & MAXWELL, P. H. 1998. Induction of endothelial PAS domain protein-1 by hypoxia: characterization and comparison with hypoxia-inducible factor-1alpha. *Blood,* 92**,** 2260-8.

WILSON, R. E., KENG, P. C. & SUTHERLAND, R. M. 1989. Drug resistance in Chinese hamster ovary cells during recovery from severe hypoxia. *J Natl Cancer Inst,* 81**,** 1235-40.

WILSTERMANN, A. M. & OSHEROFF, N. 2003. Stabilization of eukaryotic topoisomerase II-DNA cleavage complexes. *Curr Top Med Chem,* 3**,** 321-38.

WONG, G. L., WONG, V. W., TAN, G. M., IP, K. I., LAI, W. K., LI, Y. W., MAK, M. S., LAI, P. B., SUNG, J. J. & CHAN, H. L. 2008. Surveillance programme for hepatocellular carcinoma improves the survival of patients with chronic viral hepatitis. *Liver Int,* 28**,** 79-87.

WONG, L. L., LIMM, W. M., SEVERINO, R. & WONG, L. M. 2000. Improved survival with screening for hepatocellular carcinoma. *Liver Transpl,* 6**,** 320-5.

XIANG, Z. L., ZENG, Z. C., FAN, J., TANG, Z. Y., HE, J., ZENG, H. Y. & CHANG, J. Y. 2011. The expression of HIF-1alpha in primary hepatocellular carcinoma and its correlation with radiotherapy response and clinical outcome. *Mol Biol Rep,* Jun 7. Epub ahead of print.

XIE, C. Y., ZHU, H., LIN, L. P., MIAO, Z. H., GENG, M. Y., CAI, Y. J., CHEN, Y., ZHAO, H. J., LUO, H. B., ZHANG, X. W., FAN, L. M., SHEN, Y. M. & DING, J. 2007. MFTZ-1, an actinomycetes subspecies derived antitumor macrolide, functions as a novel topoisomerase II poison. *Mol Cancer Ther,* 6**,** 3059-70.

XIONG, Z. P., YANG, S. R., LIANG, Z. Y., XIAO, E. H., YU, X. P., ZHOU, S. K. & ZHANG, Z. S. 2004. Association between vascular endothelial growth factor and metastasis after transcatheter arterial chemoembolization in patients with hepatocellular carcinoma. *Hepatobiliary Pancreat Dis Int,* 3**,** 386-90.

YAMADA, R., NAKATSUKA, H., NAKAMURA, K., SATO, M., ITAMI, M., KOBAYASHI, N., MINAKUCHI, K., ONOYAMA, T., KANNO, T., MONNA, T. & YAMAMOTO, S. 1980. Hepatic artery embolization in 32 patients with unresectable hepatoma. *Osaka City Med J,* 26**,** 81-96.

YAMADA, R., SATO, M., KAWABATA, M., NAKATSUKA, H., NAKAMURA, K. & TAKASHIMA, S. 1983. Hepatic artery embolization in 120 patients with unresectable hepatoma. *Radiology,* 148**,** 397-401.

YAMAGATA, M., KANEMATSU, T., MATSUMATA, T., UTSUNOMIYA, T., IKEDA, Y. & SUGIMACHI, K. 1992. The difference in chemosensitivity to antineoplastic agents of human hepatocellular carcinoma cells under normo-oxygenated or hypoxic conditions. *Eur J Surg Oncol,* 18**,** 379-82.

YAMAUCHI, T., RAFFIN, T. A., YANG, P. & SIKIC, B. I. 1987. Differential protective effects of varying degrees of hypoxia on the cytotoxicities of etoposide and bleomycin. *Cancer Chemother Pharmacol,* 19**,** 282-6.

YAMAZAKI, Y., HASEBE, Y., EGAWA, K., NOSE, K., KUNIMOTO, S. & IKEDA, D. 2006. Anthracyclines, small-molecule inhibitors of hypoxia-inducible factor-1 alpha activation. *Biol Pharm Bull,* 29**,** 1999-2003.

YAO, J. C., PHAN, A. T., CHANG, D. Z., WOLFF, R. A., HESS, K., GUPTA, S., JACOBS, C., MARES, J. E., LANDGRAF, A. N., RASHID, A. & MERIC-BERNSTAM, F. 2008. Efficacy of RAD001 (everolimus) and octreotide LAR in advanced low- to intermediate-grade neuroendocrine tumors: results of a phase II study. *J Clin Oncol,* 26**,** 4311-8.

YATSCOFF, R. W., WANG, P., CHAN, K., HICKS, D. & ZIMMERMAN, J. 1995. Rapamycin: distribution, pharmacokinetics, and therapeutic range investigations. *Ther Drug Monit,* 17**,** 666-71.

YOUNG, R. C., OZOLS, R. F. & MYERS, C. E. 1981. The anthracycline antineoplastic drugs. *N Engl J Med,* 305**,** 139-53.

ZAREMBER, K. A. & MALECH, H. L. 2005. HIF-1alpha: a master regulator of innate host defenses? *J Clin Invest,* 115**,** 1702-4.

ZHANG, J. F., LIU, J. J., LU, M. Q., CAI, C. J., YANG, Y., LI, H., XU, C. & CHEN, G. H. 2007. Rapamycin inhibits cell growth by induction of apoptosis on hepatocellular carcinoma cells in vitro. *Transpl Immunol,* 17**,** 162-8.

ZHANG, L., YU, Q., HE, J. & ZHA, X. 2004. Study of the PTEN gene expression and FAK phosphorylation in human hepatocarcinoma tissues and cell lines. *Mol Cell Biochem,* 262**,** 25-33.

ZHONG, H., CHILES, K., FELDSER, D., LAUGHNER, E., HANRAHAN, C., GEORGESCU, M. M., SIMONS, J. W. & SEMENZA, G. L. 2000. Modulation of hypoxia-inducible factor 1alpha expression by the epidermal growth factor/phosphatidylinositol 3-kinase/PTEN/AKT/FRAP pathway in human prostate cancer cells: implications for tumor angiogenesis and therapeutics. *Cancer Res,* 60**,** 1541-5.

ZHOU, H., LUO, Y. & HUANG, S. 2010a. Updates of mTOR inhibitors. *Anticancer Agents Med Chem,* 10**,** 571-81.

ZHOU, J., WANG, Z., WU, Z. Q., QIU, S. J., YU, Y., HUANG, X. W., TANG, Z. Y. & FAN, J. 2008. Sirolimus-based immunosuppression therapy in liver transplantation for patients with hepatocellular carcinoma exceeding the Milan criteria. *Transplant Proc,* 40**,** 3548-53.

ZHOU, L., HUANG, Y., LI, J. & WANG, Z. 2009. The mTOR pathway is associated with the poor prognosis of human hepatocellular carcinoma. *Med Oncol,* 27(2), 255-61.

ZHOU, L., HUANG, Y., LI, J. & WANG, Z. 2010b. The mTOR pathway is associated with the poor prognosis of human hepatocellular carcinoma. *Med Oncol,* 27**,** 255-61.

ZHU, A. X., ABRAMS, T. A., MIKSAD, R., BLASZKOWSKY, L. S., MEYERHARDT, J. A., ZHENG, H., MUZIKANSKY, A., CLARK, J. W., KWAK, E. L., SCHRAG, D., JORS, K. R., FUCHS, C. S., IAFRATE, A. J., BORGER, D. R. & RYAN, D. P. 2011. Phase 1/2 study of everolimus in advanced hepatocellular carcinoma. *Cancer,* Apr 27. Epub ahead of print.

ZHU, H., CHEN, X. P., LUO, S. F., GUAN, J., ZHANG, W. G. & ZHANG, B. X. 2005. Involvement of hypoxia-inducible factor-1-alpha in multidrug resistance induced by hypoxia in HepG2 cells. *J Exp Clin Cancer Res,* 24**,** 565-74.

ZUNDEL, W., SCHINDLER, C., HAAS-KOGAN, D., KOONG, A., KAPER, F., CHEN, E., GOTTSCHALK, A. R., RYAN, H. E., JOHNSON, R. S., JEFFERSON, A. B., STOKOE, D. & GIACCIA, A. J. 2000. Loss of PTEN facilitates HIF-1-mediated gene expression. *Genes Dev,* 14**,** 391-6.

ZUNINO, F. & CAPRANICO, G. 1990. DNA topoisomerase II as the primary target of anti-tumor anthracyclines. *Anticancer Drug Des,* 5**,** 307-17.